

*DNA Repair Pathways in Radiation Induced Cellular Damage;*  
*a molecular approach*

DNA Repair Pathways in Radiation Induced Cellular Damage;  
a molecular approach

Van Veelen, Lieneke Rensia

Thesis Erasmus University Rotterdam.-with ref. -with summary in Dutch

ISBN 90-567-7275-9

© 2005, L.R. van Veelen

For the chapters of this thesis that are based on published papers copyright remains with the publishers.

The cover picture shows a human fibroblast immunostained with antibodies against the protein Rad51.

Layout: T.P. Henny, Rotterdam

Printed by: Thieme MediaCenter, Rotterdam

# **DNA Repair Pathways in Radiation Induced Cellular Damage; a molecular approach**

DNA reparatie mechanismen na stralingsgeïnduceerde cellulaire schade;  
een moleculair biologische analyse

## **Proefschrift**

ter verkrijging van de graad van doctor aan de  
Erasmus Universiteit Rotterdam  
op gezag van de  
Rector Magnificus

Prof.dr. S.W.J. Lamberts

en volgens besluit van het College voor Promoties.

De openbare verdediging zal plaatsvinden op  
vrijdag 4 februari 2005 om 13.30 uur

door

**Lieneke Rensia van Veelen**

geboren te Groningen

## **Promotiecommissie**

**Promotoren:** Prof.dr. R. Kanaar  
Prof.dr. P.C. Levendag

**Overige leden:** Prof.dr. P.A.E. Sillevs Smitt  
Prof.dr. A.C. Begg  
Dr. W. Vermeulen





---

## Contents

<b>Scope of the thesis</b>	9
<b>Chapter 1</b> DNA repair mechanisms and oncogenesis ( <i>review</i> )	11
<b>Chapter 2</b> Biochemical and cellular aspects of homologous recombination ( <i>review</i> )	37
<b>Chapter 3</b> Nuclear dynamics of RAD52 group homologous recombination proteins in response to DNA damage	69
<b>Chapter 4</b> Analysis of ionizing radiation-induced foci of DNA damage repair proteins	91
<b>Chapter 5</b> DNA damage response of homologous recombination proteins in recombination-impaired mammalian cell lines	115
<b>Chapter 6</b> Evaluation of ionizing radiation-induced foci formation and telomere length as predictive assays for radiosensitivity in human fibroblasts and lymphocytes	147
<b>Summary</b>	169
<b>Samenvatting</b>	177
<b>Curriculum Vitae</b>	185
<b>List of publications</b>	187
<b>Dankwoord</b>	189





## **Scope of the Thesis**

DNA damage, especially double-strand breaks, can be induced by endogenous or exogenous damaging agents, such as ionizing radiation. Repair of DNA damage is very important in maintaining genomic stability. Incorrect repair may lead to chromosomal aberrations, translocations and deletions. Consequently, incorrect repair might result in oncogenic transformation of cells, which can lead to the development of cancer. Thus, unrevealing the pathways of double-strand break repair is essential in understanding the genetic interactions that lead to oncogenic changes. Biochemical studies have provided insight into the molecular mechanisms by which various proteins involved in repair of double-strand breaks perform these essential tasks. The next step ahead is analyzing the relationship between the individual biochemical activities of double-strand break repair proteins and their coordinated action in the context of the living cell. This thesis describes the cellular behaviour and cooperation of the mammalian double-strand break repair genes Rad51, Rad52, Rad54 and Mre11 after induction of DNA damage by ionizing radiation. Furthermore, the possible use for a predictive assay that measures individual radiosensitivity in humans, based on the cellular response to DNA double-strand breaks is examined. **Chapter 1** gives an overview of the current knowledge on DNA repair mechanisms, with emphasis on the repair of double-strand breaks by homologous recombination and non-homologous end-joining. The possible role of these pathways in oncogenesis is discussed, based on cell lines and mouse models with specific mutations in DNA repair genes. **Chapter 2** describes the function of the various proteins involved in homologous recombination based on biochemical studies. Moreover, the diverse possibilities of using ionizing radiation-induced foci formation as a technique to determine the cellular properties of these proteins is discussed. An overview of the literature regarding foci formation of various repair proteins in normal and double-strand break repair deficient cell lines is given. **Chapter 3** demonstrates the dynamic behaviour and interactions between Rad51, Rad52 and Rad54 in living cells. **Chapter 4** describes a systematic analysis of a number of factors that could be responsible for the variable outcome of results with regard to ionizing radiation-induced foci formation. In these experiments Rad51 and Mre11 are used as a tool to monitor this influence. Furthermore, the relationship between Rad51 and Mre11 is studied. **Chapter 5** shows the response of Rad51, Rad52 and Rad54 upon DNA damage in radiosensitive mammalian cell lines with a mutation in various genes involved in homologous recombination, examined by ionizing radiation-induced foci formation. **Chapter 6** examines the possibility to use ionizing radiation-induced foci formation and determination of telomere length as methods that might possibly serve as a predictive assay for normal tissue response after ionizing radiation.



---

# *Chapter 1*

*DNA Repair Mechanisms and Oncogenesis*

---

# Chapter 1

## *DNA Repair Mechanisms and Oncogenesis*

L.R. van Veelen<sup>1,2</sup>, R. Kanaar<sup>1,2</sup> and D.C. van Gent<sup>1</sup>

<sup>1</sup> Department of Cell Biology and Genetics,  
Erasmus MC, University Medical Center,  
P.O. Box 1738, 3000 DR Rotterdam, The Netherlands

<sup>2</sup> Department of Radiation Oncology,  
Erasmus MC-Daniel den Hoed Cancer Center, University Medical Center,  
P.O. Box 5201, 3008 AE Rotterdam, The Netherlands

*L. Degos, D.C. Linch and B. Löwenberg, eds. Taylor and Francis Group, London, UK.  
Textbook of Malignant Haematology (2<sup>nd</sup> edition) pp. 155-164, 2005.*

## **Abstract**

Repair of DNA damage, especially of DNA double-strand breaks, is very important in maintaining genomic stability. Incorrect repair of DNA damage may lead to genomic instability and consequently oncogenic transformation of cells, which can lead to the development of cancer. In this review the relationship between defined defects in repair of DNA double-strand breaks and the formation of possible oncogenic translocations is discussed, based on research on cell lines and mouse models with specific mutations in DNA repair genes.

Proper maintenance of the genome is crucial for survival of all organisms. It is of major importance for the functioning of the cell that the information encrypted in the genome is transcribed correctly. However, endogenous and exogenous DNA damaging agents constantly threaten the integrity of the genome. When a cell detects genome injury, it can arrest the cell cycle at specific checkpoints. The activation of cell cycle checkpoints provides time to repair the DNA lesions before they can be converted into permanent mutations. In case DNA damage can not be repaired, the cell is triggered to go into apoptosis or replicative death (Fig. 1). Incorrect repair or accumulation of DNA damage results in genome instability, which may lead to impaired functioning of the cell and even to the development of cancer. Therefore, all organisms are equipped with a complex network of DNA repair mechanisms each of which is able to repair a subset of lesions. The biological significance of DNA repair mechanisms is underlined by the fact that many repair genes are conserved from yeast to humans, which are separated by more than 1.2 billion years of evolution. The importance of the DNA repair pathways is also emphasized by the fact that defects in DNA repair genes often lead to cancer predisposition in humans.

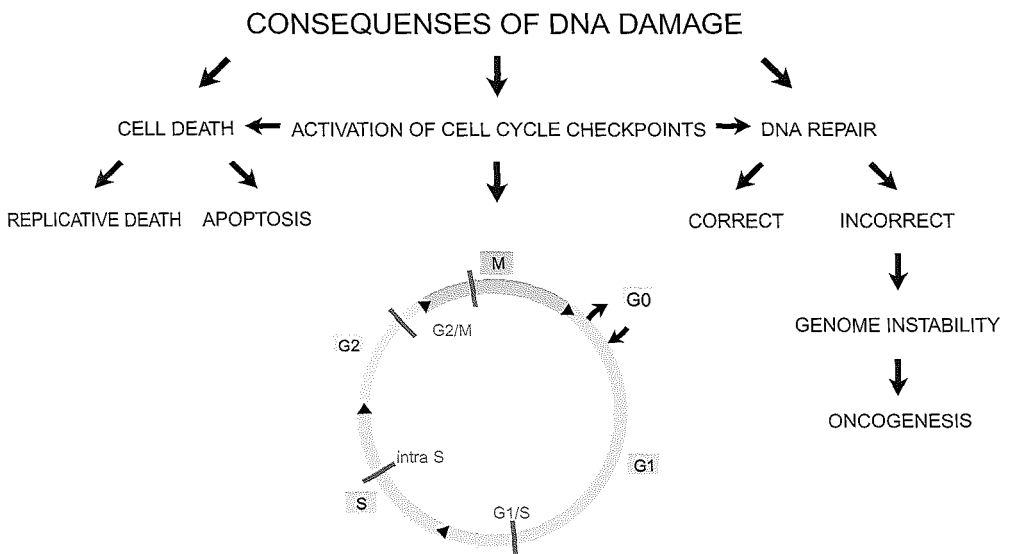


**Figure 1. Cellular consequences of damage to DNA.**

DNA damage triggers activation of cell cycle checkpoints. This can lead to cell cycle arrest at G1/S, intra-S or G2/M phases. During cell cycle arrest the DNA damage can be repaired. Incorrect repair of DNA may lead to genome instability and oncogenesis. An alternative to repair of the DNA damage is the induction of apoptosis or replicative death.

## DNA repair mechanisms

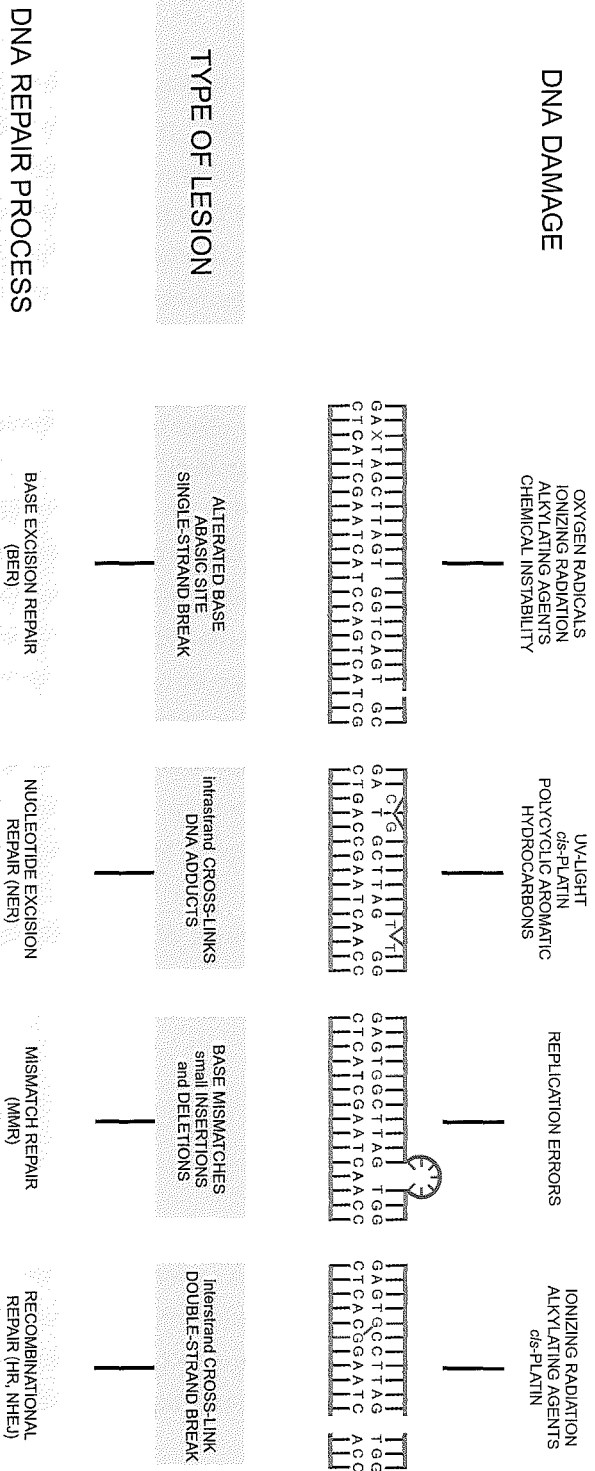
Different DNA damaging agents cause a wide variety of lesions in the DNA strands. Depending on the type of injury, a specific DNA repair mechanism will remove the damage (Fig. 2). Irrespective of the mechanism that is used to repair the lesion, there is a similar succession of events that needs to take place in order to repair the damage. The first step is to recognize the DNA lesion. Subsequently, the lesion is processed which will eventually lead to its removal. The processing of lesions frequently involves incision of DNA strands and removal of the damaged sites, including the surrounding nucleotides. Consequently, final steps in DNA damage repair are re-incorporation of the missing nucleotides and coupling of the DNA ends by a DNA ligase. Depending on the pathway used to repair the lesion and the stage of the repair reaction, a different set of proteins is required.

There are several pathways available which the cell can use to repair the damage. DNA damage can be categorized into two classes; one class in which only one of the two strands of the DNA is damaged and a second class of lesions that affects both strands of the DNA. In case only one strand is damaged, the DNA repair machinery uses the complementary DNA strand as a template for repair. Examples of this type of repair are base excision repair (BER), nucleotide excision repair (NER) and mismatch repair (MMR) (Fig. 2)<sup>1-4</sup>. Repair of a DNA double-strand break (DSB) cannot be accomplished by using the complementary strand as a template, since both strands are broken at the same site. In this case, the cell can utilize the recombinational repair pathways of non-homologous end joining (NHEJ) or homologous recombination (HR) (Fig. 2)<sup>5-7</sup>.

In the next sections the molecular mechanisms of BER, NER and MMR are reviewed briefly. Subsequently, because they are the focus of this thesis, the DSB repair pathways HR and NHEJ are discussed in more detail.

### Base Excision Repair

BER corrects small chemical alterations of bases, which are critical carriers of information in DNA (Fig. 3A). This type of damage can be due to oxygen radicals, generated during normal cellular metabolism or caused by exogenous sources such as ionizing radiation. In BER the affected base is either cut out of the helix by glycosylases, or might already be missing due to the nature of the damage<sup>3,8-10</sup>. The endonuclease Ape 1 incises the strand at the pre-existing or resulting abasic site.





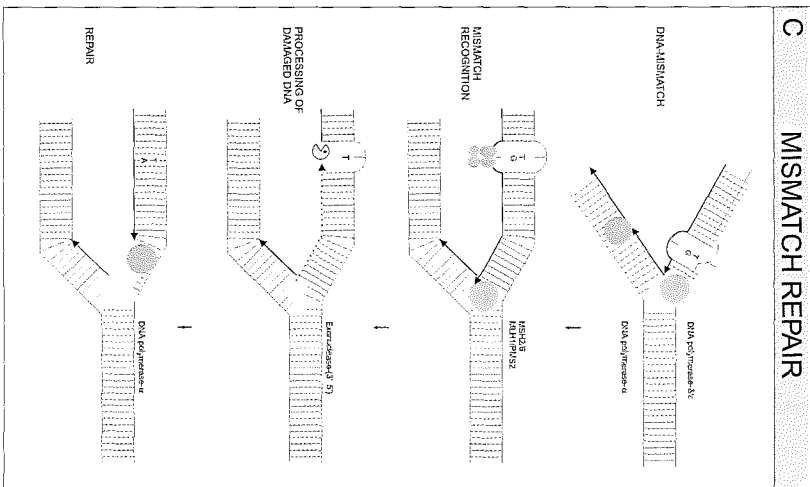
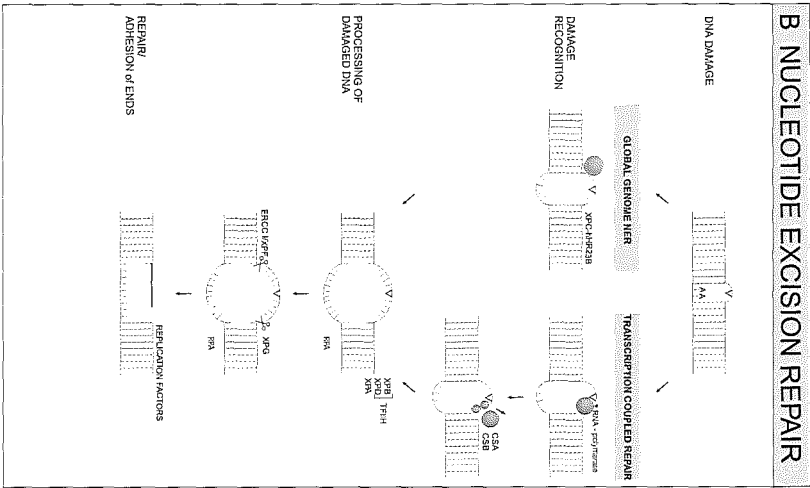
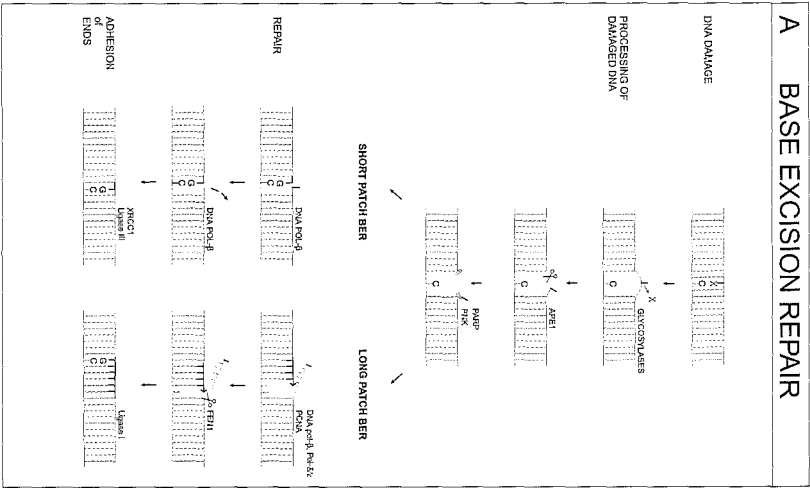
The enzymes poly (ADP-ribose) polymerase (Parp) and polynucleotide kinase (Pnk) are important to protect and trim the DNA ends for repair synthesis. After this step, the lesion can be repaired by short-patch BER, the main pathway, or long-patch BER. In short-patch BER, DNA polymerase- $\beta$  performs a one-nucleotide addition that fills the gap. The complex of Xrcc1 and DNA ligase III seals the remaining open end. In long-patch BER, DNA polymerase- $\beta$ , polymerase  $\delta/\epsilon$  and proliferating cell nuclear antigen (PCNA) are used for the repair synthesis of 2 to 10 bases. The Fen 1 structure-specific endonuclease removes the displaced DNA flap and DNA ligase I seals the remaining open end. So far, no human syndromes have been identified in which BER is deficient.

## **Nucleotide excision repair**

The NER pathway repairs helix-distorting damage that interferes with base pairing and obstructs transcription and normal replication (*Fig. 3B*). These types of lesions include thymidine dimers, induced by UV-light, or bulky DNA adducts caused by alkylating agents and cisplatin. Two subpathways of NER exist; global genome NER (GG-NER), in which the entire genome is surveyed for injuries, and transcription coupled repair (TCR) which focuses on damage that blocks elongating RNA polymerases<sup>1,4,11,12</sup>. The first step in repair through GG-NER is screening for disrupted base pairing using the Xpc-hHR23B protein complex. DNA damage recognition in TCR proceeds differently. In fact, it is the RNA polymerase, which is blocked by the lesion, that triggers the repair. This early step in TCR requires the Csa and Csb proteins. The subsequent stages of GG-NER and TCR may be identical. The transcription factor TFIIH, which contains the Xpb and Xpd helicases, opens the DNA around the damage. Xpa possibly confirms the presence of damage. The protein Rpa binds the undamaged strand, thereby stabilizing the open intermediate. Xpg and Ercc1/Xpf are endonucleases which cleave the borders of the opened damaged strand. The regular DNA replication machinery fills the gap that remains. At least three syndromes are associated with inborn defects in NER; Cockayne syndrome, xeroderma pigmentosum and trichothiodystrophy<sup>13,14</sup>. All these syndromes are characterized by extreme sensitivity to UV-light and premature aging. In particular xeroderma pigmentosum patients have a predisposition to UV-induced skin cancer.

### **Figure 2. Overview of different DNA repair pathways in mammalian cells.**

*Various types of lesions in DNA can be caused by exogenous or endogenous damaging agents. They may affect a single-strand or both strands of the DNA. Different DNA repair pathways that operate on the various lesions are indicated.*



## Mismatch repair

MMR removes nucleotides that are mispaired due to incorporation of an incorrect nucleotide during DNA replication (Fig. 3C). The mismatch is recognized by the complex Msh2 and Msh6 after which additional MMR factors like Mlh1 and Pms2 are recruited<sup>2,15,16</sup>. The newly synthesized strand containing the mis-incorporated nucleotide is identified and excised. Subsequently, the excised tract is resynthesized.

Defects in the MMR system dramatically increase the number of genes that exhibit mutations, due to the uncorrected errors during DNA replication. This replication error (RER) phenotype can easily be detected as an increased level of microsatellite instability<sup>17,18</sup>. Tumors which show this RER phenotype, are usually at a low stage of development and have a favorable prognosis. Hereditary nonpolyposis colorectal cancer (HNPCC) is an example of a genetic disorder, which is caused by a defect in MMR and is usually caused by mutations in the *Mlh1*, *Msh2* or *Msh6* genes<sup>19</sup>. Furthermore a variety of other cancers, like carcinoma of the endometrium, are associated with microsatellite instability caused by a defect in MMR.

### **Figure 3. Repair mechanisms and models of lesions affecting one DNA strand.**

#### **3A. Base excision repair.**

Damage repaired by BER may be caused by ionizing radiation, alkalyting agents and oxygen radicals. These agents cause single-strand breaks or small alterations or deletions of bases, which carry critical information in DNA. The mechanisms of repair through BER is shown in the figure and explained in the text.

#### **3B. Nucleotide excision repair.**

Damage which distorts the normal architecture of the DNA helix is repaired through NER. This type of damage is caused by UV-light, cis-platin and polycyclic aromatic hydrocarbons. Disruption of the DNA helix interferes with base-pairing and obstructs transcription and normal replication. The mechanisms of repair through NER is shown in the figure and explained in the text.

#### **3C. Mismatch repair.**

Errors made during DNA replication can cause base-mismatches or small insertions or deletions of nucleotides, which may lead to mutations. These errors are removed by MMR. A model for MMR is shown in the figure and explained in the text.

## DNA double-strand break repair

DSBs, as well as the less genotoxic single-strand breaks, can be caused by ionizing radiation, free radicals and chemicals, such as alkylating agents. Furthermore, DSBs may arise during replication of a region containing a single-strand break. Several repair mechanisms can deal with DSBs, emphasizing the importance of repairing this type of DNA damage.

The two major DSB repair pathways are HR and NHEJ. The difference between these two pathways is the use of a homologous sequence. HR uses the sister chromatid or homologous chromosome as a template for repair, whereas NHEJ simply joins the broken ends without use of a template (*Fig. 4*). This difference in repair mechanisms leads to a difference in the fidelity of repair. HR restores the original DNA sequence and is therefore a precise type of repair. NHEJ, on the other hand, often leads to addition or deletion of nucleotides at the joining site. In this way, important information may be lost, thus making NHEJ an error-prone repair pathway.

The relative contribution of these pathways to DSB repair likely depends on the cell cycle stage. In the G1-phase, when the sister chromatid is absent, a DSB is most likely to be repaired through NHEJ<sup>20,21</sup>. HR is most efficient in the S- and G2-phases of the cell cycle, when the sister chromatid is available as a template<sup>22</sup>. However, NHEJ may also occur in the S- and G2-phases<sup>23,24</sup>. The detection, processing and ligation of the break is organized by a large number of proteins, which are specific for each pathway, although some proteins may be involved in both HR and NHEJ (*Fig. 4*). The exact function of many repair proteins involved in these pathways is still unknown.

**Homologous Recombination.** HR is mediated by the so-called Rad52 group of proteins, which includes Rad50, Rad51, Rad52, Rad54, Mre11 and Nbs1<sup>6,7,25</sup>. Recognition of the broken DNA ends may occur by the Rad50/Mre11/Nbs1 complex or by Rad52<sup>26,27</sup>. Nucleolytic processing of the broken ends leads to the formation of single-stranded tails (*Fig. 4*). Rad51 proteins form a nucleoprotein filament on this single-stranded tail. The Rad51 nucleoprotein filament searches for the homologous piece of DNA<sup>28</sup>. Once the homology has been detected, a joint molecule is generated between the damaged DNA and the undamaged sister chromatid. Several proteins assist Rad51 in this complex reaction, including the breast cancer susceptibility proteins Brca1 and Brca2, five Rad51 paralogs, Rad52 and Rad54<sup>6, 29-33</sup>. The information that was lost during processing of the DNA ends is restored by DNA polymerases that synthesize new DNA using the undamaged sister chromatid as a template. Finally, the DNA strands are ligated resulting in accurate repair of the DSB. A putative link between

DNA DOUBLE-STRAND BREAK



HOMOLOGOUS RECOMBINATION

NON-HOMOLOGOUS END JOINING

DAMAGE RECOGNITION



END PROCESSING



HOMOLOGY SEARCH



DNA SYNTHESIS



LIGATION



Rad51, Rad52, Rad54  
Rad50, Mre11, Nbs1  
Rad51 paralogs  
Brca1, Brca2

Ku70, Ku80, DNA-PKcs  
Artemis  
Ligase IV, Xrcc4

**Figure 4. Major double-strand break repair pathways.**

DNA DSBs can be repaired by at least two mechanistically distinct pathways; homologous recombination (HR) and non-homologous end joining (NHEJ). This figure shows a simplification of the models for DSB repair. During HR the damaged DNA (grey lines) uses the sister chromatid or homologous chromosome (red lines) as a template to repair the DNA accurately. NHEJ repairs the damaged DNA by simply joining the DNA ends in a way that is not necessarily error-free, since no DNA template is utilized for the newly synthesized DNA at the damaged site (red lines). The succession of events that take place during repair of the damage is presented. A number of proteins involved in each pathway are indicated and discussed in the text.

reduced HR-efficiency and cancer predisposition is provided by the observation that many carriers of mutations in either Brca1 or Brca2 develop breast or ovarian cancer<sup>34</sup>.

**Non-Homologous End Joining.** Several proteins that are involved in NHEJ have been identified (Fig. 4). The Ku70/Ku80 protein complex forms a ring around the DNA ends<sup>35</sup>. End-bound Ku70/Ku80 activates the DNA-dependent protein kinase catalytic subunit (DNA-PKcs). Together they form a protein complex known as DNA-PK which is involved in the early recognition of the DSB<sup>36</sup>. Subsequently, the DNA can be processed by nucleases or polymerases. Nucleases, such as the Artemis protein, remove nucleotides from the DNA ends<sup>37</sup>. DNA polymerases synthesize new DNA, in order to prepare the DNA ends for ligation. Finally, both ends are joined by the Ligase IV/Xrcc4 complex<sup>38</sup>.

Two groups of patients with defects in NHEJ have been identified. A small subset of patients with severe combined immunodeficiency (SCID) have a mutation in the Artemis gene<sup>39</sup>. Furthermore, patients have been described in which a mutation on one allele of the *Ligase IV* gene is detected<sup>40</sup>. The phenotype of these patients is heterogeneous, although most of them suffer from immunodeficiency. It is not clear whether patients with a defect in either *Artemis* or *Ligase IV* display cancer predisposition.

## DNA rearrangements in the immune system

**V(D)J recombination.** The NHEJ repair pathway is not only used to repair DSBs which are induced by exogenous factors, but it is also involved in processing the programmed DSBs that arise during the generation of immunoglobulin and T-cell receptor genes. These programmed DSBs are natural intermediates in a specialized recombination event called V(D)J recombination<sup>41</sup>. This recombination reaction is required for the creation of functional B- and T-cells.

Mature immunoglobulin (Ig) and T cell receptor (TCR) genes are assembled from separate gene segments in B- and T-cells, respectively. The lymphoid-specific proteins Rag1 and Rag2 initiate this DNA recombination process. They bind to recombination signal sequences (Fig. 5A), which flank the variable (V), diversity (D) and joining (J) segments of the Ig and Tcr genes (Fig. 5B)<sup>41</sup>. Subsequently, a DSB is made at the border of the recombination signal sequence and the coding gene segment. The products of this cleavage reaction are blunt DNA ends at the side of the recombination signal sequence. The coding gene segment ends in a hairpin structure, in which the top strand is coupled to the bottom strand. The DNA ends are recombined such that the two coding gene segments form the coding joint, from which

the immunoglobulin or T-cell receptor genes arise, while the signal sequences are ligated in the signal joint, which is not used any further (*Fig. 5A*). For this joining process, the NHEJ machinery of the cell is used.

V(D)J recombination is a highly regulated process. In B-cell development, the Ig heavy chain locus is recombined first. If this yields a functional heavy chain polypeptide, the cell will start a proliferation phase, after which the Ig light chain loci ( $\kappa$  or  $\lambda$ ) are rearranged. These cells enter the circulation as virgin B-cells, provided that they produce functional immunoglobulins that are not autoreactive. A similar order of events leads to the formation of virgin T-cells<sup>42</sup>. A deficiency in one of the Rag proteins or in one of the components of the NHEJ process severely impairs the capacity to perform V(D)J recombination which results in low levels of mature B- and T-cells<sup>43</sup>.

**Immunoglobulin class switching.** A later step in B-cell development is immunoglobulin heavy chain class switching. This leads to expression of a different class of antibodies which are also initiated by programmed DSB formation<sup>44,45</sup>. Most circulating B-cells never encounter antigens that are recognized by the immunoglobulins on their surface. The few B-cells that are stimulated by an antigen go into a regulated differentiation scheme. These stimulated B-cells are able to change the type of immunoglobulin they produce using a DNA recombination process, called immunoglobulin heavy chain class switching (*Fig. 5B*)<sup>44,45</sup>. The mechanism of this recombination reaction is less well understood than the process of V(D)J recombination. However, it is clear that class switch recombination requires DNA-PK, which might indicate that DSBs are intermediates in this process which may be repaired by the NHEJ proteins<sup>46-48</sup>. After the B-cells have undergone the maturation program, they enter the circulation as plasma cells, which produce large amounts of secreted immunoglobulins that recognize the antigen for which they were selected. When the antigen has been removed from the system, some of these plasma cells can develop into memory cells, which survive for a very long time and react very quickly when the organism is invaded for a second time by the same antigen.

**Somatic hypermutation.** Somatic hypermutation is another process in the immune system in which the DNA sequence is altered (*Fig. 5B*). It changes the binding efficiency of immunoglobulins, by introducing point mutations in the DNA region containing the V(D)J segment<sup>49,50</sup>. It has been demonstrated that DSBs occur in hypermutating Ig genes, preferentially at mutational hotspots<sup>49,51</sup>. However, the exact function of these DSBs is still poorly understood.

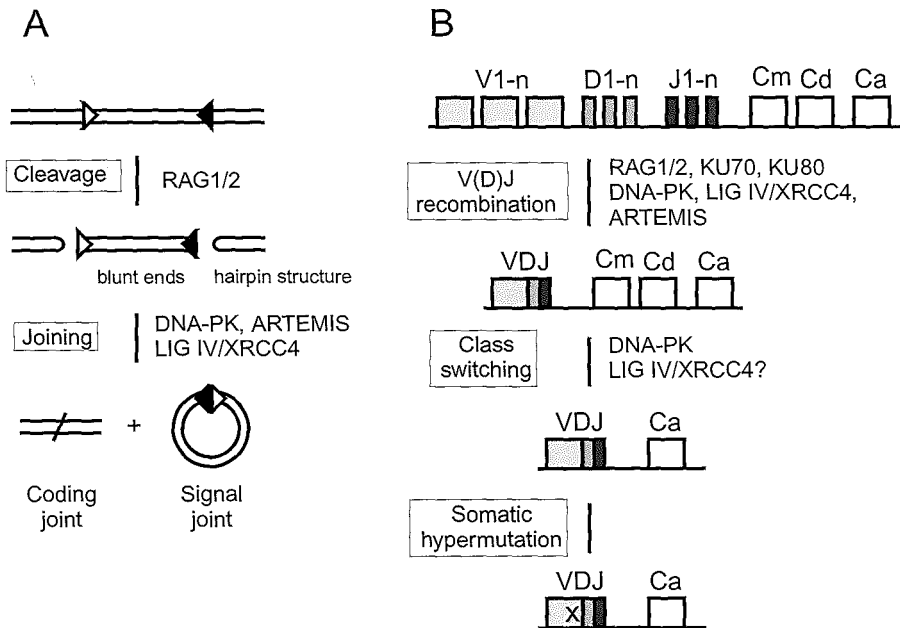


**Figure 5. DNA rearrangements in the immune system.**

**5A.** The mechanisms of V(D)J recombination.

DSBs are made by the *Rag1* and *Rag2* proteins at the border of the recombination signal sequences (triangles) that surround the V, D and J segments of the Ig and Tcr genes. Recombination signal sequences contain motifs separated by a spacer of 12 or 23 base pairs of non-conserved sequence. Recombination always takes place between one signal sequence with a 12 bp spacer and one with a 23 bp spacer (open and closed triangles). The DSBs are made in such a way that the ends form a hairpin structure in which the top strand is coupled to the bottom strand. The joining reaction is accomplished by the NHEJ machinery, which involves end recognition by the Ku/DNA-PK complex and ligation by the LigaseIV/Xrcc4 complex. The DNA hairpin intermediates are probably opened and processed by the Artemis protein. The coding joint gives rise to the functional immunoglobulin or T-cell receptor genes. The signal joint is irrelevant for the further process.

**5B.** Overview of the different types of DNA rearrangements in the immune system.

In pre-B cells, the immunoglobulin loci undergo V(D)J recombination. As an example, the IgH locus is shown. First, one of the D segments is coupled to one of the J segments, followed by V to DJ joining. After successful assembly of functional immunoglobulin genes and stimulation by antigen, a second DNA rearrangement can delete a number of constant regions (indicated by capital C with different subscripts), resulting in expression of a different immunoglobulin isotype. This class switch recombination reaction requires at least the components of the DNA-PK complex, and possibly also the Ligase IV/Xrcc4 complex. Finally, the affinity of the antibodies for the antigen can be modulated by introduction of point mutations into the VDJ exon. The mechanism of this somatic hypermutation reaction is not yet clear, although DSBs have been found at the site of hypermutation, suggesting that DSB repair mechanisms may be involved.



## Cell cycle checkpoints

DSBs are particularly dangerous lesions when they occur during replication of the genome or during mitosis when the duplicated chromosomes are divided over the daughter cells. When broken chromosomes are carried through mitosis, the chromosome fragments will not distribute evenly between the two daughter cells, thus causing chromosomal aberrations<sup>52,53</sup>. Several checkpoints can stop the cell at different points in the cell cycle when DNA damage is present. The G1/S checkpoint prevents the cell from starting DNA replication; intra-S checkpoints slow down replication and G2/M checkpoints arrest the cell before division<sup>21</sup>. Among the many proteins involved in DNA damage-induced cell cycle arrest are p53, ATM and the protein complex Mre11/Rad50/Nbs1. *P53* plays a role in a number of different checkpoints. ATM and the Mre11/Rad50/Nbs1 complex are mainly involved in the intra-S checkpoint<sup>54,55</sup>.

Several human syndromes are associated with defects in these checkpoint genes. Mutations in *ATM* or *Mre11* cause syndromes called ataxia telangiectasia (AT) or AT-like disorder (ATLD), respectively<sup>56-58</sup>. A mutation in *Nbs1* leads to the Nijmegen breakage syndrome<sup>59</sup>. These syndromes have a number of overlapping features, such as growth retardation, neurological problems, increased sensitivity to ionizing radiation and a predisposition to cancer, mainly lymphoma. A heterozygous mutation in *p53* can cause the Li-Fraumeni syndrome, a disorder that is characterized by a high tumor incidence, especially breast cancer, sarcomas, brain tumors and, to a lesser extent, hematological and adrenocortical neoplasms<sup>60</sup>. Additionally, the *p53* gene is frequently found to be mutated in tumors, which gives an indication of the tumorigenic effects of a defect in *p53*.

## Double-strand breaks and chromosomal aberrations

DSB repair plays a role in the prevention of chromosomal instability and potentially oncogenic translocations<sup>7,61</sup>. Paradoxically some proteins required for proper DSB repair, are likely to be involved in the creation of translocations as well. These translocations arise when a fusion occurs between parts of different chromosomes. A DSB is most probably the initiating DNA lesion that can result in translocations as a consequence of misrepair (*Fig. 6*). Since proteins involved in DSB repair are essential for the ligation of DNA ends, it must mean that the generation of translocations requires their activity. Translocations are a characteristic feature of many tumors and have become important markers in diagnosis and prognosis. However, little is known about the relationship between

oncogenesis and DSB repair defects in humans<sup>62</sup>. Studies involving mouse models and cell lines with mutations in DNA repair genes, have highlighted the relationship between defects in DSB repair pathways and the formation of translocations and oncogenesis (Table 1)<sup>63</sup>.

**Homologous recombination and chromosomal aberrations.** HR uses the sister chromatid or the homologous chromosome as a template for repair of the broken ends. Probably because of its proximity, the sister chromatid is commonly used as the repair template. The preference of the sister chromatid over the homologous chromosome is biologically relevant since recombination between homologous chromosomes can lead to loss of heterozygosity (LOH)<sup>64</sup>. Defects in HR, such as errors in template choice, could even be more harmful when recombination occurs between repetitive sequences, which are present throughout the genome (Fig. 6). This type of ectopic recombination may lead to chromosomal translocations.

The importance of HR is emphasized by the finding that inactivation of genes involved in HR often results in embryonic lethality. Therefore, animal models have been designed in which the effect of mutations in specific tissues can be investigated. The role of *Brca1* in genomic instability was studied by creating mice in which the *Brca1* gene was specifically inactivated in the epithelial cells<sup>65</sup>. In the mammary tumors that developed, translocations were frequently observed. Additional inactivation of the *p53* gene accelerated the formation of mammary tumors in these mice. The same results were seen in mice that carry a specific mutation in the *Brca2* gene<sup>66</sup>. *Brca2* mutant mice have an increased sensitivity to ionizing radiation, growth retardation, infertility and frequent development of thymic lymphomas and cells, derived from these mice, show spontaneous chromosomal aberrations<sup>67</sup>. Chromosomal instability was also observed in a chicken B-cell lymphoma cell line that was conditionally mutated for *Rad51*<sup>68</sup>. Results from these animal studies suggest a role for HR in the development of chromosomal translocations and oncogenesis.

**Figure 6. Translocations and loss of heterozygosity during aberrant DSB repair.**

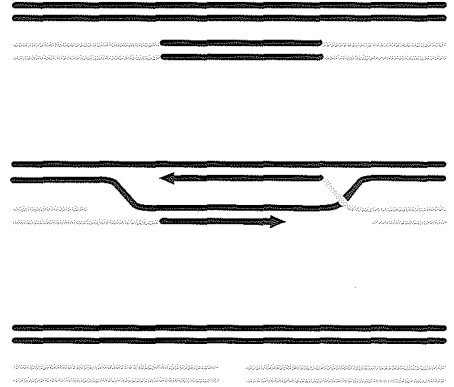
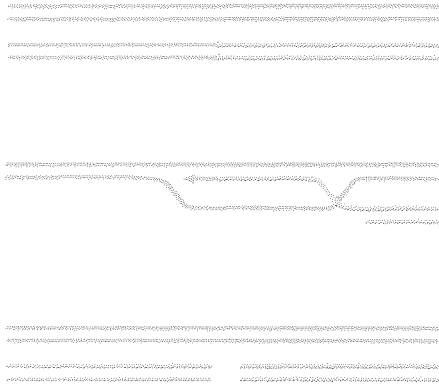
**(Upper left)** Translocations by NHEJ can occur when two DSBs on heterologous chromosomes are ligated. Unbroken heterologous chromosomes are depicted by two parallel blue and yellow lines respectively. They are shown to undergo breakage and misligation, resulting in a reciprocal translocation.

**(Upper right)** Translocations by HR can occur when a DSB is repaired using repetitive sequences located on a heterologous chromosome. In the example a combined translocational and LOH event is shown.

**(Bottom left)** Loss of heterozygosity (LOH) by NHEJ can occur when DNA sequences around a DSB are degraded before ligation. The sets of light and dark blue lines represent homologous chromosomes.

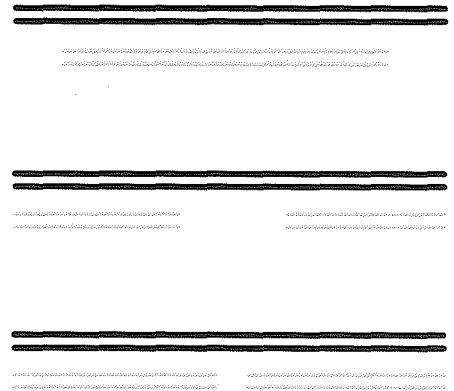
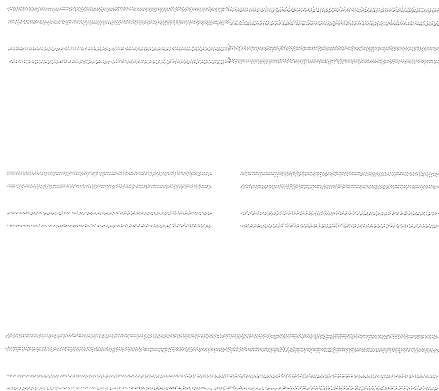
**(Bottom right)** LOH during HR can occur when the homologous chromosome instead of the sister chromatid is used for DSB repair.

HOMOLOGOUS RECOMBINATION



TRANSLOCATIONS

NON-HOMOLOGOUS END JOINING



LOSS OF HETEROZYGOSITY

**Non-homologous end joining and chromosomal aberrations.** The role of NHEJ in oncogenesis has been studied more extensively. Defects in NHEJ not only lead to genomic instability but also to impaired functioning of the V(D)J recombination process. Immunodeficiency is therefore a characteristic feature of humans and mice with defects in one of the NHEJ genes. Mice carrying mutations in NHEJ genes have been studied in more detail. The phenotypes of these mutant mice reveal similarities, like increased radiation sensitivity and immunodeficiency, but also striking differences have been observed. Mice lacking *Ku70*, *Ku80* or *DNA-PKcs* are viable and *Ku70* and possibly *DNA-PKcs* deficient mice develop T-cell lymphomas at late onset<sup>69-73</sup>. This is in contrast with *Xrcc4* or *Ligase IV* deficient mice, which die during embryogenesis due to neuronal apoptosis<sup>74-77</sup>. The lethality of the *Xrcc4* and *Ligase IV* mutant mice, together with the apoptosis and senescence phenotype of cells derived from the NHEJ mutant mice reveal that the NHEJ pathway is critical for the repair of spontaneously occurring DSBs. Cells that are deficient in one of the NHEJ genes indeed show genomic instability, particularly spontaneous chromosome and chromatid breaks (*Table 1*).

The main evidence for a role of NHEJ in tumorigenesis is seen in experiments where mice, that lack one of the NHEJ genes, are crossed with *p53* deficient mice. Interestingly the lethality, but not the V(D)J recombination capability, of the *Xrcc4* and *Ligase IV* mice is rescued by the absence of *p53*<sup>75,78</sup>. However, these viable double mutant mice, develop pro-B-cell lymphomas at early age. Pro-B-cell lymphomas are also observed in other double mutant mice, which lack *p53* and one of the other NHEJ genes (*Table 1*). A possible explanation for this additional effect of the *p53* mutation can be found in the reduced level of apoptosis in *p53* deficient mice. Damaged NHEJ-deficient cells, which would normally go into apoptosis, are not eliminated efficiently in this genetic background. The pro-B-cell lymphomas that occur in these mice have a characteristic t(12;15) translocation between the IgH locus and the c-myc locus<sup>79</sup>. The IgH locus is the first target of the Rag endonucleases in the development of B-lymphocytes. Most likely, the initiating lesion of the pro-B-cell lymphomas is a Rag-induced DSB. This hypothesis is supported by the fact that triple-mutant *DNA-PK/p53/Rag2* mice do not develop pro-B-cell lymphomas<sup>79</sup>.

**Table 1. Consequences of homozygous mutations in cell cycle checkpoint genes and genes involved in DSB repair.**

*The influence of a homozygous mutation (knock-out mutation) of these genes on genomic instability in cells and cancer predisposition in mice is indicated. An additional homozygous mutation of p53 rescues viability in several embryonic lethal mice and influences the spectrum and time of onset of tumors in these mice. The column miscellaneous represents genes which may be involved in more than one of the pathways listed above. ND = not determined*

	Genome instability	Mouse knock-out: cancer predisposition	Mouse knock-out combined with <i>p53</i> knock-out: cancer predisposition	References
<b>Cell cycle checkpoint genes</b>				
<i>ATM</i>	Chromosomal aberrations	T-cell lymphomas	Early onset B- and T-cell lymphomas	81,82
<i>p53</i>	Chromosomal aberrations	T-cell lymphomas and B-cell lymphomas	Not applicable	83-85
<b>Non-Homologous End Joining</b>				
<i>DNA-PKcs</i>				
<i>Ku70</i>	Chromosomal aberrations	No overt cancer predisposition	Early onset pro-B-cell lymphomas	71,86-88
<i>Ku80</i>	Chromosomal aberrations	T-cell lymphomas	ND	72,73,89,90
<i>Artemis</i>	Chromosomal aberrations	No cancer predisposition	Early onset pro-B-cell lymphomas	91-93
<i>Xrcc4</i>	ND	ND	ND	39
<i>Ligase IV</i>	Chromosomal aberrations	Embryonic lethal	Rescues embryonic lethality Early onset pro-B-cell lymphomas	74,78
	Chromosomal aberrations	Embryonic lethal	Rescues embryonic lethality Early onset pro-B-cell lymphomas	63,75,80
<b>Homologous recombination</b>				
<i>Rad51</i>	Chromosomal aberrations	Embryonic lethal	Embryonic lethal	68,94,95
<i>Rad52</i>	ND	No cancer predisposition	ND	96
<i>Rad54</i>	No instability	No cancer predisposition	ND	97,98
<i>Brca2</i>	Chromosomal aberrations	Embryonic lethal	Embryonic lethal	99,100
<b>Miscellaneous</b>				
<i>Brca1</i>	Chromosomal aberrations	Embryonic lethal	Embryonic lethal	30,99
<i>Rad50</i>	Not viable	Embryonic lethal	ND	101
<i>Mre11</i>	Chromosomal aberrations	Embryonic lethal	ND	102
<i>Nbs1</i>	Translocations	Embryonic lethal	ND	103
<b>V(D)J recombination genes</b>				
<i>Rag1</i>	Translocations	Unknown Mice die at early age	Early onset T-cell lymphomas	84,104,105
<i>Rag2</i>	Translocations	Unknown Mice die at early age	Early onset T-cell lymphomas	84,104,105

The development of mouse models has enabled a detailed analysis of genetic interactions between NHEJ deficiencies and mutations in other genome stability genes. Mice that are deficient for one of the NHEJ genes and heterozygous for *p53* are also prone to get solid tumors, mainly sarcomas. Although this broad spectrum of tumors can also be observed in the heterozygous *p53* mouse, the NHEJ deficiency accelerates this process, leading to development of the tumors at an earlier onset. Complementary, heterozygosity for *Ligase IV* also influences tumor development in mice, carrying a homozygous deletion in a tumor suppressor gene. These knock-out mice are predisposed to get lymphomas, but an additional heterozygous mutation in *Ligase IV* provokes development of soft tissue sarcomas which possess chromosomal amplifications, deletions and translocations<sup>80</sup>. This implies that a heterozygous mutation in an NHEJ gene by itself does not lead to an increased cancer risk. However, a combination of such a mutation and a defect in other genes involved in genome stability, may accelerate cancer development, emphasizing the importance of the genetic background in oncogenesis. The genetic background in which a mutation in one of the repair gene occurs, determines whether a tumor will develop and influences the time of onset. These findings are very important to understand the intricate genetic interactions that may influence the risk for cancer.

## **Future perspectives**

It is evident that DNA DSB repair proteins not only play an important role in the prevention, but also in the generation of genomic instability. The findings described in this chapter are just the beginning of a deeper understanding of the genetic interactions underlying oncogenic changes. The development of mouse models, which allows investigation of the effects of a combination of two or more mutations, will yield a wealth of information in the near future. In combination with genomics and proteomics, this will lead to a new view on the exact role of the genes involved in DNA repair and their involvement in the etiology of cancer.

## References

1. Svejstrup, J.Q. Mechanisms of transcription-coupled DNA repair. *Nat Rev Mol Cell Biol* **3**, 21-9. (2002).
2. Aquilina, G. & Bignami, M. Mismatch repair in correction of replication errors and processing of DNA damage. *J Cell Physiol* **187**, 145-54. (2001).
3. Lindahl, T. Keynote: past, present, and future aspects of base excision repair. *Prog Nucleic Acid Res Mol Biol* **68**, xvii-xxx. (2001).
4. Sugasawa, K. et al. A multistep damage recognition mechanism for global genomic nucleotide excision repair. *Genes Dev* **15**, 507-21. (2001).
5. Karran, P. DNA double strand break repair in mammalian cells. *Curr Opin Genet Dev* **10**, 144-50. (2000).
6. Kanaar, R., Hoeijmakers, J.H. & van Gent, D.C. Molecular mechanisms of DNA double strand break repair. *Trends Cell Biol* **8**, 483-9. (1998).
7. van Gent, D.C., Hoeijmakers, J.H. & Kanaar, R. Chromosomal stability and the DNA double-stranded break connection. *Nat Rev Genet* **2**, 196-206. (2001).
8. Memisoglu, A. & Samson, L. Base excision repair in yeast and mammals. *Mutat Res* **451**, 39-51. (2000).
9. Mol, C.D., Parikh, S.S., Putnam, C.D., Lo, T.P. & Tainer, J.A. DNA repair mechanisms for the recognition and removal of damaged DNA bases. *Annu Rev Biophys Biomol Struct* **28**, 101-28. (1999).
10. Whitehouse, C.J. et al. XRCC1 stimulates human polynucleotide kinase activity at damaged DNA termini and accelerates DNA single-strand break repair. *Cell* **104**, 107-17. (2001).
11. Buschta-Hedayat, N., Buterin, T., Hess, M.T., Missura, M. & Naegeli, H. Recognition of nonhybridizing base pairs during nucleotide excision repair of DNA. *Proc Natl Acad Sci USA* **96**, 6090-5. (1999).
12. Citterio, E., Vermeulen, W. & Hoeijmakers, J.H. Transcriptional healing. *Cell* **101**, 447-50. (2000).
13. Cleaver, J.E. & Crowley, E. UV damage, DNA repair and skin carcinogenesis. *Front Biosci* **7**, 1024-43. (2002).
14. Vermeulen, W. et al. Mammalian nucleotide excision repair and syndromes. *Biochem Soc Trans* **25**, 309-15. (1997).
15. Harfe, B.D. & Jinks-Robertson, S. DNA mismatch repair and genetic instability. *Annu Rev Genet* **34**, 359-99. (2000).
16. Kolodner, R.D. & Marsischky, G.T. Eukaryotic DNA mismatch repair. *Curr Opin Genet Dev* **9**, 89-96. (1999).
17. Atkin, N.B. Microsatellite instability. *Cytogenet Cell Genet* **92**, 177-81. (2001).
18. Sinden, R.R. Neurodegenerative diseases. Origins of instability. *Nature* **411**, 757-8. (2001).
19. Muller, A. & Fishel, R. Mismatch repair and the hereditary non-polyposis colorectal cancer syndrome (HNPCC). *Cancer Invest* **20**, 102-9. (2002).
20. Dasika, G.K. et al. DNA damage-induced cell cycle checkpoints and DNA strand break repair in development and tumorigenesis. *Oncogene* **18**, 7883-99. (1999).
21. Zhou, B.B. & Elledge, S.J. The DNA damage response: putting checkpoints in perspective. *Nature* **408**, 433-9. (2000).
22. Johnson, R.D. & Jasin, M. Sister chromatid gene conversion is a prominent double-strand break repair pathway in mammalian cells. *EMBO J* **19**, 3398-407. (2000).
23. Takata, M. et al. Homologous recombination and non-homologous end-joining pathways of DNA double-strand break repair have overlapping roles in the maintenance of chromosomal integrity in vertebrate cells. *EMBO J* **17**, 5497-508. (1998).
24. Richardson, C. & Jasin, M. Coupled homologous and nonhomologous repair of a double-strand break preserves genomic integrity in mammalian cells. *Mol Cell Biol* **20**, 9068-75. (2000).
25. Paques, F. & Haber, J.E. Multiple pathways of recombination induced by double-strand breaks in *Saccharomyces cerevisiae*. *Microbiol Mol Biol Rev* **63**, 349-404. (1999).

## Chapter 1

---

26. de Jager, M. et al. Human Rad50/Mre11 is a flexible complex that can tether DNA ends. *Mol Cell* **8**, 1129-35. (2001).
27. Van Dyck, E., Stasiak, A.Z., Stasiak, A. & West, S.C. Binding of double-strand breaks in DNA by human Rad52 protein. *Nature* **398**, 728-31. (1999).
28. Baumann, P. & West, S.C. Role of the human RAD51 protein in homologous recombination and double-stranded-break repair. *Trends Biochem Sci* **23**, 247-51. (1998).
29. Davies, A.A. et al. Role of BRCA2 in control of the RAD51 recombination and DNA repair protein. *Mol Cell* **7**, 273-82. (2001).
30. Moynahan, M.E., Cui, T.Y. & Jasin, M. Homology-directed dna repair, mitomycin-c resistance, and chromosome stability is restored with correction of a Brca1 mutation. *Cancer Res* **61**, 4842-50. (2001).
31. Moynahan, M.E., Pierce, A.J. & Jasin, M. BRCA2 is required for homology-directed repair of chromosomal breaks. *Mol Cell* **7**, 263-72. (2001).
32. Thompson, L.H. & Schild, D. Homologous recombinational repair of DNA ensures mammalian chromosome stability. *Mutat Res* **477**, 131-53. (2001).
33. Thacker, J. A surfeit of RAD51-like genes? *Trends Genet* **15**, 166-8. (1999).
34. Venkitaraman, A.R. Cancer susceptibility and the functions of BRCA1 and BRCA2. *Cell* **108**, 171-82. (2002).
35. Walker, J.R., Corpina, R.A. & Goldberg, J. Structure of the Ku heterodimer bound to DNA and its implications for double-strand break repair. *Nature* **412**, 607-14. (2001).
36. Jones, J.M., Gellert, M. & Yang, W. A Ku bridge over broken DNA. *Structure (Camb)* **9**, 881-4. (2001).
37. Ma, Y., Pannicke, U., Schwarz, K. & Lieber, M.R. Hairpin Opening and Overhang Processing by an Artemis/DNA-Dependent Protein Kinase Complex in Nonhomologous End Joining and V(D)J Recombination. *Cell* **108**, 781-94. (2002).
38. Lieber, M.R., Grawunder, U., Wu, X. & Yaneva, M. Tying loose ends: roles of Ku and DNA-dependent protein kinase in the repair of double-strand breaks. *Curr Opin Genet Dev* **7**, 99-104. (1997).
39. Moshous, D. et al. Artemis, a novel DNA double-strand break repair/V(D)J recombination protein, is mutated in human severe combined immune deficiency. *Cell* **105**, 177-86. (2001).
40. O'Driscoll, M. et al. DNA ligase IV mutations identified in patients exhibiting developmental delay and immunodeficiency. *Mol Cell* **8**, 1175-85. (2001).
41. Oettinger, M.A. V(D)J recombination: on the cutting edge. *Curr Opin Cell Biol* **11**, 325-9. (1999).
42. Schatz, D.G. & Malissen, B. Lymphocyte development. *Curr Opin Immunol* **14**, 183-5. (2002).
43. Gennery, A.R., Cant, A.J. & Jeggo, P.A. Immunodeficiency associated with DNA repair defects. *Clin Exp Immunol* **121**, 1-7. (2000).
44. Chen, X., Kinoshita, K. & Honjo, T. Variable deletion and duplication at recombination junction ends: implication for staggered double-strand cleavage in class-switch recombination. *Proc Natl Acad Sci USA* **98**, 13860-5. (2001).
45. Zhang, K. Immunoglobulin class switch recombination machinery: progress and challenges. *Clin Immunol* **95**, 1-8. (2000).
46. Rolink, A., Melchers, F. & Andersson, J. The SCID but not the RAG-2 gene product is required for S mu-S epsilon heavy chain class switching. *Immunity* **5**, 319-30. (1996).
47. Manis, J.P. et al. Class switching in B cells lacking 3' immunoglobulin heavy chain enhancers. *J Exp Med* **188**, 1421-31. (1998).
48. Casellas, R. et al. Ku80 is required for immunoglobulin isotype switching. *Embo J* **17**, 2404-11. (1998).
49. Papavasiliou, F.N. & Schatz, D.G. Cell-cycle-regulated DNA double-stranded breaks in somatic hypermutation of immunoglobulin genes. *Nature* **408**, 216-21. (2000).
50. Diaz, M. & Casali, P. Somatic immunoglobulin hypermutation. *Curr Opin Immunol* **14**, 235-40. (2002).
51. Bross, L. et al. DNA double-strand breaks in immunoglobulin genes undergoing somatic hypermutation. *Immunity* **13**, 589-97. (2000).



52. Myung, K. & Kolodner, R.D. Suppression of genome instability by redundant S-phase checkpoint pathways in *Saccharomyces cerevisiae*. *Proc Natl Acad Sci USA* **99**, 4500-7. (2002).
53. Caspari, T. & Carr, A.M. Checkpoints: how to flag up double-strand breaks. *Curr Biol* **12**, 105-7. (2002).
54. Falck, J., Petrini, J.H., Williams, B.R., Lukas, J. & Bartek, J. The DNA damage-dependent intra-S phase checkpoint is regulated by parallel pathways. *Nat Genet* **30**, 290-4. (2002).
55. Petrini, J.H. The Mre11 complex and ATM: collaborating to navigate S phase. *Curr Opin Cell Biol* **12**, 293-6. (2000).
56. Shiloh, Y. & Kastan, M.B. ATM: genome stability, neuronal development, and cancer cross paths. *Adv Cancer Res* **83**, 209-54. (2001).
57. Lavin, M.F. & Khanna, K.K. ATM: the protein encoded by the gene mutated in the radiosensitive syndrome ataxia-telangiectasia. *Int J Radiat Biol* **75**, 1201-14. (1999).
58. Stewart, G.S. et al. The DNA double-strand break repair gene hMRE11 is mutated in individuals with an ataxia-telangiectasia-like disorder. *Cell* **99**, 577-87. (1999).
59. Carney, J.P. et al. The hMre11/hRad50 protein complex and Nijmegen breakage syndrome: linkage of double-strand break repair to the cellular DNA damage response. *Cell* **93**, 477-86. (1998).
60. Kleihues, P., Schauble, B., zur Hausen, A., Esteve, J. & Ohgaki, H. Tumors associated with p53 germline mutations: a synopsis of 91 families. *Am J Pathol* **150**, 1-13. (1997).
61. Hoeijmakers, J.H. Genome maintenance mechanisms for preventing cancer. *Nature* **411**, 366-74. (2001).
62. Pierce, A.J. et al. Double-strand breaks and tumorigenesis. *Trends Cell Biol* **11**, 52-9. (2001).
63. Ferguson, D.O. & Alt, F.W. DNA double strand break repair and chromosomal translocation: lessons from animal models. *Oncogene* **20**, 5572-9. (2001).
64. Thiagalingam, S. et al. Loss of heterozygosity as a predictor to map tumor suppressor genes in cancer: molecular basis of its occurrence. *Curr Opin Oncol* **14**, 65-72. (2002).
65. Xu, X. et al. Conditional mutation of Brca1 in mammary epithelial cells results in blunted ductal morphogenesis and tumour formation. *Nat Genet* **22**, 37-43. (1999).
66. Jonkers, J. et al. Synergistic tumor suppressor activity of BRCA2 and p53 in a conditional mouse model for breast cancer. *Nat Genet* **29**, 418-25. (2001).
67. Friedman, L.S. et al. Thymic lymphomas in mice with a truncating mutation in Brca2. *Cancer Res* **58**, 1338-43. (1998).
68. Sonoda, E. et al. Rad51-deficient vertebrate cells accumulate chromosomal breaks prior to cell death. *EMBO J* **17**, 598-608. (1998).
69. Zhu, C., Bogue, M.A., Lim, D.S., Hasty, P. & Roth, D.B. Ku86-deficient mice exhibit severe combined immunodeficiency and defective processing of V(D)J recombination intermediates. *Cell* **86**, 379-89. (1996).
70. Jhappan, C., Morse, H.C., 3rd, Fleischmann, R.D., Gottesman, M.M. & Merlino, G. DNA-PKcs: a T-cell tumour suppressor encoded at the mouse scid locus. *Nat Genet* **17**, 483-6. (1997).
71. Kurimasa, A. et al. Catalytic subunit of DNA-dependent protein kinase: impact on lymphocyte development and tumorigenesis. *Proc Natl Acad Sci USA* **96**, 1403-8. (1999).
72. Gu, Y. et al. Growth retardation and leaky SCID phenotype of Ku70-deficient mice. *Immunity* **7**, 653-65. (1997).
73. Li, G.C. et al. Ku70: a candidate tumor suppressor gene for murine T cell lymphoma. *Mol Cell* **2**, 1-8. (1998).
74. Gao, Y. et al. A critical role for DNA end-joining proteins in both lymphogenesis and neurogenesis. *Cell* **95**, 891-902. (1998).
75. Frank, K.M. et al. DNA ligase IV deficiency in mice leads to defective neurogenesis and embryonic lethality via the p53 pathway. *Mol Cell* **5**, 993-1002. (2000).
76. Barnes, D.E., Stamp, G., Rosewell, I., Denzel, A. & Lindahl, T. Targeted disruption of the gene encoding DNA ligase IV leads to lethality in embryonic mice. *Curr Biol* **8**, 1395-8. (1998).

77. Gu, Y. et al. Defective embryonic neurogenesis in Ku-deficient but not DNA-dependent protein kinase catalytic subunit-deficient mice. *Proc Natl Acad Sci USA* **97**, 2668-73. (2000).
78. Gao, Y. et al. Interplay of p53 and DNA-repair protein XRCC4 in tumorigenesis, genomic stability and development. *Nature* **404**, 897-900. (2000).
79. Vanasse, G.J. et al. Genetic pathway to recurrent chromosome translocations in murine lymphoma involves V(D)J recombinase. *J Clin Invest* **103**, 1669-75. (1999).
80. Sharpless, N.E. et al. Impaired nonhomologous end-joining provokes soft tissue sarcomas harboring chromosomal translocations, amplifications, and deletions. *Mol Cell* **8**, 1187-96. (2001).
81. Xu, Y., Yang, E.M., Brugarolas, J., Jacks, T. & Baltimore, D. Involvement of p53 and p21 in cellular defects and tumorigenesis in *Atm*<sup>-/-</sup> mice. *Mol Cell Biol* **18**, 4385-90. (1998).
82. Westphal, C.H. et al. *atm* and p53 cooperate in apoptosis and suppression of tumorigenesis, but not in resistance to acute radiation toxicity. *Nat Genet* **16**, 397-401. (1997).
83. Bouffler, S.D., Kemp, C.J., Balmain, A. & Cox, R. Spontaneous and ionizing radiation-induced chromosomal abnormalities in p53-deficient mice. *Cancer Res* **55**, 3883-9. (1995).
84. Nacht, M. & Jacks, T. V(D)J recombination is not required for the development of lymphoma in p53-deficient mice. *Cell Growth Differ* **9**, 131-8. (1998).
85. Donehower, L.A. et al. Effects of genetic background on tumorigenesis in p53-deficient mice. *Mol Carcinog* **14**, 16-22. (1995).
86. Taccioli, G.E. et al. Targeted disruption of the catalytic subunit of the DNA-PK gene in mice confers severe combined immunodeficiency and radiosensitivity. *Immunity* **9**, 355-66. (1998).
87. Stackhouse, M.A. & Bedford, J.S. An ionizing radiation-sensitive mutant of CHO cells: *irs-20*. III. Chromosome aberrations, DNA breaks and mitotic delay. *Int J Radiat Biol* **65**, 571-82. (1994).
88. Nacht, M. et al. Mutations in the p53 and *SCID* genes cooperate in tumorigenesis. *Genes Dev* **10**, 2055-66. (1996).
89. Ferguson, D.O. et al. The nonhomologous end-joining pathway of DNA repair is required for genomic stability and the suppression of translocations. *Proc Natl Acad Sci USA* **97**, 6630-3. (2000).
90. Gu, Y., Jin, S., Gao, Y., Weaver, D.T. & Alt, F.W. Ku70-deficient embryonic stem cells have increased ionizing radiosensitivity, defective DNA end-binding activity, and inability to support V(D)J recombination. *Proc Natl Acad Sci USA* **94**, 8076-81. (1997).
91. Difilippantonio, M.J. et al. DNA repair protein Ku80 suppresses chromosomal aberrations and malignant transformation. *Nature* **404**, 510-4. (2000).
92. Lim, D.S. et al. Analysis of ku80-mutant mice and cells with deficient levels of p53. *Mol Cell Biol* **20**, 3772-80. (2000).
93. Vogel, H., Lim, D.S., Karsenty, G., Finegold, M. & Hasty, P. Deletion of Ku86 causes early onset of senescence in mice. *Proc Natl Acad Sci USA* **96**, 10770-5. (1999).
94. Tsuzuki, T. et al. Targeted disruption of the *Rad51* gene leads to lethality in embryonic mice. *Proc Natl Acad Sci USA* **93**, 6236-40. (1996).
95. Lim, D.S. & Hasty, P. A mutation in mouse *rad51* results in an early embryonic lethal that is suppressed by a mutation in p53. *Mol Cell Biol* **16**, 7133-43. (1996).
96. Rijkers, T. et al. Targeted inactivation of mouse *RAD52* reduces homologous recombination but not resistance to ionizing radiation. *Mol Cell Biol* **18**, 6423-9. (1998).
97. Dronkert, M.L. et al. Mouse *RAD54* affects DNA double-strand break repair and sister chromatid exchange. *Mol Cell Biol* **20**, 3147-56. (2000).
98. Essers, J. et al. Disruption of mouse *RAD54* reduces ionizing radiation resistance and homologous recombination. *Cell* **89**, 195-204. (1997).

99. Ludwig, T., Chapman, D.L., Papaioannou, V.E. & Efstratiadis, A. Targeted mutations of breast cancer susceptibility gene homologs in mice: lethal phenotypes of *Brca1*, *Brca2*, *Brca1/Brca2*, *Brca1/p53*, and *Brca2/p53* nullizygous embryos. *Genes Dev* **11**, 1226-41. (1997).
100. Suzuki, A. et al. *Brca2* is required for embryonic cellular proliferation in the mouse. *Genes Dev* **11**, 1242-52. (1997).
101. Luo, G. et al. Disruption of *mRad50* causes embryonic stem cell lethality, abnormal embryonic development, and sensitivity to ionizing radiation. *Proc Natl Acad Sci USA* **96**, 7376-81. (1999).
102. Xiao, Y. & Weaver, D.T. Conditional gene targeted deletion by Cre recombinase demonstrates the requirement for the double-strand break repair Mre11 protein in murine embryonic stem cells. *Nucleic Acids Res* **25**, 2985-91. (1997).
103. Zhu, J., Petersen, S., Tessarollo, L. & Nussenzweig, A. Targeted disruption of the Nijmegen breakage syndrome gene *NBS1* leads to early embryonic lethality in mice. *Curr Biol* **11**, 105-9. (2001).
104. Hiom, K., Melek, M. & Gellert, M. DNA transposition by the *RAG1* and *RAG2* proteins: a possible source of oncogenic translocations. *Cell* **94**, 463-70. (1998).
105. Barreto, V., Marques, R. & Demengeot, J. Early death and severe lymphopenia caused by ubiquitous expression of the *Rag1* and *Rag2* genes in mice. *Eur J Immunol* **31**, 3763-72. (2001).



---

## Chapter 2

*Biochemical and cellular aspects of homologous recombination*

---

## Chapter 2

### *Biochemical and cellular aspects of homologous recombination*

Lieneke van Veelen<sup>1,2</sup>, Joanna Wesoly<sup>1</sup> and Roland Kanaar<sup>1,2</sup>

<sup>1</sup> Department of Cell Biology and Genetics,  
Erasmus MC, University Medical Center,  
P.O. Box 1738, 3000 DR Rotterdam, The Netherlands

<sup>2</sup> Department of Radiation Oncology,  
Erasmus MC-Daniel den Hoed Cancer Center, University Medical Center,  
P.O. Box 5201, 3008 AE Rotterdam, The Netherlands

*DNA Damage Recognition, Marcel Dekker Inc., first edition. In Press*

## **Abstract**

Exchange of DNA strands between homologous DNA molecules via recombination ensures accurate genome duplication and preservation of genome integrity. Biochemical studies have provided insight into the molecular mechanisms by which homologous recombination proteins perform these essential tasks. More recent cell biological experiments are addressing the behavior of homologous recombination proteins in cells. The challenge ahead is to uncover the relationship between the individual biochemical activities of homologous recombination proteins and their coordinated action in the context of the living cell.

## Introduction

Homologous recombination, the exchange of DNA sequences between two homologous DNA molecules, is essential for the preservation of genome integrity. It contributes to the repair of a wide range of DNA lesions, including DNA double-strand breaks (DSBs) and DNA interstrand crosslinks<sup>1,2</sup>. In addition, homologous recombination plays a pivotal role in underpinning genome duplication, through its role in rebuilding DNA replication forks that have collapsed due to lesions in the template DNA<sup>3</sup>. Homologous recombination is mediated by an extensive group of proteins that need to work together in a coordinated fashion. This cooperation is necessary to choreograph the complicated DNA gymnastics which is required to accurately restore DNA damage on one molecule using information of a second homologous DNA molecule.

An extensive number of biochemical studies on the enzymes that mediate homologous recombination have provided a number of working models of how the reaction can take place in the test tube<sup>1,4</sup>. One important conclusion from these studies has been that the core of the process, homology recognition and DNA strand exchange, is remarkably conserved throughout evolution. More recent cell biology studies have begun to address the behavior of homologous recombination proteins inside cells<sup>5</sup>. The interesting challenge ahead is to link our understanding of the biochemical mechanisms of homologous recombination with its operation in the context of the living cell.

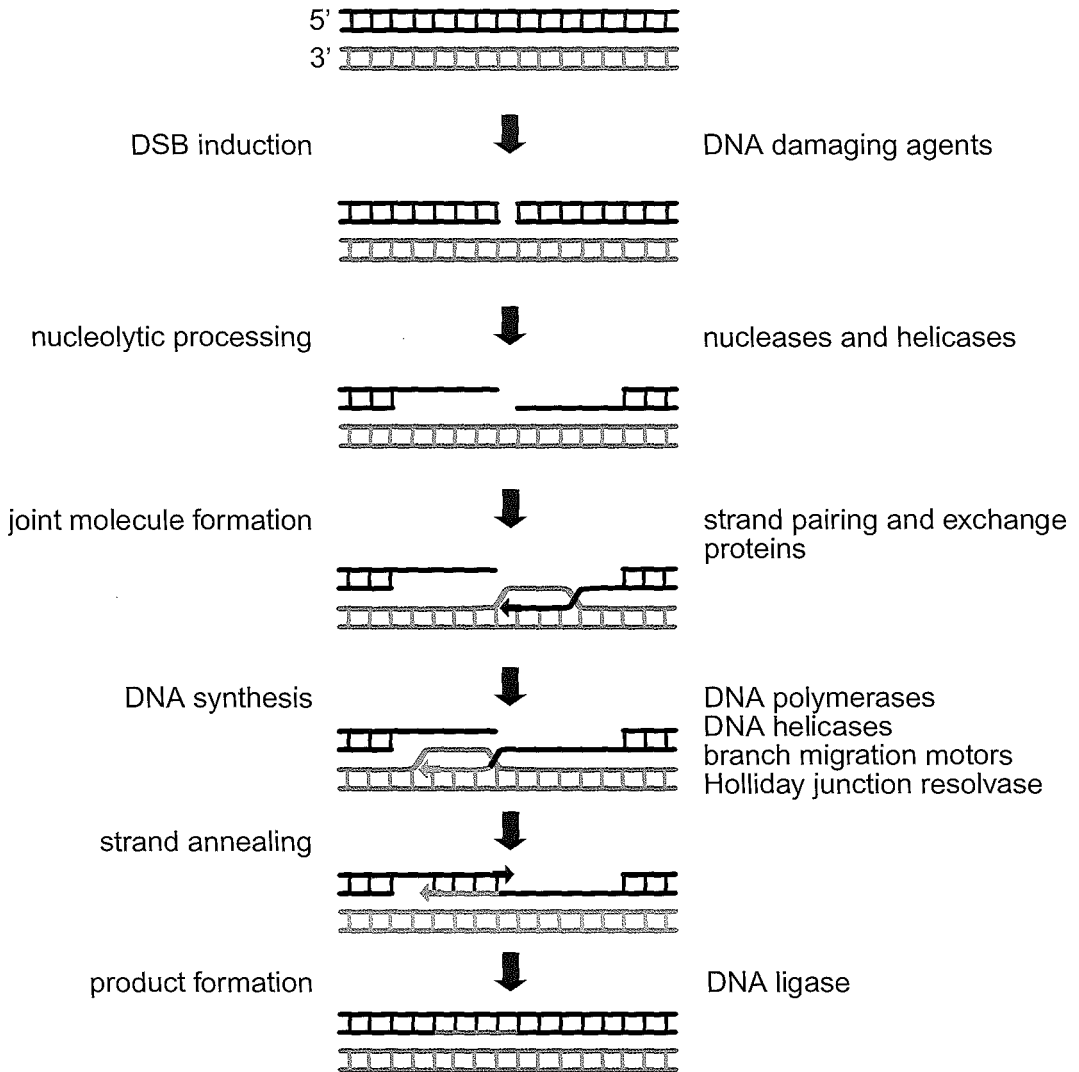


## DNA double-strand break repair through homologous recombination

The fundamentals of homologous recombination are highly conserved from phages to humans<sup>6</sup>. For the sake of brevity, we consider here an example of one model for repair of a DSB by homologous recombination. More in depth discussions of different models for homologous recombination can be found in a number of extensive reviews<sup>1,2,4</sup>. During DSB repair via homologous recombination, missing DNA is restored using the intact homologous sequence provided by the sister chromatid. In the early stage of the reaction, referred to as presynapsis, the DNA ends are processed into a 3' single-stranded overhang, by yet unidentified nucleases and/or helicases (*Fig. 1*). The single-stranded DNA tails are coated with a strand exchange protein to form a nucleoprotein filament (see below) that can recognize a homologous DNA sequence. During synapsis, the middle step of the recombination process, the nucleoprotein filament invades the homologous template DNA to form a joint heteroduplex molecule linking the broken end(s) and the undamaged template DNA. In the postsynaptic, or late stage of recombination, DNA polymerases restore the missing information and DNA ends are ligated. In this last step of the reaction, resolution of recombined molecules into separate DNA duplexes can be promoted by structure-specific endonucleases<sup>7</sup>.

### **Figure 1. A model for DSB repair through homologous recombination.**

*The black and gray double-stranded DNA, depicted as ladders, are homologous in sequence. A DSB can be generated by DNA damaging agents or replication of DNA containing a single-stranded break. The DSB is processed by the combined action of helicases and/or nucleases resulting in the generation of single-stranded DNA tails with a 3' overhang. The Mre11/Rad50/NBS1 complex has been implicated in this step, although its precise role is still unclear. The single-stranded DNA tail is bound by the Rad51 strand exchange protein to form a nucleoprotein filament. This filament can recognize homologous double-stranded DNA. DNA strand exchange generates a joint molecule between the homologous damaged DNA and undamaged DNA. In addition to Rad51, these steps require the coordinated action of the single-stranded DNA binding protein RPA (replication protein A), Rad52 and Rad54. The role of the five Rad51 paralogs, XRCC2, XRCC3, Rad51B, Rad51C and Rad51D, as well as the function of the breast cancer susceptibility proteins Brca1 and Brca2 has not yet been defined in great detail. DNA synthesis, requiring a DNA polymerase, its accessory factors and a ligase, restores the missing information. Resolution of crossed DNA strands (Holliday junctions) by a resolvase yields two intact duplex DNAs. Only one pair of possible recombination products is depicted.*



**Proteins involved**

Rad50, Mre11, NBS1  
RPA, Rad51, Rad52, Rad54  
XRCC2, XRCC3, Rad51B, Rad51C, Rad51D  
BRCA1, BRCA2

## Biochemical properties of homologous recombination proteins

Below we discuss a number of proteins involved in homologous recombination, with emphasis on the proteins involved in synapsis, the central core reaction of homologous recombination, in which the joint molecule between the broken DNA and the intact repair template is established.

**The Rad51 protein.** Rad51, conserved in all kingdoms of life, is a key protein in homologous recombination because it promotes homology recognition and DNA strand exchange. Biochemical studies have shown that Rad51 binds both single-stranded and double-stranded DNA<sup>8</sup>. Its preferred substrate is single-stranded tailed duplex DNA, which resembles a DSB repair intermediate<sup>9</sup> (Fig. 1). Rad51 polymerizes on single-stranded DNA to form a nucleoprotein filament that is capable of recognizing homologous double-stranded DNA and promotes DNA strand exchange between the double-stranded template DNA and the Rad51-coated single-stranded DNA<sup>10,11</sup>. Rad51-mediated joint molecule formation is stimulated by a number of accessory proteins; the single-stranded DNA binding protein RPA, Rad52 and Rad54<sup>10,11</sup>.

Cells from the yeast *Saccharomyces cerevisiae* that lack Rad51 are viable but display strongly reduced mitotic and meiotic recombination and are sensitive to ionizing radiation<sup>12</sup>. In vertebrates, Rad51 is essential for cell proliferation. Depletion of Rad51 from chicken DT40 cells leads to accumulation of chromosomal abnormalities and cell death<sup>13</sup>. Targeted disruption of *Rad51* in mouse cells results in early embryonic lethality<sup>14,15</sup>. Together, these observations suggest that Rad51 plays an important role in proliferation processes.

Rad51 interacts *in vitro* with a number of proteins involved in DSB repair, including RPA, Rad52, Rad54 and BRCA2. RPA is thought to remove the secondary structures on single-stranded DNA. BRCA2 was implicated in DSB repair recently and is thought to play a controlling role upstream of Rad51 function in DNA strand exchange<sup>16-21</sup>.

Both in yeast and in vertebrates paralogs of Rad51 have been identified. There are two mitotic Rad51 paralog proteins in *S. cerevisiae*; Rad55 and Rad57. They form a heterodimer that interacts with Rad51 and stimulates Rad51-mediated strand exchange. The recombination defect and ionizing radiation sensitivity of *Rad55* and *Rad57* mutants can be overcome by overexpression of Rad51 or Rad52<sup>22,23</sup>. In total, five paralogs have been discovered in mitotically dividing vertebrate cells; XRCC2, XRCC3, Rad51B, Rad51C and Rad51D<sup>24,25</sup>. The paralogs are present in two distinct complexes. One contains XRCC3 and Rad51C, while the other consists of XRCC2, Rad51B, Rad51C and Rad51D<sup>26,27</sup>. Disruption of the paralogs in chicken

cells leads to chromosomal instability, moderately increased ionizing radiation sensitivity, significantly increased sensitivity to the cross-linking agent mitomycin C and it affects homologous recombination efficiency. Similarly to *Rad51*-deficient mice, targeted disruption of *Rad51B*, *Rad51D* and *Xrcc2* results in embryonic lethality<sup>24,25</sup>.

**The Rad52 protein.** Rad52 is a central homologous recombination protein in the *S. cerevisiae*. *Rad52* mutants display the most severe recombination phenotype of all *Rad52* epistasis group mutants in yeast. The *Rad52* mutants are extremely sensitive to DNA damaging agents and almost completely deficient in all pathways of homology-mediated repair, including pathways that are independent of Rad51<sup>1,4</sup>. In vertebrates, *Rad52* mutants have only a two-fold decreased level of homologous recombination compared to wild type cells as measured by homologous gene targeting efficiency<sup>28,29</sup>. It is possible that some of the functions of Rad52 in mammals can be taken over by Rad51 paralogs<sup>6,30,31</sup>.

Furthermore, although Rad52 homologs have been identified in the yeast *S. cerevisiae* and *Schizosaccharomyces pombe*, no such proteins have been identified in vertebrates<sup>32,33</sup>.

*In vitro* Rad52 binds to single-stranded DNA, protects the ends from nucleolytic degradation and forms rings interacting with DNA<sup>5</sup>. Rad52 also interacts with Rad51 and RPA and stimulates Rad51-mediated strand exchange by overcoming the inhibitory role of RPA<sup>34,35</sup>.

**The Rad54 protein.** Rad54 belongs to the SWI2/SNF2 family of proteins involved in many biological processes such as transcriptional activation and repression, destabilization of nucleosomes, DNA repair and chromosome segregation<sup>36</sup>. In general, these proteins function by modulating protein-DNA interactions. Rad54 is an important accessory factor for Rad51<sup>37</sup>. A number of biochemical characteristics of Rad54 have been well defined for different species ranging from yeast to humans. Rad54 is a double-stranded DNA-dependent ATPase with ability to change DNA topology and chromatin structure<sup>38-41</sup>. Rad54 has been implicated to participate throughout the whole duration of the homologous recombination reaction by first stabilizing the Rad51 nucleoprotein filament, subsequently by stimulating Rad51-mediated joint molecule formation and chromatin remodeling. Finally, in the last stage of the reaction it could displace Rad51 from the product DNA<sup>42</sup>.

*Rad54*-deficient mouse embryonic stem cells show increased sensitivity to ionizing radiation, mitomycin C and methanesulfonate and have a defect in homology-dependent DSB repair<sup>42-44</sup>. Mice lacking *Rad54* are viable<sup>44</sup>. They are sensitive to the cross-linking agent mitomycin C<sup>45</sup>. In *S. cerevisiae* a homologue of *RAD54* - *RDH54/TID1* has been identified<sup>46,47</sup>. The proteins have similar biochemical properties<sup>48,49</sup>. Yeast Rad54 and Tid1 promote Rad51-mediated joint molecule formation and have ability to modify DNA topology<sup>48</sup>. Both Rad54

and Tid1 interact with Rad51<sup>46,48</sup>. In yeast there is a functional overlap between both proteins, but Rad54 is more important in mitosis, where the sister chromatid is used as a template, while Tid1 is important in meiosis directing recombination towards the homologous chromosome<sup>47,50,51</sup>. Recently, a human gene, termed Rad54B, sharing a significant homology to *Rad54* has been isolated<sup>52</sup>.

**The Rad50/Mre11/NBS1 protein complex.** The presence of Rad50/Mre11/NBS1 complex is required for proper functioning of DSB repair, although its role is still elusive<sup>4</sup>. The complex consists of two proteins, Rad50 and Mre11, conserved from yeast to human, while the third subunit, NBS1 in mammals and Xrs2 in yeast, is less conserved at the amino acid level<sup>53</sup>. In yeast, the complex is involved in non-homologous DNA end joining, sister chromatid repair by homologous recombination, telomere maintenance and formation and processing of DSBs in meiosis<sup>53</sup>. Biochemical analysis of Mre11 revealed its strand dissociation, strand annealing and 3'-5' exo/endo dsDNA nuclease activity properties<sup>53</sup>. The Rad50/Mre11 complex has been shown to bind DNA ends and tether linear DNA molecules<sup>54,55</sup>.

Conditional inactivation of *Mre11* in chicken cells causes accumulation of chromosomal breaks, increased radiosensitivity and reduced targeted integration frequencies<sup>56</sup>. NBS1-deficient chicken cells display similar defects as the *Mre11* knockout cells, with additional reduction of gene conversion levels and lower rates of sister chromatid exchanges<sup>57</sup>. *Mre11*, *Rad50* and *NBS1* null mutations in mice lead to cellular and/or embryonic lethality indicating the importance of this complex for the function of the cell<sup>58-60</sup>. Mutations in the *Mre11* gene have been found in patients with ataxia telangiectasia-like disorder, while mutations in *NBS1* cause the Nijmegen breakage syndrome<sup>61,62</sup>. Cells derived from these patients display chromosomal instability and radioresistant DNA synthesis, which is an indication of a defective intra-S checkpoint. Indeed, mammalian Mre11 and NBS1 are phosphorylated by ATM, a cell cycle checkpoint protein that is crucial in the cellular response to DSBs in response to ionizing radiation<sup>53</sup>. Ultraviolet light (UV), hydroxyurea or methylmethane sulfonate treatment also leads to phosphorylation of both proteins, most likely by the ATR kinase<sup>63,64</sup>. The presence of the Rad50/Mre11/NBS1 complex is required for proper activation of checkpoints throughout all cell cycle phases<sup>53</sup>. The complex could serve as a signal modifier by nucleolytic modification of the lesions in order to make them detectable by the checkpoint machinery.

**The Brca1 and Brca2 proteins.** Mutations in the BRCA1 and BRCA2 breast cancer susceptibility genes predispose to breast, ovarian, prostate and pancreatic cancer<sup>65</sup>. Mouse *Brca1*- and *Brca2*-deficient and human mutant cell lines display chromosomal instability and sensitivity to DNA damaging agents<sup>66</sup>. Both proteins are required for homology-directed repair and gene targeting events. In comparison to wild type cells, gene targeting is respectively 20-fold and 2-fold decreased in *Brca1* and *Brca2* mutant cells<sup>18,67</sup>. Similarly to *Rad51*, targeted disruption of *Brca1* and *Brca2* in mice leads to embryonic lethality, associated with a proliferation defect. This defect is partially suppressed by a p53 mutation<sup>68-71</sup>. While *Brca2* interacts directly with *Rad51*, the interaction between *Brca1* and *Rad51* appears to be indirect<sup>21</sup>. Crystallographic data, characterizing the conserved BRC repeats and C-terminal single-strand DNA binding folds of *Brca2* suggest that *Brca2* can recruit *Rad51* to a DSB and regulate the spatial distribution of *Rad51*<sup>20,72</sup>.

**Other proteins involved in homologous recombination.** Homologous recombination is a collection of complex processes. So far, not all proteins involved in these processes have been identified. The number of proteins known to participate in homologous recombination has significantly increased over the last years. The variety of substrates on which homologous recombination can act could explain the diversity of proteins required for its successful completion. Recently, a group of DNA helicases has been implicated in homologous recombination. Human homologs of the RecQ helicase in *Escherichia coli*; Bloom, Werner and Rothmund-Thomson proteins (BLM, WRN and Recql4, respectively), are thought to resolve abnormal replication structures after the replication forks stall or collapse<sup>73</sup>. These proteins could also promote joint molecule formation and take part in the resolution of joint molecules. The three proteins are ATP dependent 3'-5' helicases which are able to unwind forked DNA structures and synthetic Holliday junctions *in vitro*<sup>74,75</sup>. Mutations in BLM, WRN or the yeast RecQ homologue *Sgs1*, lead to chromosomal instability and an increased risk of tumor formation in patients<sup>73</sup>. Patient derived cell lines accumulate abnormal replication intermediates<sup>74</sup>. BLM mutant cells are characterized by hyperrecombination, visualized through increased numbers of sister chromatid exchanges. WRN mutant cells have increased levels of translocations and deletions<sup>74</sup>. The BLM protein interacts with *Rad51*, *Rad51D* and RPA; WRN protein with DNA-PK and RPA<sup>76-81</sup>.

## Cellular properties of homologous recombination proteins

Local accumulations of proteins involved in homologous recombination. In addition to unraveling the function of homologous recombination proteins in the test tube, it is also of great importance to understand the action mechanisms of these proteins in the context of the cell, where they have to function in chromatin and compete with other DNA metabolic processes. The response to DNA damage of a number of proteins involved in homologous recombination has been visualized inside cells using immunofluorescence<sup>5</sup>. Many of the homologous recombination proteins studied to date, including Rad51, Rad52, Rad54, Brca1, Brca2 and Rad50/Mre11/NBS1, accumulate into subnuclear structures at sites of DNA damage<sup>82-86</sup>. These subnuclear structures are referred to as foci. An overview of a number of proteins detected in foci is given in *Table 1*.

Besides this accumulation at sites of induced DNA damage, proteins involved in homologous recombination can also be observed in foci in cells that have not been treated with exogenous DNA damaging agents. These so-called 'spontaneous' foci occur specifically in S-phase cells. They represent the cytological manifestation of the link between DNA replication and homologous recombination. DSBs occur during DNA replication, for example when imperfections in the DNA template are encountered. This can lead to replication fork arrest and breakdown. The resulting DSB intermediates are acted upon by homologous recombination factors that rebuild a functional replication fork<sup>3</sup>. Usually, these DNA replication associated foci have a similar appearance as the DNA damage-induced foci of the same protein. However, cells show less spontaneous foci per nucleus probably because there are less spontaneous DSBs than DNA damage-induced DSBs.

**Detection of foci by antibodies in chemically fixed cells.** Immunostaining is a commonly used method of detecting nuclear foci of proteins of interest. After treatment of cells by damaging agents, cells are fixed, permeabilized, and foci can be detected by a fluorescent labeled antibody specific for the protein of interest. An example of ionizing radiation-induced Rad51 foci is displayed in *Figure 2A*. Immunostaining experiments can be done for many cell types. The method is relatively simple and fast, though the results depend on various factors, such as the fixation and permeabilization techniques and the cell lines and antibodies used. This variability complicates the interpretation of published data on DNA damage induced foci formation<sup>87</sup>.

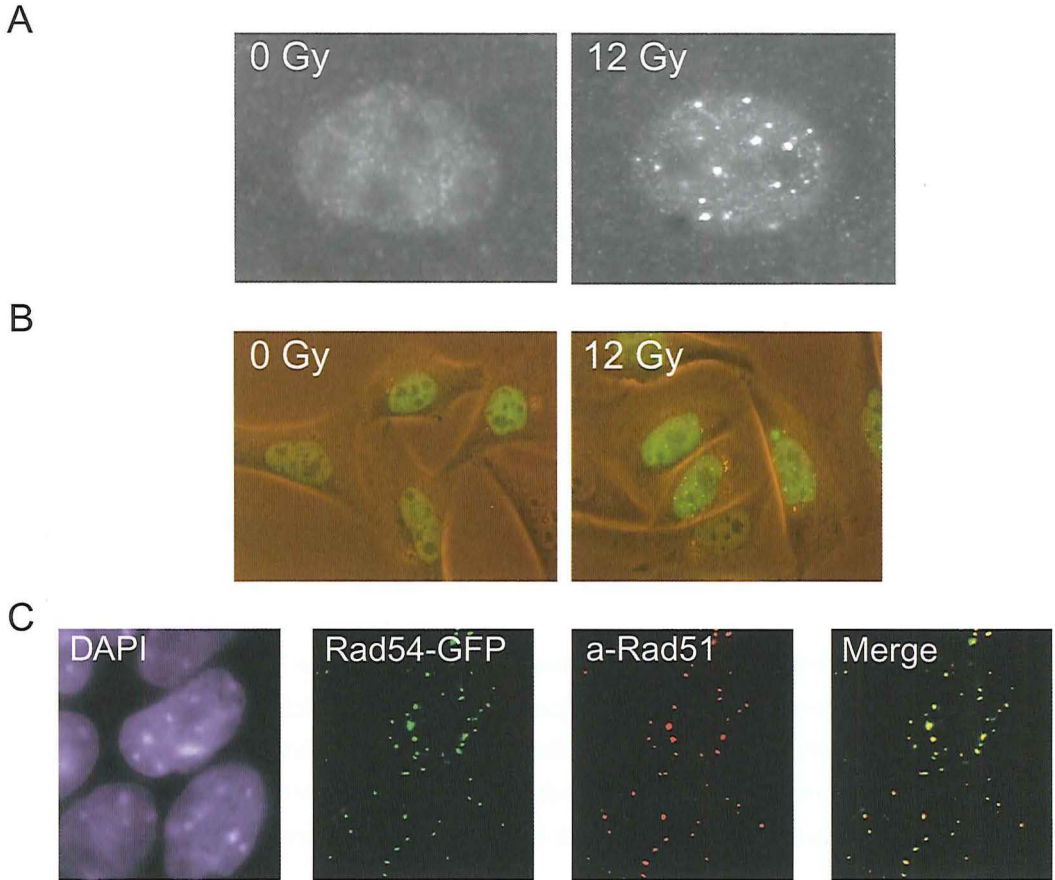


**Figure 2. Irradiation induced foci formation of homologous recombination proteins.**

**2A.** Rad51 ionizing radiation induced foci by antibody detection in fixed cells.

Chinese hamster ovary (CHO) cells were irradiated with 12 Gy and chemically fixed after 2 hours. Immunostaining was performed using antibodies against Rad51. After ionizing radiation treatment Rad51 foci appear in the nucleus.

**2B.** Rad52 ionizing radiation induced foci detected by expression of Rad52-GFP in living cells.

CHO cells expressing Rad52-GFP were irradiated with 12 Gy and investigated after 2 hours. Using a fluorescence microscope, ionizing radiation induced Rad52 foci can be observed in living cells.

**2C.** Co-localization of Rad51 and Rad54 ionizing radiation induced foci.

Wild type CHO cell lines expressing Rad54 fused to GFP were irradiated with 12 Gy and fixed at 2 hours after irradiation. Cells were counterstained with a Rad51 antibody. The first panel from the left shows the nuclei of the cells, visualized through DAPI staining. The second and third panels show ionizing radiation induced Rad54 and Rad51 foci detected through the GFP signal and the fluorescent labeled antibody, respectively. The last panel shows the merged images, resulting in a yellow focus in case of Rad51 and Rad54 colocalization. For Rad51 and Rad54 the co-localization is virtually complete.



**Detection of foci by expression of the protein of interest tagged to a fluorescent group.** Another approach to study foci formation is by stably transfecting the cDNA of the protein of interest tagged to a fluorescent group, such as one of a number of the spectral variants of the green fluorescent protein (GFP). After ascertaining that this tagged protein is functioning similarly as the endogenous protein, the transfected cells can be studied by fluorescence microscopy (*Fig. 2B*). In this manner, the behavior of the protein can be observed before and after damage induction. Foci of the tagged proteins are smaller in size than foci observed by immunostaining, though their number is usually not different<sup>88</sup>. An advantage of studying foci formation by expression of the protein of interest is that it can be done in both living and fixed cells. The unfixed cells can even be used to study the dynamic behavior of the protein in time (see below). The main disadvantage of this technique is the fact that not all cell lines are suitable for stable transfection.

**Co-localization of proteins in foci.** DNA damage induced formation of nuclear foci implicates the involvement of certain proteins during the process of DNA repair. Moreover, a possible cooperation of specific proteins in the repair of DSBs can be studied by investigating foci formation of two or more proteins at the same time in the same cell. Co-localization of foci suggests an association between the proteins of interest. They may be part of the same DNA repair complex or participate in the same cascade of proteins that are essential for repair of DSBs. Co-localization of foci can be complete (*Fig. 2C*) or partial, which may provide information about the cooperation of the proteins. It is also possible that the two proteins of interest are mutually exclusive with respect to their presence in foci. An explanation for this phenomenon might be the recruitment of specific repair proteins at different stages of the cell cycle. An example is provided in *Figure 3*. While ionizing radiation induced Rad51 foci are observed in replicating cells, Mre11 foci are detected in cells outside of S-phase. Though co-localization experiments do not provide any information about the actual interaction of the proteins of interest, the results can lead to the suggestion whether specific proteins may or may not cooperate in the repair of DSBs.

**Foci formation in DNA repair deficient mutant cell lines.** In addition to co-localization experiments, DNA repair deficient mutant cell lines can be used to establish a possible cooperation between DSB repair proteins. Cell lines with a defect in one of the DNA repair proteins may show less or more spontaneous or damage induced foci per nucleus, depending on the repair pathway that is diminished. An increase in number of foci might be due to the inability of the cell to repair the spontaneous occurring DSBs. A decrease in number of foci may occur in case the protein of interest, or one of its cooperating proteins, is not func-

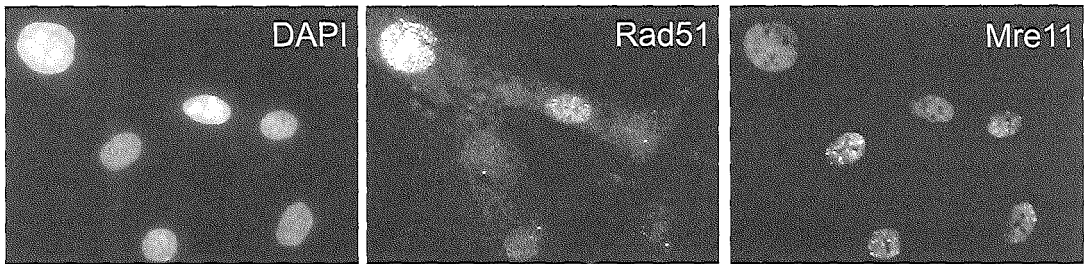


**Figure 3. Rad51 and Mre11 ionizing radiation induced foci formation depends on cell cycle stage.**

Primary human fibroblasts were irradiated with 12 Gy and incubated for 8 hours before fixation. Double immunostaining was performed using antibodies against Rad51 and Mre11. The nuclei were visualized by DAPI staining. A representative picture of each staining pattern is shown. Cells positive for Rad51 foci do usually lack Mre11 foci and vice versa. Note that cells which are positive for Rad51 IRIFs display a brighter DAPI staining, indicating that they are replicative cells.

tioning properly. This may lead to impaired complex formation at the site of the DSB, thus preventing an accumulation of the protein of interest (Table 1). Interestingly, even though Rad51 foci do not form in, for example, the Rad51 paralog mutant cell lines in response to induced DNA damage, these mutant cell lines are capable of forming the DNA replication associated spontaneous Rad51 foci. Possibly, the accessory proteins to Rad51 are not absolutely required for Rad51 foci under all circumstances. However, given that most of the mutants are hypomorphic, the proteins still retain parts of their functions. Consistent with this idea is the finding that complete knockouts for these proteins result in embryonic lethality in mice<sup>89</sup>.

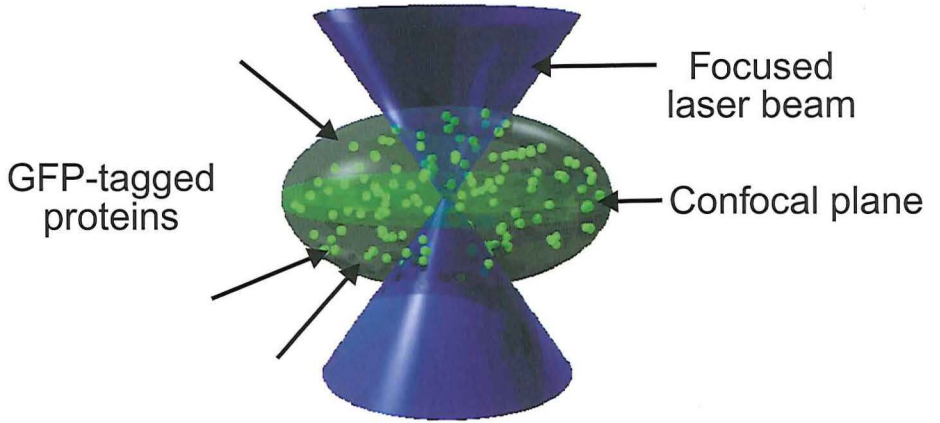
**Nuclear dynamics of homologous recombination proteins in living cells.** Cell lines expressing the protein of interest tagged to a GFP spectral variant may be utilized to study the dynamic behavior of the protein in living cells using a confocal microscope. The principle of studying the dynamic behavior is based on the rate of recovery of the fluorescent signal of the protein in an area that has been bleached by a short laser pulse (Fig. 4A)<sup>90</sup>. Fluorescence redistribution after photobleaching (FRAP) can be used to determine the diffusion rate of proteins by bleaching a small strip spanning the entire nucleus. Recovery of the fluorescence in the strip is monitored at specific time intervals. The kinetics with which the fluorescence intensity in the strip reaches the same intensity as the unbleached area relates to the diffusion rate of a protein (Fig. 4B). FRAP can also be used to study the residence times of specific proteins in the DNA damage induced foci. In this case a single focus is bleached and the

time interval between bleaching and recovery of fluorescence in the focus is measured. The time to recovery can be used to estimate the residence time of that specific protein at the damaged site (Fig. 4C)<sup>88,91</sup>.

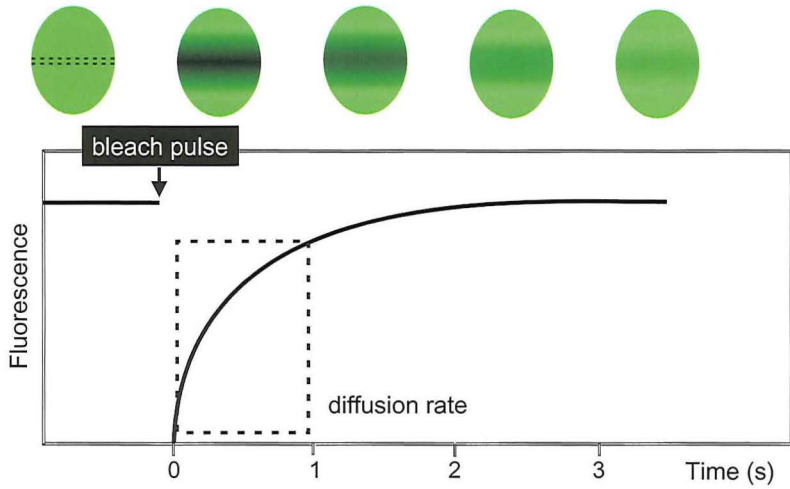
### **Implications of analysis of homologous recombination proteins in living cells.**

Investigation of the nuclear dynamics of DNA repair proteins has provided new insight in the recognition mechanisms of DNA damage and the interaction between mechanistically distinct DNA repair pathways. For example, Rad52 and Rad54 diffuse through the nucleus<sup>88</sup>. Diffusion ensures that the proteins are everywhere in the nucleus all of the time, which is a useful property of proteins that need to repair DSBs that can occur anywhere in the genome. Furthermore, diffusion rate measurements of Rad52 and Rad54 showed that these proteins have different diffusion rates before the induction of DNA damage<sup>88</sup>. Because the two proteins diffuse through the nucleus independently of each other, they cannot be part of the same pre-assembled holo-complex in the absence of DNA damage. Possibly, the affinity of the Rad52 group proteins for the DSB site compared to intact DNA might be slightly increased. This difference in affinity ensures that the Rad52 group proteins will be immobilized for a longer time at the DSB site than at other sites in the genome, resulting in a local accumulation or focus at the site of DNA damage. The large local concentration of the different proteins ensures that the reaction, that each of them mediate, can be driven to completion. Performing repair of DNA lesions by diffusible proteins that are temporarily immobilized due to the encounter of sites of increased affinity has an important advantage over the use of pre-assembled holo-complexes. In situ assembly allows greater flexibility in the components of a DNA repair complex. Because different components can reversibly interact with the DNA damage-induced structure, the correct components required for repair of a specific lesion can be selected. The reversible interaction of proteins with DNA damage-induced foci alleviates the necessity of having to disassemble a DNA repair holo-complex that does not contain all of the specialized components required to repair the lesion it is associated with. Furthermore, in situ assembly allows exchange of components between different multi-step DNA repair pathways. Multi-step DNA repair pathways can mix and match components, instead of linear DNA repair pathways in which each use a defined set of enzymes. This cross talk is biologically significant because it will lead to an increase in the diversity of DNA lesions that can be repaired.

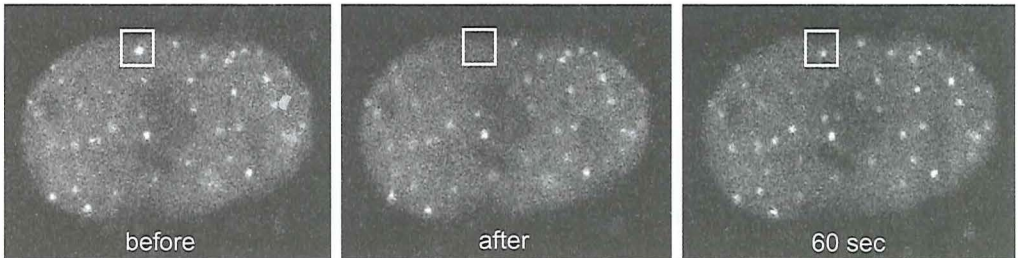
A



B



C



## Acknowledgments

The authors wish to thank Jeroen Essers for kindly providing a number of pictures used in the figures.

### **Figure 4. Methods of studying the nuclear dynamics of proteins.**

#### **4A.** *The principle of fluorescence redistribution after photobleaching (FRAP).*

*The diffusion of a protein and the fraction of mobile proteins can be determined by bleaching a small area in living cells expressing the protein of interest tagged to a fluorescent group using a focused laser beam. The recovery of fluorescence in the bleached area can be measured. This gives an indication of the mobility of proteins in the nucleus. FRAP analysis can be done for freely moving proteins (B) or proteins that are bound to DNA (C).*

#### **4B.** *The principle of strip bleaching.*

*This technique can be used to determine the diffusion rate of recombination proteins in living cells. A bleach pulse of 200 ms is given such that only a small strip spanning the entire nucleus will be bleached. After this bleach pulse the recovery of fluorescence in the strip is monitored at intervals of 100 milliseconds. After a while the fluorescence intensity in the strip will have reached the same level as the unbleached area. This represents influx of the GFP-tagged proteins from the surroundings into the bleached area. In this way the diffusion rate of a GFP-tagged protein can be measured and plotted as is shown in the graph.*

#### **4C.** *FRAP for Rad52-GFP ionizing radiation induced foci.*

*A similar analysis as described in (B) can be done for DNA damage induced foci. A single focus in the nucleus is bleached and the time interval between bleaching and recovery of the focus is measured. The picture shows an example for a Rad52-GFP focus before bleaching, immediately after bleaching and after 60 seconds. Recovery of the fluorescence at the damaged site can be observed within 60 seconds. The time to recovery of the focus relates to the residence time of the protein at the damaged site. Various repair proteins have different residence times in DNA damage induced foci.*

### **Table 1. Overview of proteins involved in spontaneous or induced foci formation.**

*The table shows an overview of recombination proteins known to form spontaneous or damage-induced subnuclear structures called foci in mitotically dividing cells. For this overview the literature from 1995 till August 2003 was surveyed. Co-localization with other proteins of interest and the influence of mutant or absent proteins on foci formation of a specific other protein is shown. In cases where contradictory results have been reported, the references are given in the Comments column.*

**Abbreviations:** APH: aphidicolin; AS: arsenic; CPT: Camptothecin; HU: hydroxyurea; IR: ionizing radiation; kd: kinase dead; LET: low energy transfer; MMC: mitomycin C; MMS: methylmethanesulfonate; NCS: neocarzinostatin; PML-NB: promyelocytic leukemia nuclear bodies; UV: ultraviolet radiation; VM26: teniposide; 4NQO: 4-nitroquinoline 1-oxide.

**Table 1. Overview of proteins involved in spontaneous or induced foci formation.**

Protein	Spontaneous foci formation	Cell cycle dependency of spontaneous or induced foci	Damage induced foci formation	Co-localization			
				Before treatment	After treatment		
					Complete	Partial	None
Core homologous recombination proteins							
RPA	yes	S-phase G2-phase	IR UV CPT	WRN BLM PML-NB Brca1 Rad51	WRN Rad51 Brca1 ATR		
Rad51	yes	S-phase G2-phase	IR MMS MMC UV-C CPT HU Cisplatin Etoposide Tetracyclin	RPA Rad54B BLM Brca1 Fanc-D2 p53	RPA Rad54B $\gamma$ -H2AX Rad54 PML-NB BrdU <sup>3</sup>	Brca1 Rad52 PCNA WRN BLM phospho-p53 Brca2	BrdU <sup>3</sup> Mre11 Rad50 Nbs1 MDC1
Rad52			IR MMS			Rad50 Rad51	
Rad54			IR		Rad51 Rad54B		
Rad54B	yes		IR	Rad51	Rad51 Rad54	Brca1	
Rad51 paralogs	no		no				
Brca proteins							
Brca1	yes	S-phase	IR MMC HU UV MMS	Bard1 Cds1 Fanc-D2 Rad51 RPA	Bard1 $\gamma$ -H2AX RPA Bach1 Fanc-D2 MDC1	Rad54B Nbs1 BLM PCNA Mre11 Rad50 Rad51	
Brca2			IR MMC		Rad51 Fanc-C		
BARD1			HU MMS UV	Brca1	Brca1	PCNA	
BACH1		S-phase G2-phase	HU		Brca1		

Foci formation influenced by a mutation						No influence on foci formation	Comments	References
Absence	Decrease		Delay	Increase				
	# of foci-positive cells	# of foci per nucleus	# of foci-positive cells	# of foci-positive cells	# of foci per nucleus			
	ATR			Brca1 *	Brca1 *	WRN ATM DNA-PK Brca2	* upon IR, not UV	78,92-99
Xrcc2 Xrcc3 Rad51B Rad51C Rad51D Brca1 <sup>1</sup> Brca2 <sup>10</sup> PML	LigaseIV WRN ** Fanconi (all 8 groups) <sup>5</sup> Fanc-D2 <sup>6</sup> Fanc-A/C/G <sup>7</sup> p21 c-Abl MSH2 ** Arg		Fanc-A/C/G <sup>7</sup> AT	ATM DNA-PK Rad54 BLM <sup>9</sup> MSH2 * WRN * Xrcc4	ATM Xrcc4	p53 Brca1 <sup>2</sup> Mre11 Nbs1 Rad52 H2AX Fanconi (all 8 groups except Fanc-D2) 53BP1 p53 BLM <sup>8</sup>	<sup>1</sup> 100,101 <sup>2</sup> 102,103 <sup>3</sup> 83 <sup>4</sup> 94 <sup>5</sup> 104 <sup>6</sup> 105 <sup>7</sup> 106 <sup>8</sup> 107 <sup>9</sup> 94,108 <sup>10</sup> S-phase foci are present  * spontaneous foci ** damage induced foci	29,56,82,83,85, 88,92-94,96,99-141
	c-Abl							88,117,142,143
				ATM				88,112,113,116
								113
	H2AX Brca1 53BP1 MDC1	53BP1 MDC1	Fanc-C <sup>1</sup>			Nbs1 DNA-PK ATM BLM Brca2 Fanconi (all 8 groups) <sup>2</sup>	<sup>1</sup> 106 <sup>2</sup> 104	87,91,97,99, 101,102,104-106,113,114, 119,125,132, 136,137,139, 141,144-157
						Brca1		99,140,141
								152,158
	Brca1							149

Protein	Spontaneous foci formation	Cell cycle dependency of spontaneous or induced foci	Damage induced foci formation	Co-localization			
				Before treatment	After treatment		
					Complete	Partial	None
Mre11 complex							
Mre11	yes	Staining pattern depends on cell cycle	IR HU CPT MMC	TRF1 BrdU PCNA PML-NB	Rad50 Nbs1 53BP1 PCNA Fanc-D2 $\gamma$ -H2AX MDC1	Brca1 PML-NB p53 p21	Rad51
Rad50	yes	no cell cycle dependency	IR HU CPT MMC MMS UV	TRF1/2 PML-NB	Mre11 Nbs1 $\gamma$ -H2AX	Brca1 Rad52 PCNA PML-NB p53	Rad51
Nbs1	yes		IR HU CPT MMC AS NCS	$\gamma$ -H2AX TRF2 PML-NB	Mre11 Rad50 53BP1 Fanc-D2 $\gamma$ -H2AX	Brca1 ATM	Rad51
MDC1	yes <sup>1</sup> no <sup>2</sup>		IR UV phleomycin		Mre11 Nbs1 $\gamma$ -H2AX 53BP1 Brca1 Chk2		Rad51
DNA helicases							
WRN	yes	S-phase	IR HU UVC CPT etoposide bleomycin 4NQO	BLM	RPA ATR	Rad51 BrdU	
BLM	yes	S-phase	IR HU etoposide	PML-NB Rad51 RPA phospho-p53 PCNA WRN	PML-NB Rad51 p53	Brca1 Mre11 Rad50 Rad51 RPA PCNA	
Cell cycle proteins							
p21		G0-phase G1-phase	LET		Mre11		PCNA
p53	rare	S-phase	IR APH HU	Rad51	Mre11 PML-NB BLM	Rad51 BrdU PCNA	



Biochemical and cellular aspects of homologous recombination

Foci formation influenced by a mutation						No influence on foci formation	Comments	References
Absence	Decrease		Delay	Increase				
	# of foci-positive cells	# of foci per nucleus	# of foci-positive cells	# of foci-positive cells	# of foci per nucleus			
Nbs1 Mre11 Ku70 Ku80 BLM * ATRkd <sup>10</sup> Fanc- A/C/G <sup>8***</sup> MSH2 H2AX MDC1	ATM <sup>6</sup> Brca1 <sup>1</sup> Fanc-D2 <sup>3</sup>				LigaseIV	DNA-PK p53 Brca1 <sup>2</sup> ATM <sup>7</sup> Fanconi (all 8 groups) <sup>4</sup> BLM ** WRN Fanc-D1 Fanc-D2 <sup>7</sup> XP-F 53BP1 ATR <sup>9</sup>	<sup>1</sup> 102 <sup>2</sup> 87,148 <sup>3</sup> 159 <sup>4</sup> 104,106 <sup>5</sup> 120,153,154,156 <sup>6</sup> 110 <sup>7</sup> 173 <sup>8</sup> 106 <sup>9</sup> 156 <sup>10</sup> 153  * upon HU, not IR ** upon IR, not HU *** upon MMC, not IR	61,62,85,87, 102,104,105, 106,110,120, 135,138,148, 153,154,156, 159-173
Nbs1 H2AX	Brca1 <sup>1</sup>					Brca2 Brca1 <sup>2</sup>	<sup>1</sup> 102 <sup>2</sup> 148	61,102,103,110 ,114,117,120, 134,142,148, 153,165,166, 168,170
Mre11 Nbs1 Rag1/2 H2AX BLM * Fanc- C/G/A <sup>3***</sup>	Brca1 <sup>1</sup> MDC1	MDC1				Brca1 <sup>2</sup> BLM Fanc-D1 Fanc- A/C/G <sup>3****</sup> 53BP1 ATM	<sup>1</sup> 102 <sup>2</sup> 87,148 <sup>3</sup> 106  * upon HU, not IR ** upon IR, not HU *** upon MMC, not IR **** upon IR, not MMC	61,62,87,91, 102,105,106, 120,125,136, 139,148,153, 154,157,161, 163,165,166, 170-177
H2AX						ATM ATR Mre11 Nbs1 DNA-PK 53BP1 Chk2 Brca1	<sup>1</sup> 157 <sup>2</sup> 138	138,155,157, 178
WRN				ATRkd	Telomerase	ATM		78,96,179,180
				ATM ATR	ATM ATR Telomerase	DNA-PK p53		94,107,108,133 ,148,153,179
						Nbs1 XPA p53 ATM		84,169
	BLM							107,133,168

Protein	Spontaneous foci formation	Cell cycle dependency of spontaneous or induced foci	Damage induced foci formation	Co-localization			
				Before treatment	After treatment		
					Complete	Partial	None
53BP1	yes		IR MMC CPT 4NQO MMS etoposide neomycin VM26 UV HU		$\gamma$ -H2AX Mre11 Nbs1 MDC1		
CHK2			IR <sup>1</sup> no <sup>2</sup>		MDC1		
ATM			IR <sup>1</sup> NCS <sup>1</sup> no <sup>2</sup>			$\gamma$ -H2AX Nbs1	
ATR	no		IR HU UVC CPT APH	PML-NB	RPA WRN Brca1		
Other							
H2AX	yes	S-phase * All phases **	IR NCS UV HU CPT	Rad51 Rad50 Brca1 Mre11	Rad51 Rad50 Mre11 Nbs1 Brca1 53BP1 PML-NB p53 MDC1	ATM PCNA	
PCNA		S-phase	IR HU UV	Mre11 $\gamma$ -H2AX	Mre11	Brca1 BLM Rad50 BARD1 BrdU $\gamma$ -H2AX BLM p53	
Fanc -D2	yes	S-phase	IR MMC UV	Brca1 Mre11 Nbs1 Rad51	Brca1 Mre11 Nbs1		
PML-NB	nuclear bodies		nuclear bodies	Mre11	Mre11 $\gamma$ -H2AX p53 Rad50		
Cds1	yes		no foci upon IR	Brca1			

Biochemical and cellular aspects of homologous recombination

Foci formation influenced by a mutation						No influence on foci formation	Comments	References
Absence	Decrease		Delay	Increase				
	# of foci-positive cells	# of foci per nucleus	# of foci-positive cells	# of foci-positive cells	# of foci per nucleus			
H2AX	ATM MDC1	MDC1	ATM	DNA-PK *		Nbs1 ATM p53 DNA-PK MDC1	* before treatment	125,138,151, 154,157,163, 172,181,182
	53BP1						<sup>1</sup> 139,178 <sup>2</sup> 91 Opposite results on Chk2 foci formation have been reported, depending on the antibody used.	91,139,178
MDC1							<sup>1</sup> 155,176 <sup>2</sup> 147,180	147,155,176, 180
	ATRkd							98,147,180
ATR Top1 *** H2AX	DNA-PK MDC1	MDC1	Ligase IV	Nbs1 + DNA-PK *		ATM HUS1 53BP1 Rad50 Mre11 Nbs1 MDC1	* untreated cells ** upon IR *** upon HU, CPT and UV	91,114,136- 139,151,155- 157,163,168, 170,174,176, 178,181,183
								107,148,151, 156,158,167, 169,184
Fanc-A/C/G Brca1						Mre11 Nbs1		132,150,173
								168
								145

## References

1. Symington, L.S. Role of RAD52 epistasis group genes in homologous recombination and double-strand break repair. *Microbiol Mol Biol Rev* **66**, 630-70. (2002).
2. Dronkert, M.L. & Kanaar, R. Repair of DNA interstrand cross-links. *Mutat Res* **486**, 217-47. (2001).
3. Cox, M.M. et al. The importance of repairing stalled replication forks. *Nature* **404**, 37-41. (2000).
4. Paques, F. & Haber, J.E. Multiple pathways of recombination induced by double-strand breaks in *Saccharomyces cerevisiae*. *Microbiol Mol Biol Rev* **63**, 349-404. (1999).
5. West, S.C. Molecular views of recombination proteins and their control. *Nat Rev Mol Cell Biol* **4**, 435-45. (2003).
6. Modesti, M. & Kanaar, R. Homologous recombination: from model organisms to human disease. *Genome Biol* **2**, Reviews1014. (2001).
7. Heyer, W.D., Ehmsen, K.T. & Solinger, J.A. Holliday junctions in the eukaryotic nucleus: resolution in sight? *Trends Biochem Sci* **28**, 548-57. (2003).
8. Baumann, P. & West, S.C. Role of the human RAD51 protein in homologous recombination and double-stranded-break repair. *Trends Biochem Sci* **23**, 247-51. (1998).
9. Mazin, A.V., Bornarth, C.J., Solinger, J.A., Heyer, W.D. & Kowalczykowski, S.C. Rad54 protein is targeted to pairing loci by the Rad51 nucleoprotein filament. *Mol Cell* **6**, 583-92. (2000).
10. Sung, P., Trujillo, K.M. & Van Komen, S. Recombination factors of *Saccharomyces cerevisiae*. *Mutat Res* **451**, 257-75. (2000).
11. Bianco, P.R., Tracy, R.B. & Kowalczykowski, S.C. DNA strand exchange proteins: a biochemical and physical comparison. *Front Biosci* **3**, 570-603. (1998).
12. Game, J.C. DNA double-strand breaks and the RAD50-RAD57 genes in *Saccharomyces*. *Semin Cancer Biol* **4**, 73-83. (1993).
13. Sonoda, E. et al. Rad51-deficient vertebrate cells accumulate chromosomal breaks prior to cell death. *Embo J* **17**, 598-608. (1998).
14. Lim, D.S. & Hasty, P. A mutation in mouse rad51 results in an early embryonic lethal that is suppressed by a mutation in p53. *Mol Cell Biol* **16**, 7133-43. (1996).
15. Tszuzuki, T. et al. Targeted disruption of the Rad51 gene leads to lethality in embryonic mice. *Proc Natl Acad Sci USA* **93**, 6236-40. (1996).
16. Shinohara, A. & Ogawa, T. Rad51/RecA protein families and the associated proteins in eukaryotes. *Mutat Res* **435**, 13-21. (1999).
17. Davies, A.A. et al. Role of BRCA2 in control of the RAD51 recombination and DNA repair protein. *Mol Cell* **7**, 273-82. (2001).
18. Moynahan, M.E., Pierce, A.J. & Jasin, M. BRCA2 is required for homology-directed repair of chromosomal breaks. *Mol Cell* **7**, 263-72. (2001).
19. Orelli, B.J. & Bishop, D.K. BRCA2 and homologous recombination. *Breast Cancer Res* **3**, 294-8. (2001).
20. Pellegrini, L. et al. Insights into DNA recombination from the structure of a RAD51-BRCA2 complex. *Nature* **420**, 287-93. (2002).
21. Venkataraman, A.R. Functions of BRCA1 and BRCA2 in the biological response to DNA damage. *J Cell Sci* **114**, 3591-8. (2001).
22. Hays, S.L., Firmenich, A.A. & Berg, P. Complex formation in yeast double-strand break repair: participation of Rad51, Rad52, Rad55, and Rad57 proteins. *Proc Natl Acad Sci USA* **92**, 6925-9. (1995).
23. Johnson, R.D. & Symington, L.S. Functional differences and interactions among the putative RecA homologs Rad51, Rad55, and Rad57. *Mol Cell Biol* **15**, 4843-50. (1995).

24. Thacker, J. A surfeit of RAD51-like genes? *Trends Genet* **15**, 166-8. (1999).
25. Schild, D., Lio, Y.C., Collins, D.W., Tsomondo, T. & Chen, D.J. Evidence for simultaneous protein interactions between human Rad51 paralogs. *J Biol Chem* **275**, 16443-9. (2000).
26. Masson, J.Y. et al. Identification and purification of two distinct complexes containing the five RAD51 paralogs. *Genes Dev* **15**, 3296-307. (2001).
27. Sigurdsson, S. et al. Mediator function of the human Rad51B-Rad51C complex in Rad51/RPA-catalyzed DNA strand exchange. *Genes Dev* **15**, 3308-18. (2001).
28. Rijkers, T. et al. Targeted inactivation of mouse RAD52 reduces homologous recombination but not resistance to ionizing radiation. *Mol Cell Biol* **18**, 6423-9. (1998).
29. Yamaguchi-Iwai, Y. et al. Homologous recombination, but not DNA repair, is reduced in vertebrate cells deficient in RAD52. *Mol Cell Biol* **18**, 6430-5. (1998).
30. Fujimori, A. et al. Rad52 partially substitutes for the Rad51 paralog XRCC3 in maintaining chromosomal integrity in vertebrate cells. *Embo J* **20**, 5513-20. (2001).
31. Sung, P. Yeast Rad55 and Rad57 proteins form a heterodimer that functions with replication protein A to promote DNA strand exchange by Rad51 recombinase. *Genes Dev* **11**, 1111-21. (1997).
32. van den Bosch, M. et al. Characterization of RAD52 homologs in the fission yeast *Schizosaccharomyces pombe*. *Mutat Res* **461**, 311-23. (2001).
33. Bai, Y. & Symington, L.S. A Rad52 homolog is required for RAD51-independent mitotic recombination in *Saccharomyces cerevisiae*. *Genes Dev* **10**, 2025-37. (1996).
34. Sugiyama, T. & Kowalczykowski, S.C. Rad52 protein associates with replication protein A (RPA)-single-stranded DNA to accelerate Rad51-mediated displacement of RPA and presynaptic complex formation. *J Biol Chem* **277**, 31663-72. (2002).
35. Hiom, K. DNA repair: Rad52 - the means to an end. *Curr Biol* **9**, R446-8. (1999).
36. Pazin, M.J. & Kadonaga, J.T. SWI2/SNF2 and related proteins: ATP-driven motors that disrupt protein-DNA interactions? *Cell* **88**, 737-40. (1997).
37. Tan, R.T.L., Kanaar, R. & Wyman, C. Rad54, a Jack of all trades in homologous recombination. *DNA Repair (Amst)* **2**, 787-94. (2003).
38. Alexeev, A., Mazin, A. & Kowalczykowski, S.C. Rad54 protein possesses chromatin-remodeling activity stimulated by the Rad51-ssDNA nucleoprotein filament. *Nat Struct Biol* **10**, 182-6. (2003).
39. Alexiadis, V. & Kadonaga, J.T. Strand pairing by Rad54 and Rad51 is enhanced by chromatin. *Genes Dev* **16**, 2767-71. (2002).
40. Jaskelioff, M., Van Komen, S., Krebs, J.E., Sung, P. & Peterson, C.L. Rad54p is a chromatin remodeling enzyme required for heteroduplex DNA joint formation with chromatin. *J Biol Chem* **278**, 9212-8. (2003).
41. Ristic, D., Wyman, C., Paulusma, C. & Kanaar, R. The architecture of the human Rad54-DNA complex provides evidence for protein translocation along DNA. *Proc Natl Acad Sci USA* **98**, 8454-60. (2001).
42. Solinger, J.A., Kiiianitsa, K. & Heyer, W.D. Rad54, a Swi2/Snf2-like recombinational repair protein, disassembles Rad51:dsDNA filaments. *Mol Cell* **10**, 1175-88. (2002).
43. Dronkert, M.L. et al. Mouse RAD54 affects DNA double-strand break repair and sister chromatid exchange. *Mol Cell Biol* **20**, 3147-56. (2000).
44. Essers, J. et al. Disruption of mouse RAD54 reduces ionizing radiation resistance and homologous recombination. *Cell* **89**, 195-204. (1997).
45. Essers, J. et al. Homologous and non-homologous recombination differentially affect DNA damage repair in mice. *Embo J* **19**, 1703-10. (2000).
46. Dresser, M.E. et al. DMC1 functions in a *Saccharomyces cerevisiae* meiotic pathway that is largely independent of the RAD51 pathway. *Genetics* **147**, 533-44. (1997).
47. Klein, H.L. RDH54, a RAD54 homologue in *Saccharomyces cerevisiae*, is required for mitotic diploid-specific recombination and repair and for meiosis. *Genetics* **147**, 1533-43. (1997).

## Chapter 2

---

48. Petukhova, G., Sung, P. & Klein, H. Promotion of Rad51-dependent D-loop formation by yeast recombination factor Rdh54/Tid1. *Genes Dev* **14**, 2206-15. (2000).
49. Tanaka, K., Kagawa, W., Kinebuchi, T., Kurumizaka, H. & Miyagawa, K. Human Rad54B is a double-stranded DNA-dependent ATPase and has biochemical properties different from its structural homolog in yeast, Tid1/Rdh54. *Nucleic Acids Res* **30**, 1346-53. (2002).
50. Arbel, A., Zenvirth, D. & Simchen, G. Sister chromatid-based DNA repair is mediated by RAD54, not by DMC1 or TID1. *Embo J* **18**, 2648-58. (1999).
51. Shinohara, M. et al. Characterization of the roles of the *Saccharomyces cerevisiae* RAD54 gene and a homologue of RAD54, RDH54/TID1, in mitosis and meiosis. *Genetics* **147**, 1545-56. (1997).
52. Hiramoto, T. et al. Mutations of a novel human RAD54 homologue, RAD54B, in primary cancer. *Oncogene* **18**, 3422-6. (1999).
53. D'Amours, D. & Jackson, S.P. The Mre11 complex: at the crossroads of dna repair and checkpoint signalling. *Nat Rev Mol Cell Biol* **3**, 317-27. (2002).
54. Chen, L., Trujillo, K., Ramos, W., Sung, P. & Tomkinson, A.E. Promotion of Dnl4-catalyzed DNA end-joining by the Rad50/Mre11/Xrs2 and Hdf1/Hdf2 complexes. *Mol Cell* **8**, 1105-15. (2001).
55. de Jager, M. et al. Human Rad50/Mre11 is a flexible complex that can tether DNA ends. *Mol Cell* **8**, 1129-35. (2001).
56. Yamaguchi-Iwai, Y. et al. Mre11 is essential for the maintenance of chromosomal DNA in vertebrate cells. *Embo J* **18**, 6619-29. (1999).
57. Tauchi, H., Matsuura, S., Kobayashi, J., Sakamoto, S. & Komatsu, K. Nijmegen breakage syndrome gene, NBS1, and molecular links to factors for genome stability. *Oncogene* **21**, 8967-80. (2002).
58. Zhu, J., Petersen, S., Tessarollo, L. & Nussenzweig, A. Targeted disruption of the Nijmegen breakage syndrome gene NBS1 leads to early embryonic lethality in mice. *Curr Biol* **11**, 105-9. (2001).
59. Xiao, Y. & Weaver, D.T. Conditional gene targeted deletion by Cre recombinase demonstrates the requirement for the double-strand break repair Mre11 protein in murine embryonic stem cells. *Nucleic Acids Res* **25**, 2985-91. (1997).
60. Luo, G. et al. Disruption of mRad50 causes embryonic stem cell lethality, abnormal embryonic development, and sensitivity to ionizing radiation. *Proc Natl Acad Sci USA* **96**, 7376-81. (1999).
61. Carney, J.P. et al. The hMre11/hRad50 protein complex and Nijmegen breakage syndrome: linkage of double-strand break repair to the cellular DNA damage response. *Cell* **93**, 477-86. (1998).
62. Stewart, G.S. et al. The DNA double-strand break repair gene hMRE11 is mutated in individuals with an ataxia-telangiectasia-like disorder. *Cell* **99**, 577-87. (1999).
63. Lim, D.S. et al. ATM phosphorylates p95/nbs1 in an S-phase checkpoint pathway. *Nature* **404**, 613-7. (2000).
64. Gatei, M. et al. ATM-dependent phosphorylation of nibrin in response to radiation exposure. *Nat Genet* **25**, 115-9. (2000).
65. Venkitaraman, A.R. Cancer susceptibility and the functions of BRCA1 and BRCA2. *Cell* **108**, 171-82. (2002).
66. Scully, R., Puget, N. & Vlasakova, K. DNA polymerase stalling, sister chromatid recombination and the BRCA genes. *Oncogene* **19**, 6176-83. (2000).
67. Moynahan, M.E., Chiu, J.W., Koller, B.H. & Jasin, M. Brca1 controls homology-directed DNA repair. *Mol Cell* **4**, 511-8. (1999).
68. Gowen, L.C., Johnson, B.L., Latour, A.M., Sulik, K.K. & Koller, B.H. Brca1 deficiency results in early embryonic lethality characterized by neuroepithelial abnormalities. *Nat Genet* **12**, 191-4. (1996).
69. Hakem, R. et al. The tumor suppressor gene Brca1 is required for embryonic cellular proliferation in the mouse. *Cell* **85**, 1009-23. (1996).
70. Ludwig, T., Chapman, D.L., Papaioannou, V.E. & Efstratiadis, A. Targeted mutations of breast cancer susceptibility gene homologs in mice: lethal phenotypes of Brca1, Brca2, Brca1/Brca2, Brca1/p53, and Brca2/p53 nullizygous embryos. *Genes Dev* **11**, 1226-41. (1997).

71. Suzuki, A. et al. Brca2 is required for embryonic cellular proliferation in the mouse. *Genes Dev* **11**, 1242-52. (1997).
72. Yang, H. et al. BRCA2 function in DNA binding and recombination from a BRCA2-DSS1-ssDNA structure. *Science* **297**, 1837-48. (2002).
73. Bachrati, C.Z. & Hickson, I.D. RecQ helicases: suppressors of tumorigenesis and premature aging. *Biochem J* **374**, 577-606. (2003).
74. Chakraverty, R.K. & Hickson, I.D. Defending genome integrity during DNA replication: a proposed role for RecQ family helicases. *Bioessays* **21**, 286-94. (1999).
75. Karow, J.K., Wu, L. & Hickson, I.D. RecQ family helicases: roles in cancer and aging. *Curr Opin Genet Dev* **10**, 32-8. (2000).
76. Braybrooke, J.P. et al. Functional interaction between the bloom's syndrome helicase and the RAD51 paralog, RAD51L3 (RAD51D). *J Biol Chem* **15**, 15 (2003).
77. Brosh, R.M., Jr. et al. Replication protein A physically interacts with the Bloom's syndrome protein and stimulates its helicase activity. *J Biol Chem* **275**, 23500-8. (2000).
78. Constantinou, A. et al. Werner's syndrome protein (WRN) migrates Holliday junctions and co-localizes with RPA upon replication arrest. *EMBO Rep* **1**, 80-4. (2000).
79. Cooper, M.P. et al. Ku complex interacts with and stimulates the Werner protein. *Genes Dev* **14**, 907-12. (2000).
80. Wu, L. & Hickson, I.D. Molecular biology. DNA ends ReQ-uire attention. *Science* **292**, 229-30. (2001).
81. Xia, S.J., Shammas, M.A. & Shmookler Reis, R.J. Elevated recombination in immortal human cells is mediated by HsRAD51 recombinase. *Mol Cell Biol* **17**, 7151-8. (1997).
82. Raderschall, E., Golub, E.I. & Haaf, T. Nuclear foci of mammalian recombination proteins are located at single-stranded DNA regions formed after DNA damage. *Proc Natl Acad Sci U S A* **96**, 1921-6. (1999).
83. Haaf, T., Golub, E.I., Reddy, G., Radding, C.M. & Ward, D.C. Nuclear foci of mammalian Rad51 recombination protein in somatic cells after DNA damage and its localization in synaptonemal complexes. *Proc Natl Acad Sci U S A* **92**, 2298-302. (1995).
84. Jakob, B., Scholz, M. & Taucher-Scholz, G. Immediate localized CDKN1A (p21) radiation response after damage produced by heavy-ion tracks. *Radiat Res* **154**, 398-405. (2000).
85. Nelms, B.E., Maser, R.S., MacKay, J.F., Lagally, M.G. & Petrini, J.H. In situ visualization of DNA double-strand break repair in human fibroblasts. *Science* **280**, 590-2. (1998).
86. Tashiro, S., Walter, J., Shinohara, A., Kamada, N. & Cremer, T. Rad51 accumulation at sites of DNA damage and in postreplicative chromatin. *J Cell Biol* **150**, 283-91. (2000).
87. Wu, X. et al. Independence of R/M/N focus formation and the presence of intact BRCA1. *Science* **289**, 11. (2000).
88. Essers, J. et al. Nuclear dynamics of RAD52 group homologous recombination proteins in response to DNA damage. *Embo J* **21**, 2030-7. (2002).
89. Thompson, L.H. & Schild, D. Homologous recombinational repair of DNA ensures mammalian chromosome stability. *Mutat Res* **477**, 131-53. (2001).
90. Houtsmuller, A.B. & Vermeulen, W. Macromolecular dynamics in living cell nuclei revealed by fluorescence redistribution after photobleaching. *Histochem Cell Biol* **115**, 13-21. (2001).
91. Lukas, C., Falck, J., Bartkova, J., Bartek, J. & Lukas, J. Distinct spatiotemporal dynamics of mammalian checkpoint regulators induced by DNA damage. *Nat Cell Biol* **5**, 255-60. (2003).
92. Gasior, S.L., Wong, A.K., Kora, Y., Shinohara, A. & Bishop, D.K. Rad52 associates with RPA and functions with rad55 and rad57 to assemble meiotic recombination complexes. *Genes Dev* **12**, 2208-21. (1998).
93. Golub, E.I., Gupta, R.C., Haaf, T., Wold, M.S. & Radding, C.M. Interaction of human rad51 recombination protein with single-stranded DNA binding protein, RPA. *Nucleic Acids Res* **26**, 5388-93. (1998).

94. Bischof, O. et al. Regulation and localization of the Bloom syndrome protein in response to DNA damage. *J Cell Biol* **153**, 367-80. (2001).
95. MacPhail, S.H. & Olive, P.L. RPA foci are associated with cell death after irradiation. *Radiat Res* **155**, 672-9. (2001).
96. Sakamoto, S. et al. Werner helicase relocates into nuclear foci in response to DNA damaging agents and co-localizes with RPA and Rad51. *Genes Cells* **6**, 421-30. (2001).
97. Choudhary, S.K. & Li, R. BRCA1 modulates ionizing radiation-induced nuclear focus formation by the replication protein A p34 subunit. *J Cell Biochem* **84**, 666-74. (2002).
98. Barr, S.M., Leung, C.G., Chang, E.E. & Cimprich, K.A. ATR kinase activity regulates the intranuclear translocation of ATR and RPA following ionizing radiation. *Curr Biol* **13**, 1047-51. (2003).
99. Tarsounas, M., Davies, D. & West, S.C. BRCA2-dependent and independent formation of RAD51 nuclear foci. *Oncogene* **22**, 1115-23. (2003).
100. Bhattacharyya, A., Ear, U.S., Koller, B.H., Weichselbaum, R.R. & Bishop, D.K. The breast cancer susceptibility gene BRCA1 is required for subnuclear assembly of Rad51 and survival following treatment with the DNA cross-linking agent cisplatin. *J Biol Chem* **275**, 23899-903. (2000).
101. Huber, L.J. et al. Impaired DNA damage response in cells expressing an exon 11-deleted murine Brca1 variant that localizes to nuclear foci. *Mol Cell Biol* **21**, 4005-15. (2001).
102. Zhong, Q. et al. Association of BRCA1 with the hRad50-hMre11-p95 complex and the DNA damage response. *Science* **285**, 747-50. (1999).
103. Yuan, S.S. et al. BRCA2 is required for ionizing radiation-induced assembly of Rad51 complex in vivo. *Cancer Res* **59**, 3547-51. (1999).
104. Digweed, M. et al. Attenuation of the formation of DNA-repair foci containing RAD51 in Fanconi anaemia. *Carcinogenesis* **23**, 1121-6. (2002).
105. Godthelp, B.C., Artwert, F., Joenje, H. & Zdzienicka, M.Z. Impaired DNA damage-induced nuclear Rad51 foci formation uniquely characterizes Fanconi anemia group D1. *Oncogene* **21**, 5002-5. (2002).
106. Pichierri, P., Averbek, D. & Rosselli, F. DNA cross-link-dependent RAD50/MRE11/NBS1 subnuclear assembly requires the Fanconi anemia C protein. *Hum Mol Genet* **11**, 2531-46. (2002).
107. Sengupta, S. et al. BLM helicase-dependent transport of p53 to sites of stalled DNA replication forks modulates homologous recombination. *Embo J* **22**, 1210-22. (2003).
108. Wu, L., Davies, S.L., Levitt, N.C. & Hickson, I.D. Potential role for the BLM helicase in recombinational repair via a conserved interaction with RAD51. *J Biol Chem* **276**, 19375-81. (2001).
109. Tashiro, S. et al. S phase specific formation of the human Rad51 protein nuclear foci in lymphocytes. *Oncogene* **12**, 2165-70. (1996).
110. Maser, R.S., Monsen, K.J., Nelms, B.E. & Petrini, J.H. hMre11 and hRad50 nuclear foci are induced during the normal cellular response to DNA double-strand breaks. *Mol Cell Biol* **17**, 6087-96. (1997).
111. Bishop, D.K. et al. Xrcc3 is required for assembly of Rad51 complexes in vivo. *J Biol Chem* **273**, 21482-8. (1998).
112. Morrison, C. et al. The controlling role of ATM in homologous recombinational repair of DNA damage. *Embo J* **19**, 463-71. (2000).
113. Tanaka, K., Hiramoto, T., Fukuda, T. & Miyagawa, K. A novel human rad54 homologue, Rad54B, associates with Rad51. *J Biol Chem* **275**, 26316-21. (2000).
114. Paull, T.T. et al. A critical role for histone H2AX in recruitment of repair factors to nuclear foci after DNA damage. *Curr Biol* **10**, 886-95. (2000).
115. Morrison, C. et al. The essential functions of human Rad51 are independent of ATP hydrolysis. *Mol Cell Biol* **19**, 6891-7. (1999).
116. Tan, T.L. et al. Mouse Rad54 affects DNA conformation and DNA-damage-induced Rad51 foci formation. *Curr Biol* **9**, 325-8. (1999).



117. Liu, Y. & Maizels, N. Coordinated response of mammalian Rad51 and Rad52 to DNA damage. *EMBO Rep* **1**, 85-90. (2000).
118. Takata, M. et al. The Rad51 paralog Rad51B promotes homologous recombinational repair. *Mol Cell Biol* **20**, 6476-82. (2000).
119. Scully, R. et al. Association of BRCA1 with Rad51 in mitotic and meiotic cells. *Cell* **88**, 265-75. (1997).
120. Mirzoeva, O.K. & Petrini, J.H. DNA damage-dependent nuclear dynamics of the Mre11 complex. *Mol Cell Biol* **21**, 281-8. (2001).
121. O'Regan, P., Wilson, C., Townsend, S. & Thacker, J. XRCC2 is a nuclear RAD51-like protein required for damage-dependent RAD51 focus formation without the need for ATP binding. *J Biol Chem* **276**, 22148-53. (2001).
122. Pichierri, P., Franchitto, A., Mosesso, P. & Palitti, F. Werner's syndrome protein is required for correct recovery after replication arrest and DNA damage induced in S-phase of cell cycle. *Mol Biol Cell* **12**, 2412-21. (2001).
123. Pichierri, P., Franchitto, A., Piergentili, R., Colussi, C. & Palitti, F. Hypersensitivity to camptothecin in MSH2 deficient cells is correlated with a role for MSH2 protein in recombinational repair. *Carcinogenesis* **22**, 1781-7. (2001).
124. Takata, M. et al. Chromosome instability and defective recombinational repair in knockout mutants of the five Rad51 paralogs. *Mol Cell Biol* **21**, 2858-66. (2001).
125. Celeste, A. et al. Genomic instability in mice lacking histone H2AX. *Science* **296**, 922-7. (2002).
126. Delacote, F., Han, M., Stamato, T.D., Jasin, M. & Lopez, B.S. An xrcc4 defect or Wortmannin stimulates homologous recombination specifically induced by double-strand breaks in mammalian cells. *Nucleic Acids Res* **30**, 3454-63. (2002).
127. Godthelp, B.C. et al. Mammalian Rad51C contributes to DNA cross-link resistance, sister chromatid cohesion and genomic stability. *Nucleic Acids Res* **30**, 2172-82. (2002).
128. Kraakman-van der Zwet, M. et al. Brca2 (XRCC11) deficiency results in radioresistant DNA synthesis and a higher frequency of spontaneous deletions. *Mol Cell Biol* **22**, 669-79. (2002).
129. Li, Y. et al. Arg tyrosine kinase is involved in homologous recombinational DNA repair. *Biochem Biophys Res Commun* **299**, 697-702. (2002).
130. Liu, N. XRCC2 is Required for the Formation of Rad51 Foci Induced by Ionizing Radiation and DNA Cross-Linking Agent Mitomycin C. *J Biomed Biotechnol* **2**, 106-113. (2002).
131. Raderschall, E. et al. Formation of higher-order nuclear Rad51 structures is functionally linked to p21 expression and protection from DNA damage-induced apoptosis. *J Cell Sci* **115**, 153-64. (2002).
132. Taniguchi, T. et al. S-phase-specific interaction of the Fanconi anemia protein, FANCD2, with BRCA1 and RAD51. *Blood* **100**, 2414-20. (2002).
133. Yang, Q. et al. The processing of Holliday junctions by BLM and WRN helicases is regulated by p53. *J Biol Chem* **277**, 31980-7. (2002).
134. Yuan, S.S., Chang, H.L. & Lee, E.Y. Ionizing radiation-induced Rad51 nuclear focus formation is cell cycle-regulated and defective in both ATM(-/-) and c-Abl(-/-) cells. *Mutat Res* **525**, 85-92. (2003).
135. Franchitto, A. et al. The mammalian mismatch repair protein MSH2 is required for correct MRE11 and RAD51 relocalization and for efficient cell cycle arrest induced by ionizing radiation in G2 phase. *Oncogene* **22**, 2110-20. (2003).
136. Petersen, S. et al. AID is required to initiate Nbs1/gamma-H2AX focus formation and mutations at sites of class switching. *Nature* **414**, 660-5. (2001).
137. Bassing, C.H. et al. Increased ionizing radiation sensitivity and genomic instability in the absence of histone H2AX. *Proc Natl Acad Sci USA* **99**, 8173-8. (2002).
138. Goldberg, M. et al. MDC1 is required for the intra-S-phase DNA damage checkpoint. *Nature* **421**, 952-6. (2003).

## Chapter 2

---

139. Wang, B., Matsuoka, S., Carpenter, P.B. & Elledge, S.J. 53BP1, a mediator of the DNA damage checkpoint. *Science* **298**, 1435-8. (2002).
140. Shin, D.S. et al. Full-length archaeal Rad51 structure and mutants: mechanisms for RAD51 assembly and control by BRCA2. *Embo J* **22**, 4566-76. (2003).
141. Chen, J. et al. Stable interaction between the products of the BRCA1 and BRCA2 tumor suppressor genes in mitotic and meiotic cells. *Mol Cell* **2**, 317-28. (1998).
142. Liu, Y., Li, M., Lee, E.Y. & Maizels, N. Localization and dynamic relocalization of mammalian Rad52 during the cell cycle and in response to DNA damage. *Curr Biol* **9**, 975-8. (1999).
143. Kitao, H. & Yuan, Z.M. Regulation of ionizing radiation-induced Rad52 nuclear foci formation by c-Abl-mediated phosphorylation. *J Biol Chem* **277**, 48944-8. (2002).
144. Jin, Y. et al. Cell cycle-dependent colocalization of BARD1 and BRCA1 proteins in discrete nuclear domains. *Proc Natl Acad Sci USA* **94**, 12075-80. (1997).
145. Lee, J.-S., Collins, K.M., Brown, A.L., Lee, C.H. & Chung, J.H. hCds1-mediated phosphorylation of BRCA1 regulates the DNA damage response. *Nature* **404**, 201-4. (2000).
146. Cortez, D., Wang, Y., Qin, J. & Elledge, S.J. Requirement of ATM-dependent phosphorylation of brca1 in the DNA damage response to double-strand breaks. *Science* **286**, 1162-6. (1999).
147. Tibbetts, R.S. et al. Functional interactions between BRCA1 and the checkpoint kinase ATR during genotoxic stress. *Genes Dev* **14**, 2989-3002. (2000).
148. Wang, Y. et al. BASC, a super complex of BRCA1-associated proteins involved in the recognition and repair of aberrant DNA structures. *Genes Dev* **14**, 927-39. (2000).
149. Cantor, S.B. et al. BACH1, a novel helicase-like protein, interacts directly with BRCA1 and contributes to its DNA repair function. *Cell* **105**, 149-60. (2001).
150. Garcia-Higuera, I. et al. Interaction of the Fanconi anemia proteins and BRCA1 in a common pathway. *Mol Cell* **7**, 249-62. (2001).
151. Ward, I.M. & Chen, J. Histone H2AX is phosphorylated in an ATR-dependent manner in response to replication stress. *J Biol Chem* **276**, 47759-62. (2001).
152. Fabbro, M., Rodriguez, J.A., Baer, R. & Henderson, B.R. BARD1 induces BRCA1 intranuclear foci formation by increasing RING-dependent BRCA1 nuclear import and inhibiting BRCA1 nuclear export. *J Biol Chem* **277**, 21315-24. (2002).
153. Franchitto, A. & Pichierri, P. Bloom's syndrome protein is required for correct relocalization of RAD50/MRE11/NBS1 complex after replication fork arrest. *J Cell Biol* **157**, 19-30. (2002).
154. Celeste, A. et al. Histone H2AX phosphorylation is dispensable for the initial recognition of DNA breaks. *Nat Cell Biol* **5**, 675-9. (2003).
155. Lou, Z., Chini, C.C., Minter-Dykhouse, K. & Chen, J. Mediator of DNA damage checkpoint protein 1 regulates BRCA1 localization and phosphorylation in DNA damage checkpoint control. *J Biol Chem* **278**, 13599-602. (2003).
156. Mirzoeva, O.K. & Petrini, J.H. DNA replication-dependent nuclear dynamics of the Mre11 complex. *Mol Cancer Res* **1**, 207-18. (2003).
157. Stewart, G.S., Wang, B., Bignell, C.R., Taylor, A.M. & Elledge, S.J. MDC1 is a mediator of the mammalian DNA damage checkpoint. *Nature* **421**, 961-6. (2003).
158. Scully, R. et al. Dynamic changes of BRCA1 subnuclear location and phosphorylation state are initiated by DNA damage. *Cell* **90**, 425-35. (1997).
159. Digweed, M. et al. SV40 large T-antigen disturbs the formation of nuclear DNA-repair foci containing MRE11. *Oncogene* **21**, 4873-8. (2002).
160. Goedecke, W., Eijpe, M., Offenbergh, H.H., van Aalderen, M. & Heyting, C. Mre11 and Ku70 interact in somatic cells, but are differentially expressed in early meiosis. *Nat Genet* **23**, 194-8. (1999).
161. Paull, T.T. & Gellert, M. The 3' to 5' exonuclease activity of Mre 11 facilitates repair of DNA double-strand breaks. *Mol Cell* **1**, 969-79. (1998).

162. Dong, Z., Zhong, Q. & Chen, P.L. The Nijmegen breakage syndrome protein is essential for Mre11 phosphorylation upon DNA damage. *J Biol Chem* **274**, 19513-6. (1999).
163. Schultz, L.B., Chehab, N.H., Malikzay, A. & Halazonetis, T.D. p53 binding protein 1 (53BP1) is an early participant in the cellular response to DNA double-strand breaks. *J Cell Biol* **151**, 1381-90. (2000).
164. Zhao, S., Renthal, W. & Lee, E.Y. Functional analysis of FHA and BRCT domains of NBS1 in chromatin association and DNA damage responses. *Nucleic Acids Res* **30**, 4815-22. (2002).
165. Zhu, X.D., Kuster, B., Mann, M., Petrini, J.H. & de Lange, T. Cell-cycle-regulated association of RAD50/MRE11/NBS1 with TRF2 and human telomeres. *Nat Genet* **25**, 347-52. (2000).
166. Desai-Mehta, A., Cerosaletti, K.M. & Concannon, P. Distinct functional domains of nibrin mediate Mre11 binding, focus formation, and nuclear localization. *Mol Cell Biol* **21**, 2184-91. (2001).
167. Maser, R.S. et al. Mre11 complex and DNA replication: linkage to E2F and sites of DNA synthesis. *Mol Cell Biol* **21**, 6006-16. (2001).
168. Carbone, R., Pearson, M., Minucci, S. & Pelicci, P.G. PML NBs associate with the hMre11 complex and p53 at sites of irradiation induced DNA damage. *Oncogene* **21**, 1633-40. (2002).
169. Jakob, B., Scholz, M. & Taucher-Scholz, G. Characterization of CDKN1A (p21) binding to sites of heavy-ion-induced damage: colocalization with proteins involved in DNA repair. *Int J Radiat Biol* **78**, 75-88. (2002).
170. Furuta, T. et al. Phosphorylation of histone H2AX and activation of Mre11, Rad50, and Nbs1 in response to replication-dependent DNA double-strand breaks induced by mammalian DNA topoisomerase I cleavage complexes. *J Biol Chem* **278**, 20303-12. (2003).
171. Lee, J.H. et al. Distinct functions of Nijmegen breakage syndrome in ataxia telangiectasia mutated-dependent responses to DNA damage. *Mol Cancer Res* **1**, 674-81. (2003).
172. Anderson, L., Henderson, C. & Adachi, Y. Phosphorylation and rapid relocalization of 53BP1 to nuclear foci upon DNA damage. *Mol Cell Biol* **21**, 1719-29. (2001).
173. Nakanishi, K. et al. Interaction of FANCD2 and NBS1 in the DNA damage response. *Nat Cell Biol* **4**, 913-20. (2002).
174. Chen, H.T. et al. Response to RAG-mediated VDJ cleavage by NBS1 and gamma-H2AX. *Science* **290**, 1962-5. (2000).
175. Zhao, S. et al. Functional link between ataxia-telangiectasia and Nijmegen breakage syndrome gene products. *Nature* **405**, 473-7. (2000).
176. Andegeko, Y. et al. Nuclear retention of ATM at sites of DNA double strand breaks. *J Biol Chem* **276**, 38224-30. (2001).
177. Yuan, S.S. et al. Arsenic-induced Mre11 phosphorylation is cell cycle-dependent and defective in NBS cells. *DNA Repair (Amst)* **1**, 137-42. (2002).
178. Lou, Z., Minter-Dykhouse, K., Wu, X. & Chen, J. MDC1 is coupled to activated CHK2 in mammalian DNA damage response pathways. *Nature* **421**, 957-61. (2003).
179. von Kobbe, C. et al. Colocalization, physical, and functional interaction between Werner and Bloom syndrome proteins. *J Biol Chem* **277**, 22035-44. (2002).
180. Pichierri, P., Rosselli, F. & Franchitto, A. Werner's syndrome protein is phosphorylated in an ATR/ATM-dependent manner following replication arrest and DNA damage induced during the S phase of the cell cycle. *Oncogene* **22**, 1491-500. (2003).
181. Rappold, I., Iwabuchi, K., Date, T. & Chen, J. Tumor suppressor p53 binding protein 1 (53BP1) is involved in DNA damage-signaling pathways. *J Cell Biol* **153**, 613-20. (2001).
182. Ward, I.M., Minn, K., Jorda, K.G. & Chen, J. Accumulation of checkpoint protein 53BP1 at DNA breaks involves its binding to phosphorylated histone H2AX. *J Biol Chem* **278**, 19579-82. (2003).
183. Rothkamm, K. & Lobrich, M. Evidence for a lack of DNA double-strand break repair in human cells exposed to very low x-ray doses. *Proc Natl Acad Sci USA* **100**, 5057-62. (2003).
184. Balajee, A.S. & Geard, C.R. Chromatin-bound PCNA complex formation triggered by DNA damage occurs independent of the ATM gene product in human cells. *Nucleic Acids Res* **29**, 1341-51. (2001).



---

## Chapter 3

*Nuclear dynamics of RAD52 group homologous recombination  
proteins in response to DNA damage*

---

## Chapter 3

### *Nuclear dynamics of RAD52 group homologous recombination proteins in response to DNA damage*

Jeroen Essers<sup>1\*</sup>, Adriaan B. Houtsmuller<sup>2\*</sup>, Lieneke van Veelen<sup>1,3</sup>, Coen Paulusma<sup>1</sup>, Alex L. Nigg<sup>2</sup>, Albert Pastink<sup>4</sup>, Wim Vermeulen<sup>1</sup>, Jan H.J. Hoeijmakers<sup>1</sup> and Roland Kanaar<sup>1,3</sup>

\*These authors contributed equally.

<sup>1</sup> Department of Cell Biology and Genetics, <sup>2</sup>Department of Pathology, Erasmus MC, University Medical Center, P.O. Box 1738, 3000 DR Rotterdam, The Netherlands

<sup>3</sup> Department of Radiation Oncology, Erasmus MC-Daniel den Hoed Cancer Center, University Medical Center, P.O. Box 5201, 3008 AE Rotterdam, The Netherlands

<sup>4</sup> Department of Radiation Genetics and Chemical Mutagenesis, Leiden University Medical Center, P.O. Box 9503, 2300 RF Leiden, The Netherlands

*The EMBO Journal*, Vol. 21, no. 8, pp.2030-2037, 2002.

## **Abstract**

Recombination between homologous DNA molecules is essential for the proper maintenance and duplication of the genome and for repair of exogenously induced DNA damage such as double-strand breaks. Homologous recombination requires the RAD52 group proteins, including Rad51, Rad52 and Rad54. Upon treatment of mammalian cells with ionizing radiation, these proteins accumulate into foci at sites of DNA damage induction. Here we show that these foci are dynamic structures of which Rad51 is a stably associated core component, whereas Rad52 and Rad54 rapidly and reversibly interact with the structure. Furthermore, we show that the majority of the proteins are not part of the same multi-protein complex in the absence of DNA damage. Executing DNA transactions through dynamic multi-protein complexes, rather than stable holo-complexes, allows flexibility. In case of DNA repair, for example, it will facilitate cross-talk between different DNA repair pathways and coupling to other DNA transactions, such as replication.

## Introduction

Homologous recombination plays a pivotal role in genome duplication and in providing genome stability. Furthermore, it is involved in repair of exogenously induced DNA damage such as double-strand breaks (DSBs)<sup>1</sup>. Homologous recombination requires, among others, the *RAD52* group proteins, including Rad51, Rad52 and Rad54, and the breast cancer susceptibility proteins Brca1 and Brca2<sup>2</sup>. Immunofluorescence experiments with fixed mammalian cells have revealed that in response to DNA damage *RAD52* group proteins appear into sub-nuclear structures referred to as foci<sup>3-5</sup>. These foci form at the site of DNA damage<sup>6</sup> and contain, in addition to homologous recombination proteins, proteins involved in DNA metabolism in general, such as the single-stranded DNA binding protein RPA<sup>7</sup>. Mutant cell lines defective in the formation of Rad51-containing DNA damage-induced foci are sensitive to DNA damaging agents and display chromosomal instability<sup>8-12</sup>.

A critical intermediate in the repair of DSBs is a joint molecule between the broken DNA and a homologous double-stranded repair template. Biochemical analyses have revealed that joint molecule formation requires close co-operation between the *RAD52* group proteins<sup>13-15</sup>. Rad51 assembles into a nucleoprotein filament on the processed broken DNA, which subsequently pairs with homologous DNA aided by the Rad52 and Rad54 proteins. Physical interactions among the *RAD52* group proteins have been demonstrated biochemically and with the use of yeast two-hybrid and co-immunoprecipitation experiments<sup>13-19</sup>. These interactions have led to the suggestion that *RAD52* group proteins exist in a multi-protein complex, referred to as a 'recombinosome'<sup>17</sup>. Here we explore the spatio-temporal association between human Rad51, Rad52 and Rad54 in living cells where the proteins have to mediate homologous recombination in the context of chromatin and amid other nuclear structures and processes.

## Materials and methods

### DNA constructs and cell lines

Plasmids EGFP-Rad51, EGFP-Rad52, Rad54-EGFP were generated by inserting cDNAs encoding the respective human *RAD52* group proteins in pEGFP-C1, pEGFP-C3 and pEGFP-N1 (Clontech), respectively. The constructs were transfected into CHO9 and V79 Chinese hamster ovary cells and in mouse embryonic stem cells. Stable clones were selected using G418



or puromycin. Upon immunoblot analysis the nuclear expression levels of Rad51-GFP (Fig. 1E) and Rad54-GFP (data not shown) were found to be similar to level of the endogenous proteins. Quantitation of the nuclear fluorescence intensity of cells expression Rad52-GFP and Rad54-GFP showed that both proteins were expressed to similar levels. Taken together, these data indicate that none the nuclear GFP-tagged RAD52 group proteins are overexpressed.

### **Epifluorescence microscopy, cell survival assays and immunoblotting**

Cells were treated with ionizing radiation using a  $^{137}\text{Cs}$  source and fixed with 2 % paraformaldehyde. Endogenous Rad51 was detected using indirect immunofluorescence with a polyclonal antibody raised against human Rad51 in rabbits<sup>3</sup>. The signal from GFP-tagged proteins was observed directly by fluorescence microscopy. Quantitation of DNA damage-induced foci and cell survival assays were performed as described previously<sup>3,20</sup>. Control cell lines used in the survival assays were *irs1*<sup>21,22</sup> and *Rad54*<sup>-/-20</sup>. Cell lines stably expressing Rad51-GFP were analyzed for the presence of Rad51 using immunoblotting after cellular fractionation into nuclear and cytoplasmic fractions<sup>23,24</sup>. Five-fold more nuclear compared to cytoplasmic fraction was transferred to the blots. We believe that high local concentrations of Rad51 that could be observed in the cytoplasm (Fig. 1A) reflect the presence of Rad51 in a cytoplasmic organelle. The structures were present before irradiation and did not increase upon irradiation.

### **Confocal microscopy**

Cells were treated with ionizing radiation and subjected to photobleaching experiments 2 hrs after irradiation. Confocal images of living cells expressing GFP-tagged RAD52 group proteins were obtained using a Zeiss LSM 410 microscope equipped with a 200 mW Ar-laser at 488 nm and a 40x, 1.3 n.a. oil immersion lens. Images of single nuclei were taken at a lateral sample interval of 100 nm. GFP fluorescence was detected using a dichroic beamsplitter (488/543 nm) and an additional 515-540 nm bandpass emission filter placed in front of the photo multiplier tube.

### **Photobleaching experiments**

To determine the effective diffusion coefficient ( $D_{eff}$ ) of freely mobile GFP-labeled RAD52 group proteins, a small region with a width of 2  $\mu\text{m}$  and spanning the entire nucleus was bleached for 200 ms at high laser intensity (100% of the 488 nm line of a 200 mW Ar-laser)<sup>25-</sup>

<sup>27</sup>. Subsequently, the recovery of fluorescence in the region was monitored at intervals of 100 ms at 3% of the laser intensity applied for bleaching.  $D_{\text{eff}}$  was estimated by calculating relative fluorescence  $FR_{\text{diff}}$  at several time points, after small corrections for monitor bleaching:  $FR_{\text{diff}}(t) = (I_t - I_0) / (I_{\infty} - I_0)$ , where  $I_{\infty}$  is the fluorescence intensity measured after complete recovery,  $I_0$  is the fluorescence intensity immediately after bleaching and  $I_t$  is the measured fluorescence intensity at 100 ms intervals.  $D_{\text{eff}}$  was calculated as the value of  $D$  in the theoretical equation for one-dimensional diffusion  $FT(t) = 1 - (w^2 * [w^2 + 4\pi Dt]^{-1})^{1/2}$ <sup>27</sup> for which  $\sum (FR_{\text{diff}}(t) - FT(t))^2$  is minimal (least squares fitting). For visualization and estimation of a potentially present immobile fraction, relative fluorescence was calculated, after small corrections for monitor bleaching, as  $FR_{\text{imm}}(t) = (I_t - I_0) / (I_{t<0} - I_0)$ , where  $I_{t<0}$  is the intensity immediately before bleaching. The immobile fraction ( $N_{\text{immobile}} / N_{\text{tot}}$ ) was calculated from  $N_{\text{immobile}} / N_{\text{tot}} = 1 - FR_{\text{imm}}(\infty) * (1 - N_{\text{mobile,bleached}} / N_{\text{tot}})^{-1}$  where  $N_{\text{mobile,bleached}} / N_{\text{tot}}$  is the fraction of mobile molecules bleached by the pulse.

To determine the residence time of *RAD52* group proteins in foci formed upon  $\gamma$ -irradiation FRAP and FLIP experiments were applied. Foci, induced by treatment of cells with 12 Gy of ionizing radiation, were analyzed 2 h after irradiation. In FRAP experiments the fluorescence recovery of foci bleached for 1 s (at 100% intensity) was monitored (at 3% intensity) with time intervals as indicated. Relative fluorescence in each focus (spot) was calculated as  $FR_{\text{spot}}(t) = (I_{\text{spot},t} - I_{\text{spot},0}) / ([I_{\text{nuc1},t<0} / I_{\text{nuc1},\infty}] * [I_{\text{spot},t<0} - I_{\text{spot},0}])$ , where  $I_{\text{nuc1}}$  is the fluorescence intensity in the vicinity of the foci and  $I_{\text{spot}}$  is the intensity in the focus after subtraction of  $I_{\text{nuc1}}$  ( $I_{\text{spot}} = I_{\text{measured}} - I_{\text{nuc1}}$ ). The time required for recovery of half of the relative fluorescence intensity was used as a measure for the residence time of individual proteins. In FLIP measurements, the loss of fluorescence was monitored in foci (at 3% laser power) in between repetitive bleach pulses (1 s at 100% laser intensity with 5 s intervals) at a distant region in the same nucleus. Relative fluorescence was calculated, after small corrections for monitor bleaching, as  $FR_{\text{spot}}(t) = (I_{\text{spot},t} - I_{\text{nuc1},t}) / (I_{\text{spot},0} - I_{\text{nuc1},0})$  and the difference in relative fluorescence between the nucleoplasm and the foci was plotted against time. The longer apparent residence time for the proteins measured using the multi-bleach pulse FLIP protocol compared to FRAP is due the time required to diffuse from the bleached area to the DNA damage-induced structure.

In the simultaneous FRAP and FLIP assay one half of the nucleus is bleached for 2 s at 50% laser intensity (Fig. 5A). Subsequently, the redistribution of fluorescence in the nucleoplasm and the exchange of bleached and unbleached molecules between foci and nucleoplasm were monitored by taking confocal images at fixed time intervals (3 s for Rad54 and 12 s for Rad51 and Rad52). The relative intensity  $I_R$  of the foci in the bleached half and in the

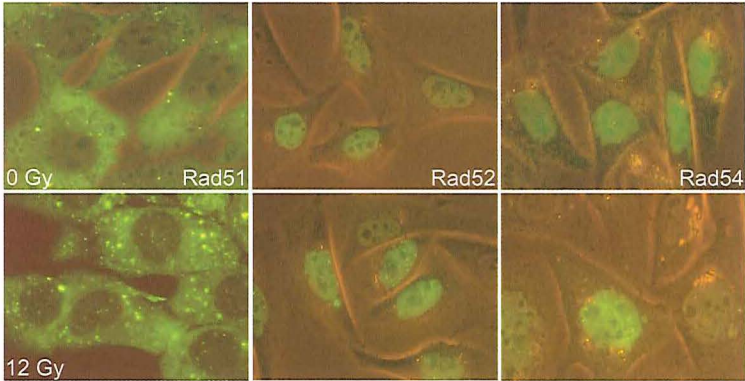
unbleached half of the cell were calculated separately as  $I_R = (I_t - I_0) / (I_{t<0} - I_0)$ , where  $I_t$  is the intensity of the foci measured at consecutive timepoints,  $I_0$  is the intensity of the bleached foci immediately after bleaching and  $I_{t<0}$  is the intensity of the foci before bleaching. If a fraction of the fluorescent molecules is stably associated with the foci, the size of this fraction is given by  $F_{\text{stably bound}} = |I_{R, \text{bleached}} - I_{R, \text{unbleached}}|$ . If the curves reach the same level ( $I_{R, \text{bleached}} = I_{R, \text{unbleached}}$ ) there is no stably bound fraction.

## Results

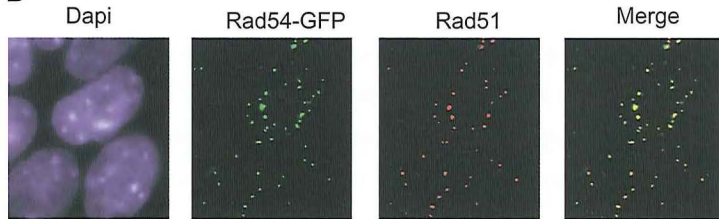
### DNA damage response of RAD52 group proteins in living cells

The characteristic DNA damage response of *RAD52* group proteins observed in fixed cells was reproduced in living cells using the human Rad51, Rad52, and Rad54 proteins tagged with the green fluorescent protein (GFP). After treatment of the cells with ionizing radiation, nuclear foci containing GFP-tagged Rad51, Rad52, and Rad54 were observed (Fig. 1A). We infer biologically relevant behavior of the GFP-tagged *RAD52* group proteins from the following experiments. By combining the detection of the GFP fluorescence with immunofluorescence we showed pair-wise colocalization of the three proteins in the DNA damage-induced foci (Fig. 1B and data not shown). The example shown in Figure 1B revealed quantitative colocalization of Rad54-GFP and endogenous Rad51 after irradiation. Furthermore, the kinetics and dose response of DNA damage-induced Rad51-GFP foci formation was similar to that of endogenous Rad51 as detected by immunofluorescence (Fig. 1C and 1D). Similar kinetics as those observed for Rad51 foci formation were observed for Rad52-GFP and Rad54-GFP foci upon irradiation (Fig. 1C). Recently, the presence of Rad51 in the nucleus, as well as in the cytoplasm has been demonstrated<sup>23,24</sup>. We observed a similar subcellular localisation for Rad51-GFP (Fig. 1A). Importantly, immunoblot analysis of nuclear and cytoplasmic fractions of the Rad51-GFP expressing cells showed that the expression levels of nuclear endogenous and GFP-tagged Rad51 were similar (Fig. 1E). Significantly, the presence of Rad51-GFP did not have a negative effect on the survival of cells with respect to irradiation (Fig. 1F). The biological activity of Rad52-GFP has recently been revealed by the demonstration that the fusion protein increases the resistance of cells towards DNA damaging agents<sup>4</sup>. Furthermore, the *Saccharomyces cerevisiae* Rad52 protein fused to GFP is fully functional in DNA repair and recombination<sup>28</sup>. Finally, Rad54-GFP corrected the ionizing radiation sensitivity of *Rad54* knockout mouse embryonic stem cells (Fig. 1G).

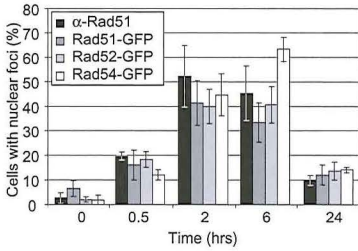
A



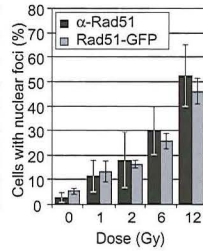
B



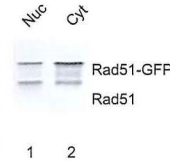
C



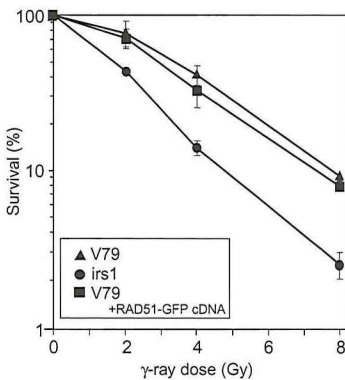
D



E



F



G

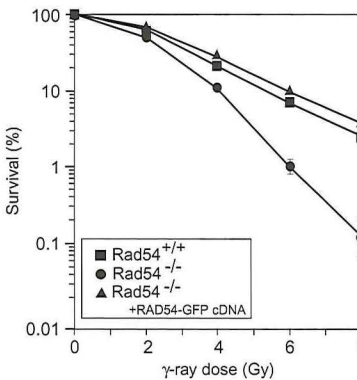


**Figure 1. DNA damage response of the human RAD52 group proteins in living cells.**

**1A.** Detection of Rad51-GFP, Rad52-GFP and Rad54-GFP in living Chinese hamster ovary (CHO) cells before treatment with ionizing radiation by a combination of fluorescence and phase contrast microscopy (0 Gy; upper panels). All three proteins formed nuclear foci upon treatment with ionizing radiation (12 Gy; lower panels). Images were taken 2 h after irradiation.

**1B.** DNA damage-induced colocalization of Rad51 and Rad54-GFP. Rad54-GFP expressing cells were fixed 2 h after treatment with ionizing radiation (12 Gy). Nuclei were visualized by Dapi staining. The signal from the Rad54-GFP protein, shown in green, was observed directly by fluorescence microscopy. Endogenous Rad51, shown in red, was detected by indirect immunofluorescence using antibodies against Rad51. Colocalization of Rad51 and Rad54-GFP, in yellow, is evident in the merged image.

**1C.** Kinetics of endogenous Rad51, Rad51-GFP, Rad52-GFP, and Rad54-GFP DNA damage-induced foci formation. CHO cells or their derivatives expressing the indicated GFP-tagged RAD52 group proteins were fixed at the indicated times after treatment with ionizing radiation (12 Gy). Detection of foci was done as described in panel B. The percentage of cells containing nuclear foci of endogenous Rad51, Rad51-GFP, Rad52-GFP, or Rad54-GFP was determined in three independent experiments.

**1D.** Dose response of endogenous and GFP-tagged Rad51 foci. CHO cells and their derivative expressing Rad51-GFP were fixed 2 h after treatment with the indicated doses of ionizing radiation. Detection of foci was done as described above.

**1E.** Immunoblot of endogenous and GFP-tagged Rad51. Cell-free extracts prepared from V79 cells stably expressing Rad51-GFP were fractionated into nuclear (nuc) and cytoplasmic (cyt) fractions that were analyzed for the presence of endogenous Rad51 and Rad51-GFP by immunoblotting using antibodies against Rad51.

**1F.** Clonogenic survival assays of V79 cells and its indicated derivatives. V79 cells and V79 cells expressing Rad51-GFP were equally sensitive to ionizing radiation as measured by colony forming ability after irradiation. A derivative of V79 (*irs1*), defective in the Rad51 paralogue *Xrcc2*, served as a control for irradiation.

**1G.** Clonogenic survival assays of the Rad54-proficient and -deficient cells after treatment ionizing radiation. The ionizing radiation sensitivity of Rad54<sup>-/-</sup> mouse embryonic stem cells was corrected to wild type levels by the expression of Rad54-GFP.

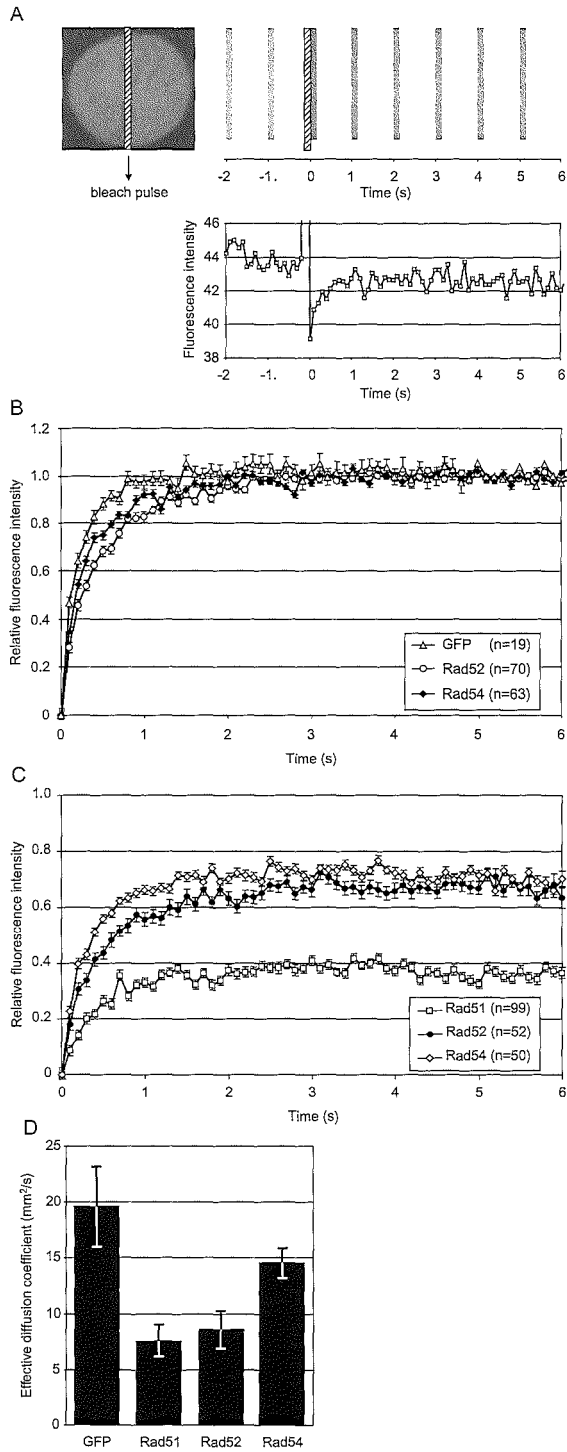


**Figure 2. Fluorescence redistribution after photobleaching analyses of RAD52 group proteins in CHO cells.**

Cells stably expressing Rad51, Rad52 and Rad54 fused to GFP were subjected to a local bleach pulse and the kinetics of fluorescence recovery in the bleached area was determined.

**2A.** An example of the primary data obtained using the photobleaching protocol on a cell nucleus, shown left, containing GFP-tagged Rad54. The fluorescence in a small strip, indicated by the hatched rectangle, spanning the entire nucleus was bleached with a 200 ms high intensity laser pulse. The recovery of fluorescence in the strip was monitored at intervals of 100 ms. For clarity, only strips obtained every second are shown above the time scale of the experiment. The measured fluorescence intensities over time are plotted below.

**2B.** The photobleaching protocol was applied to a number ( $n$ ) of cells containing GFP and GFP-tagged Rad52 and Rad54. The fluorescence intensity immediately after bleaching was set to zero and the final post-bleach pulse fluorescence intensity measured was set to one. The normalized data is plotted.

**2C.** The photobleaching protocol was applied to a number ( $n$ ) of cells containing GFP-tagged Rad51, Rad52 and Rad54. In this case the final measured fluorescence intensity was normalized to the pre-bleach pulse fluorescence intensity.

**2D.** The effective diffusion coefficients ( $D_{eff}$ ) of the RAD52 group proteins were determined by fitting the experimentally obtained curves, shown in B and C, to a mathematical model describing diffusion (see Materials and methods).

Measurements were performed in triplicate and consistent results were obtained among different sets of experiments.

Error bars indicate twice the standard error of the mean.

**Mobility of RAD52 group proteins in the nucleus**

To ascertain whether the RAD52 group proteins are constituents of the same pre-assembled DNA repair complex in living cells, we analyzed the dynamic behavior of the proteins using fluorescence redistribution after photobleaching (FRAP)<sup>26,29,30</sup>. The effective diffusion coefficient ( $D_{eff}$ ) of the proteins and the fraction of the proteins that was mobile were determined by measuring the kinetics of fluorescence recovery in a nuclear area that had been photobleached (Fig. 2). The fluorescence in a small strip spanning the width of the entire nucleus was bleached using a 200 ms high intensity laser pulse<sup>25-27</sup>. Subsequently, the recovery of fluorescence in the strip was monitored at intervals of 100 ms. Figure 2A shows the primary data for a single cell containing GFP-tagged Rad54. Measurements were performed on over 60 cells for Rad52 and Rad54. For estimation of the  $D_{eff}$ , the final post-bleach pulse fluorescence intensity measured was set to one and the fluorescence intensity immediately after the bleach pulse was set to zero (see Materials and methods) (Fig. 2D below). The normalized data are shown in Figure 2B.

The bleaching protocol employed above led to the irreversible bleaching of about 30% of all fluorescent proteins in the cell due to the ratio between the nuclear volume irra-

diated with the laser to the total nuclear volume and the diffusion of the proteins during the laser pulse. In the experiment shown in *Figure 2C* the final measured fluorescence intensity was normalized to the pre-bleach pulse fluorescence intensity. The fluorescence in the bleached area recovered to approximately 70% for both the Rad52 and Rad54 proteins. This behavior was similar to that of free GFP in our experimental set-up and indicates that all of the detected Rad52 and Rad54 molecules in the cell were mobile<sup>26,27,29-31</sup>. In contrast, Rad51 behaved differently, in that it was present in two distinct kinetic pools. Approximately half of the Rad51 proteins were immobile within the time-scale of the measurements.

The fluorescence recovery curves were used to calculate  $D_{eff}$  of the mobile fraction of the RAD52 group proteins (*Fig. 2D*). All three recombination proteins had a lower mobility than free GFP and in turn Rad51 and Rad52 has a lower mobility than Rad54. The observed differences in the dynamic behavior of the RAD52 group proteins in the absence of DNA damage indicate that even though they colocalize in DNA damage-induced foci, the majority of the proteins are not constituents of the same pre-assembled multi-protein complex in undamaged cells. These observations are consistent with the inability to co-immunoprecipitate RAD52 group proteins under physiological conditions in the absence of DNA damage<sup>3</sup> (*data not shown*). Interestingly, in irradiated cells the diffusion rates of the Rad52 and Rad54 proteins in the nucleoplasm did not differ from those in unirradiated cells (*data not shown*).

### **Turnover of RAD52 group proteins in DNA damage-induced foci**

Next we addressed the nature of the DNA damage-induced foci formed by the RAD52 group proteins. It is not known whether these subnuclear structures form due to long-lived protein-protein interactions between their constituents or whether they are dynamic structures in which the RAD52 group proteins turnover. Therefore, we photobleached a single Rad52-containing focus in cells treated with ionizing radiation (*Fig. 3A*). Interestingly, the fluorescence of the focus recovered over time, indicating that unbleached Rad52 molecules from the nucleoplasm were exchanging with bleached Rad52 molecules in the DNA damage-induced structure. We quantitated the fluorescence recovery of individual foci for the Rad51, Rad52 and Rad54 proteins. Intriguingly, the different RAD52 group proteins displayed a very different residence time in the DNA damage-induced structures (*Fig. 3B*). Half of the original fluorescence intensity recovered in 0.5 s for Rad54 and 26 s Rad52. In contrast to Rad52 and Rad54, Rad51 fluorescence hardly recovered over time, implying that it resides in the DNA damage-induced structures much longer.



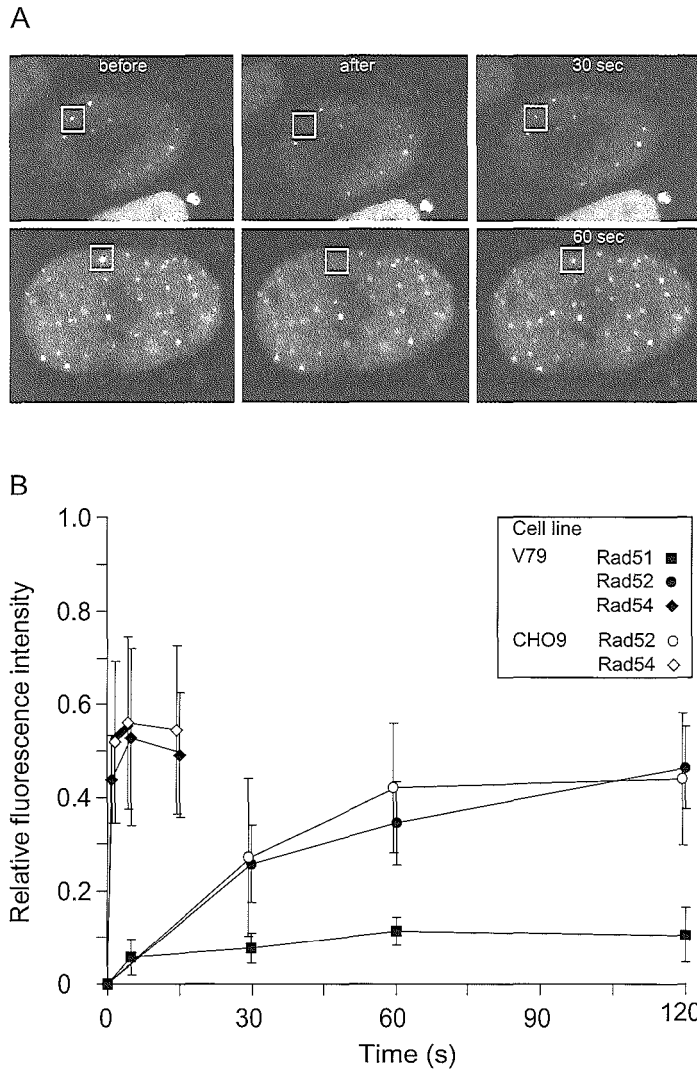


**Figure 3. Different residence times of RAD52 group proteins in DNA damage-induced foci.**

**3A.** Individual DNA damage-induced foci, marked by the square, in cells stably expressing Rad52-GFP were photobleached. Images were collected before, immediately after, and at the indicated times after the bleach pulse.

**3B.** Quantitative FRAP analysis of DNA damage-induced Rad51-GFP, Rad52-GFP and Rad54-GFP foci. Recovery of fluorescence was measured at the indicated time points after the bleach pulse. All data points represent the mean of at least 10 different measurements and the error bars indicate twice the standard error of the mean. The results were independent of the cell line used because similar results were obtained with V79 and CHO9 cells. The major cause of fluctuations in fluorescence intensity of the foci was due to cellular movement.

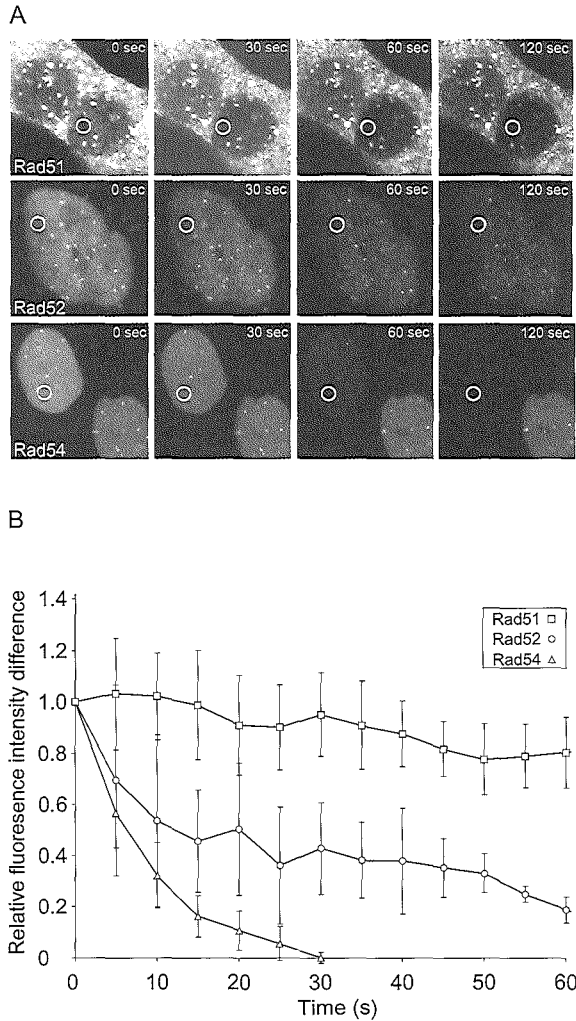


**Figure 4. Fluorescence loss in photobleaching in DNA damage-induced Rad51-GFP, Rad52-GFP and Rad54-GFP foci.**

**4A.** A region, indicated by the circle, in the nucleoplasm of ionizing radiation-treated (12 Gy) Rad51-GFP, Rad52-GFP or Rad54-GFP expressing cells was repeatedly bleached 2 h after the irradiation. Cells were imaged between bleach pulses at the indicated times after the initial bleach pulse.

**4B.** Quantitative FLIP analysis of DNA damage-induced Rad51-GFP, Rad52-GFP and Rad54-GFP containing foci. The difference between the loss in fluorescence of the DNA damage-induced foci and that of the nucleoplasm was determined at the indicated time points after the initial bleach pulse. The resulting curves were corrected for background bleaching due to monitoring of the cells. For each data point at least 5 different cells and 5 foci per cell were analyzed. Error bars indicate twice the standard error of the mean.

To obtain independent confirmation of the dynamic behavior of the *RAD52* group proteins in the DNA damage-induced structures, we examined them using fluorescence loss in photobleaching (FLIP)<sup>26,29-31</sup>. In these experiments the laser pulse used for bleaching fluorescence was not aimed at the structures. Instead, an area in the nucleoplasm, devoid of foci, was repeatedly bleached. The fluorescence intensity of the nucleoplasm, in a region away from the bleached area, and of the DNA damage-induced structures in the cells were measured after every bleach pulse (*Fig. 4*). The observed relative loss of fluorescence in the structures demonstrated their dynamic nature, because it is due to the equilibrium between dissociation of unbleached proteins (and later also of bleached proteins) and association of (un)bleached proteins. Bleaching was specific for the cells on which the laser was aimed, as can be seen from the fluorescence signal in the control cells shown for Rad51 and Rad54 which hardly changed over time except for a low amount of bleaching due to monitoring of the cells (*Fig. 4A*). Quantitation of these FLIP experiments revealed a qualitatively similar result as found in the FRAP experiment (*Fig. 4B*). The residence time of Rad54 in the DNA damage-induced structures was shorter than the residence time of Rad52, while Rad51 was a much more long-lived component of the structures with little turnover and therefore a long residence time.

### **Absence of immobile Rad52 and Rad54 in DNA damage-induced foci**

The FRAP and FLIP experiments clearly revealed that the majority of Rad51 molecules is stably associated with the DNA damage-induced structures. In contrast, Rad52 and Rad54 were not stably associated with the structures. However, we could not rule out, from the FRAP and FLIP experiments by themselves, that a minor fraction of these proteins was stably associated. To address this issue we performed a set of experiments in which FRAP and FLIP techniques were applied simultaneously in the same cell (*Fig. 5*). One half of a cell containing DNA damage-induced structures was bleached (*Fig. 5A*). Subsequently, the recovery of the fluorescence was monitored in a number of foci in the bleached half of the cell, while loss of fluorescence was monitored in a number of foci in the unbleached half of the same cell. The change in fluorescence intensity of Rad51, Rad52 and Rad54 containing foci was quantitated over time (*Fig. 5B*). If a stably associated fraction of the *RAD52* group proteins with the DNA damage-induced structures would be present, the FRAP and FLIP curve would not converge. This is because in the bleached DNA damage-induced structures a fraction of the bleached proteins would not be replaced, while in the unbleached structures a fraction of the fluorescent proteins would not be replaced. Consistent with a long residence time, the FRAP and

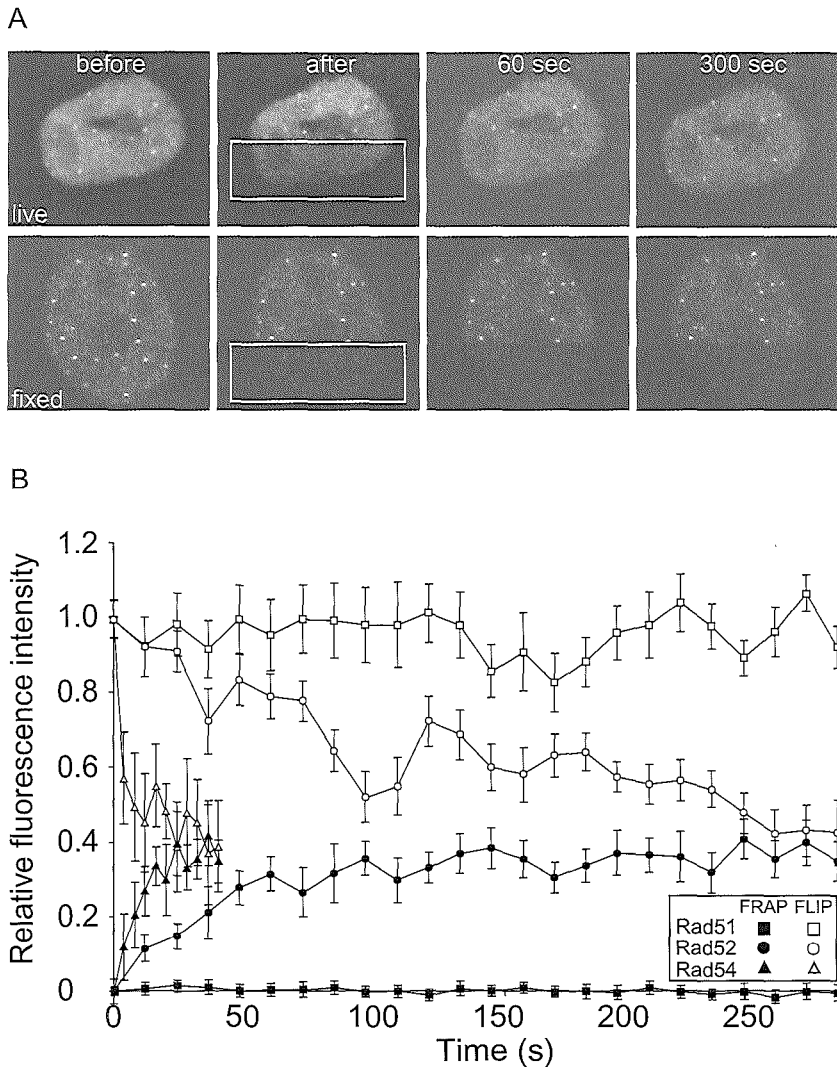


**Figure 5. Fluorescence loss in photobleaching and fluorescence redistribution after photobleaching in DNA damage-induced Rad51-GFP, Rad52-GFP and Rad54-GFP foci.**

**5A.** A region, indicated by the rectangle, of a cell containing Rad52-GFP foci was bleached by a single laser pulse (upper panels). The cell was imaged at the indicated times after bleaching. FLIP was measured in foci in the unbleached half of the cell, while FRAP was measured in foci in the bleached half of the same cell. The same experimental protocol applied to a fixed cell demonstrates the requirement for protein mobility to observe FRAP and FLIP (lower panels).

**5B.** Quantitation of the simultaneous FRAP and FLIP experiment on DNA damage-induced Rad51-GFP, Rad52-GFP and Rad54-GFP foci. Error bars indicate twice the standard error of the mean.

FLIP curves for Rad51 hardly changed over time. Significantly, for Rad52 and Rad54 the curves for the FRAP and FLIP experiments completely converged, showing the absence of a long-lived immobile fraction of either of the two proteins in the DNA damage-induced structures. Finally, the simultaneous FLIP/FRAP experiment demonstrated that the bleaching itself did not affect the dynamic behavior of the GFP-tagged *RAD52* group proteins since both the 'flipped' and the 'frapped' side of the cell returned to the same fluorescence intensity, as did the fluorescence intensity ratio between the nucleoplasm and the DNA damaged-induced structures.

## **Discussion**

### **Different mobilities of RAD52 group protein in the nucleus**

The results of our experiments suggest that the major fraction of the *RAD52* group proteins are not part of the same pre-assembled holo-complex in the absence of DNA damage. Instead, the majority of the proteins are diffusing through the nucleus independently. Once a DSB arises it might represent a site with a slightly increased affinity for one of the *RAD52* group proteins compared to intact DNA. In this regard, Rad52 itself is a good candidate protein because it preferentially binds to DNA ends<sup>32</sup>. The difference in affinity ensures that Rad52 will be immobilized for a longer time at the DSB site than at other sites in the genome. Therefore, on average, Rad52 will accumulate at the DSB site. From the observed fluorescence intensity of the Rad52 protein in the DNA damage-induced structures, we suspect that these structures do not represent a single Rad52 heptamer bound to a single DSB end<sup>33</sup>. Because fewer DNA damage-induced structures are observed compared to the number of DSBs generated by a given dose of ionizing radiation, it is possible that these structures represent sites where multiple DSBs are processed. Alternatively, or in addition, multiple Rad52 heptamers might be required to process a DNA lesion. Accumulation of Rad52 at the DSB sites might, in turn, generate sites of increased affinity for the other *RAD52* group proteins, such as Rad51. The reason why Rad51 is the most stable component of DNA damage-induced structures could be due to the fact that this protein is part of a higher order structure, the nucleoprotein filament, in which it could be kept through co-operative interactions<sup>34</sup>. Although we cannot rule out the possibility that the GFP tag influences the residence time of Rad51 in the DNA damage-induced structures, we believe this to be unlikely because the dose response and the kinetics of appearance and disappearance of DNA damage-induced structures containing endogenous Rad51 and Rad51-GFP are the same (*Fig. 1C and 1D*).

A scenario in which the DNA repair proteins diffuse through the nucleus in relatively small complexes, and assemble 'on-the-spot' in DNA repair complexes may be favorable to holo-complex formation prior to binding to damage, because small complexes have more efficient access than bulky holo-complexes to DNA damage located in condensed (hetero)chromatin regions<sup>26,35</sup>. Moreover, the observed homogeneous distribution of freely mobile DNA repair proteins, probably due to free diffusion<sup>36</sup>, ensures that all required factors are always present in the vicinity of DNA lesions wherever they occur, allowing rapid and efficient detection and subsequent repair. The observation that the induction of DNA damage does not influence the diffusion rates of the Rad52 and Rad54 proteins that are located in the nucleoplasm (as oppose to the proteins in the DNA damage-induced structures) argues that potential complexes between Rad52 and Rad54 do not pre-assemble away from the DNA damage-induced structures.

### **Cross-talk between DNA repair pathways**

Performing repair of DNA lesions by freely diffusing proteins that are temporarily immobilized due to the encounter of sites of increased affinity has an additional important advantage over a mechanism involving pre-assembled holo-complexes<sup>37</sup>. *In situ* assembly allows a greater flexibility in the composition of a DNA repair complex. Because different components can rapidly and reversibly interact with the DNA damage-induced structure, the specific components required for repair of a particular lesion can be selected. For example, while both the repair of a DSB and an interstrand DNA cross-link through homologous recombination require Rad51, repair of an interstrand DNA cross-link requires, in addition, structure-specific endonucleases, such as ERCC1/XPF<sup>38</sup>. ERCC1/XPF is also involved in nucleotide excision repair, but the other components of this DNA repair pathway do not play a major role in mammalian interstrand DNA cross-link repair. The rapid and reversible interaction of proteins with DNA damage-induced structures, alleviates the necessity of having to disassemble a DNA repair holo-complex that does not contain all of the specialized components required to repair the lesion it is associated with. Furthermore, *in situ* assembly allows exchange of components between different multi-step DNA repair pathways. This cross-talk is biologically significant because it will lead to an increase in the diversity of DNA lesions that can be repaired and provides a mechanism to link DNA repair with other DNA transactions, such as replication.

## **Acknowledgements**

We thank T. Cervelli, K. Mattern and C. Beerens for their contributions to this work. This work was supported by grants from the Dutch Organisation for Scientific Research (NWO), the Dutch Cancer Society (KWF) and the Association for International Cancer Research.

## References

1. Flores-Rozas, H. & Kolodner, R.D. Links between replication, recombination and genome instability in eukaryotes. *Trends Biochem Sci* **25**, 196-200 (2000).
2. Modesti, M. & Kanaar, R. Homologous recombination: from model organisms to human disease. *Genome Biol* **2**, (2001).
3. Tan, T.L. et al. Mouse Rad54 affects DNA conformation and DNA-damage-induced Rad51 foci formation. *Curr Biol* **9**, 325-8. (1999).
4. Liu, Y. & Maizels, N. Coordinated response of mammalian Rad51 and Rad52 to DNA damage. *EMBO Rep* **1**, 85-90. (2000).
5. Haaf, T., Golub, E.I., Reddy, G., Radding, C.M. & Ward, D.C. Nuclear foci of mammalian Rad51 recombination protein in somatic cells after DNA damage and its localization in synaptonemal complexes. *Proc Natl Acad Sci USA* **92**, 2298-302 (1995).
6. Tashiro, S., Walter, J., Shinohara, A., Kamada, N. & Cremer, T. Rad51 accumulation at sites of DNA damage and in postreplicative chromatin. *J Cell Biol* **150**, 283-91. (2000).
7. Raderschall, E., Golub, E.I. & Haaf, T. Nuclear foci of mammalian recombination proteins are located at single-stranded DNA regions formed after DNA damage. *Proc Natl Acad Sci USA* **96**, 1921-6. (1999).
8. Bishop, D.K. et al. Xrcc3 is required for assembly of Rad51 complexes in vivo. *J Biol Chem* **273**, 21482-8 (1998).
9. Takata, M. et al. The Rad51 paralog Rad51B promotes homologous recombinational repair. *Mol Cell Biol* **20**, 6476-82. (2000).
10. Takata, M. et al. Chromosome instability and defective recombinational repair in knockout mutants of the five Rad51 paralogs. *Mol Cell Biol* **21**, 2858-66. (2001).
11. Yu, V.P. et al. Gross chromosomal rearrangements and genetic exchange between nonhomologous chromosomes following BRCA2 inactivation. *Genes Dev* **14**, 1400-6 (2000).
12. O'Regan, P., Wilson, C., Townsend, S. & Thacker, J. XRCC2 is a nuclear RAD51-like protein required for damage-dependent RAD51 focus formation without the need for ATP binding. *J Biol Chem* **276**, 22148-53. (2001).
13. Baumann, P. & West, S.C. Role of the human RAD51 protein in homologous recombination and double-stranded-break repair. *Trends Biochem Sci* **23**, 247-51 (1998).
14. Paques, F. & Haber, J.E. Multiple pathways of recombination induced by double-strand breaks in *Saccharomyces cerevisiae*. *Microbiol Mol Biol Rev* **63**, 349-404 (1999).
15. Sung, P., Trujillo, K.M. & Van Komen, S. Recombination factors of *Saccharomyces cerevisiae*. *Mutat Res* **451**, 257-75. (2000).
16. Johnson, R.D. & Symington, L.S. Functional differences and interactions among the putative RecA homologs Rad51, Rad55, and Rad57. *Mol Cell Biol* **15**, 4843-50 (1995).
17. Hays, S.L., Firmenich, A.A. & Berg, P. Complex formation in yeast double-strand break repair: participation of Rad51, Rad52, Rad55, and Rad57 proteins. *Proc Natl Acad Sci USA* **92**, 6925-9 (1995).
18. Golub, E.I., Kovalenko, O.V., Gupta, R.C., Ward, D.C. & Radding, C.M. Interaction of human recombination proteins Rad51 and Rad54. *Nucleic Acids Res* **25**, 4106-10 (1997).
19. Chen, G. et al. Radiation-induced assembly of Rad51 and Rad52 recombination complex requires ATM and c-Abl. *J Biol Chem* **274**, 12748-52 (1999).
20. Essers, J. et al. Disruption of mouse RAD54 reduces ionizing radiation resistance and homologous recombination. *Cell* **89**, 195-204 (1997).



21. Cartwright, R., Tambini, C.E., Simpson, P.J. & Thacker, J. The XRCC2 DNA repair gene from human and mouse encodes a novel member of the recA/RAD51 family. *Nucleic Acids Res* **26**, 3084-9 (1998).
22. Liu, N. et al. XRCC2 and XRCC3, new human Rad51-family members, promote chromosome stability and protect against DNA cross-links and other damages. *Mol Cell* **1**, 783-93 (1998).
23. Davies, A.A. et al. Role of BRCA2 in control of the RAD51 recombination and DNA repair protein. *Mol Cell* **7**, 273-82. (2001).
24. Kraakman-van der Zwet, M. et al. Brca2 (XRCC11) deficiency results in radioresistant DNA synthesis and a higher frequency of spontaneous deletions. *Mol Cell Biol* **22**, 669-79. (2002).
25. Houtsmuller, A.B. et al. Action of DNA repair endonuclease ERCC1/XPF in living cells. *Science* **284**, 958-61 (1999).
26. Houtsmuller, A.B. & Vermeulen, W. Macromolecular dynamics in living cell nuclei revealed by fluorescence redistribution after photobleaching. *Histochem Cell Biol* **115**, 13-21. (2001).
27. Ellenberg, J. et al. Nuclear membrane dynamics and reassembly in living cells: targeting of an inner nuclear membrane protein in interphase and mitosis. *J Cell Biol* **138**, 1193-206 (1997).
28. Lisby, M., Rothstein, R. & Mortensen, U.H. Rad52 forms DNA repair and recombination centers during S phase. *Proc Natl Acad Sci USA* **98**, 8276-82. (2001).
29. Misteli, T. Protein dynamics: implications for nuclear architecture and gene expression. *Science* **291**, 843-7 (2001).
30. White, J. & Stelzer, E. Photobleaching GFP reveals protein dynamics inside live cells. *Trends Cell Biol* **9**, 61-5 (1999).
31. Pederson, T. Protein mobility within the nucleus-what are the right moves? *Cell* **104**, 635-8 (2001).
32. Van Dyck, E., Stasiak, A.Z., Stasiak, A. & West, S.C. Binding of double-strand breaks in DNA by human Rad52 protein. *Nature* **398**, 728-31. (1999).
33. Stasiak, A.Z. et al. The human Rad52 protein exists as a heptameric ring. *Curr Biol* **10**, 337-40. (2000).
34. De Zutter, J.K. & Knight, K.L. The hRad51 and RecA proteins show significant differences in cooperative binding to single-stranded DNA. *J Mol Biol* **293**, 769-80 (1999).
35. Cremer, T. & Cremer, C. Chromosome territories, nuclear architecture and gene regulation in mammalian cells. *Nat Rev Genet* **2**, 292-301. (2001).
36. Phair, R.D. & Misteli, T. High mobility of proteins in the mammalian cell nucleus. *Nature* **404**, 604-9 (2000).
37. Kowalczykowski, S.C. Some assembly required. *Nat Struct Biol* **7**, 1087-9 (2000).
38. Dronkert, M.L. & Kanaar, R. Repair of DNA interstrand cross-links. *Mutat Res* **486**, 217-47. (2001).



---

## Chapter 4

*Analysis of ionizing radiation-induced foci  
of DNA damage repair proteins*

---

## Chapter 4

### *Analysis of ionizing radiation-induced foci of DNA damage repair proteins*

Lieneke R. van Veelen<sup>1,2</sup>, Tiziana Cervelli<sup>3</sup>, Mandy W.M.M. van de Rakt<sup>1</sup>, Arjan F. Theil<sup>1</sup>,  
Jeroen Essers<sup>1</sup>, Roland Kanaar<sup>1,2</sup>

<sup>1</sup> Department of Cell Biology and Genetics, Erasmus MC,  
University Medical Center, P.O. Box 1738, 3000 DR Rotterdam, The Netherlands

<sup>2</sup> Department of Radiation Oncology, Erasmus MC-Daniel den Hoed Cancer Center,  
University Medical Center, P.O. Box 5201, 3008 AE Rotterdam, The Netherlands

<sup>3</sup> Laboratory of Gene and Molecular Therapy, Institute of Clinical Physiology,  
CNR, 56124 Pisa, Italy

*Mutation Research, In Press ( 2005)*

## **Abstract**

Repair of DNA double-strand breaks by homologous recombination requires an extensive set of proteins. Among these proteins are Rad51 and Mre11, which are known to re-localize to sites of DNA damage into nuclear foci. Ionizing radiation-induced foci can be visualized by immunostaining. Published data show a large variation in the number of foci-positive cells and amount of foci per nucleus for specific DNA repair proteins. The experiments described here demonstrate that the time after induction of DNA damage influenced not only the number of foci-positive cells, but also the size of the individual foci. The dose of ionizing radiation influenced both the number of foci-positive cells and the amount of foci per nucleus. However, based on the predicted number of induced double-strand breaks, the amount of foci per nucleus was always less than expected according to the dose administered. Furthermore, ionizing radiation-induced foci formation depended on the cell cycle stage of the cells and the protein of interest that was investigated. Rad51 and Mre11 foci seemed to be mutually exclusive, though a small subset of cells did show co-localization of these proteins, which suggests cooperation at a specific moment during DNA repair.

## Introduction

DNA damage can be induced by a variety of physiological and pathological events. A specific type of damage is the DNA double-strand break (DSB). DSBs may be caused by ionizing radiation but can also arise during replication, for example when a replication fork passes through a region containing a single-strand break<sup>1</sup>. DSBs are particularly dangerous when they arise in proliferating cells, since incorrect repair of DNA may give rise to genomic instability. Therefore, when a DSB occurs, replication of the cell is stopped by one of the checkpoints in the cell cycle<sup>2</sup>. During this cell cycle arrest the cell is allowed time to repair the damage. For this repair two major pathways are used<sup>3</sup>. One of these pathways is called homologous recombination, a mechanism which uses homologous DNA as a repair template. Because this repair mechanism demands the presence of a sister chromatid, homologous recombination is most efficient in the S- and G2 phases of the cell cycle. The other pathway for repair of DSBs is called non-homologous end-joining. In this pathway the DNA broken ends are simply joined without the use of a template. Non-homologous end-joining can operate efficiently during G1 phase because it does not require the presence of a sister chromatid. A large number of proteins are required for repair of a DSB, which are specific for each pathway, though some proteins may be involved in both homologous recombination and non-homologous end-joining.

The Rad51 protein plays a key role in the pathway of homologous recombination<sup>4</sup>. It promotes DNA strand exchange, through its assembly into a nucleoprotein filament on the processed single-stranded ends of the broken DNA. In this way a joint molecule is generated between the damaged DNA and the undamaged homologous position on the sister chromatid. The importance of *Rad51* is emphasized by the fact that inactivation of the gene results in chromosomal instability and embryonic lethality<sup>5-7</sup>.

Mre11 is a component of a protein complex containing Rad50 and Nbs1. This complex plays a role in many processes involved in maintaining genome stability<sup>8</sup>. Though its precise function is still unclear, the Mre11 complex is known to be involved in cell cycle checkpoint activation and repair of DSBs, possibly in both homologous recombination and non-homologous end-joining<sup>9</sup>. The Mre11 complex plays a pivotal role in preventing genomic instability during DNA replication and DNA repair. Inactivation of one of the genes of the Mre11 complex results in cellular or embryonic lethality<sup>10-13</sup>. However, hypomorphic mutations in Mre11 or Nbs1 are known to lead to the chromosomal instability- and radiosensitivity syndromes Ataxia-Telangiectasia-Like Disorder and Nijmegen Breakage Syndrome in humans<sup>14</sup>.

Both Rad51 and Mre11 re-localize into subnuclear structures upon the induction of DNA damage by ionizing radiation, the so-called ionizing radiation-induced foci (IRIF)<sup>15,16</sup>. These IRIF are known to form at the site of DNA damage<sup>17-19</sup>. Though their similar response to DNA damage may suggest a joint role for Rad51 and Mre11 in the repair of DSBs, no clear mechanistic connection between these two proteins has been established<sup>20</sup>.

IRIF can be visualized indirectly through immunostaining with antibodies against the protein of interest, or directly through expression of the protein tagged to a fluorescent protein. The results of experiments regarding IRIF for various proteins in the literature deviate to a large extent. The reported results differ in number of IRIF-positive cells, amount of foci per cell, size and staining pattern. This might be due to different techniques of visualizing DNA damage-induced foci, but other factors may play a role as well.

The experiments described here had a dual intent. First, a systematic analysis of a number of factors that could be responsible for the variable outcome of results with regard to IRIF formation is reported. In these experiments Rad51 and Mre11 were used as a tool to monitor this influence because of their widespread use in IRIF experiments. The influence of incubation time and radiation dose on number of IRIF-positive cells and amount of IRIF per cell was measured. Second, the relationship between Rad51 and Mre11 was studied, since Rad51 and Mre11 are both essential in DNA replication and repair. Using proliferating cell nuclear antigen (PCNA) as a cell cycle stage marker the correlation between DNA damage-induced Rad51 foci, Mre11 foci and PCNA staining pattern was investigated.

## **Materials and Methods**

### **Cell lines and tissue culture**

Chinese hamster derived cell lines CHO9 and V79 were cultured in Dulbecco's modified Eagle's medium (DMEM) (Bio Whittaker Europe), supplemented with 10% fetal calf serum (FCS), penicillin (100 U/ml) and streptomycin (100 µg/ml). HeLa cells were cultured in 45% Ham's F10 (Bio Whittaker Europe) and 45% DMEM, 10% FCS, penicillin and streptomycin. Primary human fibroblasts, C5RO (passage 20-30), from a skin biopsy of a healthy volunteer and the same human fibroblasts immortalized through infection with a hTert retroviral vector (passage 20-30), were cultured in Ham's F10 medium supplemented with 15% FCS, penicillin and streptomycin.

### **DNA constructs**

The plasmid eGFP-PCNA was generated by inserting a cDNA encoding the human PCNA into pEGFP-C1 (Clontech). Primary human fibroblasts were transiently transfected with PCNA-GFP cDNA and FACS-sorted 24 hours after transfection. After sorting, the cells were used for experiments within 48 hours.

Wild type primary human fibroblasts (C5RO) were infected with a retrovirus expressing hTert (using pBabe as a vector and Phoenix A cells as packaging cell line)<sup>21</sup>. Expression of hTert in the fibroblasts was demonstrated by RT-PCR (data not shown). The same method was used for the incorporation of GFP-PCNA in the hTert immortalized human fibroblasts. GFP-PCNA was expressed in a 1:3 ratio compared to the endogeneous protein in the human fibroblasts (data not shown).

The plasmid eGFP-Mre11 was generated by inserting the cDNA encoding human Mre11 into pEGFP-N2. The construct was transfected into Chinese hamster cells. Stable clones were selected using G418.

### **Immunostaining**

Cells were grown on glass coverslips and irradiated using a <sup>137</sup>Cs source. After various time points they were fixed with 2% para-formaldehyde. Cells were washed with BSA (0.5%) and glycine (0.15%) in PBS and permeabilized with 0.1% Triton X-100 in PBS. The following antibodies were used:  $\alpha$ -hRad51 (nr.2307, rabbit polyclonal antibody)<sup>22</sup>,  $\alpha$ -hMre11 (nr. 2244, rabbit polyclonal antibody)<sup>23</sup>,  $\alpha$ -hMre11 (12D7, Genetex, mouse monoclonal antibody) and  $\alpha$ -hRad50 (13B3, Genetex, mouse monoclonal antibody). The antibodies against the proteins of interest were applied separately or combined in case of double staining. The coverslips were incubated for 90 minutes. Again, the cells were washed with BSA and glycine in PBS and extracted with 0.1% Triton X-100 in PBS. The secondary antibodies tagged to a fluorescent group (Alexa Fluor 594 or 488, goat  $\alpha$ -rabbit IgG and/or goat  $\alpha$ -mouse IgG, Molecular Probes Inc.) were applied. Cells were incubated for 60 minutes and subsequently washed with 0.1% Triton X-100 in PBS and PBS. Coverslips were put on object glasses covered with DAPI/DAPCO/Vectashield and sealed.

### **Fluorescence microscopy analysis**

Analysis of foci formation was performed using a Leica DMRBE fluorescent microscope connected to a Hamamatsu dual mode cooled CCD camera C4480. To visualize the fluorescence pattern the following filtersets (Chroma Technology Corp.) were used: 31000, 31004, 41001



and 83000. The number of cells containing foci was determined by counting 150-500 cells per experiment. To determine co-localization of different proteins, pictures through various filters were taken. Using a photo-editing program these pictures were merged.

## **Results**

### **Rad51 IRIF formation depends on time and dose**

IRIF formation of Rad51 was investigated in wild type Chinese hamster cells (V79 or CHO9), HeLa cells and primary human fibroblasts. In all types of cell lines Rad51 foci could be detected, using the fixation and permeabilization technique described in the materials and methods section. To determine the kinetics of Rad51 IRIF formation and the duration of detectable foci after irradiation, foci formation was investigated at different time points after ionizing radiation (*Fig. 1A*). As soon as 30 minutes after irradiation with 12 Gy, Rad51 foci could be detected in all 3 cell lines. The number of primary fibroblasts positive for Rad51 foci increased in time with a maximum at 8 hours after irradiation. The Chinese hamster cells displayed a faster increase in IRIF with a maximum at 2 hours and a decline thereafter. For the HeLa cells the peak in foci positive cells appeared at 8 hours, after a slow rise in the first hours. After 24 hours all cell lines still showed an increased level of foci in the cells that were foci-positive (*Fig. 1B*). Although a clear rise in the number of foci per nucleus was observed after induction of DNA damage, the mean number of IRIF per nucleus in treated cells did not differ significantly among later time points (*Fig. 1B*). In *Figure 1C* the appearance of the IRIF is displayed. Though the amount of foci per nucleus was comparable for all time points after irradiation, the foci did show different characteristics. Foci appeared to increase in size; from small foci after 30 minutes, to large foci at 24 hours. For Chinese hamster cells the size of the foci reached a maximum at 8 hours, while after 24 hours most cells contained very small foci or both small and large foci.

To determine the influence of radiation dose on IRIF formation, cell lines were irradiated with various doses and fixed at time points at which a maximum amount of foci positive cells was detected (*Fig. 2A*), as determined from the time course experiment (*Fig. 1A*). For all cell lines the number of foci positive cells increased with higher dose. In primary fibroblasts and HeLa cells this number seemed to reach a plateau at 6 Gy, while the number of foci positive Chinese hamster cells reached its maximum at 12 Gy. The number of foci per nucleus was also influenced by the irradiation dose (*Fig. 2B*). This number increased with increasing dose for all cell lines, while the size of the foci did not depend on the dose administered (*Fig. 2C*).

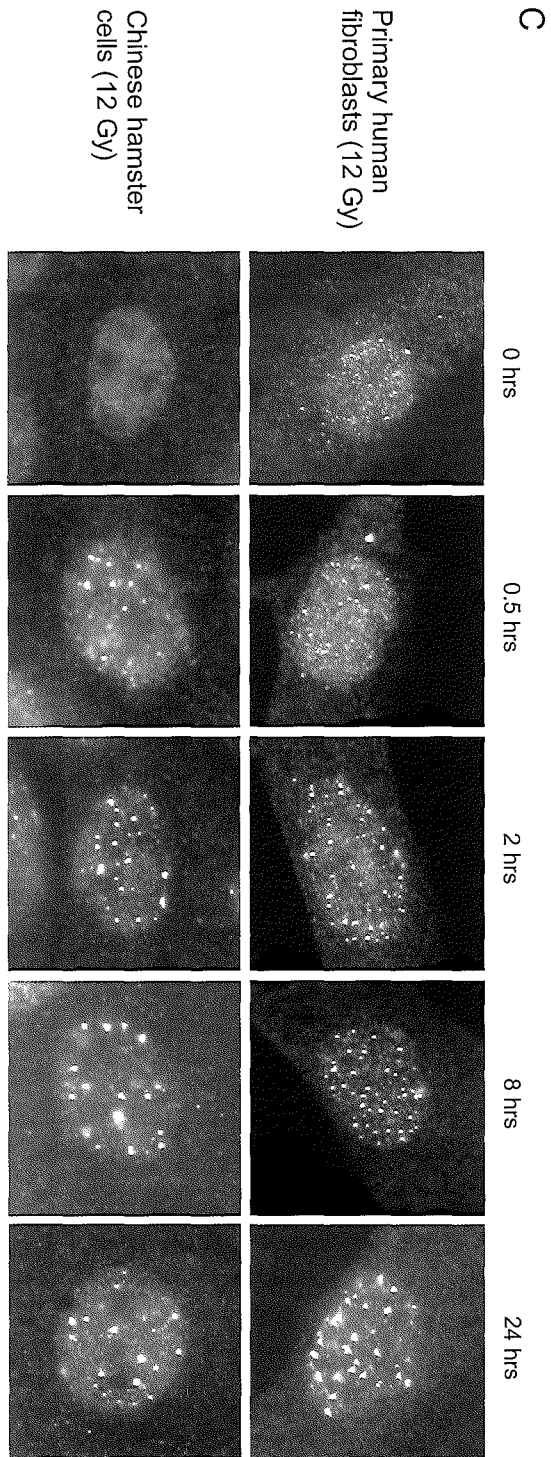
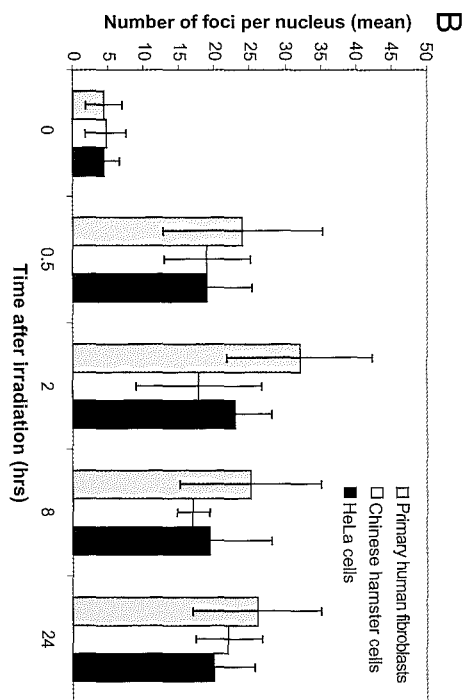
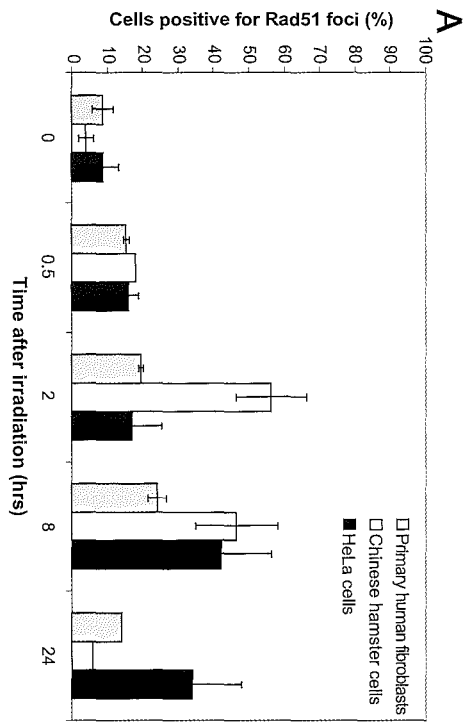


**Figure 1. Time dependency of Rad51 IRIF.**

Primary human fibroblasts, Chinese hamster and HeLa cells were irradiated with 12 Gy, fixed after 0, 0.5, 2, 8 and 24 hours, after which immunostaining using antibodies against Rad51 was performed. Cells with  $\geq 1$  focus per nucleus were considered positive for foci formation. The error bars represent the 95% confidence interval.

**1A.** The percentage of foci positive cells was determined by counting at least 200 cells per experiment. The experiment was performed 2-4 times for all cell lines.

**1B.** The number of foci per foci-positive cell was determined by counting at least 50 cells with  $\geq 1$  focus per nucleus per experiment.

**1C.** Representative pictures of primary human fibroblasts and Chinese hamster cells at indicated time points after irradiation with a dose of 12 Gy.

**Mre11 IRIF formation depends on time and dose**

The same time- and dose experiments were performed for Mre11 IRIF. Mre11 foci could be detected upon ionizing radiation treatment of primary human fibroblasts. In Chinese hamster cells and HeLa cells no Mre11 foci could be visualized by immunostaining with the protocol employed, regardless of the type of antibodies used. These antibodies however, did detect Mre11 on immunoblots of Chinese hamster and HeLa cell lines. Furthermore, Mre11 IRIF could be detected in Chinese hamster cells after stable introduction of a construct expressing Mre11-GFP. This means that Chinese hamster cells do form Mre11 foci upon irradiation, but they could not be visualized by immunostaining under the conditions used.

Time dependency of Mre11 foci formation was investigated by irradiation of primary human fibroblasts with 12 Gy and fixation of the cells after various time-points (*Fig. 3A, 3B*). Mre11 foci were detectable in 10% of the cells before irradiation. The amount of these foci per nucleus however, was always limited to one. Thirty minutes after irradiation, this single large focus had disappeared in nearly all cells. At 2 hours small foci appeared in 28% of the cells, after which the number of foci positive cells increased in time. Once foci were detectable, the amount of foci per nucleus seemed independent of the time after irradiation, though the size of the foci expanded with increasing incubation time (*Fig. 3E, top row*).

The dose-dependence of Mre11 foci formation was investigated after an incubation period of 8 hours with different doses of irradiation (*Fig. 3C*). The number of foci positive cells increased with increasing dose, with a maximum of 75% foci positive cells at 6 Gy. The number of foci per nucleus showed an increase up to 12 Gy (*Fig. 3D*). The size of the foci was independent of the dose administered (*Fig. 3E, bottom row*).

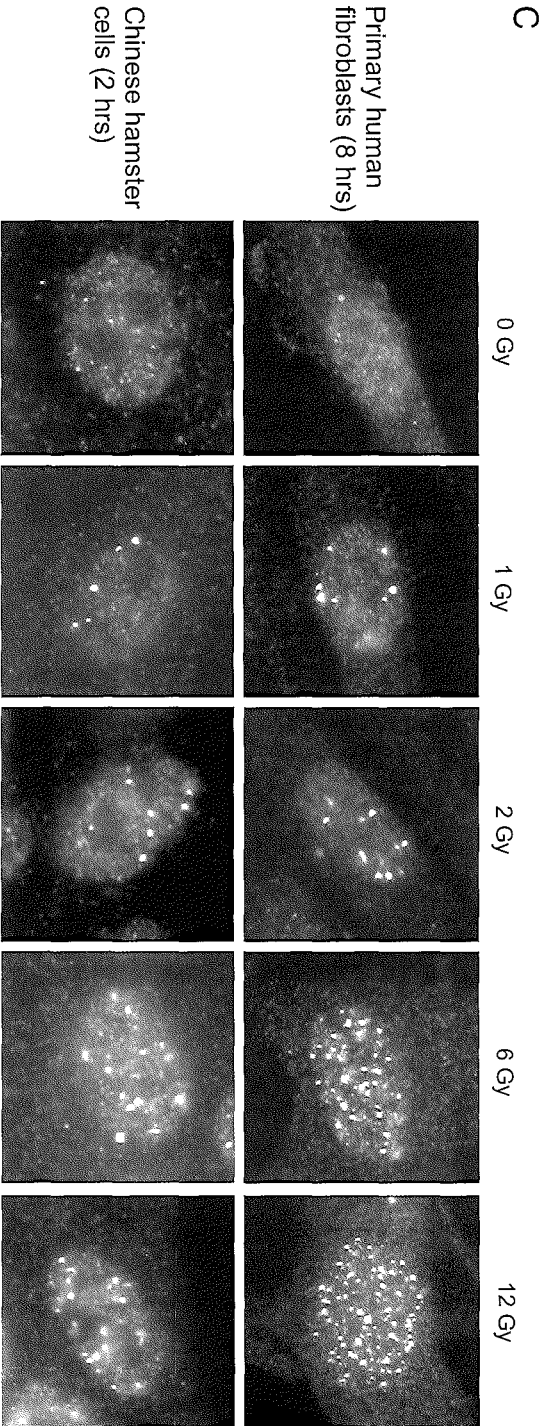
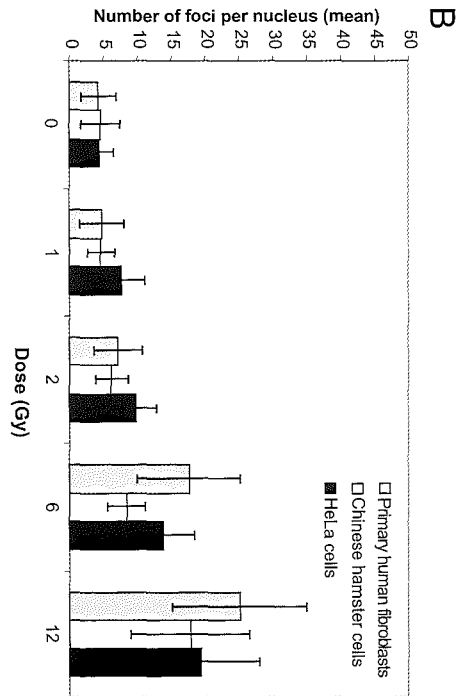
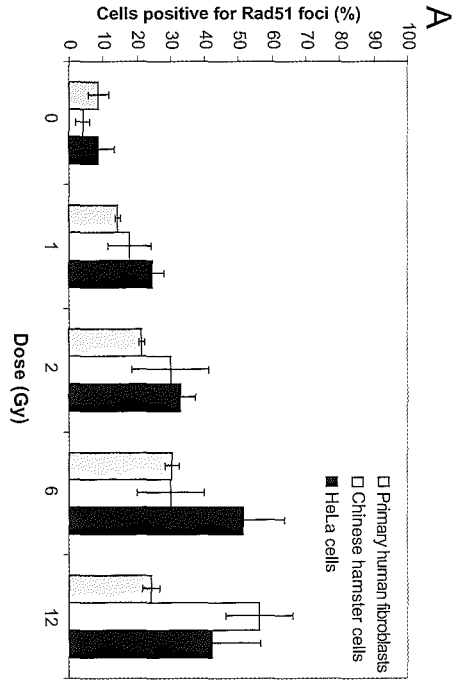


**Figure 2. Dose dependency of Rad51 IRIF.**

Primary human fibroblasts, Chinese hamster and HeLa cells were irradiated with 0, 1, 2, 6 and 12 Gy, fixed after 2 hours (Chinese hamster cells) or 8 hours (primary fibroblasts and HeLa cells) after which immunostaining with antibodies against Rad51 was performed. Cells with  $\geq 1$  focus per nucleus were considered positive for foci formation. The error bars represent the 95% confidence interval.

**2A.** The percentage of foci positive cells was determined by counting at least 200 cells per experiment. The experiment was performed 2-4 times for all cell lines.

**2B.** The number of foci per foci-positive cell was determined by counting at least 50 cells with  $\geq 1$  focus per nucleus per experiment.

**2C.** Representative pictures of primary fibroblasts and Chinese hamster cells at indicated dose points, 8 hours (primary fibroblasts) or 2 hours (Chinese hamster cells) after irradiation.

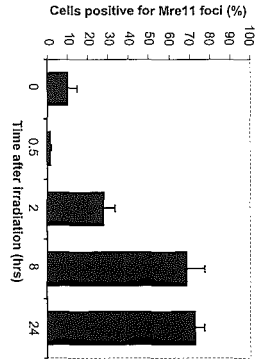
**Correlation between Rad51 and Mre11 IRIF formation in primary human fibroblasts**

Since the induction of Rad51 IRIF and Mre11 IRIF seemed to show distinct patterns, it was tested whether Rad51 and Mre11 foci formation are mutually exclusive. Therefore, Rad51 and Mre11 IRIF formation was analyzed simultaneously by double immunostaining in primary human fibroblasts. In general, cells that displayed Rad51 IRIF did not show Mre11 foci and vice versa (Fig. 4). Occasionally, both Rad51 and Mre11 foci could be distinguished in one cell. However, this occurred in less than 1% of the cells. Usually the Mre11 foci in these cells were smaller than in cells lacking Rad51 foci, while the Rad51 foci had a normal appearance. In case of simultaneous appearance of Rad51 and Mre11 IRIF, a partial co-localization of IRIF was observed (Fig. 5A), which could be reproduced for double immunostaining with Rad51 and Rad50 (Fig. 5B). Furthermore, similar results were seen in Chinese hamster cells stably transfected with Mre11-GFP cDNA and immunostained for Rad51 (Fig. 5C).

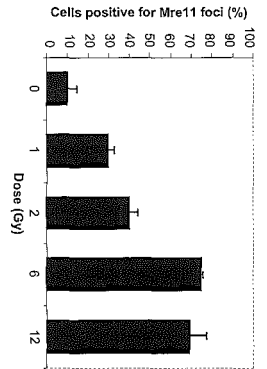
**Distinct PCNA staining patterns and Rad51 and Mre11 IRIF**

In an attempt to correlate the influence of cell cycle stage to Rad51 or Mre11 IRIF PCNA patterns were determined before irradiation in primary human fibroblasts expressing PCNA-GFP (Fig. 6, Table 1). After irradiation a significant change in a number of cells with PCNA foci was detected. Interestingly, the appearance of this pattern was somewhat different from the pattern seen in untreated fibroblasts, since size and number of the PCNA foci was smaller than in the regular early S phase cells. Either these cells were arrested in early S phase after treatment, or the PCNA foci were induced by irradiation in G1-phase. Given the percentages of

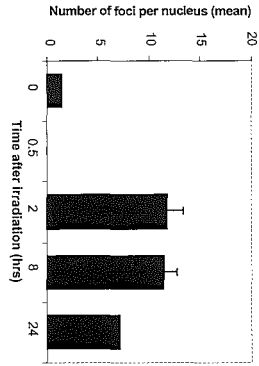
A



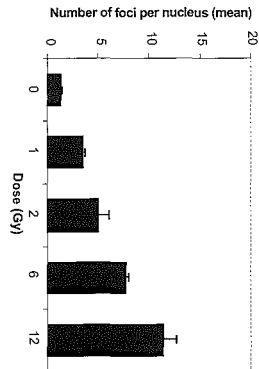
C



B



D



E

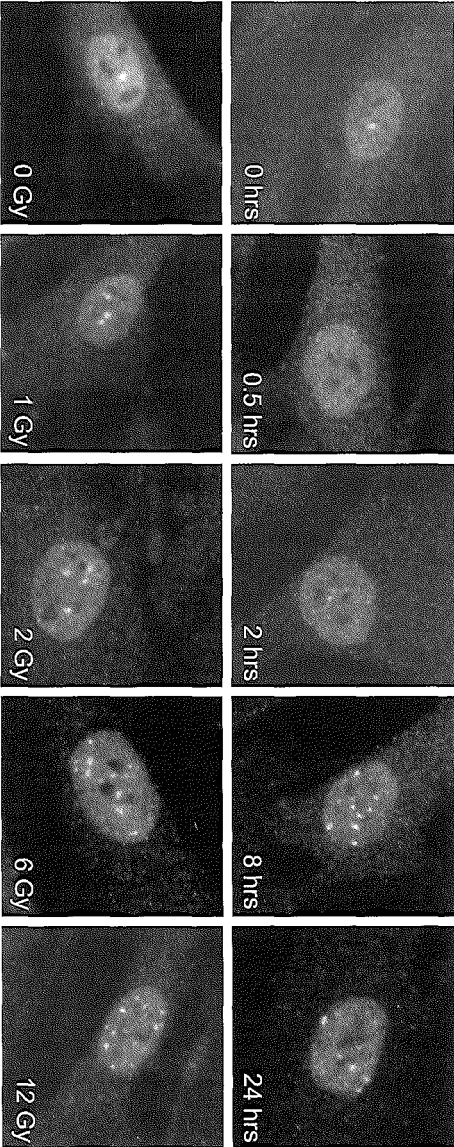


**Figure 3. Time- and dose dependency of Mre11 IRIF.**

**3A.** Primary human fibroblasts were irradiated with 12 Gy, fixed after 0, 0.5, 2, 8 and 24 hours and immunostaining using antibodies against Mre11 was performed. Cells with  $\geq 1$  focus per nucleus were considered positive for foci formation. The percentage foci positive cells was determined by counting at least 250 cells per experiment. The experiment was performed 3 times.

**3B.** Primary human fibroblasts were irradiated with 12 Gy and fixed after 0, 0.5, 2, 8 and 24 hours. The number of foci per foci-positive cell was determined by counting at least 100 cells with  $\geq 1$  focus per nucleus per experiment.

**3C.** Primary human fibroblasts were irradiated with 0, 1, 2, 6 and 12 Gy and fixed after 8 hours. Cells with  $\geq 1$  focus per nucleus were considered positive for foci formation. The percentage of foci positive cells was determined by counting at least 250 cells per experiment. The experiment was performed 3 times.

**3D.** Primary human fibroblasts were irradiated with 0, 1, 2, 6 and 12 Gy and fixed after 8 hours. The number of foci per foci-positive cell was determined by counting at least 100 cells with  $\geq 1$  focus per nucleus per experiment.

The error bars represent the 95% confidence interval.

**3E.** Representative pictures of primary human fibroblasts at indicated time points after irradiation with 12 Gy (upper panel) and at indicated dose points, 8 hours after irradiation (lower panel).

cells with the different PCNA patterns before and after irradiation, the latter possibility is more likely (Table 1). However, at present we can not discriminate between the two possibilities. Therefore the use of PCNA as a cell cycle marker after irradiation is not useful at this stage.

To determine a possible cooperation between Rad51 and PCNA or Mre11 and PCNA, co-localization experiments were performed using PCNA-GFP expressing primary fibroblasts and Chinese hamster cells. No co-localization was observed for Rad51 foci and Rad51 IRIF with PCNA foci in primary fibroblasts. The very few cells in S phase that showed Mre11 foci did not exhibit any co-localization with PCNA before irradiation. However, in fibroblasts with the specific PCNA foci pattern seen after irradiation (Fig. 6) co-localization with Mre11 IRIF was frequently observed (Fig. 7). This co-localization was complete for PCNA, though some Mre11 IRIF did not show an overlap with PCNA foci.

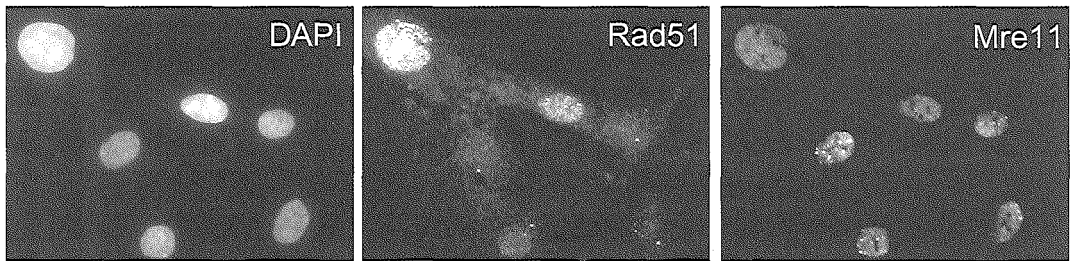


**Figure 4. Rad51 and Mre11 IRIF are frequently mutually exclusive.**

Primary human fibroblasts were irradiated with 12 Gy and incubated for 8 hours before fixation. Double immunostaining was performed using antibodies against Rad51 and Mre11. The nuclei were visualized by DAPI staining. A representative picture is shown of each staining pattern. Cells positive for Rad51 foci do usually lack Mre11 foci and vice versa. Note that cells which are positive for Rad51 IRIF display a brighter DAPI staining, indicating that these cells are undergoing replication.

## Discussion

### Time dependence of Rad51 and Mre11 IRIF

Results from this study establish the influence of time after induction of DNA damage on IRIF. Both Rad51 and Mre11 IRIF show a correlation between number of foci-positive cells and the time period after DNA damage (Fig. 1A, 3A). A time-dependent increase in foci formation is seen in all investigated cell lines; however, the percentages of foci-positive cells varies, depending on the cell line and the protein of interest. In general, Chinese hamster cell lines, from which most cells are in S phase, not only show a faster increase and decrease but also a higher percentage of Rad51 foci-positive cells than cell lines with a longer doubling time. Furthermore, a clear difference between the number of Rad51 and Mre11 foci-positive cells is observed: the percentage of cells with Mre11 IRIF is higher than cells with Rad51 IRIF. This could be explained by the cell cycle characteristic appearance of Rad51 and Mre11 IRIF. Since the function of Rad51 depends on the availability of a sister chromatid to repair the damage, it is likely that Rad51 IRIF will appear in S phase or G2 cells only<sup>24</sup>. In contrast to Rad51, Mre11



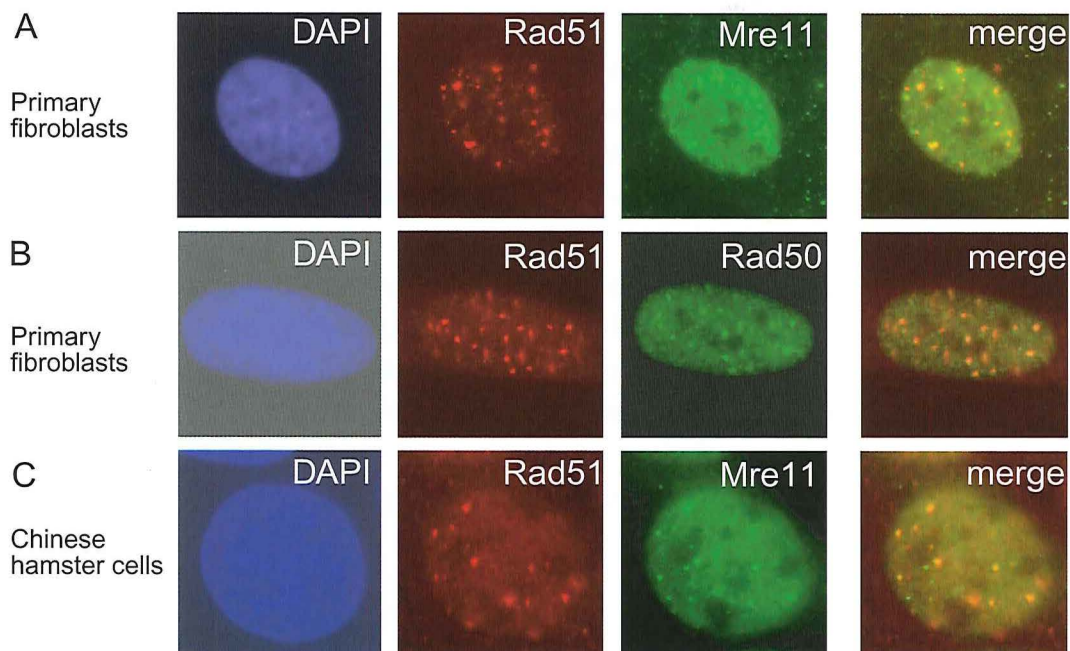


**Figure 5. Co-localization of Rad51 with Mre11 and Rad50 IRIF.**

**5A.** Primary human fibroblasts were irradiated with 12 Gy and fixed after 8 hours. Double immunostaining was performed using antibodies against Rad51 and Mre11. Some cells with Rad51 IRIF were observed which showed a partial co-localization with small Mre11 foci.

**5B.** Primary human fibroblasts were irradiated with 12 Gy and fixed after 8 hours. Double immunostaining was performed using antibodies against Rad51 and Rad50. Some cells with Rad51 IRIF showed a partial co-localization with Rad50 foci.

**5C.** Chinese hamster cells (CHO9) expressing Mre11-GFP were irradiated with 12 Gy and fixed after 2 hours. Immunostaining was performed using antibodies against Rad51. Cells with both Rad51 and Mre11 IRIF could be observed, in which the Rad51 foci partially co-localized with Mre11 foci.

likely functions in both homologous recombination and non-homologous end-joining and will therefore also operate in G1.

No influence of time after irradiation on number of foci per nucleus has been detected in all investigated cell lines for both Rad51 and Mre11 IRIF. An increase in amount of foci per nucleus is seen after treatment compared to non-irradiated cells, but this number does not differ significantly between the various time points (*Fig. 1B, 3B*). However, an interesting change in the appearance of foci is observed during the time-course because the size of the individual foci increases (*Fig. 1C, 3E*). Shortly after irradiation, Mre11 foci disappear completely while Rad51 foci are very small and can hardly be discriminated from the background staining. After a few hours, the size of the foci of both Rad51 and Mre11 gradually expands until they reach a large size after 24 hours, which can easily be distinguished. An explanation for this phenomenon could be that the DSBs which are still present at 24 hours after damage-induction are difficult to repair, which might result in an accumulation of more DNA repair proteins at the damaged site. Another explanation might be that the DNA damage has been repaired, but the signal for recruiting repair proteins is still present. Therefore, these proteins keep being attracted to the site of the original DNA damage.

PCNA pattern	foci	periferal	aggregated	homogeneous
Radiation dose				
0 Gy	6 % (early S)	1 % (mid S)	2 % (late S)	91 % (G1/G2)
12 Gy	41 % (?)	0 % (mid S)	2 % (late S)	57 % (G1/G2)

**Table 1. PCNA pattern in untreated and irradiated primary fibroblasts.**

Primary human fibroblasts, transiently transfected with PCNA-GFP and FACS sorted, were irradiated with 12 Gy and incubated for 8 hours after irradiation. The various PCNA patterns of the cells were determined<sup>29</sup>. For each experiment 200 cells per slide were counted. The results show the mean percentage of 2 experiments with comparable results.

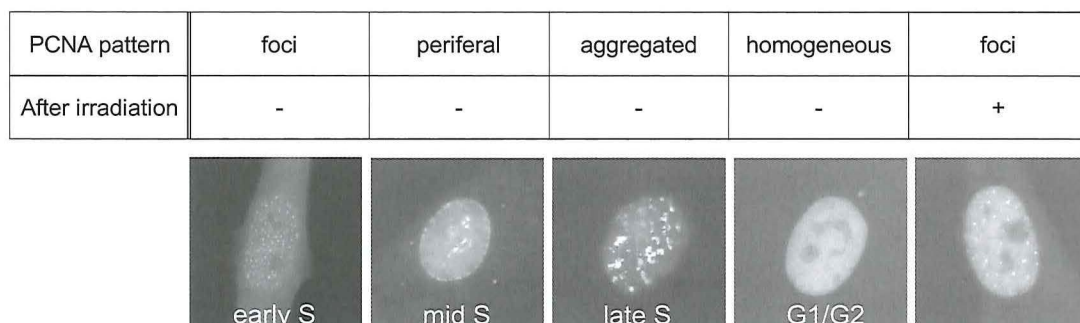


**Figure 6. PCNA patterns before and after irradiation in primary fibroblasts.**

The various cell cycle stages of hTert immortalized human fibroblasts infected with PCNA-GFP are shown. The first 3 pictures demonstrate cells in 3 different stages of S phase: early-, mid- and late S phase with 3 different patterns. The 4th picture shows a cell in either G1 or G2 phase which shows a homogeneous staining pattern. The last picture displays an example of a cell after irradiation with 12 Gy and an 8 hours incubation period before fixation, in which small nuclear foci on a bright nuclear background were observed. The cell cycle stage of cells showing this pattern is uncertain.

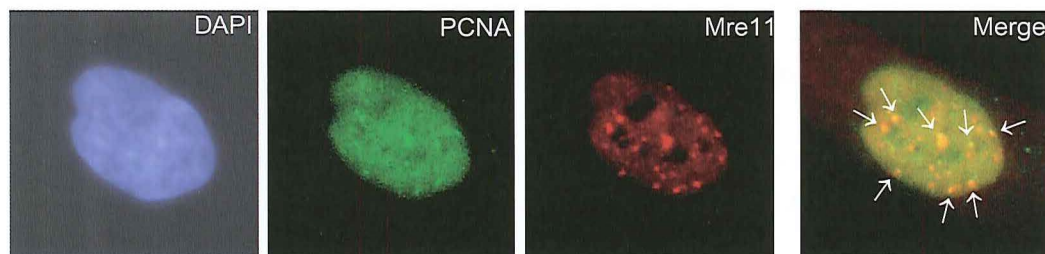


**Figure 7. Co-localization of Mre11 IRIF and PCNA foci.**

PCNA-GFP expressing human fibroblasts were irradiated with 12 Gy and fixed after 16 hours. Immunostaining was performed using antibodies against Mre11. A substantial number of Mre11 IRIF positive cells showed co-localization with the PCNA foci after irradiation. White arrows indicate the sites of co-localization.

### **Dose dependence of Rad51 and Mre11 IRIF**

The same influence for number of foci-positive cells that has been established for the time-course, is observed for the dose of ionizing radiation that is administered (*Fig. 2A, 3C*). For both Rad51 and Mre11 and in all investigated cell lines an increasing number of foci-positive cells is seen with increasing dose, though this number seems to reach a plateau at 6 Gy. Probably, at this dose most cells will have a certain damage-load and are arrested in their cell cycle, since nearly all cells are positive for either Rad51 or Mre11 IRIF. Doses over 6 Gy do therefore not increase the number of foci-positive cells any further.

The amount of foci per nucleus does also depend on the given dose (*Fig. 2B, 3D*). This dose-dependency does not reach a plateau phase. At the highest dose tested, the largest number of Rad51 and Mre11 foci per nucleus are detected. The amount of foci per nucleus though, is always less than the number of breaks expected according to the dose administered<sup>25</sup>. Furthermore, the amount of Mre11 foci per nucleus is always less than Rad51 foci for primary fibroblasts. Unlike the time course, the size of the foci does not depend on the dose of ionizing radiation. All foci observed have the same size, though Rad51 foci are always smaller than Mre11 foci (*Fig. 2C, 3E*).

The findings described here on the influence of time and dose on number of IRIF-positive cells confirm the results that have been established earlier for primary fibroblasts<sup>16</sup>. The increase of IRIF in a time- and dose dependent manner is also found in other cell lines than fibroblasts, but the percentage of cells that are positive at each time- or dose-point depends on the specific cell line and the protein of interest. The observation that the amount of foci per nucleus is only dose, but not time-dependent raises the question whether each focus represents one site of DNA damage or a repair site where multiple breaks can be repaired<sup>26</sup>. If one focus would be the site of one DSB, a larger number of foci would be expected than is observed. Moreover, the amount of foci would be expected to inversely correlate with time, since repair proteins would no longer be needed at the sites where DSBs have been repaired. Alternatively, there might be a fraction of DSBs that are rapidly repaired, for example by the non-homologous DNA end joining pathway<sup>27</sup> and these DSBs will therefore be missed by the analysis of IRIF.

### **Rad51 and Mre11 in relation to cell cycle stage**

PCNA is a processivity factor for the DNA polymerases  $\delta$  and  $\epsilon$ . It clamps onto DNA and slides along the DNA during replication<sup>28</sup>. Replicating DNA can therefore be detected through visualization of PCNA. PCNA is known to form specific patterns in early-, mid-, and

late S phase and no discernible pattern in G1/G2 phase<sup>29</sup>. PCNA may thus be used to determine the cell cycle stage of individual cells at a specific moment and correlate it to the activity of other proteins. The results of determination of the cell cycle stage based on the PCNA pattern of primary human fibroblasts expressing PCNA-GFP before irradiation reveal a low percentage of cells in S-phase and a high percentage of cells with homogeneous staining, which is likely to be mostly G1 in primary fibroblasts (*Fig. 6, Table 1*). Interestingly radiation causes a high percentage of cells to get PCNA foci. Since this is unlikely to represent an accumulation of cells in S phase, it is possible that these foci are induced in G1-phase, since even outside S phase polymerase action is needed for DNA repair. However, this uncertainty makes PCNA a less suitable marker for cell cycle stage after irradiation. The experiments on Rad51 and Mre11 foci formation with regard to PCNA staining pattern, reveal that Rad51 IRIF generally do not co-localize with PCNA. These observations are consistent with the findings in yeast, where DNA polymerase action could not advance before Rad51 was removed from the DNA<sup>30</sup>. For Mre11 IRIF on the contrary, co-localization with PCNA foci was frequently observed (*Fig. 7*).

Although Rad51 and Mre11 IRIF are in general mutually exclusive (*Fig. 4*), occasionally nuclei can be observed which contain co-localizing Rad51 and Mre11 IRIF (*Fig. 5*)<sup>16,20</sup>. These results show that there is a correlation between Mre11 and Rad51 foci in a small subset of cells, which can not be further defined or related to a cell cycle stage due to the difficulties of using PCNA as a marker after irradiation.

The results presented here demonstrate that the incubation period after ionizing radiation treatment, the dose administered and the specific cell cycle characteristics of the cell line of interest have a large influence on the number of IRIF positive cells, the amount of foci per nucleus and the features of the foci. It is therefore very important to be careful in the interpretation of data on IRIF. Results from experiments on IRIF formation of a certain protein in a specific cell line may not directly be extrapolated or compared to other cell lines. Furthermore, the results demonstrate that despite the fact that Rad51 and Mre11 IRIF are mostly mutually exclusive there might be a certain moment during replication or DSB repair at which these proteins do cooperate.

## **Acknowledgements**

This work was supported by grants from the Dutch Organization for Scientific Research (NWO), the Dutch Cancer Society, the European Union and an EMBO short-term fellowship to T. Cervelli.

## References

1. Kanaar, R. & Hoeijmakers, J.H. Recombination and joining: different means to the same ends. *Genes Funct* **1**, 165-74. (1997).
2. van Veelen, L.R., Wesoly, J. & Kanaar, R. Biochemical and Cellular aspects of homologous recombination. DNA damage recognition, Marcel Dekker, INC., New York, NY. In Press.
3. van Gent, D.C., Hoeijmakers, J.H. & Kanaar, R. Chromosomal stability and the DNA double-stranded break connection. *Nat Rev Genet* **2**, 196-206. (2001).
4. Symington, L.S. Role of RAD52 epistasis group genes in homologous recombination and double-strand break repair. *Microbiol Mol Biol Rev* **66**, 630-70 (2002).
5. Sonoda, E. et al. Rad51-deficient vertebrate cells accumulate chromosomal breaks prior to cell death. *EMBO J* **17**, 598-608. (1998).
6. Lim, D.S. & Hasty, P. A mutation in mouse rad51 results in an early embryonic lethal that is suppressed by a mutation in p53. *Mol Cell Biol* **16**, 7133-43. (1996).
7. Tsuzuki, T. et al. Targeted disruption of the Rad51 gene leads to lethality in embryonic mice. *Proc Natl Acad Sci USA* **93**, 6236-40. (1996).
8. de Jager, M. & Kanaar, R. Genome instability and Rad50(S): subtle yet severe. *Genes Dev* **16**, 2173-8. (2002).
9. D'Amours, D. & Jackson, S.P. The Mre11 complex: at the crossroads of dna repair and checkpoint signalling. *Nat Rev Mol Cell Biol* **3**, 317-27. (2002).
10. Yamaguchi-Iwai, Y. et al. Mre11 is essential for the maintenance of chromosomal DNA in vertebrate cells. *EMBO J* **18**, 6619-29. (1999).
11. Zhu, J., Petersen, S., Tessarollo, L. & Nussenzweig, A. Targeted disruption of the Nijmegen breakage syndrome gene NBS1 leads to early embryonic lethality in mice. *Curr Biol* **11**, 105-9. (2001).
12. Xiao, Y. & Weaver, D.T. Conditional gene targeted deletion by Cre recombinase demonstrates the requirement for the double-strand break repair Mre11 protein in murine embryonic stem cells. *Nucleic Acids Res* **25**, 2985-91. (1997).
13. Luo, G. et al. Disruption of mRad50 causes embryonic stem cell lethality, abnormal embryonic development, and sensitivity to ionizing radiation. *Proc Natl Acad Sci USA* **96**, 7376-81. (1999).
14. Shiloh, Y. ATM and related protein kinases: safeguarding genome integrity. *Nat Rev Cancer* **3**, 155-68. (2003).
15. Haaf, T., Golub, E.I., Reddy, G., Radding, C.M. & Ward, D.C. Nuclear foci of mammalian Rad51 recombination protein in somatic cells after DNA damage and its localization in synaptonemal complexes. *Proc Natl Acad Sci USA* **92**, 2298-302. (1995).
16. Maser, R.S., Monsen, K.J., Nelms, B.E. & Petrini, J.H. hMre11 and hRad50 nuclear foci are induced during the normal cellular response to DNA double-strand breaks. *Mol Cell Biol* **17**, 6087-96. (1997).
17. Nelms, B.E., Maser, R.S., MacKay, J.F., Lagally, M.G. & Petrini, J.H. In situ visualization of DNA double-strand break repair in human fibroblasts. *Science* **280**, 590-2. (1998).
18. Tashiro, S., Walter, J., Shinohara, A., Kamada, N. & Cremer, T. Rad51 accumulation at sites of DNA damage and in postreplicative chromatin. *J Cell Biol* **150**, 283-91. (2000).
19. Aten, J.A. et al. Dynamics of DNA double-strand breaks revealed by clustering of damaged chromosome domains. *Science* **303**, 92-5. (2004).
20. Mirzoeva, O.K. & Petrini, J.H. DNA damage-dependent nuclear dynamics of the Mre11 complex. *Mol Cell Biol* **21**, 281-8. (2001).

## Chapter 4

---

21. Ouellette, M.M., McDaniel, L.D., Wright, W.E., Shay, J.W. & Schultz, R.A. The establishment of telomerase-immortalized cell lines representing human chromosome instability syndromes. *Hum Mol Genet* **9**, 403-11. (2000).
22. Essers, J. et al. Analysis of mouse Rad54 expression and its implications for homologous recombination. *DNA Repair (Amst)* **1**, 779-93. (2002).
23. de Jager, M. et al. DNA-binding and strand-annealing activities of human Mre11: implications for its roles in DNA double-strand break repair pathways. *Nucleic Acids Res* **29**, 1317-25. (2001).
24. Tashiro, S. et al. S phase specific formation of the human Rad51 protein nuclear foci in lymphocytes. *Oncogene* **12**, 2165-70. (1996).
25. Prise, K.M. et al. A review of dsb induction data for varying quality radiations. *Int J Radiat Biol* **74**, 173-84. (1998).
26. Lisby, M., Mortensen, U.H. & Rothstein, R. Colocalization of multiple DNA double-strand breaks at a single Rad52 repair centre. *Nat Cell Biol* **5**, 572-7. (2003).
27. Essers, J. et al. Nuclear dynamics of RAD52 group homologous recombination proteins in response to DNA damage. *EMBO J* **21**, 2030-7. (2002).
28. Warbrick, E. The puzzle of PCNA's many partners. *Bioessays* **22**, 997-1006. (2000).
29. Leonhardt, H. et al. Dynamics of DNA replication factories in living cells. *J Cell Biol* **149**, 271-80. (2000).
30. Sugawara, N., Wang, X. & Haber, J.E. In vivo roles of Rad52, Rad54, and Rad55 proteins in Rad51-mediated recombination. *Mol Cell* **12**, 209-19 (2003).







---

## Chapter 5

*DNA damage response of homologous recombination proteins  
in recombination-impaired mammalian cell lines*

---

# Chapter 5

## *DNA damage response of homologous recombination proteins in recombination-impaired mammalian cell lines*

Lieneke R. van Veelen<sup>1,2</sup>, Jeroen Essers<sup>1</sup>, Mandy W.M.M. van de Rakt<sup>1</sup>, Hanny Odijk<sup>1</sup>,  
Coen C. Paulusma<sup>1</sup>, Roland Kanaar<sup>1,2</sup>

<sup>1</sup> Department of Cell Biology and Genetics, Erasmus MC,  
University Medical Center, P.O. Box 1738, 3000 DR Rotterdam, The Netherlands

<sup>2</sup> Department of Radiation Oncology, Erasmus MC-Daniel den Hoed Cancer Center,  
University Medical Center, P.O. Box 5201, 3008 AE Rotterdam, The Netherlands

*Based on: Mutation Research, In Press ( 2005)*

## **Abstract**

Homologous recombination is of major importance for the prevention of genomic instability during chromosome duplication and repair of DNA damage, especially double-strand breaks. Biochemical experiments have revealed that during the process of homologous recombination the *RAD52* group proteins, including Rad51, Rad52 and Rad54, are involved in an essential step: formation of a joint molecule between the broken DNA and the intact repair template. Accessory proteins for this reaction include the Rad51 paralogs and Brca2. The significance of homologous recombination for the cell is underscored by the evolutionary conservation of the Rad51, Rad52 and Rad54 proteins from yeast to humans. Upon treatment of cells with ionizing radiation, the *RAD52* group proteins accumulate at the sites of DNA damage into so-called foci. For the yeast *S. cerevisiae* foci formation of Rad51 and Rad54 is abrogated in the absence of Rad52, while Rad51 foci formation does occur in the absence of the Rad51 paralog Rad55. By contrast, we show here that in mammalian cells Rad52 is not required for foci formation of Rad51 and Rad54. Furthermore, radiation-induced foci formation of Rad51 and Rad54 is impaired in all Rad51 paralog- and Brca2 mutant cell lines tested, while Rad52 foci formation is not influenced by a mutation in any of these recombination proteins. Despite their evolutionary conservation and biochemical similarities, *S. cerevisiae* and mammalian Rad52 appear to differentially contribute to the DNA damage response. Additionally, the results bring forward that spontaneously arising DNA damage is not appropriately processed in the absence of Rad54 ATPase activity.

## Introduction

Homologous recombination plays a crucial role in proper maintenance of the genome. It is involved in the correction of errors that occur during chromosome duplication and in repair of DNA double-strand breaks (DSBs), thereby providing genomic stability. Homologous recombination is a precise mechanism of repairing DSBs. The intact DNA of the sister chromatid or, more rarely, the homologous chromosome, is used as a template to repair the broken DNA<sup>1</sup>. A critical step in homologous recombination is the formation of a nucleoprotein filament; a protein-DNA complex that recognizes a homologous piece of DNA. After the homologous DNA is detected, a joint molecule is generated between the damaged DNA and the undamaged sister chromatid. Many proteins are involved in homology recognition and joint molecule formation. The *RAD52* group proteins, including Rad51, Rad52 and Rad54 and the Rad51 paralogs all cooperate in this important process<sup>2</sup>. Furthermore, the breast cancer susceptibility proteins Brca1 and 2 are also involved in homologous recombination.

Rad51 plays a key role in homologous recombination since it promotes DNA strand exchange. Rad51 assembles into a nucleoprotein filament on the processed single-stranded ends of the broken DNA<sup>3</sup>. Rad52 stimulates this reaction by facilitating homologous pairing and increasing the efficiency of annealing between the single-stranded DNA and homologous template DNA<sup>4-8</sup>. Rad54, an ATP dependent DNA translocating motor protein<sup>9</sup>, has several activities important in homologous recombination<sup>10</sup>. It stabilizes the Rad51 filaments on single-stranded DNA, an action that does not require ATP hydrolysis<sup>11</sup>. Rad54 is also involved in chromatin remodeling by which the accessibility of template DNA is altered<sup>12-14</sup>. Furthermore, it promotes Rad51-mediated joint-molecule formation<sup>15-17</sup> and destabilizes the filaments on double-stranded DNA, which does require ATP hydrolysis<sup>18</sup>. Although the precise function of the *RAD52* group proteins is not completely understood, it is clear that a close cooperation between the three proteins is required for the formation of a joint molecule during homologous recombination.

The Rad51 paralogs, Xrcc2, Xrcc3, Rad51B, Rad51C and Rad51D are known to play an important role in recombination and in providing genome stability<sup>19-25</sup>. The Rad51 paralogs form two distinct complexes<sup>26,27</sup>. One complex includes Rad51B, Rad51C, Rad51D and Xrcc2. The other complex contains Rad51C and Xrcc3. The Rad51 paralogs are thought to facilitate the action of Rad51 in homologous recombination, but their exact biological function is still unknown<sup>25,28-30</sup>. Recent evidence suggests that Rad51C and Xrcc3 are also important in Holliday junction resolution, a late step in homologous recombination<sup>31</sup>.

The breast cancer susceptibility protein Brca2 binds single-stranded DNA and regulates

the activity of Rad51 *in vitro*<sup>32</sup>. The BRC repeats in Brca2 are involved in complex formation with the RecA-homology domain of Rad51. This domain in Rad51 serves as an interface for oligomerization between individual Rad51 monomers. Because the BRC repeats in Brca2 imitate this domain on Rad51 it might be able to control the assembly of the Rad51 nucleoprotein filament, since the Rad51 monomers bound to Brca2 will not be able to self associate<sup>33,34</sup>. Interaction between an isolated BRC repeat and Rad51 results in an inability of Rad51 to form a nucleoprotein filament<sup>35</sup>. Furthermore, some mutations in Brca2 affect the nuclear localization of Rad51, thus preventing Rad51 from functioning properly<sup>35</sup>. Little is known about the function of Brca1, though it is certain to play a role in genomic stability and recombinational repair. *Brca1*-deficient cells are impaired in the repair of DSBs by homologous recombination<sup>36,37</sup>. Additionally, Brca1 has the ability to bind to DNA in areas of the genome that are undergoing damage induced replication and recombinational repair, but the relevance of this activity needs to be determined<sup>38</sup>.

The *RAD52* group proteins and the Brca proteins are known to form subnuclear structures, called foci, upon the induction of DNA damage by ionizing radiation or specific genotoxic agents<sup>39-41</sup>. These foci form at the site of DNA damage<sup>42,43</sup>. Cell lines that are defective in homologous recombination, generally show an increased sensitivity to ionizing radiation. Moreover, some mutant cell lines lacking recombinational repair proteins are defective in DNA damage-induced Rad51 foci formation, indicating that these proteins are essential for the irradiation-induced increased local concentration of Rad51<sup>19,20,25,44-47</sup>. Here, the genetic requirements for ionizing radiation-induced foci formation by Rad51, Rad52 and Rad54 are determined in cell lines in which homologous recombination is impaired through mutations in *Xrcc2*, *Xrcc3*, *Rad51C*, *Brca2*, *Rad52* or *Rad54*.

## Materials and methods

### Cell lines and tissue culture

The radiation sensitive Chinese Hamster cell lines Irs1, an *Xrcc2* mutant cell line derived from V79 cells<sup>48-50</sup>; Irs1SF, an *Xrcc3* mutant cell line derived from AA8 cells<sup>49,51</sup>; V-C8, a Brca2 mutant cell line derived from V79 cells<sup>52,53</sup>; CL-V4B, a *Rad51C* mutant cell line derived from V79B cells<sup>20</sup> and the control cell line V79, were cultured in Dulbecco's modified Eagle's medium (DMEM) (Bio Whittaker Europe), supplemented with 10% fetal calf serum (FCS), penicillin (100 U/ml) and streptomycin (100 µg/ml). The embryonic stem (ES) cells E14<sup>54</sup>, a wild type

cell line derived from mouse strain 129; *Rad54*<sup>-/HA</sup>, a cell line carrying one disrupted *Rad54* allele and one *RAD54* allele expressing HA-tagged *Rad54* protein<sup>55,56</sup>; *Rad52*<sup>-/57</sup> and *Rad54*<sup>-/</sup> ES cells<sup>58</sup>, all derived from E14, were cultured in ES medium containing: 45 % DMEM, 45 % Buffalo rat liver cell conditioned DMEM, 10 % FCS, penicillin (100 U/ml) and streptomycin (100 µg/ml), 0.2 mM non-essential amino acids, 0.1 mM β-mercapto-ethanol and 1000 U/ml leukemia inhibitory factor.

### **DNA constructs**

The plasmids peGFP-, peYFP- and peCFP-*Rad51*, peGFP- and peYFP-*Rad52* and peGFP- and peYFP-*Rad54* were generated by inserting the cDNAs encoding the respective human *Rad51*, *Rad52* and *Rad54* proteins into peGFP-C1, peYFP-C1 and peCFP-C1, peGFP-C3 and peYFP-C3 and peGFP-N1 and peYFP-N1 (Clontech), respectively. The constructs were transfected into V79 cells and the Chinese hamster mutant cell lines. Stable clones were selected using G418 and FACS sorting (FACS Vantage, Becton, Dickinson and Company, USA).

For expression in ES cells, the human *Rad52*-eGFP cDNA was placed under control of the PGK promotor. The construct pPGK-*Rad52*-eGFP was stably transfected in the *Rad54*<sup>-/HA</sup> and *Rad54*<sup>-/</sup> mouse ES cell lines. The human *Rad54*-eGFP cDNA was also placed under control of the PGK promotor and the construct pPGK-*Rad54*-eGFP was stably transfected in the *Rad52*<sup>-/</sup> and *Rad54*<sup>-/</sup> mouse ES cell lines.

The constructs pPGK-h*Rad54*<sup>K189A</sup>-eGFP and pPGK-h*Rad54*<sup>K189R</sup>-eGFP were generated by site directed mutagenesis at position 189 using pPGK-*Rad54*-eGFP. This resulted in a single amino acid substitution in which the invariant lysine residue at position 189, which is in the Walker A box nucleotide binding motif, was changed in an alanine (K189A) or arginine (K189R) residue. The constructs pPGK-h*Rad54*<sup>K189A</sup>-eGFP and pPGK-h*Rad54*<sup>K189R</sup>-eGFP were stably transfected in the *Rad54*<sup>-/</sup> mouse ES cell line. For all transfections into mouse ES cell lines stable clones were selected using puromycin.

### **Immunoblotting**

Whole cell extracts of the abovementioned Chinese hamster and ES cell lines were prepared, ran on a SDS-PAGE gel and transferred to a nitrocellulose transfer membrane. The proteins of interest were visualized using the following antibodies: α-h*Rad51* (a rabbit polyclonal antibody)<sup>56</sup>; α-h*Rad52* (a rabbit polyclonal antibody, Santa Cruz biotechnology); α-h*Rad54* (a rabbit polyclonal antibody)<sup>58</sup>; α-green fluorescent protein (GFP) (a mouse monoclonal antibody, Roche) and goat α-rabbit/α-mouse IgG, alkaline phosphatase conjugate (Biosource Int.).



### **Immunostaining**

Cells were grown on (gelatinized) glass cover slips and irradiated using a  $^{137}\text{Cs}$  source. Two different fixation methods were employed. In all cases, with the exception of the experiments shown in the left-hand panels of *Figure 3*, cells were fixed with 2% para-formaldehyde. Cells were washed with BSA (0.5%) and glycine (0.15%) in PBS and permeabilized with 0.1% Triton X-100 in PBS. The antibody against the protein of interest (as described above) was applied and the cover slips were incubated for 90 minutes. Again, the cells were washed and permeabilized and the secondary antibody tagged to a fluorescent group (Alexa Fluor 594 or 488 goat a-rabbit IgG, Molecular Probes Inc.) was applied. Cells were incubated for 60 minutes and subsequently washed with 0.1% Triton X-100 in PBS and PBS. For the experiments shown in the left-hand panels of *Figure 3*, cells were fixed with methanol/acetone for 20 minutes at  $-20\text{ }^{\circ}\text{C}$  and permeabilized with cold acetone at various time points after irradiation. Cells were washed three times with PBS and incubated for 1 hour with PBS containing 10% FCS at room temperature. Cover slips were incubated for 1.5 hours at room temperature with the antibody against the protein of interest, followed by an 1.5 hours incubation period with the secondary antibody. The cover slips were put on object glasses covered with DAPI/DAPCO/Vectashield and sealed.

### **Fluorescence microscopy analysis**

Analysis of foci was performed using a Leica DMRBE fluorescent microscope connected to a Hamamatsu dual mode cooled CCD camera C4480. To visualize the fluorescence pattern the following filtersets were used (Chroma Technology Corp.): 31000, 31004, 41001, 31044 V2, 41028 and 83000. The number of cells containing foci was determined by counting 150-250 cells per slide. For some experiments a cut off level of number of foci per nucleus was used as described in the legends. To examine co-localization of different proteins, pictures through various filters were taken. Using a photo-editing program these pictures were merged.

## **Results**

### **Generation and characterization of Chinese hamster cell lines expressing GFP-tagged Rad52 group proteins**

The cDNAs encoding the human Rad51, Rad52 and Rad54 proteins tagged with GFP were stably transfected into wild type and mutant Chinese hamster cells. Furthermore, a wild type

Chinese hamster cell line was generated that expressed both Rad51-CFP and Rad52-YFP. The expression of all tagged proteins was analyzed by immunoblotting using antibodies against the proteins of interest and against GFP (Fig. 1A, 2A). The expression levels of the endogenous Rad51 and Rad54 proteins and their GFP-tagged derivatives were similar. This feature could not unambiguously be established for Rad52 due to the low reactivity of the Rad52 antibody. The immunoblotting analysis also revealed that the full-length protein fused to GFP was present in all cell lines used in this study. The Rad52 group GFP fusion proteins display biological relevant behavior as is evident from a number of previously published experiments. In the wild type control cell line the presence of Rad51-GFP has no effect on the survival of cells after ionizing radiation treatment, ruling out a dominant negative effect of the Rad51 fusion protein. Furthermore, the kinetics of foci formation after ionizing radiation is similar for Rad51-GFP and endogenous Rad51 detected through immunofluorescence staining<sup>39</sup>. The Rad52-GFP protein is fully functional in DSB repair in *S. cerevisiae*<sup>59,60</sup>. In addition, in mammalian cells the fusion protein is biologically active because it increases the resistance of cells to DNA damaging agents<sup>61</sup>. Rad54-GFP corrects the ionizing radiation sensitivity of *Rad54*<sup>-/-</sup> mouse ES cells<sup>39</sup>. Furthermore, upon exposure to ionizing radiation the kinetics of foci formation in wild type Chinese hamster cells are similar for both Rad54-GFP and endogenous Rad54 (data not shown).

### **Formation of Rad51, Rad52 and Rad54 foci in homologous recombination impaired Chinese hamster cell lines**

The *RAD52* group proteins form nuclear foci in response to DNA damage caused by ionizing radiation. Rad51 foci formation is regulated by several other proteins involved in homologous recombination such as the Rad51 paralogs and the Brca proteins. However, the role of these proteins in Rad52 and Rad54 irradiation induced foci formation is unknown. Therefore, irradiation induced foci formation of Rad52 group proteins was examined in Chinese hamster cells mutated in *Xrcc2*, *Xrcc3*, *Rad51C* or *Brca2*.

Rad51 foci formation was assessed in various recombination deficient Chinese hamster cell lines determined by both immunostaining of endogeneous Rad51 protein and by detection of the Rad51-GFP fusion protein. Both approaches showed comparable results for all cell lines examined (Table 1). Before irradiation all cell lines showed a low percentage of cells (1-6%) with Rad51 foci (data not shown). Two hours after irradiation 59% of the wild type (V79) cells formed Rad51 foci, as determined for both endogeneous and Rad51-GFP protein. The number of cells positive for Rad51 foci, as well as the amount of foci per cell increased nota-

bly after irradiation. However, in cell lines deficient in Xrcc2, Xrcc3, Rad51C and Brca2 no change in foci formation was seen before and after irradiation (Fig. 1B). To rule out the possibility that Rad51 foci formation does occur in these cell lines but with delayed kinetics, the same experiment was repeated 24 hours after irradiation. Whereas in the wild type cells a considerable number of cells were positive for Rad51 foci (45%), the mutant cell lines did not show any change in Rad51 foci formation after 24 hours as compared to the situation before treatment (data not shown). These results imply that the ability of Rad51 to form nuclear foci upon DNA damage depends on functional Xrcc2, Xrcc3, Rad51C and Brca2.

The involvement of Xrcc2, Xrcc3, Rad51C and Brca2 in Rad52 foci formation was studied by transfection of the Rad52-GFP cDNA in the aforementioned wild type and mutant Chinese hamster cell lines. In untreated cell lines 6-13% of the cells were positive for Rad52 foci. After irradiation the number of positive cells increased in all cell lines (30-63%) (Table 1).

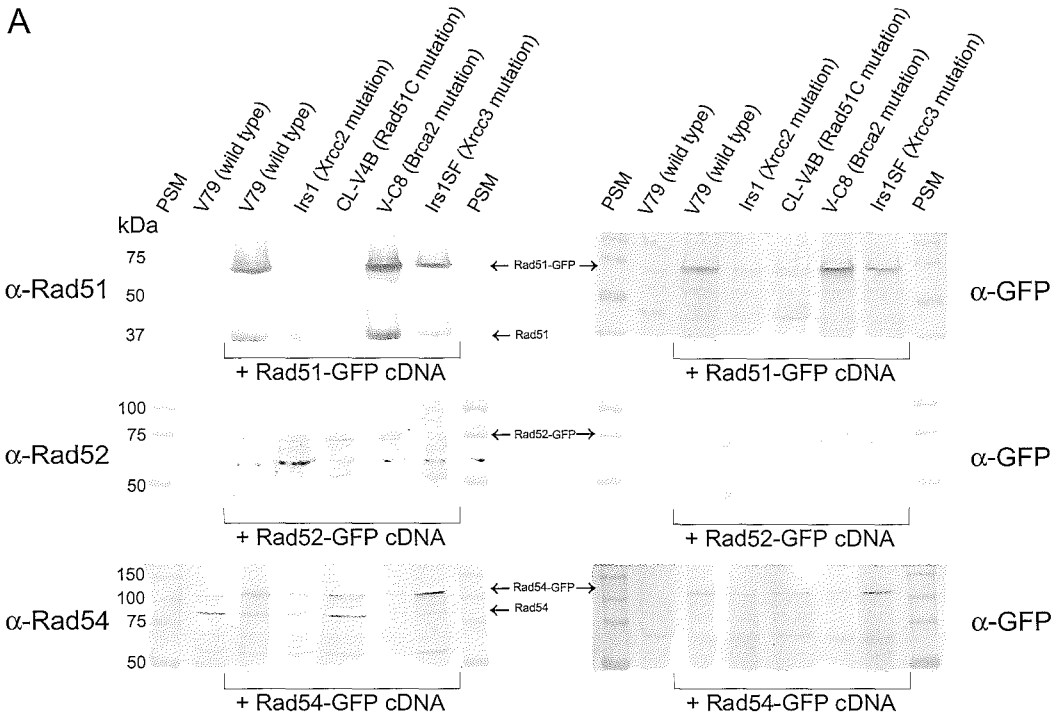
**Figure 1. Rad51, Rad52 and Rad54 ionizing radiation induced foci in recombination impaired Chinese hamster cell lines.**

**1A.** Immunoblots detecting endogeneous Rad51, Rad51-GFP, Rad52-GFP, endogeneous Rad54 and Rad54-GFP. Whole cell extracts of V79 cells (negative control) and V79, Irs1, CL-V4B, V-C8 and Irs1SF cells, stably expressing the above-mentioned proteins, were analyzed for presence of the endogeneous and GFP-tagged protein by immunoblotting, using antibodies against human Rad51, Rad52, Rad54 and GFP. The position of the endogeneous and Rad52 group GFP-fusion proteins is indicated. The molecular size of the pre-stained marker (PSM) proteins is indicated in kDa.

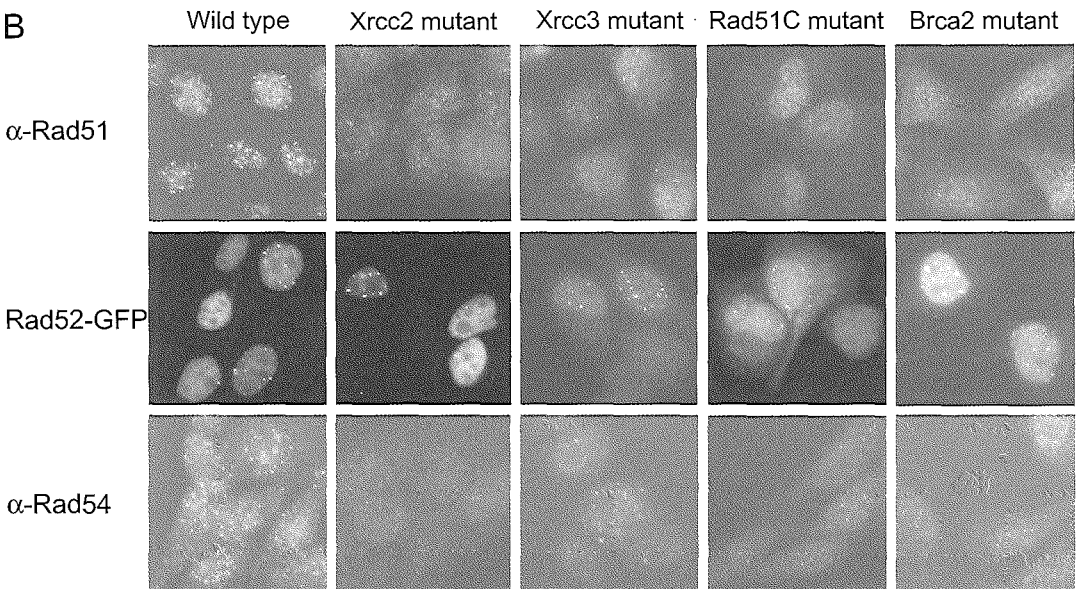
**1B.** Ionizing radiation induced foci of the Rad52 group proteins in a wild type and four recombination impaired Chinese hamster cell lines. Foci were detected using antibodies against the protein of interest (Rad51 and Rad54) or through expression of Rad52 fused to GFP. Cells were irradiated with 12 Gy and fixed after 2 hours. The first row shows the results for Rad51. No ionizing radiation induced foci were seen in the mutant cell lines. In the second row the results for Rad52 are displayed. The mutations had no influence on Rad52 foci formation because all studied cell lines showed Rad52 foci after ionizing radiation. In the last row the results for Rad54 are shown. As for Rad51, no Rad54 foci could be detected in the recombination impaired cell lines.

**1C.** Irradiation induced foci were examined for Rad51, Rad52 and Rad54 content by co-localization experiments. Wild type Chinese hamster cell lines expressing Rad52 or Rad54 fused to GFP were irradiated with 12 Gy and fixed 2 hours after irradiation. Cells were counterstained with a Rad51 or Rad54 antibody. The first column shows the nuclei of the cells, visualized through DAPI staining. The second and third column show the GFP and antibody signal, as indicated. The last column shows the merged image. Co-localization is indicated by a yellow color and white arrows. All three proteins demonstrated co-localization with the other proteins. For Rad52 co-localization with Rad51 and Rad54 was partial, while practically all foci of Rad51 and Rad54 co-localized.

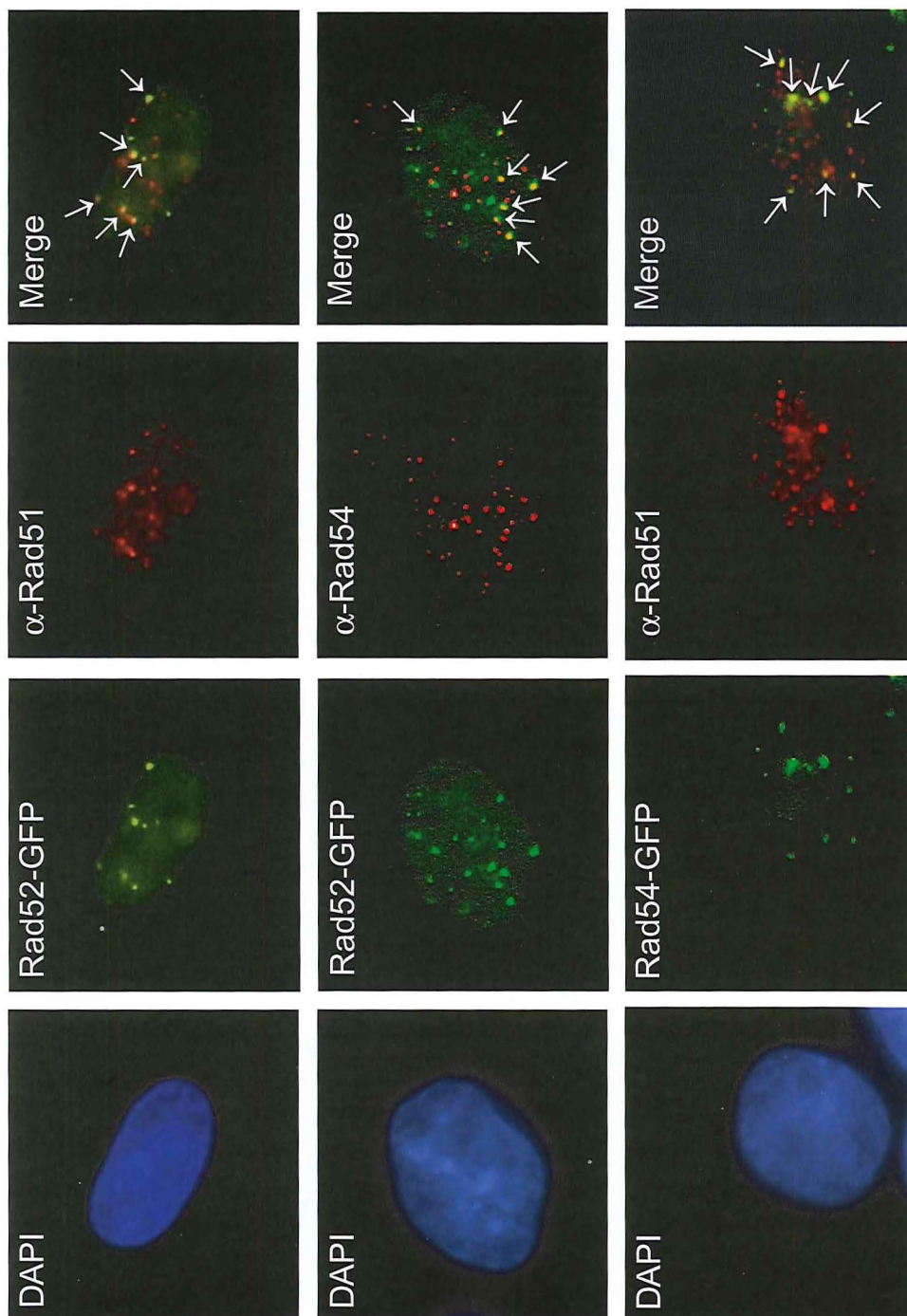
A



B



C



In addition, the amount of foci per cell increased (*Fig. 1B*). Even 24 hours after irradiation all cell lines displayed an increased number of cells positive for Rad52 foci (50% for V79) (data not shown). This result shows that Rad52 foci formation does not depend on the presence of Xrcc2, Xrcc3, Rad51C and Brca2.

Rad54 foci formation in wild type and mutant Chinese hamster cell lines was determined for both endogenous Rad54 and in cell lines expressing Rad54-GFP. Both approaches showed similar results (*Table 1*). Before irradiation all cell lines showed a low percentage of cells (1-15%) with Rad54 foci. After irradiation the number of foci-positive cells increased to 69% in the wild type cell line. Furthermore, the amount of foci per cell increased. The mutant cell lines did not show an increase in number of foci positive cells, nor in amount of foci per cell (*Fig. 1B*). Even 24 hours after ionizing radiation no increase in Rad54 foci was detected in the mutant cell lines, while in the wild type cell line a considerable number of cells (51%) were still positive for Rad54 foci (data not shown). These data imply that the ability of Rad54 to form radiation induced foci, like Rad51 but unlike Rad52, relies on functional Xrcc2, Xrcc3, Rad51C and Brca2.

### **Co-localization of Rad51, Rad52 and Rad54 in a wild type Chinese hamster cell line**

Next, the relation between the RAD52 group proteins in response to DNA damage was assessed by studying co-localization in wild type Chinese hamster cells, stably expressing either Rad51-GFP, Rad52-GFP or Rad54-GFP protein. Co-localization was determined by GFP detection and indirect immunostaining using Rad51 or Rad54 antibodies. The results are shown in *Table 2*. All three proteins co-localized with each other, albeit to a different extent (*Fig. 1C*). Most cells positive for Rad52 foci showed very little overlap with Rad51 or Rad54 foci, whereas essentially all Rad51 and Rad54 foci co-localized.

### **Kinetics of Rad51-CFP/Rad52-YFP irradiation induced foci formation in wild type Chinese hamster cells**

Since Rad51 and Rad52 foci only partially overlapped after irradiation, the kinetics of foci formation of the two proteins together in one cell line was investigated in a time and dose dependent manner. The results are graphed in *Figure 2B* for a dose of 12 Gy. After irradiation Rad51 showed a very fast response in foci formation. As early as 5 minutes after irradiation an increase in Rad51 foci positive cells was detected. The response of Rad52 foci formation to ionizing radiation was slower than for Rad51 and the peak in number of foci

Chinese hamster cell line	Rad51	Rad51-GFP	Rad52-GFP	Rad54	Rad54-GFP
V79 Wild type	+	+	+	+	+
Irs1 <i>Xrcc2</i> mutation	-	-	+	-	-
Irs1SF <i>Xrcc3</i> mutation	-	-	+	-	-
CL-V4B <i>Rad51C</i> mutation	-	-	+	-	-
V-C8 <i>Brca2</i> mutation	-	-	+	-	-

**Table 1. Ionizing radiation induced foci formation of homologous recombination proteins in Chinese hamster cell lines.**

The indicated Chinese hamster cell lines were irradiated with 12 Gy and fixed after 2 or 24 hours. Foci formation was determined using either antibodies to detect the endogenous protein or by using cell lines that express the protein of interest fused to GFP. For each experiment the number of foci-positive cells was determined by counting at least 150 cells. A cell was considered positive for Rad51 foci in case of  $\geq 5$  foci/nucleus, positive for Rad52 foci if  $\geq 1$  foci/nucleus and positive for Rad54 foci in case of  $> 1$  foci/nucleus. Cell lines that showed 1-15 % foci positive cells were considered negative (-) for irradiation induced foci formation, since this percentage corresponds to the percentage of foci positive cells before irradiation. Cell lines that were considered positive for irradiation induced foci formation (+) showed 30-80% foci containing cells. Each experiment was performed three times with similar results.

positive cells appeared 2 hours later. Foci could be detected up to at least 36 hours after irradiation.

In *Figure 2C* the number of foci positive cells is subdivided into cells containing either no foci, only Rad51 or Rad52 foci, or both Rad51 and Rad52 foci. During the first hours after irradiation most cells showed only Rad51 foci. After 2 hours an increase in cells positive for both Rad51 and Rad52 was detected, which peaked at 10 hours after irradiation and gradually declined up till 36 hours after irradiation. Apart from the cells with both Rad51 and Rad52 foci, a substantial number of cells still showed Rad51 foci only during the first 10 hours, while the number of cells positive for Rad52 foci only stayed at a very low level during

the whole time period (0-14%).

This experiment was repeated with a dose of 2 Gy and time-points to 10 hours (data not shown). The same trend for Rad51 foci was observed as in the 12 Gy experiment, though the amount of foci per cell was less. Rad52 on the other hand, showed a reduced response to the low dose of 2 Gy: only a few cells displayed both Rad52 and Rad51 foci (max. 11%) or Rad52 foci only (max. 6%).

### Formation of Rad51, Rad52 and Rad54 foci in Rad52<sup>-/-</sup> and Rad54<sup>-/-</sup> mouse ES cell lines

The results on Rad51, Rad52 and Rad54 foci formation demonstrate that a mutation in one of the Rad51 paralogs or in Brca2 leads to impaired foci formation for Rad51 and Rad54,

	Rad51	Rad51-G(C)FP	Rad52-YFP	Rad54	Rad54-YFP
Rad51	NA	ND	±	+	+
Rad51-G(C)FP	ND	NA	±	+	+
Rad52-YFP	±	±	NA	±	ND
Rad54	+	+	±	NA	+
Rad54-YFP	+	+	ND	+	NA

**Table 2. Co-localization of Rad51, Rad52 and Rad54 ionizing radiation induced foci in a wild type Chinese hamster cell line.**

V79 cells were irradiated with 12 Gy and fixed after 2 hours. Foci formation for the different proteins of interest was detected by performing immunostaining with the antibodies indicated on cell lines that expressed the specified proteins. Using different fluorescent microscope filter sets for the various proteins, co-localization could be determined. Pictures were taken from cells that contained foci of both proteins of interest (at least 20 cells per slide). Using a photo-editing computer program co-localization was assessed. Cells were considered positive when at least 3 individual foci showed co-localization. For Rad52, mostly partial co-localization (±) was observed (i.e. not all foci for both proteins of interest co-localized). For Rad51 and Rad54, however, co-localization was essentially complete (+). ND, not determined; NA, not applicable.



but does not influence irradiation induced Rad52 foci formation. To investigate the reciprocal influence of Rad52 or Rad54 on the Rad52 group proteins, ionizing radiation induced Rad51, Rad52 and Rad54 foci formation was studied in *Rad52*<sup>-/-</sup> and *Rad54*<sup>-/-</sup> mouse ES cells (Table 3).

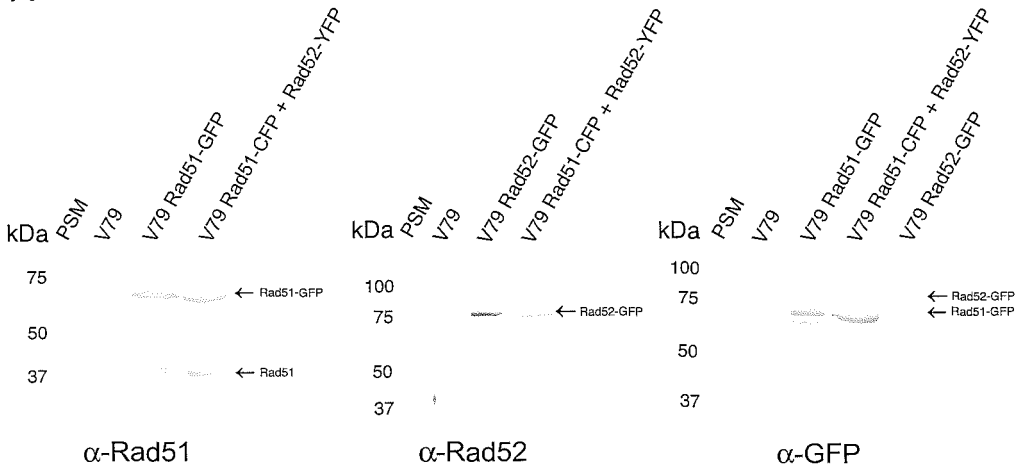
Previously we reported the inability to detect DNA damage-induced Rad51 foci in *Rad54*<sup>-/-</sup> ES cells<sup>55</sup>. However, in the chicken-derived DT40 cell line Rad51 foci could be detected in the absence of Rad54<sup>19</sup>. The difference between these studies was in the fixation method applied to the cells; methanol/acetone for the former and para-formaldehyde for the latter. Therefore, we compared both fixation methods side-by-side (Fig. 3). While no ionizing radiation induced Rad51 foci can be detected in *Rad54*<sup>-/-</sup> ES cells when the cells are fixed with the methanol/acetone method, they are detected upon fixation with para-formaldehyde. In the presence of Rad54, DNA damage-induced Rad51 foci can be detected with the methanol/acetone fixation method (Fig. 3). Possibly, the stability of the Rad51 foci is affected in the absence of Rad54, such that they can be cross-linked with para-formaldehyde, but are not resistant to methanol/acetone treatment.

In both wild type, *Rad52*<sup>-/-</sup> and *Rad54*<sup>-/-</sup> ES cells Rad51 foci were detected by immunostaining before irradiation using the para-formaldehyde fixation method (Fig. 4A). For all three cell lines, the number of cells displaying foci increased after irradiation and more foci per cell were present after irradiation (<15 before vs >25 after irradiation). As the Rad51 behavior after irradiation was similar for all three cell lines, we conclude that there is no significant influence of a *Rad52*<sup>-/-</sup> or *Rad54*<sup>-/-</sup> background on Rad51 foci formation.

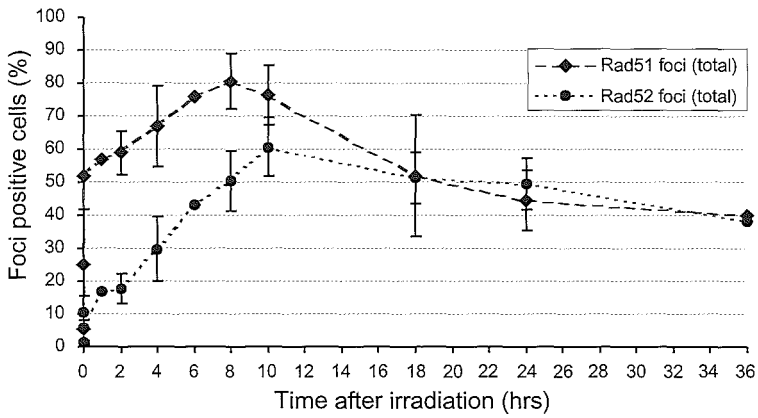
Rad52 foci formation was studied by introducing Rad52-GFP in wild type and *Rad54*<sup>-/-</sup> ES cells. Before irradiation both cell lines showed few cells with Rad52 foci. After irradiation the number of foci positive cells and the amount of foci per cell was increased. Though a difference in number of Rad52 foci positive cells between the wild type and the *Rad54*<sup>-/-</sup> cells was detected (80 vs 33 %) after irradiation, this might not be a significant result, since it was difficult to determine the exact number of Rad52-GFP expressing cells in the different cell populations. The amount of foci per cell was equal in both cell lines. From these data we conclude that a *Rad54*<sup>-/-</sup> background most likely does not influence Rad52 foci formation.

Subsequently, Rad54 ionizing radiation induced foci formation was studied in *Rad52*<sup>-/-</sup> ES cells using immunostaining (Fig. 4B). A *Rad54*-proficient ES cell line functioned as positive control, the *Rad54*<sup>-/-</sup> ES cell line was used as a negative control. Rad54 foci were detected in both wild type and *Rad52*<sup>-/-</sup> ES cells. As was seen for Rad51 foci, a considerable number of

A



B



C

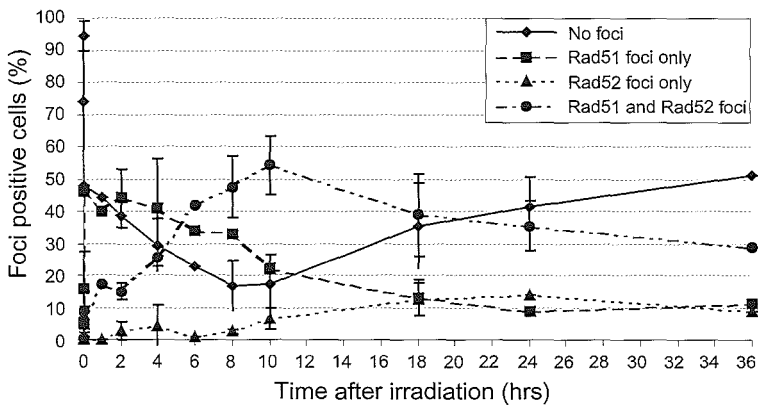


**Figure 2. Time course of Rad51 and Rad52 ionizing radiation induced foci formation in wild type Chinese hamster cells.**

**2A.** Immunoblots detecting endogenous Rad51, Rad51-CFP and Rad52-YFP. A whole cell extract of V79 cells stably expressing both of the abovementioned proteins, was analyzed for presence of the endogenous and GFP-tagged proteins by immunoblotting, using antibodies against Rad51, Rad52 and GFP. The position of the endogenous- and Rad51 GFP-fusion protein and the Rad52 GFP-fusion protein is indicated. The molecular size of the pre-stained marker (PSM) proteins is indicated in kDa.

**2B.** Wild type Chinese hamster cells stably expressing both Rad51-CFP and Rad52-YFP were irradiated with 12 Gy and fixed after indicated time-points. Foci formation was determined using specific microscopic filter sets for the abovementioned constructs. For each experiment the number of foci-positive cells was determined after counting at least 150 cells. A cell was considered positive for Rad51 or Rad52 foci in case of  $\geq 1$  foci/nucleus. The graph is showing the total number of Rad51 and Rad52 positive cells. For both proteins the amount of foci-positive cells increased in time and decreased after 10 hours. For all time points before 18 hours more Rad51 than Rad52 foci were present. At the time points later than 18 hours the percentages approach.

**2C.** The same time course as in 2B, in which the number of cells without Rad51 and Rad52 foci, with Rad51 foci only, Rad52 foci only or both Rad51 and Rad52 foci are displayed. Most cells positive for Rad52 foci showed Rad51 foci as well, but not all cells positive for Rad51 foci showed Rad52 foci. The number of cells positive for both Rad51 and Rad52 increased in time and decreased after 10 hours. Most cells that were positive for both Rad51 and Rad52 showed a partial co-localization of foci.

cells displayed few Rad54 foci before irradiation. Both the number of foci positive cells and the amount of foci per cell increased after irradiation ( $<15$  before vs  $>25$  after irradiation). No significant influence of the *Rad52*<sup>-/-</sup> background on Rad54 foci formation could be detected before and after irradiation regarding to number of foci positive cells and the amount of foci per nucleus. Thus, Rad52 is not necessary in the ionizing radiation induced response of Rad54 with regard to foci formation.

**The influence of ATP hydrolysis on Rad54 foci formation**

In order to study whether the response of Rad54 to DNA damage is ATP dependent, GFP-tagged, ATPase deficient Rad54 was expressed in *Rad54*<sup>-/-</sup> ES cells. Therefore, two constructs were designed with site-specific mutations in Rad54. In pPGK-hRad54<sup>K189R</sup>-GFP the lysine at position 189 was replaced by arginine, thus permitting ATP to bind to Rad54, though the subsequent hydrolysis of ATP is severely impaired. In pPGK-hRad54<sup>K189A</sup>-GFP, the lysine was replaced by alanine, blocking ATP binding altogether. Both these constructs and pPGK-

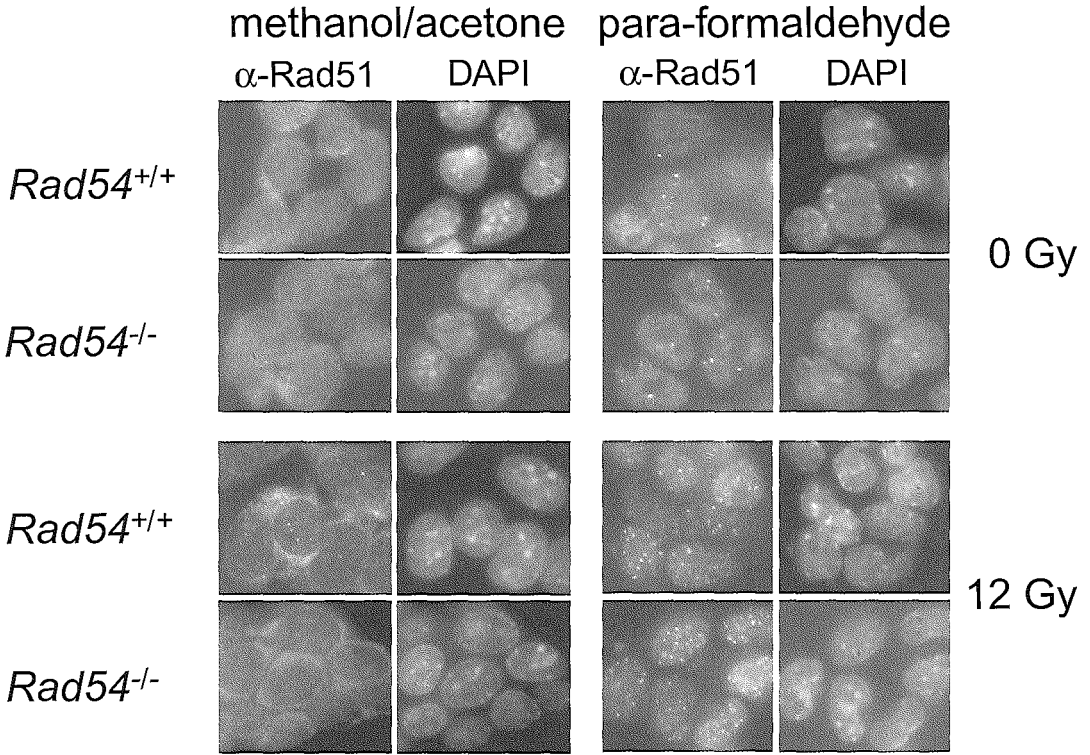


**Figure 3. Comparison of different fixation methods for the detection of Rad51 irradiation induced foci.** *Rad54<sup>+/+</sup>* and *Rad54<sup>-/-</sup>* mouse ES cells were either untreated (upper left and right panels) or irradiated with 12 Gy (lower left and right panels) and fixed after 2 hours with either methanol/acetone (upper and lower left panels) or 2% para-formaldehyde (upper and lower right panels) as described in the materials and methods. Using an antibody against Rad51, foci formation was compared in untreated cells (upper panels) and irradiated cells (lower panels). To discriminate between the different cells the nuclei are visualized by DAPI staining, shown next to the Rad51 staining. Before irradiation hardly any Rad51 foci can be discriminated after methanol/acetone fixation (left-hand panels) in both cell lines, while after fixation with para-formaldehyde (right-hand panels) most nuclei of both *Rad54<sup>+/+</sup>* and *Rad54<sup>-/-</sup>* ES cells show several foci. After ionizing radiation the *Rad54<sup>+/+</sup>* ES cells fixed with methanol/acetone show Rad51 foci, while they cannot be detected in *Rad54<sup>-/-</sup>* ES cells. After fixation with para-formaldehyde irradiated cells demonstrate numerous Rad51 foci in both *Rad54<sup>+/+</sup>* and *Rad54<sup>-/-</sup>* ES cells.

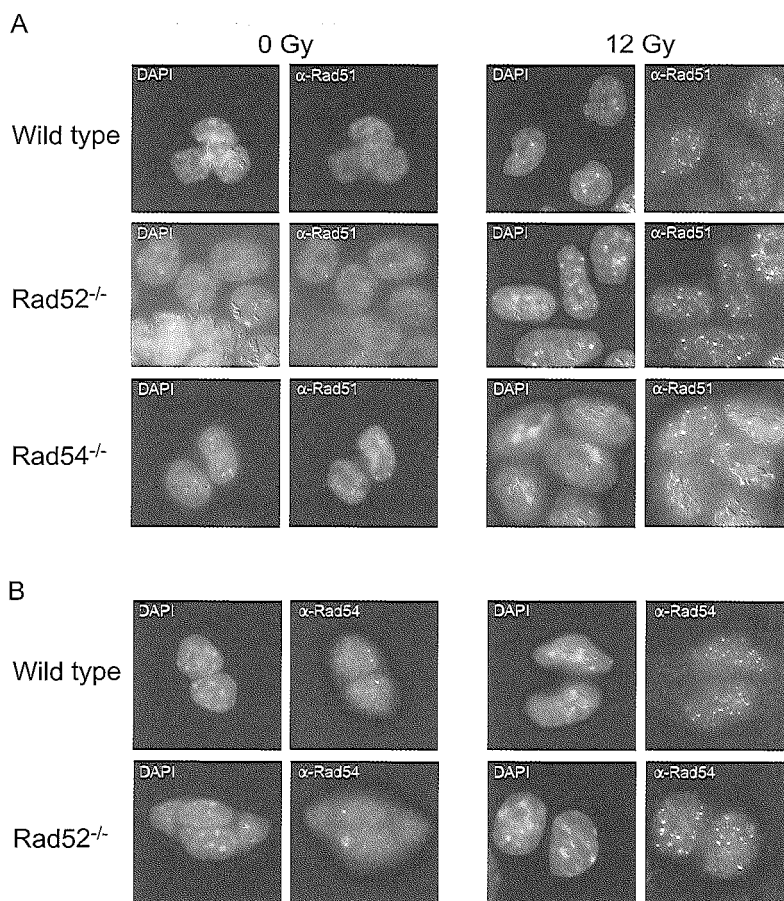


**Figure 4. Rad51 and Rad54 ionizing radiation induced foci formation in Rad54 proficient- and recombination deficient ES cells.**

*Rad54<sup>+/HA</sup>*, a Rad54-proficient mouse ES cell line that has wild type DNA repair characteristics<sup>55</sup>, Rad52<sup>-/-</sup> and Rad54<sup>-/-</sup> mouse ES cells were irradiated with 12 Gy and fixed after 2 hours. Immunostaining was performed using a Rad51 or Rad54 antibody. Cells were analyzed by fluorescence microscopy and a characteristic picture of each slide is shown. The first two columns show cells before, and the last two columns after irradiation.

**4A.** In the upper row the situation for Rad51 in the Rad54-proficient cells is demonstrated. The middle panel shows the results for Rad52<sup>-/-</sup> cells and the lower panel for Rad54<sup>-/-</sup> cells. In all three cell lines the same results were observed; a few foci in untreated cells and a considerable increase in the amount of Rad51 foci per nucleus after irradiation.

**4B.** In the upper row the situation in the Rad54-proficient cells is displayed and the second row shows the results for Rad52<sup>-/-</sup> cells. The Rad54-proficient and Rad52<sup>-/-</sup> cell lines displayed the same results; the number of Rad54 foci per nucleus increased substantially after irradiation.

hRad54-GFP were stably transfected into *Rad54*<sup>-/-</sup> ES cells (Fig. 5A). A clonogenic survival assay showed that, as established earlier, expression of Rad54-GFP corrected the ionizing radiation sensitivity of the *Rad54*<sup>-/-</sup> ES cells to wild type levels<sup>62</sup>. Expression of the Rad54<sup>K189R</sup>-GFP and Rad54<sup>K189A</sup>-GFP proteins resulted in hardly any rescue of the ionizing radiation sensitivity of mouse *Rad54*<sup>-/-</sup> ES cells (data not shown).

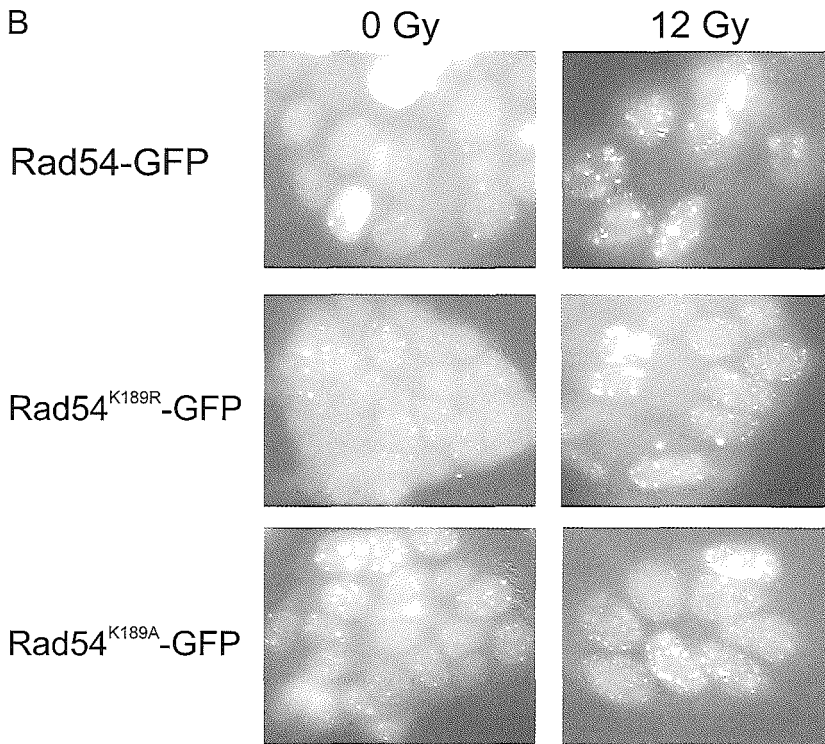
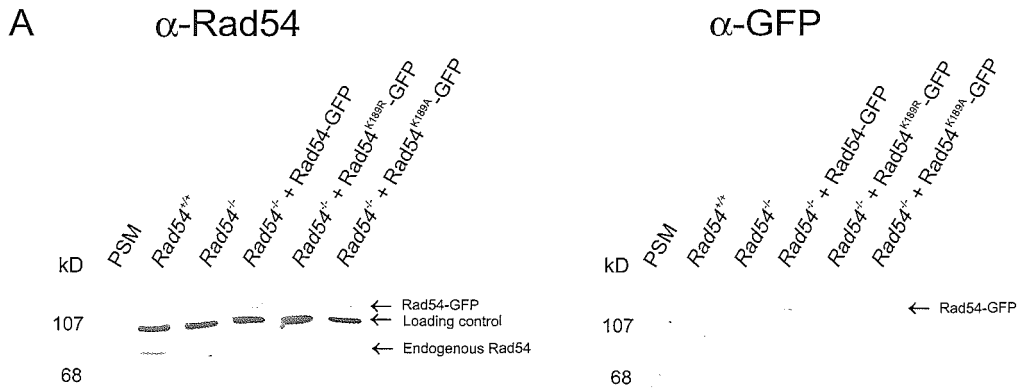
When ionizing radiation induced Rad54 foci formation was studied in *Rad54*<sup>-/-</sup> cells expressing Rad54<sup>K189R</sup>-GFP and Rad54<sup>K189A</sup>-GFP, a striking result was observed (Fig. 5C). Both cell lines showed numerous Rad54 foci in most cells already before irradiation. After irradiation only a slight increase in foci positive cells was seen. Not only the number of foci-positive cells was increased before irradiation in the *Rad54*<sup>-/-</sup> cell lines expressing the mutant Rad54-GFP, but also the amount of foci per cell was very high and comparable to the level observed after irra-

**Figure 5. Rad54 foci formation in *Rad54*<sup>-/-</sup> ES cells expressing Rad54-GFP, Rad54<sup>K189R</sup>-GFP and Rad54<sup>K189A</sup>-GFP.**

**5A.** Immunoblot analysis of endogenous Rad54 and Rad54-GFP in ES cells. Whole cell extracts of *Rad54*<sup>+/+</sup> ES cells (positive control), *Rad54*<sup>-/-</sup> ES cells (negative control) and *Rad54*<sup>-/-</sup> ES cells stably expressing Rad54-GFP, Rad54<sup>K189R</sup>-GFP and Rad54<sup>K189A</sup>-GFP, were analyzed for the presence of endogenous Rad54 and Rad54-GFP by immunoblotting, using antibodies against Rad54 and GFP.

**5B.** *Rad54*<sup>-/-</sup> mouse ES cells were stably transfected with the Rad54-GFP (upper panel), Rad54<sup>K189R</sup>-GFP (middle panel) and Rad54<sup>K189A</sup>-GFP (lower panel) cDNAs. Cells were irradiated with 12 Gy and fixed after 2 hours. Rad54 foci formation was determined before irradiation (first column) and after irradiation (last column). A characteristic picture of each slide is shown. *Rad54*<sup>-/-</sup> ES cells regained their original phenotype with respect to Rad54 foci formation after stable transfection with Rad54-GFP. Before irradiation less than 50% of the cells showed a few Rad54 foci, while after irradiation this number increased substantially and most of the cells had a large amount of Rad54 foci. After transfection with the construct Rad54<sup>K189R</sup>-GFP, 75% of the cells showed numerous foci already before irradiation, which increased to 99% after irradiation. Most cells transfected with the Rad54<sup>K189A</sup>-GFP construct displayed a large amount of foci already before irradiation. This number remained practically unchanged after irradiation.

**5C.** The *Rad54*<sup>-/-</sup> ES cell lines expressing Rad54-GFP, Rad54<sup>K189R</sup>-GFP or Rad54<sup>K189A</sup>-GFP were irradiated with 12 Gy and fixed after 2 hours. Ionizing radiation induced foci formation was determined by counting at least 150 cells for each experiment. A cell was considered positive in case of 1 or more focus per cell. The results were compared with the non-irradiated cells. The *Rad54*<sup>-/-</sup> ES cell line expressing Rad54-GFP showed a few Rad54 foci in less than 50% of the cells before irradiation. However, the *Rad54*<sup>-/-</sup> ES cell lines expressing Rad54<sup>K189R</sup>-GFP or Rad54<sup>K189A</sup>-GFP displayed foci in most cells both before and after irradiation. Furthermore, the amount of foci per cell showed the same high number both before and after irradiation in these cell lines (>25 foci/cell).



**C**

ES cell line	<i>Rad54</i> -GFP		<i>Rad54</i> <sup>K189R</sup> -GFP		<i>Rad54</i> <sup>K189A</sup> -GFP	
	0 Gy	12 Gy	0 Gy	12 Gy	0 Gy	12 Gy
<i>Rad54</i> <sup>+</sup>	46%	95%	75%	99%	90%	99%

ES cell line	Rad51		Rad52-GFP		Rad54	
	0 Gy	12 Gy	0 Gy	12 Gy	0 Gy	12 Gy
<b>Rad54-proficient</b>	70 %	98 %	2 %	80 %	57 %	95 %
<b>Rad54<sup>-/-</sup></b>	66 %	97 %	1 %	33 %	0 %	0 %
<b>Rad52<sup>-/-</sup></b>	48 %	90 %	ND	ND	40 %	90 %

**Table 3. Ionizing radiation induced foci formation of homologous recombination proteins in ES cell lines.**

*Rad54*-proficient, *Rad54*<sup>-/-</sup> and *Rad52*<sup>-/-</sup> mouse ES cell lines were irradiated with 12 Gy and fixed after 2 hours. Foci formation was determined using either antibodies to detect the endogeneous proteins or by using cell lines that express the proteins of interest fused to GFP. As a positive control a *Rad54*-proficient cell line with a wild type DNA repair phenotype was used. For each experiment the number of foci-positive cells was determined by counting at least 200 cells. A cell was considered positive (+) in case of one or more foci per cell. Most cell lines showed foci both before and after irradiation. The number of foci per nucleus, however, was considerably higher after irradiation (<15 foci/cell vs. >25 foci/cell). ND, not determined.

diation (Fig. 5B). Therefore, no significant difference in foci formation could be detected in these *Rad54* deficient cell lines before and after irradiation. The *Rad54*<sup>K189R</sup>-GFP and *Rad54*<sup>K189A</sup>-GFP expressing cell lines showed the same characteristics before, as wild type ES cells after exposure to ionizing radiation. Furthermore, the ionizing radiation induced *Rad54* foci co-localized completely with *Rad51* foci both before and after irradiation in all three cell lines.



## Discussion

The *RAD52* group proteins are required for the formation of a joint molecule between the broken DNA and the intact repair template. This essential step in DNA repair by homologous recombination requires a close cooperation between Rad51, Rad52 and Rad54. Indeed, Rad52 stimulates Rad51-mediated strand-exchange *in vitro*<sup>5-8,63-65</sup>. Furthermore a relationship between Rad51 and Rad52 has been demonstrated at a cellular level because of the partial overlap of DNA damage induced foci<sup>66</sup>. Interaction between Rad51 and Rad54 has been detected biochemically in yeast and in mammalian cells after introducing DNA damage by ionizing radiation or DNA damaging agents<sup>10,64,65</sup>. Interaction between Rad52 and Rad54 has not been demonstrated so far. Analysis of the genetic requirement for ionizing radiation-induced foci formation of homologous recombination proteins in the yeast *S. cerevisiae* has shown that Rad52 is required for foci formation of Rad51 and Rad54<sup>73</sup>. The placement of Rad52 upstream in the response of homologous recombination to DNA damage is consistent with chromatin immuno-precipitation experiments showing that Rad52 is required for Rad51 binding near the break site on DNA<sup>65</sup>.

We have analyzed ionizing radiation-induced foci formation of Rad51, Rad52 and Rad54 in mammalian cells. Our results demonstrate that the genetic requirements for Rad52 ionizing radiation induced foci formation are different from that of Rad51 and Rad54. Mammalian Rad52 can form nuclear foci in *Xrcc2*, *Xrcc3*, *Rad51C* and *Brca2* mutant Chinese hamster cell lines upon ionizing radiation induced DSBs, whereas Rad51 and Rad54 cannot. Even though Rad52 is known to be able to substitute partially for *Xrcc3*<sup>67</sup>, no increase in foci formation was observed in the *Xrcc3* mutant Chinese hamster cell line compared to wild type cells. Furthermore, mammalian Rad52 is not required for ionizing radiation-induced foci formation of Rad51 and Rad54. Our results argue for a differential distribution of tasks between Rad52 and the Rad51 paralogs in yeast and mammalian cells. *S. cerevisiae* Rad52, but not mammalian Rad52, is required for Rad51 and Rad54 foci formation, while the mammalian Rad51 paralogs are required for Rad51 foci formation and the yeast Rad51 paralog Rad55 is not<sup>73</sup>.

Our experiments in recombination-proficient cells on co-localization of damage-induced foci of the *RAD52* group proteins reveal that all three proteins can co-localize, but that a striking quantitative distinction can be made between co-localization of Rad52 with either Rad51 or Rad54 and the co-localization of Rad51 and Rad54 foci. Co-localization of Rad51 or Rad54 with Rad52 is generally limited, only a part of the foci of these proteins show over-

lap. In contrast, co-localization of Rad51 with Rad54 foci is complete. From the experiments on the kinetics of Rad51 and Rad52 foci formation it also appears that foci formation of Rad51 and Rad52 are possibly separate processes. Rad51 foci are induced at earlier time points than Rad52 foci and more cells are positive for Rad51 than for Rad52 foci. Furthermore, the results show that many cells have Rad51 foci only, whereas cells are rarely positive for Rad52 foci, but not Rad51 foci. This might be explained by either subsequent involvement of Rad52 in the sequence of events in repair of DSBs, or involvement of Rad52 in different DNA repair subpathways or different DNA transactions altogether. In this context it is of interest to note that recently a homologous recombination independent role of Rad52 has been discovered in suppression of retroviral integration<sup>74</sup>. However, it is not clear whether this process involves Rad52 foci formation.

The results of the experiments on *Rad52*<sup>-/-</sup> ES cells have revealed another distinct difference in the role of Rad52 in the DNA damage response between *S. cerevisiae* and mammalian cells. Absence of mammalian Rad52 does not lead to an inability of Rad51 and Rad54 to accumulate in ionizing radiation-induced foci. In contrast, in *S. cerevisiae*, Rad52 is essential for Rad51 and Rad54 foci formation<sup>73</sup>. With respect to Rad54, ionizing radiation-induced foci formation assays in *Rad54*<sup>-/-</sup> ES cells show that Rad54 is not required for Rad52 and Rad51 foci formation. However, this does not mean that foci formation by these protein is not affected. For Rad51 we previously detected an effect of the absence of Rad54 on Rad51 foci formation. Using methanol/acetone fixation of cells, we found that in mouse ES cells lacking Rad54, Rad51 foci cannot be detected<sup>55</sup>. Comparison of methanol/acetone and para-formaldehyde fixation methods shows that *Rad54*<sup>-/-</sup> ES cells are not inherently deficient in ionizing radiation induced Rad51 foci formation. Given the protein-protein interaction between Rad51 and Rad54, it is possible that Rad51 foci are less stable in the absence of Rad54. We believe that para-formaldehyde fixation stabilizes Rad51 foci to a greater extent than methanol/acetone fixation, based on the observation that a higher percentage of wild type ES cells display spontaneous Rad51 foci using the para-formaldehyde fixation method instead of the methanol/acetone fixation method (70% versus 10%). Differential stability of Rad51 foci in the absence and presence of Rad54 is consistent with biochemical observations showing that Rad54 can stabilize Rad51 nucleoprotein filaments<sup>11</sup>.

Our results suggest a differential role of Rad52 in the DNA damage response in yeast and mammalian cells. This notion is supported by other features of Rad52. Deletion of Rad52 in *S. cerevisiae* cells causes the most severe recombination-associated phenotypes compared to deletion of other *RAD52* group genes<sup>4</sup>. By contrast, unlike cells with mutations in other pro-

teins known to function in homologous recombination, *Rad52*<sup>-/-</sup> ES cells and chicken B-cells are not hypersensitive to ionizing radiation or cross linking agents and the *Rad52*<sup>-/-</sup> cells show only a marginal reduction in gene targeting frequency<sup>57,68</sup>. Furthermore, *Rad52* knock-out mice do not show any phenotypic changes compared to wild type mice<sup>57</sup>. Taken together, the results suggest that notwithstanding the evolutionary conservation and biochemical similarities between *S. cerevisiae* and mammalian *Rad52*, the protein contributes dramatically different to DNA damage response DNA damage in the context of *S. cerevisiae* and mammalian cells.

### **Reduction of ATPase activity of Rad54 leads to the induction of spontaneous Rad54 foci**

*Rad54* deficiency causes increased ionizing radiation sensitivity and decreased homologous recombination in ES cells<sup>58</sup>. *Rad54* is known to have several activities<sup>10</sup>. First, its function in stabilizing the *Rad51* filament on single-stranded DNA does not require ATP hydrolysis<sup>11</sup>. Furthermore, *Rad54* is involved in chromatin remodeling by altering the accessibility of template DNA<sup>12-14</sup>. Third, *Rad54* is involved in stimulating *Rad51* mediated D-loop formation<sup>6-8,69</sup>, and fourth, *Rad54* may destabilize the filaments on double-stranded DNA, which does require ATP hydrolysis<sup>9,15,18,70-72</sup>. To investigate which of these functions is responsible for the formation of ionizing radiation induced foci, ES cell lines were generated which expressed *Rad54* with mutations in the Walker A motif, which is involved in ATP binding and hydrolysis. Our results demonstrate that these mutations hardly rescued the radiation hypersensitivity of the *Rad54*<sup>-/-</sup> ES cells. Interestingly, spontaneous foci of the mutant *Rad54* proteins were observed in 75-90% of the cells before DNA damage was induced. Furthermore the foci co-localized completely with *Rad51* foci, both before and after ionizing radiation. These results show that ATP hydrolysis influences *Rad54* foci formation. The spontaneous accumulation of mutant *Rad54* into foci could be explained by an increased affinity of the protein for DNA because destabilization by ATP hydrolysis cannot take place after spontaneous arising DNA damage. In that case *Rad54* will remain on the processed DNA and accumulate into foci. Another explanation might be that spontaneously arising genomic DNA damage cannot be processed properly in the absence of ATP hydrolysis. This explanation is more likely, since *Rad51* also shows an increase in foci in the *Rad54* mutant cells and co-localizes completely with *Rad54*. Furthermore, ES cells which express the ATPase mutant *Rad54* are not able to completely rescue the radiation hypersensitivity of *Rad54*<sup>-/-</sup> cells. Following this hypothesis, the spontaneous accumulation of *Rad54* and *Rad51* foci could represent increased genomic instability. Decreased *Rad54* ATPase activity could therefore be more threatening to the genome than a complete absence of *Rad54*.

## **Acknowledgements**

We thank Dr. M.Z. Zdzienicka, Dept. of Radiation Genetics and Chemical Mutagenesis, Leiden University Medical Center, for providing us with the CL-V4B and V-C8 cell lines. This work was supported by grants from the Dutch Organization for Scientific Research (NWO), the Dutch Cancer Society (KWF), the Human Frontier Science Program Organization and the European Union.

## References

1. van Gent, D.C., Hoeijmakers, J.H. & Kanaar, R. Chromosomal stability and the DNA double-stranded break connection. *Nat Rev Genet* **2**, 196-206. (2001).
2. van den Bosch, M., Lohman, P.H. & Pastink, A. DNA double-strand break repair by homologous recombination. *Biol Chem* **383**, 873-92. (2002).
3. Symington, L.S. Role of RAD52 epistasis group genes in homologous recombination and double-strand break repair. *Microbiol Mol Biol Rev* **66**, 630-70. (2002).
4. Kanaar, R., Hoeijmakers, J.H. & van Gent, D.C. Molecular mechanisms of DNA double strand break repair. *Trends Cell Biol* **8**, 483-9. (1998).
5. Shinohara, A., Shinohara, M., Ohta, T., Matsuda, S. & Ogawa, T. Rad52 forms ring structures and co-operates with RPA in single-strand DNA annealing. *Genes Cells* **3**, 145-56. (1998).
6. Benson, F.E., Baumann, P. & West, S.C. Synergistic actions of Rad51 and Rad52 in recombination and DNA repair. *Nature* **391**, 401-4. (1998).
7. New, J.H., Sugiyama, T., Zaitseva, E. & Kowalczykowski, S.C. Rad52 protein stimulates DNA strand exchange by Rad51 and replication protein A. *Nature* **391**, 407-10. (1998).
8. Sung, P. Function of yeast Rad52 protein as a mediator between replication protein A and the Rad51 recombinase. *J Biol Chem* **272**, 28194-7. (1997).
9. Ristic, D., Wyman, C., Paulusma, C. & Kanaar, R. The architecture of the human Rad54-DNA complex provides evidence for protein translocation along DNA. *Proc Natl Acad Sci USA* **98**, 8454-60. (2001).
10. Tan, R.T.L., Kanaar, R. & Wyman, C. Rad54, a Jack of all trades in homologous recombination. *DNA Repair (Amst)* **2**, 787-94. (2003).
11. Mazin, A.V., Alexeev, A.A. & Kowalczykowski, S.C. A novel function of Rad54 protein. Stabilization of the Rad51 nucleoprotein filament. *J Biol Chem* **278**, 14029-36. (2003).
12. Jaskelioff, M., Van Komen, S., Krebs, J.E., Sung, P. & Peterson, C.L. Rad54p is a chromatin remodeling enzyme required for heteroduplex DNA joint formation with chromatin. *J Biol Chem* **278**, 9212-8. (2003).
13. Alexeev, A., Mazin, A. & Kowalczykowski, S.C. Rad54 protein possesses chromatin-remodeling activity stimulated by the Rad51-ssDNA nucleoprotein filament. *Nat Struct Biol* **10**, 182-6. (2003).
14. Alexiadis, V. & Kadonaga, J.T. Strand pairing by Rad54 and Rad51 is enhanced by chromatin. *Genes Dev* **16**, 2767-71. (2002).
15. Petukhova, G., Stratton, S. & Sung, P. Catalysis of homologous DNA pairing by yeast Rad51 and Rad54 proteins. *Nature* **393**, 91-4. (1998).
16. Mazin, A.V., Bornarth, C.J., Solinger, J.A., Heyer, W.D. & Kowalczykowski, S.C. Rad54 protein is targeted to pairing loci by the Rad51 nucleoprotein filament. *Mol Cell* **6**, 583-92. (2000).
17. Van Komen, S., Petukhova, G., Sigurdsson, S., Stratton, S. & Sung, P. Superhelicity-driven homologous DNA pairing by yeast recombination factors Rad51 and Rad54. *Mol Cell* **6**, 563-72. (2000).
18. Solinger, J.A., Kiiianitsa, K. & Heyer, W.D. Rad54, a Swi2/Snf2-like recombinational repair protein, disassembles Rad51:dsDNA filaments. *Mol Cell* **10**, 1175-88. (2002).
19. Takata, M. et al. The Rad51 paralog Rad51B promotes homologous recombinational repair. *Mol Cell Biol* **20**, 6476-82. (2000).
20. Godthelp, B.C. et al. Mammalian Rad51C contributes to DNA cross-link resistance, sister chromatid cohesion and genomic stability. *Nucleic Acids Res* **30**, 2172-82. (2002).
21. Brenneman, M.A., Wagener, B.M., Miller, C.A., Allen, C. & Nickoloff, J.A. XRCC3 controls the fidelity of homologous recombination: roles for XRCC3 in late stages of recombination. *Mol Cell* **10**, 387-95. (2002).

22. Deans, B., Griffin, C.S., Maconochie, M. & Thacker, J. Xrcc2 is required for genetic stability, embryonic neurogenesis and viability in mice. *EMBO J* **19**, 6675-85. (2000).
23. Havre, P.A., Rice, M.C., Noe, M. & Kmiec, E.B. The human REC2/RAD51B gene acts as a DNA damage sensor by inducing G1 delay and hypersensitivity to ultraviolet irradiation. *Cancer Res* **58**, 4733-9. (1998).
24. Pittman, D.L. & Schimenti, J.C. Midgestation lethality in mice deficient for the RecA-related gene, Rad51d/Rad5113. *Genesis* **26**, 167-73. (2000).
25. Takata, M. et al. Chromosome instability and defective recombinational repair in knockout mutants of the five Rad51 paralogs. *Mol Cell Biol* **21**, 2858-66. (2001).
26. Masson, J.Y. et al. Identification and purification of two distinct complexes containing the five RAD51 paralogs. *Genes Dev* **15**, 3296-307. (2001).
27. Liu, N., Schild, D., Thelen, M.P. & Thompson, L.H. Involvement of Rad51C in two distinct protein complexes of Rad51 paralogs in human cells. *Nucleic Acids Res* **30**, 1009-15. (2002).
28. Sung, P. Yeast Rad55 and Rad57 proteins form a heterodimer that functions with replication protein A to promote DNA strand exchange by Rad51 recombinase. *Genes Dev* **11**, 1111-21. (1997).
29. Sigurdsson, S. et al. Mediator function of the human Rad51B-Rad51C complex in Rad51/RPA-catalyzed DNA strand exchange. *Genes Dev* **15**, 3308-18. (2001).
30. French, C.A. et al. Role of mammalian RAD51L2 (RAD51C) in recombination and genetic stability. *J Biol Chem* **277**, 19322-30. (2002).
31. Liu, Y., Masson, J.Y., Shah, R., O'Regan, P. & West, S.C. RAD51C is required for Holliday junction processing in mammalian cells. *Science* **303**, 243-6 (2004).
32. Yang, H. et al. BRCA2 function in DNA binding and recombination from a BRCA2-DSS1-ssDNA structure. *Science* **297**, 1837-48. (2002).
33. Pellegrini, L. et al. Insights into DNA recombination from the structure of a RAD51-BRCA2 complex. *Nature* **420**, 287-93. (2002).
34. Powell, S.N., Willers, H. & Xia, F. BRCA2 keeps Rad51 in line. High-fidelity homologous recombination prevents breast and ovarian cancer? *Mol Cell* **10**, 1262-3. (2002).
35. Davies, A.A. et al. Role of BRCA2 in control of the RAD51 recombination and DNA repair protein. *Mol Cell* **7**, 273-82. (2001).
36. Snouwaert, J.N. et al. BRCA1 deficient embryonic stem cells display a decreased homologous recombination frequency and an increased frequency of non-homologous recombination that is corrected by expression of a brca1 transgene. *Oncogene* **18**, 7900-7. (1999).
37. Moynahan, M.E., Chiu, J.W., Koller, B.H. & Jasin, M. Brca1 controls homology-directed DNA repair. *Mol Cell* **4**, 511-8. (1999).
38. Paull, T.T., Cortez, D., Bowers, B., Elledge, S.J. & Gellert, M. Direct DNA binding by Brca1. *Proc Natl Acad Sci USA* **98**, 6086-91. (2001).
39. Essers, J. et al. Nuclear dynamics of RAD52 group homologous recombination proteins in response to DNA damage. *EMBO J* **21**, 2030-7. (2002).
40. Chen, J.J., Silver, D., Cantor, S., Livingston, D.M. & Scully, R. BRCA1, BRCA2, and Rad51 operate in a common DNA damage response pathway. *Cancer Res* **59**, 1752s-1756s. (1999).
41. Choudhary, S.K. & Li, R. BRCA1 modulates ionizing radiation-induced nuclear focus formation by the replication protein A p34 subunit. *J Cell Biochem* **84**, 666-74. (2002).
42. Tashiro, S., Walter, J., Shinohara, A., Kamada, N. & Cremer, T. Rad51 accumulation at sites of DNA damage and in postreplicative chromatin. *J Cell Biol* **150**, 283-91. (2000).
43. Aten, J.A. et al. Dynamics of DNA double-strand breaks revealed by clustering of damaged chromosome domains. *Science* **303**, 92-5 (2004).
44. Bishop, D.K. et al. Xrcc3 is required for assembly of Rad51 complexes in vivo. *J Biol Chem* **273**, 21482-8. (1998).

45. Bhattacharyya, A., Ear, U.S., Koller, B.H., Weichselbaum, R.R. & Bishop, D.K. The breast cancer susceptibility gene BRCA1 is required for subnuclear assembly of Rad51 and survival following treatment with the DNA cross-linking agent cisplatin. *J Biol Chem* **275**, 23899-903. (2000).
46. O'Regan, P., Wilson, C., Townsend, S. & Thacker, J. XRCC2 is a nuclear RAD51-like protein required for damage-dependent RAD51 focus formation without the need for ATP binding. *J Biol Chem* **276**, 22148-53. (2001).
47. Yuan, S.S. et al. BRCA2 is required for ionizing radiation-induced assembly of Rad51 complex in vivo. *Cancer Res* **59**, 3547-51. (1999).
48. Cartwright, R., Tambini, C.E., Simpson, P.J. & Thacker, J. The XRCC2 DNA repair gene from human and mouse encodes a novel member of the recA/RAD51 family. *Nucleic Acids Res* **26**, 3084-9. (1998).
49. Cui, X. et al. The XRCC2 and XRCC3 repair genes are required for chromosome stability in mammalian cells. *Mutat Res* **434**, 75-88. (1999).
50. Thacker, J., Tambini, C.E., Simpson, P.J., Tsui, L.C. & Scherer, S.W. Localization to chromosome 7q36.1 of the human XRCC2 gene, determining sensitivity to DNA-damaging agents. *Hum Mol Genet* **4**, 113-20. (1995).
51. Tebbs, R.S. et al. Correction of chromosomal instability and sensitivity to diverse mutagens by a cloned cDNA of the XRCC3 DNA repair gene. *Proc Natl Acad Sci USA* **92**, 6354-8. (1995).
52. Overkamp, W.J. et al. Genetic diversity of mitomycin C-hypersensitive Chinese hamster cell mutants: a new complementation group with chromosomal instability. *Somat Cell Mol Genet* **19**, 431-7. (1993).
53. Kraakman-van der Zwet, M. et al. Brca2 (XRCC11) deficiency results in radioresistant DNA synthesis and a higher frequency of spontaneous deletions. *Mol Cell Biol* **22**, 669-79. (2002).
54. Mombaerts, P., Clarke, A.R., Hooper, M.L. & Tonegawa, S. Creation of a large genomic deletion at the T-cell antigen receptor beta-subunit locus in mouse embryonic stem cells by gene targeting. *Proc Natl Acad Sci USA* **88**, 3084-7. (1991).
55. Tan, T.L. et al. Mouse Rad54 affects DNA conformation and DNA-damage-induced Rad51 foci formation. *Curr Biol* **9**, 325-8. (1999).
56. Essers, J. et al. Analysis of mouse Rad54 expression and its implications for homologous recombination. *DNA Repair (Amst)* **1**, 779-93. (2002).
57. Rijkers, T. et al. Targeted inactivation of mouse RAD52 reduces homologous recombination but not resistance to ionizing radiation. *Mol Cell Biol* **18**, 6423-9. (1998).
58. Essers, J. et al. Disruption of mouse RAD54 reduces ionizing radiation resistance and homologous recombination. *Cell* **89**, 195-204. (1997).
59. Lisby, M., Mortensen, U.H. & Rothstein, R. Colocalization of multiple DNA double-strand breaks at a single Rad52 repair centre. *Nat Cell Biol* **5**, 572-7. (2003).
60. Lisby, M., Rothstein, R. & Mortensen, U.H. Rad52 forms DNA repair and recombination centers during S phase. *Proc Natl Acad Sci USA* **98**, 8276-82. (2001).
61. Liu, Y. & Maizels, N. Coordinated response of mammalian Rad51 and Rad52 to DNA damage. *EMBO Rep* **1**, 85-90. (2000).
62. Swagemakers, S.M., Essers, J., de Wit, J., Hoeijmakers, J.H. & Kanaar, R. The human RAD54 recombinational DNA repair protein is a double-stranded DNA-dependent ATPase. *J Biol Chem* **273**, 28292-7. (1998).
63. Krejci, L. et al. Interaction with Rad51 is indispensable for recombination mediator function of Rad52. *J Biol Chem* **277**, 40132-41. (2002).
64. Wolner, B., van Komen, S., Sung, P. & Peterson, C.L. Recruitment of the recombinational repair machinery to a DNA double-strand break in yeast. *Mol Cell* **12**, 221-32. (2003).
65. Sugawara, N., Wang, X. & Haber, J.E. In vivo roles of Rad52, Rad54, and Rad55 proteins in Rad51-mediated recombination. *Mol Cell* **12**, 209-19. (2003).
66. Gasior, S.L., Wong, A.K., Kora, Y., Shinohara, A. & Bishop, D.K. Rad52 associates with RPA and functions

- with rad55 and rad57 to assemble meiotic recombination complexes. *Genes Dev* **12**, 2208-21. (1998).
67. Fujimori, A. et al. Rad52 partially substitutes for the Rad51 paralog XRCC3 in maintaining chromosomal integrity in vertebrate cells. *EMBO J* **20**, 5513-20. (2001).
68. Yamaguchi-Iwai, Y. et al. Homologous recombination, but not DNA repair, is reduced in vertebrate cells deficient in RAD52. *Mol Cell Biol* **18**, 6430-5. (1998).
69. Shinohara, A. & Ogawa, T. Stimulation by Rad52 of yeast Rad51-mediated recombination. *Nature* **391**, 404-7. (1998).
70. Petukhova, G., Van Komen, S., Vergano, S., Klein, H. & Sung, P. Yeast Rad54 promotes Rad51-dependent homologous DNA pairing via ATP hydrolysis-driven change in DNA double helix conformation. *J Biol Chem* **274**, 29453-62. (1999).
71. Solinger, J.A. & Heyer, W.D. Rad54 protein stimulates the postsynaptic phase of Rad51 protein-mediated DNA strand exchange. *Proc Natl Acad Sci USA* **98**, 8447-53. (2001).
72. Solinger, J.A., Lutz, G., Sugiyama, T., Kowalczykowski, S.C. & Heyer, W.D. Rad54 protein stimulates heteroduplex DNA formation in the synaptic phase of DNA strand exchange via specific interactions with the pre-synaptic Rad51 nucleoprotein filament. *J Mol Biol* **307**, 1207-21. (2001).
73. M. Lisby, J.H. Barlow, R.C. Burgess, R. Rothstein. Choreography of the DNA damage response: spatiotemporal relationships among checkpoint and repair proteins. *Cell* **118**, 699-713. (2004).
74. A. Lau, R. Kanaar, S.P. Jackson, M.J. O'Connor. Suppression of retroviral infection by the RAD52 DNA repair protein. *EMBO J* **23**, 3421-29. (2004).







---

## Chapter 6

*Evaluation of ionizing radiation-induced foci formation  
and telomere length as predictive assays  
for radiosensitivity in human fibroblasts and lymphocytes*

---

## Chapter 6

*Evaluation of ionizing radiation-induced foci formation  
and telomere length as predictive assays for radiosensitivity  
in human fibroblasts and lymphocytes*

L.R. van Veelen<sup>1,2</sup>, A. Zeilemaker<sup>3</sup>, K.A. Mattern<sup>3</sup>, J.M.J.M. Zijlmans<sup>3</sup>, A.N. van Geel<sup>4</sup>,  
P.C. Levendag<sup>2</sup>, R. Kanaar<sup>1,2</sup>

- <sup>1</sup> Department of Cell Biology and Genetics, Erasmus MC,  
University Medical Center, P.O. Box 1738, 3000 DR Rotterdam, The Netherlands
- <sup>2</sup> Department of Radiation Oncology, Erasmus MC-Daniel den Hoed Cancer Center,  
University Medical Center, P.O. Box 5201, 3008 AE Rotterdam, The Netherlands
- <sup>3</sup> Department of Haematology, Erasmus MC,  
University Medical Center, P.O. Box 1738, 3000 DR Rotterdam, The Netherlands
- <sup>4</sup> Department of Surgical Oncology, Erasmus MC-Daniel den Hoed Cancer Center,  
University Medical Center, P.O. Box 5201, 3008 AE Rotterdam, The Netherlands

## **Abstract**

In radiotherapy there is a great need for functional assays that predict normal tissue reaction of individuals, since the maximum radiation dose prescribed is limited by normal tissue tolerance. However, commonly used assays for predictive tests such as clonogenic survival assays show variable results and can therefore not be used routinely. We examined alternative possibilities for measuring individual radiosensitivity that rely on the cellular response to DNA double-strand breaks introduced by ionizing radiation. Upon irradiation several DNA double-strand break (DSB) repair proteins accumulate at sites of DNA damage into subnuclear structures called foci. The ability of fibroblasts from control patients, patients overreacting to radiotherapy and selected severe combined immunodeficiency (SCID) patients to form ionizing radiation-induced DSB repair protein foci was tested by immunostaining using antibodies against Rad51, Rad54, Mre11,  $\gamma$ -H2AX and Brca1. No major differences between the control and overreacting group of patients were observed. However, aberrant foci formation was observed in cells from one of the radiosensitive SCID patients. A second method tested for its ability to predict normal tissue response was determination of telomere length in lymphocytes and fibroblasts. Again, no significant differences were found between the control and overreacting group of patients, nor the SCID patients. We conclude that ionizing radiation-induced foci formation and telomere length measurements do not provide a functional assay to predict normal tissue response to radiotherapy.

## Introduction

In radiotherapy the maximum radiation dose prescribed for curative treatment is limited by normal tissue tolerance. This maximum dose is based on clinical experience such that at most a few percent of patients will suffer serious side effects of the treatment. If it would be possible to identify subgroups of patients with a high risk of severe acute or late normal tissue overreaction, dose prescriptions for radiotherapy could be individualized. A higher dose, and as a consequence a higher probability of local tumor control, could be prescribed for those patients who have a minor chance of serious complications. On the other hand, treatment can be adjusted to a lower dose for patients who will have an increased risk of severe toxicity. Therefore, there is a great need for functional assays that predict normal tissue reaction of individuals. Most predictive tests are based on cellular radiosensitivity tested by clonogenic survival assays or experiments that measure residual DNA damage by comet assay or pulsed field gel electrophoresis. However, these predictive assays show variable results and can therefore not be used routinely<sup>1-8</sup>. The purpose of this study was to evaluate other methods to measure individual radiosensitivity. This was done by screening fibroblasts of control and radiosensitive patients for possible DNA double-strand break (DSB) repair defects by examining ionizing radiation-induced foci (IRIF) formation and determining telomere length.

Ionizing radiation causes DNA damage, especially (DSBs). Incorrect repair or accumulation of DNA damage results in genome instability, which could lead to impaired functioning of the cell. There are two major DSB repair mechanisms that counteract the deleterious effects of DSBs; the pathway of homologous recombination (HR) and non-homologous end-joining (NHEJ)(*Chapter 1*). The difference between these two pathways is the use of a homologous sequence. HR uses the sister chromatid or homologous chromosome as a template for repair, whereas NHEJ simply joins the broken ends without use of a template. The detection, processing and ligation of the breaks are organized by a large number of proteins, which are specific for each pathway, although some proteins may be involved in both HR and NHEJ. A mutation in one of the genes involved in DSB repair may cause increased sensitivity to ionizing radiation. Several radiosensitive cell lines have been established with defects in one of the HR genes. For genes involved in NHEJ two groups of patients with mutations have been identified. A small subset of patients with severe combined immunodeficiency (SCID) have a mutation in the Artemis gene<sup>9</sup>. Furthermore, patients have been described with a defect in the LigaseIV gene<sup>10</sup>.

The response to DNA damage of a number of proteins involved in repair of DSBs has been visualized inside cells using immunostaining. Many of the proteins involved in DSB repair accumulate into subnuclear structures at sites of DNA damage after treatment with ionizing radiation<sup>11-15</sup>. These subnuclear structures are referred to as foci. Foci can be detected by a fluorescently labeled antibody specific for the protein of interest after treatment of cells by irradiation, fixation and permeabilization. Cell lines with a defect in one of the DNA repair proteins may show less or more damage induced foci per nucleus and/or foci positive cells. An increase in number of foci might be due to the inability of the cell to repair the spontaneous or treatment induced DSBs. A decrease in number of foci may occur in case the protein of interest, or one of its cooperating proteins, is not functioning properly. This may lead to impaired complex formation at the site of the DSB, thus preventing an accumulation of the protein of interest. For example, cells defective in the HR protein Brca2 (breast cancer associated gene)<sup>2</sup> fail to form IRIF of Rad51, a central HR protein<sup>16</sup>. Since increased sensitivity to ionizing radiation might be caused by a mutation in one of the DNA repair genes, immunostaining with antibodies against specific DNA repair proteins could possibly be used to identify the patients with an increased risk of severe toxicity upon treatment. Immunostaining experiments can be done for many cell types and the method is relatively simple and fast. Therefore, it would be suitable as a predictive assay for normal tissue response after radiotherapy. In this study fibroblasts of patients with an overreaction to irradiation were tested for their ability to form IRIF and compared to foci formation in fibroblasts of patients with a normal reaction upon treatment. Furthermore, IRIF formation was tested in fibroblasts of SCID patients with unknown mutations or a mutation in the Artemis gene, which is involved in NHEJ. The proteins of interest were Rad51 and Rad54, involved in HR; Mre11, most likely involved in both HR and NHEJ;  $\gamma$ -H2AX, a DSB-induced phosphorylation protein of the histone H2A variant H2AX which responds early in reaction to DNA damage and Brca1, involved in repair through HR and cell cycle checkpoint regulation<sup>17,18</sup>.

Determination of telomere length is another method that could possibly be used as a

**Table 1. Patient characteristics.**

*Overview of patient characteristics and information on dose and fractionation schedules of each patient. In each group 14 patients were included. Mean age is 50 years in the control group and 57 years in the hypersensitive group. Toxicity of the tissues and organs involved in the radiation field is scored according to the RTOG acute and late radiation morbidity scoring criteria. In case organs within the irradiated area are not mentioned, no specific acute or late side effects were seen (score is 0).*

**Table 1. Patient characteristics.**

Control patients	Gender	Age at treatment	Cancer type	Irradiation site	Maximum dose	Fraction dose	Acute toxicity score	Late toxicity score
1	F	73	breast	breast R	66 Gy	2 Gy	skin: gr. 1	skin: gr. 1 subcutaneous tissue: gr. 1
2	F	47	breast	breast R	66 Gy	2 Gy	skin: gr. 2	skin: gr. 1 subcutaneous tissue: gr. 2
3	F	69	breast	breast R	66 Gy	2 Gy	skin: gr. 1	skin: gr. 1 subcutaneous tissue: gr. 2
4	M	73	rectum	pelvis	60 Gy (including FIT)	2 Gy FIT: 1 x 10 Gy	skin: gr. 2 bowel: gr. 1	skin: gr. 1 subcutaneous tissue: gr. 2
5	F	52	breast	breast R	66 Gy	2 Gy	skin: gr. 1	skin: gr. 1 subcutaneous tissue: gr. 2
6	M	60	lung	lung and mediastinum	46 Gy	2 Gy	esophagus: gr. 2	skin: gr. 1 subcutaneous tissue: gr. 2 lung: gr. 2
7	F	36	melanoma	groin L	50 Gy (including 4 x hyperthermia)	2.5 Gy	skin: gr. 2	skin: gr. 0 subcutaneous tissue: gr. 2
8	F	42	breast	breast R	64 Gy	2 Gy	skin: gr. 1	skin: gr. 1 subcutaneous tissue: gr. 1
9	F	45	breast	breast L	70 Gy	2 Gy and boost 2.5 Gy	skin: gr. 1	skin: gr. 2 subcutaneous tissue: gr. 2
10	F	23	sarcoma	arm R	70 Gy	2 Gy	skin: gr. 2	skin: gr. 1 subcutaneous tissue: gr. 2
11	F	51	breast	breast R	66 Gy	2 Gy	skin: gr. 2	skin: gr. 1 subcutaneous tissue: gr. 2
12	F	54	lung	lung and mediastinum	56 Gy (including FIT)	2 Gy FIT: 1 x 10 Gy	skin: gr. 2 esophagus: gr. 2 lung: gr. 0	skin: gr. 0 lung: gr. 1 subcutaneous tissue: gr. 2
13	F	26	malignant peripheral nerve-sheath tumor	cal R	68 Gy	2 Gy	skin: gr. 1	skin: gr. 0 subcutaneous tissue: gr. 2
14	F	51	head and neck	floor of mouth	60 Gy	2 Gy (6 x week)	skin: gr. 2 mucous membrane: gr. 2	skin: gr. 1 mucous membrane: gr. 1



IRIF formation and telomere length as predictive assays for radiosensitivity

Hypersensitive patients	Gender	Age at treatment	Cancer type	Irradiation site	Maximum dose	Fraction dose	Acute toxicity score	Late toxicity score
1	F	57	breast	breast L	66 Gy	2 Gy	skin: gr. 2	skin: gr. 2 subcutaneous tissue: gr. 3
2	M	48	head and neck	soft palate and neck	mouth 91 Gy (including brachytherapy) neck 50 Gy	2 Gy brachytherapy: 3 Gy (7 fractions)	skin: gr. 2 mucous membrane: gr. 3 salivary glands: gr. 2	skin: gr. 3 subcutaneous tissue: gr. 3 mucous membrane: gr. 2 salivary glands: gr. 1
3	F	66	breast	chest wall and axilla L	46 Gy	2 Gy	skin: gr. 1	skin: gr. 3 subcutaneous tissue: gr. 3 joint: gr. 3
4	F	51	breast	breast L	70 Gy	2 Gy and boost 2.5 Gy	skin: gr. 2	skin: gr. 3 subcutaneous tissue: gr. 3
5	M	64	fibromatosis	axilla L	60 Gy	2 Gy	skin: gr. 2	skin: gr. 1 subcutaneous tissue: gr. 3
6	M	47	head and neck	floor of mouth and neck	60 Gy	2 Gy	skin: gr. 2 mucous membrane: gr. 2	skin: gr. 2 subcutaneous tissue: gr. 3
7	F	43	breast	breast L	66 Gy	2 Gy	skin: gr. 2	skin: gr. 2 subcutaneous tissue: gr. 3
8	F	68	breast	breast L	70 Gy	2 Gy and boost 2.5 Gy	skin: gr. 1	skin: gr. 2 subcutaneous tissue: gr. 3
9	F	56	breast	chest wall L	50 Gy	2 Gy	skin: gr. 1	skin: gr. 3 subcutaneous tissue: gr. 3
10	F	61	head and neck	nasopharynx and neck	Nasopharynx 83 Gy (including brachytherapy) Neck 48 Gy	2 Gy Brachytherapy: 3 Gy (6 fractions) and 5 Gy (1 fraction)	skin: gr. 2 mucous membrane: gr. 2 ear: gr. 0 upper GI: gr. 2 salivary glands: gr. 2	skin: gr. 3 subcutaneous tissue: gr. 3 mucous membrane: gr. 3 mucous membrane: gr. 3 salivary glands: gr. 3 larynx: gr. 3
11	F	42	breast	chest wall and axilla L	46 Gy	2.5 Gy axilla 3 Gy chest wall	skin: gr. 2	skin: gr. 4 bone: gr. 4
12	F	60	cervix	pelvis including para-aortal nodes	78.9 Gy (including iridium template in bladder 21.8 Gy and brachytherapy)	1.8 Gy Brachytherapy: 1 x 8.5 Gy (Point A)	skin: gr. 2 upper GI: gr. 3 stomach: ulceration lower GI: gr. 1	skin: gr. 4 bone: gr. 4 bladder: gr. 3 rectum: gr. 4
13	F	63	breast	breast R	66 Gy	2 Gy	skin: gr. 2	skin: gr. 3 subcutaneous tissue: gr. 3
14	F	74	cervix	pelvis	59 Gy (including brachytherapy)	2 Gy Brachytherapy: 1 x 7 Gy and 1 x 6 Gy (point A)	upper GI: gr. 2 lower GI: gr. 2	rectum: gr. 3 bladder: gr. 2

predictive assay for normal tissue response. Telomeres cap the ends of chromosomes, thereby allowing cells to distinguish natural chromosome ends from damaged chromosomes. In this way, telomeres protect the chromosome ends from degradation and fusion<sup>19-21</sup>. After each cell cycle telomeric DNA decreases in length, which would ultimately lead to the loss of all telomeric sequences and subsequently of essential genetic information. Therefore, most cells use the telomerase enzyme to maintain telomeres. Recent evidence suggest a correlation between telomere maintenance, DNA damage response and radiosensitivity<sup>22-25</sup>. Significantly reduced telomere length is observed in radiosensitive murine lymphoma cells and mice deficient in telomerase<sup>26</sup>. In lymphocytes from breast cancer patients telomere length is inversely correlated with chromosomal radiosensitivity<sup>27</sup>. Shortening of telomeres by a defect in telomerase may cause the ends of chromosomes to be recognized as DSBs. Cells with these dysfunctional telomeres would be more sensitive to ionizing radiation generating DSBs. As a second objective in this study we examined whether telomere length is associated with an increased normal tissue reaction and could therefore be used as a predictive assay in radiotherapy.

## **Materials and Methods**

### **Patient selection**

Control patients were selected randomly in our institution and were treated for various types of cancer at different localizations. All control patients were treated with radiotherapy combined with surgery, never combined with chemotherapy. The control patients had acute and/or late toxicity of at most grade 1 or 2, based on the Radiation Therapy Oncology Group (RTOG) Acute Morbidity Scoring Scheme and the RTOG/EORTC Late Radiation Morbidity Scoring Scheme<sup>28</sup>. Patients defined as hypersensitive to ionizing radiation were treated for various types of cancer at different localizations with either radiotherapy combined with surgery or radiotherapy as a single modality, never combined with chemotherapy. The selection criteria for hypersensitive patients were: acute and/or late toxicity grade 3 or 4 after radiotherapy using a conventional schedule for an intentional curative treatment, without known co-morbidity and no combined treatment with chemotherapy. Based on our hypothesis that hypersensitivity to ionizing radiation might be due to a problem in genes involved in DNA repair or telomere length maintenance, which should result in a systemic defect independent of the type of tissue irradiated, no selection was made based on the treated area. All patients

gave informed consent to take a 4 mm skin biopsy outside the treated area and a 14 ml blood sample. Patient characteristics are shown in *Table 1*.

Fibroblasts from 5 T<sup>-</sup>B<sup>-</sup>NK<sup>+</sup> SCID patients without RAG gene mutations; 2 of which have a mutation in the Artemis gene and increased radiosensitivity, the third, called RS-SCID-B, with a mutation in the LigaseIV gene which also shows increased radiosensitivity, and the other two with no known mutations, were kindly provided by the Department of Immunology, Erasmus MC, Rotterdam<sup>29</sup>.

### **Cells and tissue culture**

Skin biopsies were cut into small pieces and cultured in Ham's F10 medium (Bio Whittaker, Europe), supplemented with 15% fetal calf serum, penicillin (100 U/ml) and streptomycin (100 µg/ml) until fibroblasts were growing. The fibroblasts were trypsinized and expanded. Other cell cultures used in this study were fibroblasts grown from skin biopsies of 5 juvenile SCID patients, 180BR with a mutation in LigaseIV<sup>30</sup> and the control fibroblasts VH10, FN1 and C5RO from skin biopsies of healthy volunteers. All cell cultures were grown in Ham's F10 medium supplemented with 15% fetal calf serum, penicillin (100 U/ml) and streptomycin (100 µg/ml) and were regularly tested for mycoplasma infections.

Lymphocytes were isolated by spinning from PBS-diluted blood samples after adding Lymphoprep (Nycomed Pharma AS, Norway). The buffy coat was removed from the Ficoll layer and washed in PBS. Cells were frozen in liquid nitrogen until further use. Lymphocytes were cultured in RPMI medium (Bio Whittaker, Europe) with 10% fetal calf serum, penicillin (100 U/ml) and streptomycin (100 µg/ml). The first 3 days lymphocyte growth was stimulated with phytohemagglutinin (1 µg/ml) (Glaxo Wellcome UK Ltd). After stimulation, Interleukin 2 (1 U/ml) (Strathmann Biotech GMBH) was added to the medium as a lymphoid growth factor.

### **Immunostaining**

Fibroblasts were grown on glass coverslips and irradiated using a <sup>137</sup>Cs source. After 8 hours they were fixed with 2% para-formaldehyde. Cells were washed with BSA (0.5%) and glycine (0.15%) in PBS and permeabilized with 0.1% Triton X-100 in PBS. The antibody against the protein of interest ( $\alpha$ -Mre11 (rabbit polyclonal antibody)<sup>31</sup>;  $\alpha$ -Rad51 (rabbit polyclonal antibody)<sup>32</sup>;  $\alpha$ -Rad54 (rabbit polyclonal antibody)<sup>33</sup>;  $\alpha$ - $\gamma$ -H2AX (rabbit polyclonal antibody, Upstate Group Inc., MA);  $\alpha$ -Brca1 (mouse monoclonal antibody, AB-1, Oncogene Science, Cambridge, MA)) was applied and the coverslips were incubated for 90 minutes. Again, the

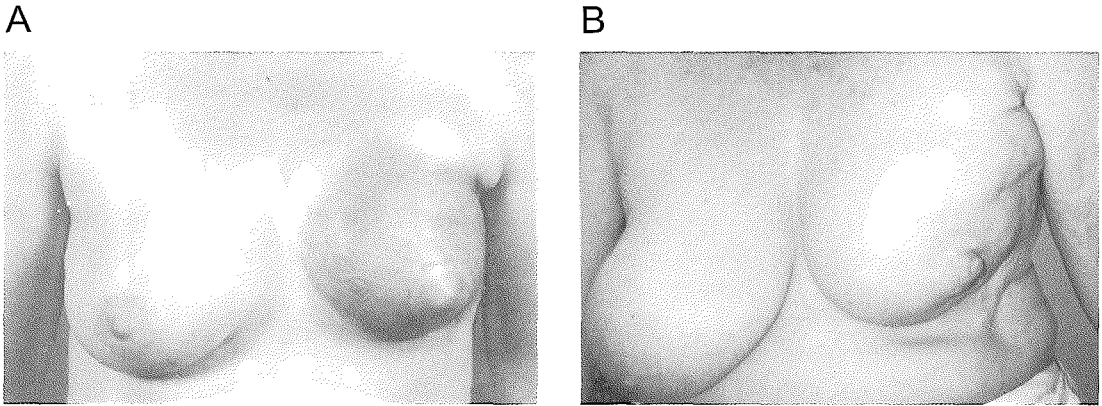


**Figure 1. Examples of patients with severe late side effects.**

Examples of 2 patients from the hypersensitive group with severe late toxicity after breast irradiation (atrophy and pigmentation change of the skin (A) and severe induration, loss of subcutaneous tissue and field contracture (A and B)).

Published with permission of both patients.

cells were washed and permeabilized and the secondary antibody tagged to a fluorescent group (Alexa Fluor 594 goat  $\alpha$ -rabbit/goat  $\alpha$ -mouse IgG, Molecular Probes Inc.) was applied. Cells were incubated for 60 minutes and subsequently washed with 0.1% Triton X-100 in PBS and regular PBS. Coverslips were put on object glasses covered with DAPI/DAPCO/Vectashield and sealed. Analysis of foci was performed using a Leica DMRBE fluorescent microscope connected to a Hamamatsu dual mode cooled CCD camera C4480. To visualize the fluorescence pattern the filtersets 31000 (Dapi), 31004 (Texas-Red) and the triple filter 83000 (Dapi-FITC-Texas-red) were used.

### **Determination of Telomere length**

Telomere length in lymphocytes of the control and hypersensitive patients was determined by a flow FISH assay and FACS analysis as described earlier<sup>34</sup>. Per patientsample  $2.4 \times 10^6$  cells were used. All experiments were done in triplo. Samples were analyzed using a FACS Calibur flow cytometer. To control for daily variations in the linearity of the flow cytometer, laser intensity and alignment, Quantumk 24 Low Level FITC beads (Bangs Laboratories INC., Fishers, IN, USA) in PBS with 0.1% BSA were analyzed at the beginning and end of each experiment. The resulting calibration curve was used to convert arbitrary fluorescence units to measurable equivalents of soluble fluorochrome (MESF). Results of telomere measure-

ments in these lymphocytes were analysed using SPSS 10 statistical software. A Mann-Whitney test was performed to calculate the p-value.

Since no lymphocytes were available of the 5 SCID and 180BR patients, telomere length in these patients was measured by Southern blot analysis using genomic DNA pellets from fibroblasts (passage numbers 7-17)<sup>35</sup>. Normal primary human fibroblasts (VH10 and C5RO) were used as positive controls. Genomic DNA was digested with *Hinfl* and *RsaI* overnight. Three microgram of DNA was used for gel electrophoresis. After denaturing in NaOH/NaCl the gel was blotted overnight and hybridized with a  $\gamma^{32}\text{P}$ -telomeric DNA probe. After scanning the blot using a Phosphor Imager, average Telomeric Restriction Fragment (TRF) length of the samples was calculated by the migrating distance of the smear corrected by intensity using ImageQuant software.

## **Results**

### **Patient groups**

For both the control and hypersensitive group 14 patients were included with similar characteristics considering age, gender and tumor type (*Table 1*). The majority of patients suffered from breast cancer. The follow up period was at least 4 years post-treatment. The maximum acute and late toxicity score in the control group was grade 2. In the hypersensitive group all patients suffered from grade 3-4 late toxicity of organs and/or tissues, while 2 patients had grade 3 acute toxicity as well. Pictures of two patients suffering from severe late side effects after breast irradiation are shown in Figure 1.

Material of 5 young (5-18 months) patients suffering from  $\text{T}^{-}\text{B}^{-}\text{NK}^{+}$  SCID without RAG gene mutations was acquired. A clonogenic survival assay showed increased sensitivity to ionizing radiation in 3 patients. Two of these patients turned out to have a mutation in the Artemis gene<sup>29</sup>, the third patient, called RS-SCID-B, has a mutation in the LigaseIV gene (unpublished results). Both these genes are involved in the NHEJ pathway of DNA repair.

### **Ionizing radiation induced foci formation**

Several radiosensitive cell lines with a mutation in one of the DNA repair genes show an decreased or increased ability to form IRIF of specific DSB repair proteins. Therefore, IRIF formation was tested in fibroblasts from the control and hypersensitive patients, a normal cell culture (C5RO), 180BR and SCID cell cultures. IRIF were detected by immunostaining using

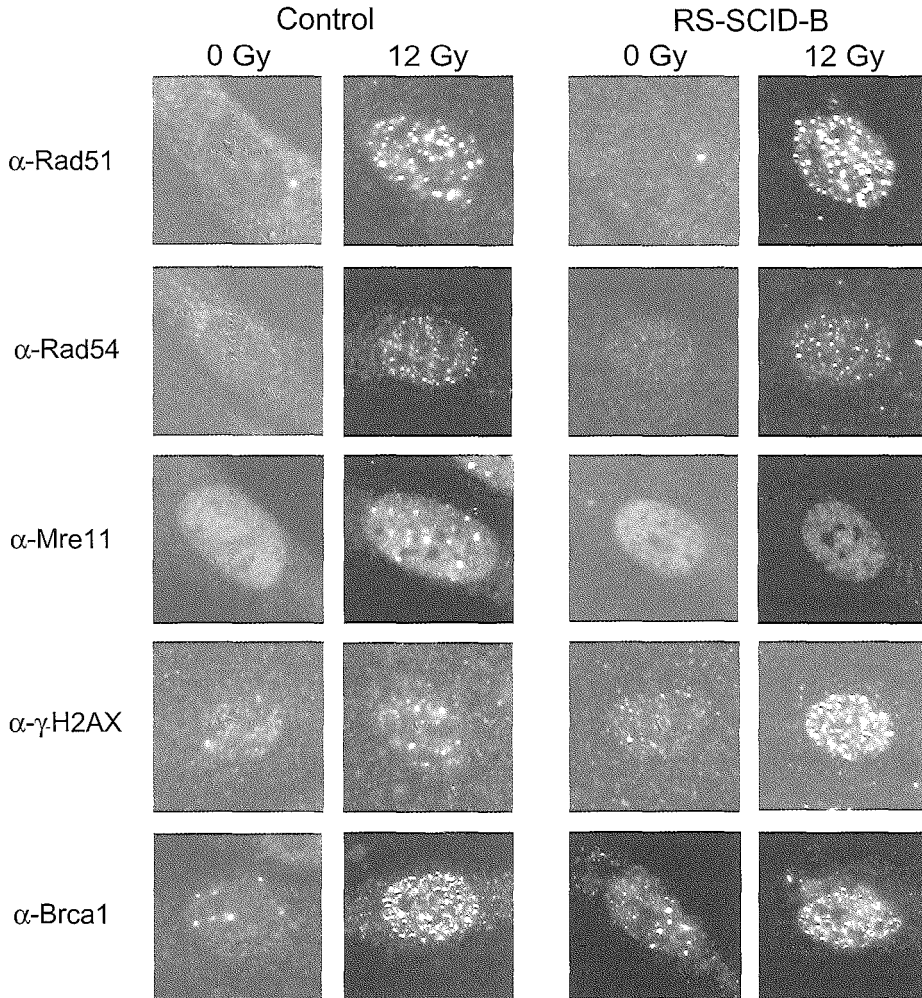


**Figure 2. Ionizing radiation induced foci formation of Rad51, Mre11,  $\gamma$ -H2AX and Brca1 in control and RS-SCID-B fibroblasts.**

Control primary human fibroblasts and RS-SCID-B primary fibroblasts were irradiated with 12 Gy and fixed after an incubation period of 8 hours. Immunostaining was performed using antibodies against Rad51, Rad54, Mre11,  $\gamma$ -H2AX and Brca1. Representative pictures of the cells before and after irradiation are shown for each antibody staining. No difference in IRIF formation was observed between control cells and RS-SCID-B cells after immunostaining for Rad51, Rad54 and Brca1. However, the appearance of the Mre11 IRIF was very different for RS-SCID-B compared to the control cells: foci were much smaller in the SCID cells though their quantity was much larger than in the control cells. The same feature was observed for  $\gamma$ -H2AX IRIF, although to a lesser extent: foci in RS-SCID-B cells were smaller than in the control cells, though their amount did not differ.

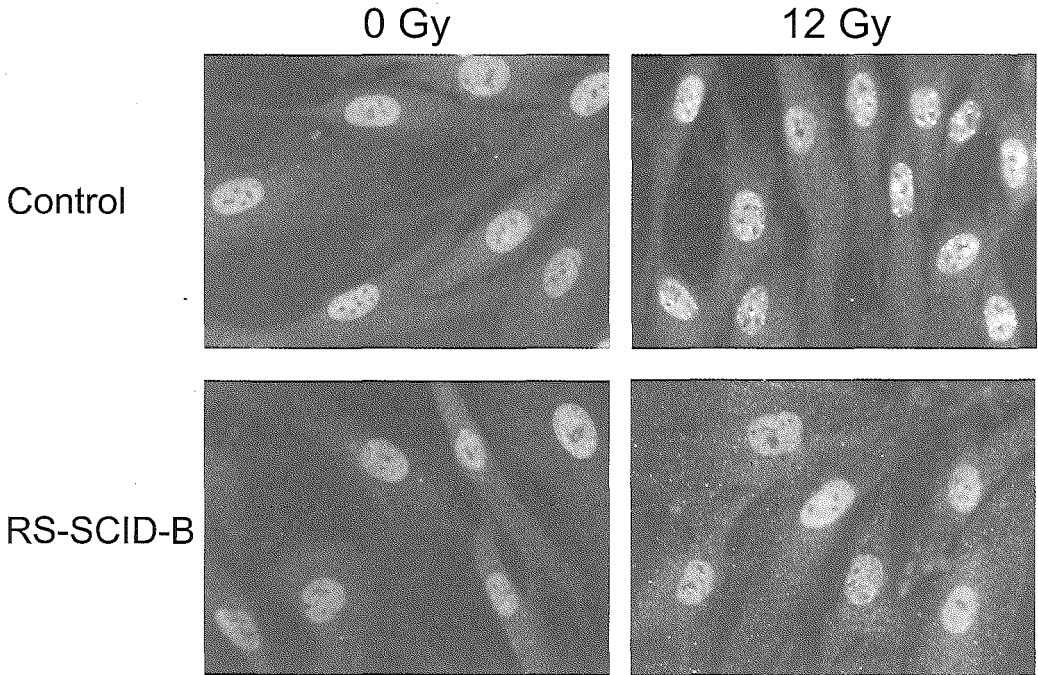


**Figure 3. Overview of Mre11 ionizing radiation induced foci in control and RS-SCID-B fibroblasts.**

Representative overview of Mre11 staining in control and RS-SCID-B cells before and after irradiation with 12 Gy and an incubation period of 8 hours. Very small and numerous, and therefore hardly discernable, Mre11 IRIF were observed in RS-SCID-B cells in contrast to the clearly detectable Mre11 IRIF in control cells.

antibodies against Rad51, Rad54, Mre11,  $\gamma$ -H2AX and Brca1 (Fig. 2). All cell cultures used had a passage number between 4 and 10.

Before irradiation no obvious difference was seen for Rad51 and Rad54 IRIF in all cell cultures. The cell cultures showed a few Rad51 foci and hardly any Rad54 foci. After treatment with ionizing radiation slight differences in IRIF formation of Rad51 and Rad54 were observed between the cell cultures. The number of Rad54 IRIF positive cells was always less than for Rad51 IRIF. Some distinction could be made in size of the foci and in lesser extent in number of foci per nucleus and number of positive cells. This slight difference in appearance was seen in both the control and hypersensitive patient cells. However, these differences were too small for reliable and routine use as a predictive assay. For the SCID cells only one radio-sensitive cell culture with a mutation in Artemis showed a difference in Rad51 and Rad54 IRIF: this cell culture showed less foci positive cells after irradiation compared to the second radio-

sensitive cell culture with an Artemis mutation and the other SCID cell cultures. The same result was seen for the 180BR cells compared to the patient cell cultures: less Rad51 and Rad54 foci positive cells were observed after irradiation.

For Mre11 no difference in IRIF formation was seen between cell cultures of the control and hypersensitive patients, both before irradiation, when hardly any Mre11 foci were seen, and after treatment, when a clear induction of foci was discernable. However, for the 180BR cell culture more small foci per nucleus were observed after ionizing radiation. Mre11 IRIF formation was also clearly altered in the other cell culture with a mutation in LigaseIV, the radiosensitive RS-SCID-B cells. As for 180BR, Mre11 foci were very small and numerous after irradiation and present in most cells (Fig. 2, 3). In none of the other cell cultures this altered appearance of Mre11 IRIF was observed.

$\gamma$ -H2AX IRIF were seen sporadic before irradiation, whereas all cell cultures showed a large number of foci after treatment. No major differences were observed between the cell

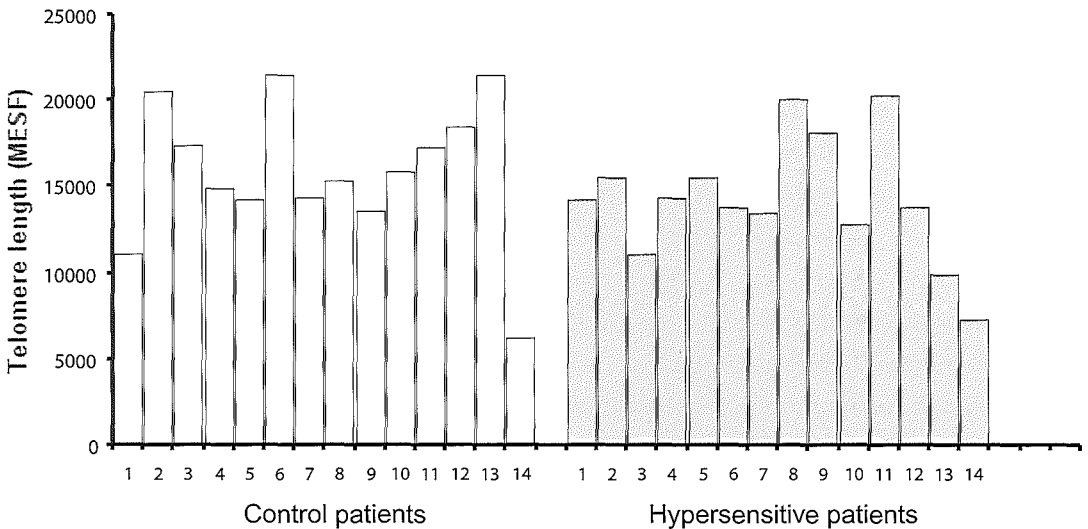


**Figure 4. Telomere length measurements in lymphocytes from control and hypersensitive patients.**

Telomere length in lymphocytes of the control and hypersensitive patients was determined by a flow FISH assay. Samples were analyzed using a FACS flow cytometer. The results are expressed in measurable equivalents of soluble fluorochrome (MESF) on the Y-axis. The individual score of each patient is shown, in subgroups of control and hypersensitive patients, on the X-axis. Numbers used are equivalent to the number of each patient used in Table 1. All experiments were done in triplo.



cultures, except for RS-SCID-B (*Fig.2*). In fibroblasts from this SCID patient  $\gamma$ -H2AX IRIF were smaller and seemed more numerous compared to the other cell cultures. However, as for Mre11 IRIF, it was not possible to easily objectively quantitate the results due to the small size and large number of the  $\gamma$ -H2AX IRIF.

The results for Brca1 IRIF formation were very heterogeneous. Before treatment all cell cultures showed a reasonable number (5-15) of foci. In most cell cultures this number did not obviously change after ionizing radiation, though the size of the foci did alter. Before treatment they appeared larger than after irradiation. However, due to the fact that both the number and the size of the foci was very dissimilar in all cell cultures it is anticipated that the predictive power of this assay will be limited.

### **Telomere length**

Several studies suggest the possibility of a link between radiosensitivity and telomere maintenance in mammalian cells<sup>26</sup>. Therefore, telomere length was measured by flow FISH in lymphocytes of the control and hypersensitive patients and by southern blotting in fibroblasts of the SCID and 180BR patients.

For the radiosensitive patient group (n = 14) mean telomere length was shorter than for the control group (n = 14): 12320 vs 16680 MESF (*Fig. 4*). However, after statistical analysis this difference turned out to be not significant with a p-value of 0.161. In this study the overall telomere length of radiosensitive patients is not significantly shorter than for control patients.

Telomere length in fibroblasts (passage numbers 7-17) from the 5 SCID patients, 180BR patient and 2 control patients varied little. For the SCID cell cultures from 6.9 to 9.8 kb and for the control patients from 6.6 to 8.4 kb. For the cell culture 180BR the telomere length was 6.6 kb. Again, these differences are too small to be of any significance.

### **Discussion**

In the present study an attempt was made to establish new methods that could be used as a predictive assay for normal tissue response in radiotherapy. We examined IRIF formation of various proteins involved in DSB repair in fibroblasts from hypersensitive patients and selected SCID patients. Furthermore telomere length was measured in lymphocytes and fibroblasts of the same patient groups.

Fibroblasts from patients with known defects in a number of the DNA repair genes show an increased sensitivity to ionizing radiation<sup>5,29,36-39</sup>. Murine cell cultures with mutations in genes involved in repair of DSBs by HR are radiosensitive as well. Moreover, Rad51 and Rad54 IRIF formation is diminished in these cell cultures<sup>40-46</sup>. Based on these results IRIF formation was determined in cells from patients overreacting to radiotherapy. Quantification of the number of foci positive cells and number of foci per nucleus is very time consuming and shows a large intra- and inter- observer variation due to the difficulty of discriminating foci by eye in all planes of a microscopical slide. Therefore, the amount of foci positive cells was estimated and compared to the other cell cultures examined. The results in this study on Rad51 and Rad54, two proteins involved in the DNA repair pathway of HR, show comparable numbers of foci positive cells after irradiation of cells from both the control and hypersensitive patient group. However, 180BR cells with a mutation in the LigaseIV gene and one of the SCID cell cultures with a mutation in Artemis, both involved in NHEJ, showed a reduced number of Rad51 and Rad54 IRIF positive cells. This has been described earlier for 180BR cells<sup>47</sup>. The results for Brca1, a cell cycle checkpoint and DNA repair protein, Mre11, most likely involved in both HR and NHEJ, and  $\gamma$ -H2AX, a DSB induced phosphorylation on histone H2AX are also not conclusive. Again, for both the hypersensitive and control group of patients the results show no major differences or are too heterogeneous to allow unambiguous conclusions. Surprisingly, the appearance of Mre11 and  $\gamma$ -H2AX IRIF was altered in the radiosensitive RS-SCID-B cells. Foci in this cell culture were much smaller and more numerous. A similar effect is seen for Mre11 in 180BR cells<sup>14,48</sup>. This might imply that, though Mre11 and  $\gamma$ -H2AX have the potential to form foci, either DSB repair is inefficient in these cells, leading to a large number of remaining unrepaired breaks, or that more DSBs are induced by ionizing radiation compared to cells from normal patients. From these results we conclude that aberrant IRIF formation of DSB repair proteins can be observed in cells from patients with proven increased cellular radiosensitivity and a known defect in one of the DNA repair genes. However, this method is less suitable as a screening method for normal tissue response after radiotherapy, due to the variability in number of foci and in their appearance. Since it is very difficult to quantitate foci, only gene defects that cause a complete deficiency of IRIF of specific DNA repair proteins can easily be detected. The same conclusion has been drawn by Olive *et al.* for  $\gamma$ -H2AX IRIF formation in mouse normal and tumor cells and by Qvarnstrom *et al.* in human skin biopsies. In these studies significant differences in the kinetics of loss of  $\gamma$ -H2AX IRIF for normal tissues have been found, but the relevance of these differences to intrinsic radiosensitivity still needs to be determined<sup>49,50</sup>.

The results on telomere length measurements in lymphocytes of the patients show no significant correlation between telomere length and increased radiosensitivity. This could be explained by the fact that telomere length in humans shows a considerable inter-individual variation and is also correlated with age and replicative senescence of cells<sup>51</sup>. Furthermore, telomere function in addition to telomere length is also an important determinant for increased radiosensitivity and could thereby account for the fact that no correlation between telomere length and radiosensitivity has been found in the cells investigated<sup>52</sup>. This could be the problem for the 180BR and SCID fibroblasts, where also no shortening of telomere length is found. Since these cells have proven and potential mutations in one of the genes involved in NHEJ, it is likely that they have dysfunctional instead of shortened telomeres, based on the observations in SCID mice where elongated telomeres are observed, with as a consequence increased levels of telomeric fusions<sup>53,54</sup>. From our results on telomere measurements we conclude that this method is not suitable as a predictive test for normal tissue reactions in radiotherapy due to a large variation between individuals.

Most research on predictive assays on normal tissues to date, has been based on the radiosensitivity of normal lymphocytes and fibroblasts as determined by clonogenic cell survival assays. Studies comparing the radiosensitivity of these cells with acute or late radiation damage have reported variable results. Consequently, clonogenic assays to predict radiation response are of limited clinical use<sup>8</sup>. Therefore, we examined alternative methods as IRIF formation and measurements of telomere length for their ability to predict normal tissue response, based on the hypothesis that increased radiosensitivity may be caused by a defect in one of the DSB repair genes. However, no significant correlation is found between IRIF formation of various DNA repair proteins or telomere length and hypersensitivity to ionizing radiation. There are several possibilities that might explain these negative findings. First, the selected patients in this study usually suffered from grade 3 and rarely grade 4 late toxicity in specific tissues. In case these patients would have a mutation in one of the genes involved in DSB repair, a different pattern of acute and severe toxicity could have been expected. Patients with known defects in one of the DNA repair genes usually show a catastrophic or even lethal reaction to treatment with ionizing radiation. These patients usually demonstrate severe acute and late toxicity which develops in all tissues involved, since cells in all organs will have a decreased ability to repair the DNA damage. None of our patients demonstrated such a severe reaction and therefore it is not likely that they will have a mutation in one of the repair genes.

The underlying hypothesis of predictive assay studies in normal and hypersensitive patients is that patients with a greater cellular radiosensitivity should have a higher risk of developing a severe normal tissue reaction. Dikomey *et al.* challenged this hypothesis by calculating that the variation of individual radiosensitivity is described by a normal distribution and all patients, not a subgroup, have a constant risk of developing late complications<sup>55</sup>. According to the study of Dikomey, our patients should have been analyzed separately and follow-up periods after radiotherapy should have been identical for each patient.

Another explanation for our non-conclusive findings could be the fact that experiments were performed on fibroblasts or lymphocytes, whereas the patients had complications in various tissues. For example, when studying radiosensitivity of fibroblasts, a relationship could be established with fibrosis, but not with telangiectasia or bone necrosis, since these tissues have completely different cell types. Therefore, it might be necessary to study the cells from the tissue that shows the toxicity in testing predictive assays<sup>3,4</sup>. Differential contributions of DSB repair pathways to radiosensitivity of different cell types has been established with the use of mouse models<sup>56</sup>. For example, fibrosis or vascular injury could be characterized by a common pathway in different tissues. However, since many different cell types are involved in radiation tissue injury it will be difficult to establish methods that measure radiosensitivity of specific cell types in heterogeneous tissues<sup>57</sup>.

In conclusion, it is important to understand the molecular mechanisms underlying acute and late normal tissue reactions in order to understand why there is a great variation in normal tissue reaction between individuals. Though IRIF formation and telomere length measurements do not seem suitable methods for a functional assay to predict normal tissue response, these methods might be used to understand the molecular background for differences in radiosensitivity between individuals.

## **Acknowledgements**

We thank P.A. Jeggo, Genome Damage and Stability Centre, University of Sussex, Falmer, Brighton, UK, for providing us with the 180BR human fibroblast cell culture. This work was supported by grants from the Dutch Organization for Scientific Research (NWO) and the European Commission.

## References

1. Twardella, D. et al. Personal characteristics, therapy modalities and individual DNA repair capacity as predictive factors of acute skin toxicity in an unselected cohort of breast cancer patients receiving radiotherapy. *Radiother Oncol* **69**, 145-53 (2003).
2. Dikomey, E., Borgmann, K., Peacock, J. & Jung, H. Why recent studies relating normal tissue response to individual radiosensitivity might have failed and how new studies should be performed. *Int J Radiat Oncol Biol Phys* **56**, 1194-200. (2003).
3. Kiltie, A.E. et al. A correlation between residual radiation-induced DNA double-strand breaks in cultured fibroblasts and late radiotherapy reactions in breast cancer patients. *Radiother Oncol* **51**, 55-65 (1999).
4. Kiltie, A.E. et al. Lack of correlation between residual radiation-induced DNA damage, in keratinocytes assayed directly from skin, and late radiotherapy reactions in breast cancer patients. *Int J Radiat Oncol Biol Phys* **43**, 481-7 (1999).
5. Zhou, P.K. et al. The radiosensitivity of human fibroblast cell lines correlates with residual levels of DNA double-strand breaks. *Radiother Oncol* **47**, 271-6 (1998).
6. Raaphorst, G.P. et al. Skin fibroblasts in vitro radiosensitivity can predict for late complications following AVM radiosurgery. *Radiother Oncol* **64**, 153-6 (2002).
7. Dikomey, E. et al. Molecular mechanisms of individual radiosensitivity studied in normal diploid human fibroblasts. Indicators of late normal tissue response after radiotherapy for head and neck cancer: fibroblasts, lymphocytes, genetics, DNA repair, and chromosome aberrations. *Toxicology* **193**, 125-35. (2003).
8. Leong, T., Borg, M. & McKay, M. Clinical and cellular radiosensitivity in inherited human syndromes. *Clin Oncol (R Coll Radiol)* **16**, 206-9 (2004).
9. Moshous, D. et al. Artemis, a novel DNA double-strand break repair/V(D)J recombination protein, is mutated in human severe combined immune deficiency. *Cell* **105**, 177-86. (2001).
10. O'Driscoll, M. et al. DNA ligase IV mutations identified in patients exhibiting developmental delay and immunodeficiency. *Mol Cell* **8**, 1175-85. (2001).
11. Raderschall, E., Golub, E.I. & Haaf, T. Nuclear foci of mammalian recombination proteins are located at single-stranded DNA regions formed after DNA damage. *Proc Natl Acad Sci USA* **96**, 1921-6. (1999).
12. Haaf, T., Golub, E.I., Reddy, G., Radding, C.M. & Ward, D.C. Nuclear foci of mammalian Rad51 recombination protein in somatic cells after DNA damage and its localization in synaptonemal complexes. *Proc Natl Acad Sci USA* **92**, 2298-302. (1995).
13. Jakob, B., Scholz, M. & Taucher-Scholz, G. Immediate localized CDKN1A (p21) radiation response after damage produced by heavy-ion tracks. *Radiat Res* **154**, 398-405. (2000).
14. Nelms, B.E., Maser, R.S., MacKay, J.F., Lagally, M.G. & Petrini, J.H. In situ visualization of DNA double-strand break repair in human fibroblasts. *Science* **280**, 590-2. (1998).
15. Tashiro, S., Walter, J., Shinohara, A., Kamada, N. & Cremer, T. Rad51 accumulation at sites of DNA damage and in postreplicative chromatin. *J Cell Biol* **150**, 283-91. (2000).
16. Kraakman-van der Zwet, M. et al. Brca2 (XRCC11) deficiency results in radioresistant DNA synthesis and a higher frequency of spontaneous deletions. *Mol Cell Biol* **22**, 669-79. (2002).
17. Ward, I.M. & Chen, J. Histone H2AX is phosphorylated in an ATR-dependent manner in response to replicational stress. *J Biol Chem* **276**, 47759-62. (2001).
18. West, S.C. Molecular views of recombination proteins and their control. *Nat Rev Mol Cell Biol* **4**, 435-45. (2003).
19. Blackburn, E.H. Switching and signaling at the telomere. *Cell* **106**, 661-73 (2001).

20. Chan, S.R. & Blackburn, E.H. Telomeres and telomerase. *Philos Trans R Soc Lond B Biol Sci* **359**, 109-21 (2004).
21. Greider, C.W. Telomeres do D-loop-T-loop. *Cell* **97**, 419-22 (1999).
22. d'Adda di Fagagna, F., Teo, S.H. & Jackson, S.P. Functional links between telomeres and proteins of the DNA-damage response. *Genes Dev* **18**, 1781-99 (2004).
23. Slijepcevic, P. Is there a link between telomere maintenance and radiosensitivity? *Radiat Res* **161**, 82-6 (2004).
24. Bouffler, S.D., Blasco, M.A., Cox, R. & Smith, P.J. Telomeric sequences, radiation sensitivity and genomic instability. *Int J Radiat Biol* **77**, 995-1005 (2001).
25. Wong, K.K. et al. Telomere dysfunction impairs DNA repair and enhances sensitivity to ionizing radiation. *Nat Genet* **26**, 85-8 (2000).
26. Goytisolo, F.A. et al. Short telomeres result in organismal hypersensitivity to ionizing radiation in mammals. *J Exp Med* **192**, 1625-36 (2000).
27. McIlrath, J. et al. Telomere length abnormalities in mammalian radiosensitive cells. *Cancer Res* **61**, 912-5 (2001).
28. Cox, J.D., Stetz, J. & Pajak, T.F. Toxicity criteria of the Radiation Therapy Oncology Group (RTOG) and the European Organization for Research and Treatment of Cancer (EORTC). *Int J Radiat Oncol Biol Phys* **31**, 1341-6. (1995).
29. Noordzij, J.G. et al. Radiosensitive SCID patients with Artemis gene mutations show a complete B-cell differentiation arrest at the pre-B-cell receptor checkpoint in bone marrow. *Blood* **101**, 1446-52. (2003).
30. Riballo, E. et al. Identification of a defect in DNA ligase IV in a radiosensitive leukaemia patient. *Curr Biol* **9**, 699-702. (1999).
31. de Jager, M. et al. DNA-binding and strand-annealing activities of human Mre11: implications for its roles in DNA double-strand break repair pathways. *Nucleic Acids Res* **29**, 1317-25. (2001).
32. Essers, J. et al. Analysis of mouse Rad54 expression and its implications for homologous recombination. *DNA Repair (Amst)* **1**, 779-93. (2002).
33. Essers, J. et al. Disruption of mouse RAD54 reduces ionizing radiation resistance and homologous recombination. *Cell* **89**, 195-204. (1997).
34. Rufer, N., Dragowska, W., Thornbury, G., Roosnek, E. & Lansdorp, P.M. Telomere length dynamics in human lymphocyte subpopulations measured by flow cytometry. *Nat Biotechnol* **16**, 743-7 (1998).
35. van Steensel, B. & de Lange, T. Control of telomere length by the human telomeric protein TRF1. *Nature* **385**, 740-3 (1997).
36. Smith, P.J. & Paterson, M.C. Enhanced radiosensitivity and defective DNA repair in cultured fibroblasts derived from Rothmund Thomson syndrome patients. *Mutat Res* **94**, 213-28. (1982).
37. Borg, M.F., Olver, I.N. & Hill, M.P. Rothmund-Thomson syndrome and tolerance of chemoradiotherapy. *Australas Radiol* **42**, 216-8. (1998).
38. Rogers, P.B., Plowman, P.N., Harris, S.J. & Arlett, C.F. Four radiation hypersensitivity cases and their implications for clinical radiotherapy. *Radiother Oncol* **57**, 143-54. (2000).
39. Riballo, E. et al. Cellular and biochemical impact of a mutation in DNA ligase IV conferring clinical radiosensitivity. Identification of a defect in DNA ligase IV in a radiosensitive leukaemia patient. *J Biol Chem* **276**, 31124-32. (2001).
40. Takata, M. et al. The Rad51 paralogue Rad51B promotes homologous recombinational repair. *Mol Cell Biol* **20**, 6476-82. (2000).
41. Takata, M. et al. Chromosome instability and defective recombinational repair in knockout mutants of the five Rad51 paralogs. *Mol Cell Biol* **21**, 2858-66. (2001).

42. Godthelp, B.C. et al. Mammalian Rad51C contributes to DNA cross-link resistance, sister chromatid cohesion and genomic stability. *Nucleic Acids Res* **30**, 2172-82. (2002).
43. Bishop, D.K. et al. Xrcc3 is required for assembly of Rad51 complexes in vivo. *J Biol Chem* **273**, 21482-8. (1998).
44. Bhattacharyya, A., Ear, U.S., Koller, B.H., Weichselbaum, R.R. & Bishop, D.K. The breast cancer susceptibility gene BRCA1 is required for subnuclear assembly of Rad51 and survival following treatment with the DNA cross-linking agent cisplatin. *J Biol Chem* **275**, 23899-903. (2000).
45. O'Regan, P., Wilson, C., Townsend, S. & Thacker, J. XRCC2 is a nuclear RAD51-like protein required for damage-dependent RAD51 focus formation without the need for ATP binding. *J Biol Chem* **276**, 22148-53. (2001).
46. Yuan, S.S. et al. BRCA2 is required for ionizing radiation-induced assembly of Rad51 complex in vivo. *Cancer Res* **59**, 3547-51. (1999).
47. Maser, R.S., Monsen, K.J., Nelms, B.E. & Petrini, J.H. hMre11 and hRad50 nuclear foci are induced during the normal cellular response to DNA double-strand breaks. *Mol Cell Biol* **17**, 6087-96. (1997).
48. Mirzoeva, O.K. & Petrini, J.H. DNA damage-dependent nuclear dynamics of the Mre11 complex. *Mol Cell Biol* **21**, 281-8. (2001).
49. Olive, P.L. & Banath, J.P. Phosphorylation of histone H2AX as a measure of radiosensitivity. *Int J Radiat Oncol Biol Phys* **58**, 331-5. (2004).
50. Qvarnstrom, O.F., Simonsson, M., Johansson, K.A., Nyman, J. & Turesson, I. DNA double strand break quantification in skin biopsies. *Radiother Oncol* **72**, 311-7 (2004).
51. Baird, D.M. & Kipling, D. The extent and significance of telomere loss with age. *Ann N Y Acad Sci* **1019**, 265-8 (2004).
52. Fannon, P., Wong, H.P., Silver, A.R., Slijepcevic, P. & Bouffler, S.D. Long but dysfunctional telomeres correlate with chromosomal radiosensitivity in a mouse AML cell line. *Int J Radiat Biol* **77**, 1151-62 (2001).
53. Gilley, D. et al. DNA-PKcs is critical for telomere capping. *Proc Natl Acad Sci USA* **98**, 15084-8 (2001).
54. Hande, P. et al. Elongated telomeres in scid mice. *Genomics* **56**, 221-3 (1999).
55. Jung, H., Beck-Bornholdt, H.P., Svoboda, V., Alberti, W. & Herrmann, T. Quantification of late complications after radiation therapy. *Radiother Oncol* **61**, 233-46 (2001).
56. Essers, J. et al. Homologous and non-homologous recombination differentially affect DNA damage repair in mice. *EMBO J* **19**, 1703-10. (2000).
57. Kruse, J.J., te Poele, J.A., Russell, N.S., Boersma, L.J. & Stewart, F.A. Microarray analysis to identify molecular mechanisms of radiation-induced microvascular damage in normal tissues. *Int J Radiat Oncol Biol Phys* **58**, 420-6 (2004).





## Summary

Proper maintenance of the genome is crucial for survival of all organisms. It is of major importance for the functioning of the cell that the information encrypted in the genome is transcribed correctly. However, endogenous and exogenous DNA damaging agents constantly threaten the integrity of the genome. Incorrect repair or accumulation of DNA damage results in genome instability, which may lead to impaired functioning of the cell. Therefore, all organisms are equipped with a complex network of DNA repair mechanisms, each of which is able to repair a subset of lesions. Among the most threatening lesions are DNA double-strand breaks (DSBs), which can be caused by ionizing radiation. DSBs are particularly dangerous when they occur during replication of the genome or during mitosis when the duplicated chromosomes are divided over the daughter cells. When broken chromosomes are carried through mitosis, the chromosome fragments will not distribute evenly between the two daughter cells, thus causing chromosomal aberrations. Several checkpoints can stop the cell at different points in the cell cycle when DNA damage is present, to allow time to repair the damage. In case DSBs are repaired incorrectly, it may lead to the origination of cancer, for example through loss of heterozygosity or development of translocations. In order to get more insight in the biological consequences of exposure to ionizing radiation in normal tissues, knowledge of repair mechanisms of DSBs in mammals is very important.

**Chapter 1** describes several types of DNA damage and the mechanisms by which these lesions can be repaired. DNA damage can be categorized into two classes. One class in which only one of the two DNA strands is damaged, such as alteration of bases. These type of lesions are repaired by use of the complementary strand as a template for repair. The second class of damage involves both strands of the DNA, such as in case of a double-strand break. Two major mechanisms can be used to repair DNA DSBs. The first repair pathway of homologous recombination (HR) uses the sister chromatid or homologous chromosome as a template to repair the damage. The second pathway, non-homologous end joining (NHEJ), simply joins the broken ends of the DNA without use of a template. Since the original DNA sequence is restored in HR, this type of repair is very precise, whereas NHEJ often leads to the addition or deletion of nucleotides at the joining site. In NHEJ important information may be lost, thus making this an error prone pathway. The relative contribution of these pathways to DSB repair likely depends on the cell cycle stage. The detection, processing and ligation of the break is organized by a large number of proteins, which are generally specific for each pathway, although some proteins may be involved in both HR and NHEJ.

---

The NHEJ repair pathway is not only used to repair DSBs which are induced by exogenous factors, but it is also involved in processing the programmed DSBs that arise during the generation of immunoglobulin and T-cell receptor genes. These programmed DSBs are natural intermediates in a specialized recombination event called V(D)J recombination. The lymphoid-specific proteins Rag1 and Rag2 initiate this DNA recombination reaction which is required for the creation of functional B- and T-cells. A deficiency in one of the Rag proteins or in one of the components of the NHEJ process severely impairs the capacity to perform V(D)J recombination which results in low levels of mature B- and T-cells.

In order to explore the relationship between oncogenesis and DSB repair defects in humans, studies involving cell lines and mouse models with mutations in DNA repair genes are performed. The importance of HR is emphasized by the finding that inactivation of genes involved in HR often results in embryonic lethality. Therefore, animal models have been designed in which the effect of mutations in specific tissues can be investigated. Results from these animal studies suggest a role for HR in the development of chromosomal translocations and oncogenesis. Defects in NHEJ not only lead to genomic instability but also to impaired functioning of the V(D)J recombination process. Immunodeficiency is therefore a characteristic feature of humans and mice with defects in one of the NHEJ genes. Depending on the specific gene, mice carrying mutations in NHEJ genes can be viable or die during embryogenesis. As main phenotype they show increased radiation sensitivity and immunodeficiency. In mice that carry mutations in one of the NHEJ genes and have a deficiency for p53, a cell cycle checkpoint gene, the lethality is rescued, but these mice are prone to develop lymphomas. Thus, a combination of a mutation in one of the DNA repair genes and a defect in other genes involved in genome stability, may accelerate cancer development, emphasizing the importance of the genetic background in oncogenesis.

In **Chapter 2** the biochemical activities of homologous recombination proteins and their coordinated action in the context of the living cell are described. Biochemical studies on the enzymes that mediate homologous recombination have provided a number of working models of how the reaction might take place in vitro, while recent cell biology studies have begun to address the behaviour of homologous recombination proteins inside cells. In one model for repair of a DSB by homologous recombination the missing DNA is restored using the intact homologous sequence provided by the sister chromatid. In the early stage of the reaction the DNA ends are processed into a 3' single-stranded overhang. The single-stranded DNA tails are coated with a strand exchange protein to form a nucleoprotein filament that

can recognize a homologous DNA sequence. The nucleoprotein filament invades the homologous template DNA to form a joint heteroduplex molecule linking the broken ends and the undamaged template DNA. In the late stage of recombination, DNA polymerases restore the missing information and DNA ends are ligated. In this chapter the function of a number of proteins involved in HR are discussed, with emphasis on the Rad52 group proteins; Rad51, Rad52 and Rad54, the five Rad51 paralogs, the Rad50/Mre11/NBS1 complex and the Brca1 and Brca2 proteins.

Rad51 is a key protein in HR because it forms a nucleoprotein filament that is able to recognize strand homology and it promotes DNA strand exchange. In total, five paralogs of Rad51 have been discovered; Xrcc2, Xrcc3, Rad51B, Rad51C and Rad51D. A mutation in one of the paralogs leads to chromosomal instability and it affects the efficiency of HR. Rad52 interacts with Rad51 and stimulates Rad51-mediated strand exchange. Rad52 mutants show a severe phenotype in yeast, whereas the phenotype of a Rad52 mutation in mammals is very subtle. Rad54 has been implicated to participate throughout the whole duration of the HR reaction by first stabilizing the Rad51 nucleoprotein filament, subsequently by stimulating Rad51-mediated joint molecule formation and chromatin remodeling. Finally, in the last stage of the reaction it could displace Rad51 from the product DNA. The precise function of the Rad50/Mre11/NBS1 complex is still unknown. Rad50 and Mre11 have shown to bind DNA ends and tether linear DNA molecules *in vitro*, while in yeast the complex is involved in NHEJ, sister chromatid repair by HR, telomere maintenance and formation and processing of DSBs in meiosis. Brca1 and Brca2 are required for homology-directed repair and gene targeting events. Biochemical data suggest that Brca2 can recruit Rad51 to a DSB and regulate the spatial distribution of Rad51. While Brca2 interacts directly with Rad51, the interaction between Brca1 and Rad51 appears to be indirect.

One way to study the behaviour of HR proteins at a cellular level is by the use of immunofluorescence. Many of the HR proteins accumulate into subnuclear structures, called foci, at sites of DNA damage. Foci can occur spontaneously during DNA replication or after treatment with DNA damaging agents. Immunofluorescence with use of an antibody against the protein of interest, is a commonly used method of detecting nuclear foci of proteins. Another approach to study foci formation is by stably transfecting the cDNA of the protein of interest tagged to a fluorescent group. In this manner, the behaviour of the protein can be observed before and after damage induction. A possible cooperation of specific proteins in DSB repair can be studied by investigating foci formation of two or more proteins at the same time in the same cell. Co-localization of foci suggests an association between the proteins of interest.

---

Though co-localization does not provide any information about the actual interaction of the proteins of interest, the results can lead to the suggestion whether specific proteins cooperate in the repair of DSBs. DNA repair deficient mutant cell lines can also be used to establish a possible cooperation between DSB repair proteins. Cell lines with a defect in one of the DNA repair proteins may show less or more spontaneous or damage induced foci, depending on the repair pathway that is diminished. An increase in number of foci might be due to the inability of the cell to repair the spontaneous occurring DSBs. A decrease in number of foci may occur in case the protein of interest, or one of its cooperating proteins, is not functioning properly. Table 1 in this chapter shows an extensive overview of the literature regarding foci formation of various repair proteins in normal and DSB repair deficient cell lines.

The principle of studying the dynamic behaviour of recombination proteins in living cells is based on the rate of recovery of the fluorescent signal of the protein in an area that has been bleached by a short laser pulse. The dynamic behaviour of Rad51, Rad52 and Rad54 in the nucleus is described in **Chapter 3**. The mobility of the Rad52 group proteins was studied by using fluorescence redistribution after photobleaching (FRAP) techniques. FRAP can be used to determine the diffusion rate of proteins by bleaching a small strip spanning the entire nucleus. Recovery of the fluorescence in the strip is monitored and the kinetics with which the fluorescence intensity in the strip reaches the same intensity as the unbleached area relates to the diffusion rate of a protein. FRAP can also be used to study the residence times of specific proteins in the DNA damage induced foci.

First, cooperation between Rad51, Rad52 and Rad54 was established using immunostaining in fixed cells. Pair-wise co-localization in DNA damage induced foci was observed for the Rad52 group proteins. Next, to ascertain whether the Rad52 group proteins are constituents of the same pre-assembled DNA repair complex in living cells, the dynamic behaviour of the proteins was studied using FRAP. The results show that all three proteins had a different mobility in the nucleus in undamaged cells. The experiments on dynamic behaviour of the Rad52 group proteins in ionizing radiation induced foci show that foci are dynamic structures of which Rad51 is a stably associated core component, whereas Rad52 and Rad54 rapidly and reversibly interact with the structure. The results of this study suggest that the major fraction of the Rad52 group proteins are not part of the same pre-assembled complex in the absence of DNA damage. Instead, the majority of the proteins are diffusing through the nucleus independently. The fact that the DNA repair proteins diffuse through the nucleus and assemble 'on-the-spot' in DNA repair complexes may have an advantage to complex for-

mation prior to DNA damage, because small complexes have more efficient access to DNA damage than bulky complexes. Furthermore, the observed homogeneous distribution of freely mobile DNA repair proteins ensures that all required factors are always present in the vicinity of DNA lesions wherever they occur, allowing rapid and efficient detection and subsequent repair.

In **Chapter 4** a systematic analysis of a number of factors that could be responsible for the variable outcome of results with regard to ionizing radiation-induced foci formation is performed. In these experiments Rad51 and Mre11 were used as a tool to monitor this influence. The results of the experiments show an increase in number of foci-positive cells for both Mre11 and Rad51 dependent on the time period after DNA damage. Furthermore, the size of the foci was positively correlated with the time after treatment of cells. The dose of ionizing radiation that is administered influenced the number of foci-positive cells as well. More foci-positive cells were seen after treatment with a higher dose, but also more foci per nucleus were observed. The increase of ionizing radiation-induced foci in a time- and dose dependent manner was found various cell lines, though the percentages of cells that are positive at each time- or dose-point depended on the specific cell line and the protein of interest. Although Rad51 and Mre11 ionizing radiation-induced foci were in general mutually exclusive, occasionally nuclei could be observed which contained co-localizing foci, which means that there is a correlation between Mre11 and Rad51 foci in a small subset of cells. The results presented in Chapter 4 demonstrate that the incubation period after ionizing radiation treatment, the dose administered and the specific cell cycle characteristics of the cell line of interest have a large influence on the number of foci positive cells, the amount of foci per nucleus and the features of the foci. Furthermore, the results demonstrate that despite the fact that Rad51 and Mre11 IRIF are mostly mutually exclusive there might be a certain moment during replication or DSB repair at which these proteins do cooperate.

**Chapter 5** describes the response of the Rad52 group proteins to DNA damage in radio-sensitive mammalian cell lines with a mutation in various genes involved in HR, examined by ionizing radiation induced foci formation. The results show that mammalian Rad52 can form nuclear foci in Xrcc2, Xrcc3, Rad51C and Brca2 mutant Chinese hamster cell lines upon ionizing radiation induced DSBs, whereas Rad51 and Rad54 cannot. Furthermore, mammalian Rad52 is not required for ionizing radiation-induced foci formation of Rad51 and Rad54. Further experiments in recombination-proficient cells reveal that all three proteins co-localize,

---

but that a distinction can be made between co-localization of Rad52 with either Rad51 or Rad54, which is generally limited, and co-localization of Rad51 and Rad54 foci, which is usually complete. Moreover, the kinetics of Rad52 ionizing radiation-induced foci formation is different from Rad51. Unlike yeast, where Rad52 is required for Rad51 and Rad54 foci formation, mammalian Rad52 is not required for ionizing radiation-induced foci formation of Rad51 and Rad54. Despite their evolutionary conservation and biochemical similarities, yeast and mammalian Rad52 appear to differentially contribute to the DNA damage response.

The protein Rad54 is known to have several functions in HR. To investigate which of the functions is responsible for ionizing radiation induced foci formation, embryonic stem cell lines were created with a specific mutation in Rad54 leading to decreased ATP binding. Cell lines with these mutant Rad54 proteins showed largely increased spontaneous Rad51 and Rad54 foci formation. One explanation could be that spontaneously arising DNA damage is not appropriately processed in the absence of Rad54 ATPase activity.

In **Chapter 6** the possibility to use ionizing radiation-induced foci formation as a functional assay in a clinical setting is examined. In an attempt to find an assay that is able to predict the normal tissue reaction of individuals upon irradiation, alternative possibilities for measuring individual radiosensitivity were examined that rely on the cellular response to DNA double-strand breaks introduced by ionizing radiation. This study was performed by screening cells of control and radiosensitive cancer patients and selected patients suffering from severe combined immunodeficiency (SCID) for possible defects in DNA double-strand break repair by examining ionizing radiation-induced foci formation of the proteins Rad51, Rad54, Mre11,  $\gamma$ -H2AX and Brca1. The results show that aberrant ionizing radiation-induced foci formation of DSB repair proteins can be observed in cells from patients with proven increased cellular radiosensitivity and a known defect in one of the DNA repair genes. However, this method turned out to be less suitable as a screening method for normal tissue response after radiotherapy, due to a large variability between patients in number of foci and in their appearance.

Determination of telomere length is another method that can possibly serve as a predictive assay for normal tissue response, since recent evidence suggest a correlation between telomere maintenance and radiosensitivity. Telomeres cap the ends of chromosomes, thereby allowing cells to distinguish natural chromosome ends from damaged chromosomes. In this way, telomeres protect the chromosome ends from degradation and fusion. In this study the association of telomere length and an increased normal tissue reaction to irradiation was exa-

mined. However, no correlation between telomere length and radiosensitivity could be found in the patient cell cultures.

From these experiments we conclude that ionizing radiation induced foci formation and telomere length measurements do not seem suitable methods for a functional assay to predict normal tissue response.





## Samenvatting

Nauwkeurige instandhouding van het genoom, dat het volledige erfelijk materiaal van een cel bevat, is essentieel voor de overleving van alle organismen. Daarom is het zeer belangrijk voor het functioneren van de cel dat de informatie die in het genoom ligt opgeslagen op een juiste wijze wordt gekopieerd. De intrinsieke structuur van het genoom wordt echter continu bedreigd door endogene en exogene factoren die het DNA beschadigen. Een opeenstapeling van DNA schade of verkeerde reparatie van het DNA resulteert in instabiliteit van het genoom, wat kan leiden tot verminderd functioneren van de cel. Alle organismen zijn daarom voorzien van een aantal mechanismen dat het DNA kan repareren. Elk van deze mechanismen kan een bepaald soort schade herstellen. Eén van de meest bedreigende vormen van DNA schade zijn de DNA dubbelstrengs breuken (DSBs), die kunnen worden veroorzaakt door ioniserende straling, zoals bij radiotherapie. DSBs zijn met name gevaarlijk wanneer ze ontstaan tijdens replicatie van het genoom of tijdens de deling van cellen, wanneer de verdubbelde chromosomen over de twee dochtercellen worden verdeeld. Indien een gebroken chromosoom deling ondergaat, worden de chromosoomfragmenten niet gelijkelijk over de dochtercellen verdeeld, waardoor chromosomale afwijkingen ontstaan. Daarom kan de cel, wanneer het DNA is beschadigd, op verschillende punten tijdens de celcyclus stoppen met vermenigvuldigen, zodat er tijd is om het DNA te herstellen. Wanneer DSBs niet goed worden gerepareerd kan dit leiden tot het ontstaan van kanker. Om meer inzicht te krijgen in de biologische processen die in gang worden gebracht in de normale weefsels na blootstelling aan ioniserende straling, is kennis van de verschillende mechanismen die DSBs kunnen herstellen onmisbaar.

**Hoofdstuk 1** beschrijft de verschillende soorten schade die aan het DNA kunnen ontstaan en de mechanismen die deze schade kunnen repareren. DNA schade kan in twee categorieën worden verdeeld. In de eerste categorie is slechts één van de twee DNA strengen beschadigd. Dit type schade wordt hersteld door de tegenoverliggende identieke DNA streng te gebruiken als een soort mal. Bij de tweede soort DNA schade zijn beide strengen van het DNA gebroken, zoals het geval is bij DSBs. Er zijn twee systemen die deze schade kunnen herstellen. Het eerste systeem, de homologe recombinatie (HR), gebruikt de tweede onbeschadigde kopie van het DNA met dezelfde DNA volgorde als een mal voor de reparatie. Bij het tweede systeem, de DNA eind-verbinding (NHEJ), wor-

---

den de gebroken uiteinden van het DNA simpelweg met elkaar verbonden, zonder dat hiervoor een mal wordt gebruikt. HR is een nauwkeurige manier om DNA te repareren, omdat hierbij de originele DNA volgorde wordt hersteld. Reparatie door middel van NHEJ is minder precies, omdat hierbij nucleotiden, waaruit het DNA bestaat, verloren kunnen gaan of kunnen worden toegevoegd. Herstel van DSBs via NHEJ is derhalve niet altijd foutloos, waardoor belangrijke informatie van het DNA verloren kan gaan. Een groot aantal eiwitten organiseert het signaleren, herstellen en verbinden van de DSBs. Deze eiwitten zijn over het algemeen verschillend voor de beide herstelsystemen, hoewel sommigen mogelijk betrokken zijn bij zowel HR als NHEJ.

NHEJ wordt niet alleen gebruikt bij het herstel van DSBs als gevolg van schade van buiten de cel, maar is ook betrokken bij het verwerken van de geprogrammeerde DSBs die optreden tijdens het maken van de genen die nodig zijn voor het immuunsysteem. Het ontstaan van deze DSBs treedt normaal op tijdens de zogenaamde V(D)J recombina-tie. Het V(D)J recombina-tie proces is noodzakelijk voor het aanmaken van de B- en T-cel-len die betrokken zijn bij de afweer.

Om de relatie tussen defecten in de reparatie van DSBs en het ontstaan van kanker te onderzoeken, worden veel studies verricht waarbij gebruik wordt gemaakt van cellijnen en muismodellen die mutaties bevatten in DNA reparatiegenen. Hierbij is vastgesteld dat inactivatie van genen die betrokken zijn bij HR, veelvuldig leidt tot het sterven van de muizen in de embryonale fase. Het grote belang van HR wordt hiermee nog eens bena-drukt. Er zijn speciale muismodellen ontwikkeld waarbij mutaties van HR genen in bepaalde weefsels kan worden onderzocht. De resultaten van onderzoek aan deze muis-modellen toont dat HR betrokken is bij het ontstaan van chromosomale afwijkingen en kanker. Afwijkingen in genen die betrokken zijn bij NHEJ leiden niet alleen tot instabiliteit van het genoom, maar ook tot het verminderd functioneren van het proces van V(D)J recombina-tie. Een defect in één van de NHEJ eiwitten leidt dan ook tot problemen met het immuunsysteem. Muizen met een mutatie in één van de NHEJ genen kunnen ofwel levensvatbaar zijn, of sterven in de embryonale fase, afhankelijk van het gen dat defect is. De muizen die levensvatbaar zijn tonen vrijwel altijd een hoge gevoeligheid voor bestraling en immuundeficiëntie. Bij muizen die zowel een defect hebben in één van de NHEJ genen, als in p53, een gen betrokken bij de celcyclus, wordt de letaliteit hersteld. Deze muizen hebben echter aanleg tot het ontwikkelen van lymfomen. Een combinatie van een mutatie in een DNA reparatiegen en een defect in een ander gen, wat betrokken is bij het instandhouden van het genoom, kan daarom het ontstaan van kanker versnellen.

In **Hoofdstuk 2** worden de biochemische kenmerken beschreven van de eiwitten die betrokken zijn bij HR en de samenwerking van deze eiwitten in levende cellen. Dankzij biochemische studies naar de eiwitten die HR reguleren is een aantal modellen ontwikkeld die het proces van HR in vitro beschrijven, terwijl recente celbiologische studies zich richten op het gedrag van deze eiwitten in de cel. In één van de modellen voor reparatie van DSBs door middel van HR, wordt het ontbrekende DNA hersteld met behulp van de tweede intacte kopie van het DNA die aanwezig is op het zuster-chromatide. Deze reparatie begint met het bewerken van de breukuiteinden. Deze breukuiteinden worden vervolgens bedekt door een eiwit wat de identieke DNA volgorde op het zuster-chromatide kan herkennen. Hierbij wordt het DNA wat de mal vormt gebonden aan de gebroken DNA uiteinden. Het ontbrekende DNA wordt hersteld naar voorbeeld van de mal door DNA polymerasen, waarna de gerepareerde DNA uiteinden met elkaar worden verbonden door een ligase. De functie van de verschillende eiwitten die betrokken zijn bij HR worden in dit hoofdstuk bediscussieerd.

Rad51 is het sleuteleiwit in HR, omdat dit eiwit de identieke DNA volgorde op het zuster-chromatide herkent en de uitwisseling van DNA strengen tot stand kan brengen. Er zijn in totaal vijf paraloge eiwitten van Rad51 ontdekt: Xrcc2, Xrcc3, Rad51B, Rad51C en Rad51D. Een mutatie in één van deze paralogen leidt tot afwijkingen van de chromosomen en heeft invloed op de efficiëntie van reparatie door HR. Rad52 werkt samen met Rad51 en stimuleert de door Rad51 gereguleerde uitwisseling van DNA strengen. Een mutatie van Rad52 in gist veroorzaakt ernstige afwijkingen, terwijl een mutatie van Rad52 in zoogdieren slechts tot geringe problemen leidt. Rad54 levert een bijdrage gedurende het hele proces van HR. Het stabiliseert de binding van Rad51 aan het DNA, vervolgens stimuleert het Rad51 bij de binding van het gebroken DNA aan het DNA wat als mal dient en het rangschikken van het chromatine. In de laatste fase van HR kan Rad54 helpen bij het loskoppelen van Rad51 van het DNA. De exacte functie van het Rad50/Mre11/Nbs1 complex is nog onduidelijk. In vitro zijn Rad50 en Mre11 in staat om de uiteinden van DNA te binden en vast te houden. In gist lijkt het complex betrokken te zijn bij NHEJ, reparatie van het zuster-chromatide tijdens HR, het onderhouden van de telomeren en het verwerken van DSBs tijdens meiose. Brca1 en Brca2 zijn onmisbaar tijdens reparatie door HR. Resultaten van biochemische experimenten lijken erop te wijzen dat Brca2 Rad51 kan aantrekken tot de DSB en de verdeling van Rad51 over het gebroken DNA kan reguleren. Brca1 daarentegen heeft waarschijnlijk alleen indirect invloed op het functioneren van Rad51.

---

Eén van de manieren om het gedrag van de eiwitten die betrokken zijn bij HR te bestuderen op cellulair niveau is door middel van immunofluorescentie. Veel HR eiwitten vormen kleine structuren in de kern die foci worden genoemd en zich bevinden op plaatsen waar DNA schade is opgetreden. Deze foci kunnen spontaan optreden tijdens de celdeling of na blootstelling aan factoren die het DNA beschadigen. Immunofluorescentie is één van de technieken die veelvuldig wordt gebruikt om foci te detecteren. Een andere methode om de vorming van foci te bestuderen is door het betreffende eiwit te koppelen aan een fluorescerende groep en in het DNA te integreren. Het gedrag van dit eiwit kan daardoor zowel voor als na behandeling worden bestudeerd in levende cellen. Om een mogelijke samenwerking van bepaalde eiwitten te onderzoeken kan de vorming van foci van twee of meer eiwitten in dezelfde cel op hetzelfde tijdstip worden onderzocht. Co-localisatie, waarbij de eiwitten zich tegelijkertijd op dezelfde plaats bevinden, kan duiden op een verband tussen deze eiwitten. Alhoewel co-localisatie geen uitsluitel geeft over de specifieke interactie tussen de eiwitten, kan het wel een aanwijzing zijn dat bepaalde eiwitten samenwerken tijdens de reparatie van DSBs. Cellijnen met een defect in één van de DNA reparatie eiwitten kunnen meer of minder foci bevatten. Een vermindering in het aantal foci kan ontstaan wanneer het eiwit dat wordt onderzocht, of een eiwit waar deze mee samenwerkt, niet goed functioneert. Een toename van het aantal foci kan het gevolg zijn van een verminderd vermogen van de cel om de DNA schade te herstellen. Tabel 1 in dit hoofdstuk toont een uitgebreid overzicht van de literatuur met betrekking tot de vorming van foci door de verschillende eiwitten die betrokken zijn bij het herstel van DNA schade in normale cellijnen en cellijnen met een mutatie.

Het principe van het bestuderen van het dynamische gedrag van eiwitten die betrokken zijn bij HR in levende cellen is gebaseerd op de snelheid van het herstel van een fluorescerende signaal dat aan een eiwit is gebonden in een gebied dat is 'gebleekt' door een laserpulse. Het dynamische gedrag van Rad51, Rad52 en Rad54 in de celkern wordt beschreven in **Hoofdstuk 3**. De mobiliteit van deze eiwitten werd bestudeerd met behulp van de 'redistributie van fluorescentie na bleking' (FRAP) techniek. FRAP kan worden gebruikt om de diffusiesnelheid van eiwitten te meten door middel van het bleken van een strook die de gehele celkern overbrugt. De snelheid van het herstel van de intensiteit van de fluorescentie geeft een indicatie over de diffusiesnelheid van het betreffende eiwit. FRAP kan ook worden gebruikt om te bestuderen hoe lang bepaalde eiwitten zich in de door DNA schade geïnduceerde foci bevinden.

Allereerst werd samenwerking tussen Rad51, Rad52 en Rad54 vastgesteld door middel van immunofluorescentie, waarbij co-localisatie van deze eiwitten ter plaatse van de foci kon worden geobserveerd. Vervolgens werd het dynamische gedrag van deze eiwitten bestudeerd met behulp van FRAP, teneinde vast te stellen of Rad51, Rad52 en Rad54 mogelijk deel uitmaken van een samengesteld complex van reparatie-eiwitten dat reeds aanwezig is voordat DNA schade ontstaat. De resultaten tonen dat deze drie eiwitten zich allemaal met een verschillende snelheid voortbewegen in de kernen van onbeschadigde cellen. Wanneer dezelfde experimenten in de door DNA schade geïnduceerde foci werden verricht, werd gezien dat deze foci dynamische structuren zijn waarbij Rad51 de stabiele component is terwijl Rad52 en Rad54 slechts kortdurend aanwezig zijn in deze structuren. De resultaten van deze studie suggereren dat het merendeel van de Rad51, Rad52 en Rad54 eiwitten geen deel uitmaken van een samengesteld complex van reparatie-eiwitten wanneer er geen schade aan het DNA is. Integendeel, het grootste deel van de eiwitten beweegt zich onafhankelijk door de celkern. Een voordeel van het feit dat de DNA reparatie-eiwitten zich vrijelijk door de kern bewegen in plaats van een complex te vormen voordat DNA schade is ontstaan, zou kunnen zijn dat kleine eiwitcomplexen gemakkelijker toegang hebben tot de plaats van DNA schade dan volumineuze complexen. Bovendien is het een voordeel dat de benodigde factoren voor herstel van DNA altijd snel in de buurt van de schade kunnen zijn wanneer de eiwitten zich vrijelijk door de kern bewegen, waardoor snelle en efficiënte herkenning van schade en vervolgens reparatie kan plaatsvinden.

In **Hoofdstuk 4** is een systematische analyse verricht naar een aantal factoren dat van invloed kan zijn op de resultaten van onderzoek door middel van stralingsgeïnduceerde foci. In de experimenten is gebruik gemaakt van Rad51 en Mre11 om de invloed van deze factoren te kunnen bepalen. De resultaten van deze proeven tonen aan dat een toename in het aantal cellen dat foci bevat afhankelijk is van de tijdsduur na de bestraling. Daarbij nam ook de grootte van de foci toe naarmate er meer tijd verstreek na bestraling. De dosis ioniserende straling was ook van invloed op het aantal foci-positieve cellen. Echter, na behandeling van de cellen met een hogere dosis straling werden niet alleen meer foci-positieve cellen waargenomen, maar ook het aantal foci per celkern was toegenomen. Het percentage foci-positieve cellen op een bepaald tijdstip en dosis was afhankelijk van de cellijn en het eiwit dat werd onderzocht. Hoewel Rad51 en Mre11 foci zich over het algemeen nooit in dezelfde kernen op hetzelfde moment bevinden, werden af en toe toch cel-

---

len gezien waarin Rad51 en Mre11 foci co-localisatie vertoonden. Dit kan betekenen dat er een correlatie is tussen deze twee eiwitten in een klein deel van de cellen. De resultaten die in hoofdstuk 4 worden beschreven tonen aan dat de incubatietijd na behandeling met bestraling, de dosis straling en de specifieke eigenschappen met betrekking tot de celcyclus van de betreffende cellijn invloed hebben op het aantal foci-positieve cellen, het aantal foci per celkern en de kenmerken van de foci. Bovendien laten de resultaten zien dat Rad51 en Mre11 op een bepaald moment tijdens de reparatie van DNA samenwerken, hoewel deze eiwitten normaliter geen foci vormen in dezelfde cellen.

**Hoofdstuk 5** beschrijft de reactie van Rad51, Rad52 en Rad54 op DNA schade in cellijnen die overgevoelig zijn voor straling en een defect in één van de genen bevatten die betrokken zijn bij de reparatie van DSBs via HR. Dit is onderzocht met behulp van stralingsgeïnduceerde vorming van foci. De resultaten laten zien dat Rad52 in staat is om foci te vormen na DNA beschadiging in hamstercellen met een mutatie in Xrcc2, Xrcc3, Rad51C of Brca2, terwijl Rad51 en Rad54 hiertoe niet in staat waren. Bovendien bleek Rad52 niet noodzakelijk te zijn voor stralingsgeïnduceerde Rad51 en Rad54 foci. Aanvullende experimenten in normale cellijnen tonen aan dat de foci van deze drie eiwitten allen co-localiseren, maar dat de co-localisatie tussen Rad52 en Rad51 of Rad54 beperkt is, terwijl Rad51 en Rad54 foci elkaar volledig overlappen. Daarbij vertonen Rad52 foci een andere kinetiek dan Rad51 foci. In tegenstelling tot in gist, waar Rad52 onmisbaar is voor de vorming van Rad51 en Rad54 foci, is Rad52 in zoogdieren niet noodzakelijk voor stralingsgeïnduceerde vorming van Rad51 en Rad54 foci. Ondanks het feit dat Rad52 in gist en in zoogdieren biochemisch dezelfde eigenschappen vertoont en de DNA volgorde sterk overeenkomt, lijkt de bijdrage van gist Rad52 en zoogdier Rad52 aan de respons op DNA schade sterk verschillend.

Het eiwit Rad54 heeft verschillende functies tijdens de reparatie van DNA schade via HR. Om te onderzoeken welke van deze functies verantwoordelijk is voor het ontstaan van stralingsgeïnduceerde foci werden embryonale stamcellen met een specifieke mutatie in Rad54 gemaakt. Deze mutatie leidde tot verminderde binding van het ATP. Cellijnen met deze mutante Rad54 eiwitten vertoonden een sterke stijging in het aantal spontane Rad51 en Rad54 foci. Een verklaring hiervoor kan zijn dat de spontaan optredende DNA schade niet goed kan worden bewerkt in afwezigheid van Rad54 ATPase activiteit.

In **Hoofdstuk 6** is de mogelijkheid onderzocht om de proeven met stralingsgeïnduceerde vorming van foci te gebruiken vanuit het oogpunt van de kliniek. Om te proberen een manier te vinden die het effect van bestraling op de normale weefsels van patiënten kan voorspellen, werd naar een nieuwe methode gezocht om de individuele stralingsgevoeligheid te meten. Door middel van het screenen van cellen van een controlegroep, een groep stralingsgevoelige kankerpatiënten en een geselecteerde groep patiënten met severe combined immunodeficiency (SCID), werd getracht om mogelijke defecten in de DNA DSB reparatiemechanismen op te sporen met behulp van de vorming van foci van de eiwitten Rad51, Rad54, Mre11,  $\gamma$ -H2AX en Brca1. De resultaten laten zien dat een afwijkend patroon in stralingsgeïnduceerde vorming van foci kan worden waargenomen in cellen van patiënten met een verhoogde gevoeligheid voor bestraling en een bewezen defect in een reparatiegen. Deze methode was echter minder geschikt als screeningsmethode om de reactie van de normale weefsels op bestraling te voorspellen, als gevolg van de variabiliteit in het aantal foci en de grootte van de foci.

Het bepalen van telomeerlengte is een andere methode die mogelijk zou kunnen dienen als screeningsmethode om de reactie van bestraling op de normale weefsels te voorspellen, aangezien recente studies een verband aantonen tussen het onderhoud van de telomeren en stralingsgevoeligheid. Telomeren bedekken de uiteinden van de chromosomen, waardoor de cel onderscheid kan maken tussen normaal voorkomende uiteinden van chromosomen en beschadigde uiteinden zoals het geval is bij DSBs. Op deze manier beschermen telomeren de chromosoomuiteinden tegen verval. In dit hoofdstuk werd het verband tussen telomeerlengte en een verhoogde gevoeligheid voor bestraling onderzocht. Er kon echter geen correlatie tussen stralingsgevoeligheid en telomeerlengte worden vastgesteld in de cellen van de onderzochte patiënten.

Uit deze experimenten kunnen we concluderen dat de vorming van stralingsgeïnduceerde foci van bepaalde eiwitten in cellen en het meten van de telomeerlengte geen geschikte methoden zijn om de respons van de normale weefsels op bestraling te voorspellen.





## Curriculum Vitae

- Name: Lieneke van Veelen
- Date of birth: September 20th 1969, Groningen
- 1981-1987: Gymnasium- $\beta$ , Stedelijk Gymnasium, Leeuwarden
- 1987-1996: Medical School, Leiden University
- Graduation project on the "Potential use of 'immediate early' gene expression in the assessment of tumor cell killing". Department of Medicine and the Cancer Center, University of California, San Diego. Supervision by Prof. S.B. Howell, MD.PhD.
- Special internship at the Department of Pediatric Oncology, Emma Children's Hospital and Academic Medical Center, University of Amsterdam. Study on the urinary profile of DOPA-metabolites in patients with neuroblastoma. Supervision by Prof. H.N. Caron, MD.PhD.
- Retrospective study at the treatment outcome for non-seminoma. Supervision by Prof. F.J. Cleton, MD.PhD., Department of Oncology, Leiden University Medical Center.
- 1996-1997: Resident internal medicine, Meander Medical Center, Amersfoort.
- 1997-2004: Resident radiation oncology (AGIKO), Department of Radiation Oncology, Erasmus MC-Daniel den Hoed Cancer Center, University Medical Center, Rotterdam. Head of the Department: Prof. P.C. Levendag, MD.PhD. Registered radiation oncologist in 2004.
- 1999-2002: PhD project on DNA repair mechanisms (AGIKO). Department of Cell Biology and Genetics, Erasmus MC, University Medical Center. Supervision by Prof. R. Kanaar, PhD.
- 2005: From March 2005 appointed for a combined function as radiation oncologist and researcher at the Department of Radiation Oncology, VU University Medical Center, Amsterdam.



## **List of publications**

- van Veelen LR, Essers J, van de Rakt MWMM, Odijk H, Paulusma CC, Kanaar R.  
Ionizing radiation-induced foci formation of mammalian Rad51 and Rad54 depends on the Rad51 paralogs, but not on Rad52.  
*Mutation Research*, In Press (2005)
- van Veelen LR, Cervelli T, van de Rakt MWMM, Theil AF, Essers J, Kanaar R.  
Analysis of ionizing radiation-induced foci of DNA damage repair proteins.  
*Mutation Research*, In Press (2005)
- van Veelen LR, Wesoly J, Kanaar R.  
Biochemical and cellular aspects of homologous recombination.  
*DNA Damage Recognition*, Marcel Dekker Inc., first edition. In Press
- van Veelen LR, Kanaar R, van Gent DC.  
DNA repair and malignant hematopoiesis.  
L. Degos, D.C. Linch and B. Löwenberg, eds., Taylor & Francis Group, London, UK. *Textbook of Malignant Haematology* (2nd Edition), (2005): 155-164.
- Noordzij JG, Verkaik NS, Van Der Burg M, Van Veelen LR, De Bruin-Versteeg S, Wiegant W, Vossen JM, Weemaes CM, De Groot R, Zdzienicka MZ, van Gent DC, van Dongen JJ.  
Radiosensitive SCID patients with Artemis gene mutations show a complete B-cell differentiation arrest at the pre-B-cell receptor checkpoint in bone marrow.  
*Blood*. 2003 Feb 15;101(4):1446-1452.
- Essers J, Houtsmuller AB, van Veelen L, Paulusma C, Nigg AL, Pastink A, Vermeulen W, Hoeijmakers JH, Kanaar R.  
Nuclear dynamics of RAD52 group homologous recombination proteins in response to DNA damage.  
*EMBO J*. 2002 Apr 15;21(8):2030-2037.
- van Veelen LR, Steyerberg EW, Cleton FJ, Keizer HJ.  
Results of 15 years of treatment of nonseminoma testicular cancer: 84% 5-year survival rate.  
*Ned Tijdschr Geneeskd*. 1999 Mar 13;143(11):564-568. Dutch.



## Dankwoord

Met veel plezier schrijf ik de laatste pagina's van dit proefschrift omdat het mij in de gelegenheid stelt iedereen te bedanken die hieraan heeft bijgedragen. Basaal wetenschappelijk onderzoek doen tijdens de opleiding tot radiotherapeut vraagt van alle betrokkenen veel inzet en flexibiliteit. De steun en medewerking die ik hiervoor van iedereen heb ontvangen is daarom van onschatbare waarde geweest.

Allereerst wil ik graag mijn promotoren Roland Kanaar en Peter Levendag bedanken. Roland, ik denk dat ik mij geen betere begeleider had kunnen wensen. Ondanks je eerste bedenkingen om in zee te gaan met een 'onwetende' arts, heb je veel tijd en energie gestoken in mijn onderzoek en proefschrift. Van je precisie en kritische wetenschappelijke houding heb ik erg veel geleerd, zo ook van je instelling om met minder geen genoegen te nemen. Peter, dank voor het vertrouwen in het feit dat laboratoriumonderzoek doen en een opleiding tegelijkertijd wel degelijk samen kunnen gaan. Veel dank voor je steun om deze AGIKO constructie te bewerkstelligen en je hulp om deze tot een goed einde te brengen.

Prof.dr. J.H.J. Hoeijmakers; dank voor de mogelijkheid die u mij hebt geboden om binnen uw vakgroep promotie-onderzoek te doen.

De leden van de beoordelingscommissie; prof.dr. P.A.E. Sillevius Smitt, prof.dr. A.C. Begg en dr. W. Vermeulen dank ik hartelijk voor het kritisch beoordelen van het manuscript.

Alle collega's uit het lab; Asia, Coen, Martijn, Alex, Mauro, Dejan, Claire, Raoul, Ellen, Nicole, Erik, Anja, Sheba, Gusia, Katsuhiko, Koos, Hanny, Linda en Esther wil ik bedanken voor hun hulp, gezelligheid en belangstelling, ook toen ik alweer 'aan de overkant' zat. Mandy, veel dank voor alle tellingen. Cecile, niemand doet ooit tevergeefs een beroep op je, veel dank voor je hulp op alle fronten. Dik, bedankt voor het onderricht in de grondbeginselen van de moleculaire biologie. Jeroen, ik vond het heel fijn om met je samen te werken en te discussiëren over de resultaten. Heel veel dank voor je hulp en het meelezen van het manuscript. Ik hoop dat we elkaar in de toekomst weer tegen gaan komen in het grijze gebied van de 'translational research'.

Sjozef, Ton, Pim, Jan-Jos in het lab en Bart Kanis in de Daniel den Hoed kliniek, wil ik bedanken voor hun hulp op het gebied van de automatisering. Marieke, Jasperina, Rita en Melle voor hun administratieve ondersteuning en Jan de Wit voor zijn hulp op het gebied van celkweken.

---

I would like to thank Professor Ralph Weichselbaum and Helena Mauceri from the University of Chicago, Department of Radiation Oncology, for giving me the opportunity to perform a number of experiments in their laboratory and giving me a warm welcome.

Het klinische deel van het onderzoek had nooit tot stand kunnen komen zonder de vrijwillige deelname van patiënten. Ik wil hen dan ook danken voor het feit dat zij geheel belangeloos bereid waren deel te nemen aan mijn onderzoek en dr. A.N. van Geel voor het verzamelen van het patiëntenmateriaal.

Onderzoek doen tijdens de opleiding kan niet zonder de bereidheid van collega's om een deel van het klinische werk op zich te nemen. Mijn collega arts-assistenten dank ik daarom hartelijk voor hun steun, interesse, gezelligheid en het spontaan overnemen van diensten en patiëntenzorg wanneer dat nodig was. In het bijzonder wil ik Karen, Karin en Marijël bedanken voor de leuke (wetenschappelijke) discussies. De stafleden van de afdeling radiotherapie dank ik eveneens voor hun interesse en flexibiliteit met betrekking tot de nodige supervisie. De secretaresses van de afdeling radiotherapie wil ik bedanken voor hun hulp. Met name Jeannette, Natasja en in het bijzonder Henny; jullie hebben er altijd voor gezorgd dat de organisatie rondom de patiëntenzorg vlekkeloos verliep, en daarbij kon ik op hectische dagen bij jullie altijd even op adem komen voor een gezellig gesprek en een kop thee.

Ilse en Karen, het is een hele eer om twee van zulke wijze en lieve dames aan mijn zijde te hebben tijdens de promotie. Ik ben er trots op dat jullie mijn paranimf willen zijn.

Lieve familie en vrienden, ondanks het feit dat ik het de laatste jaren vaak heb laten afweten op belangrijke gebeurtenissen, hebben jullie altijd begrip kunnen opbrengen voor de situatie en zijn jullie geïnteresseerd gebleven in mijn doen en laten. Heel veel dank hiervoor.

Mijn ouders hebben mij de basis gegeven om dit proefschrift te kunnen schrijven en mij altijd gestimuleerd om door te zetten. Lieve pap, mam, Petra, Eveline en Niek, bedankt voor alles wat jullie de afgelopen jaren voor mij hebben gedaan en voor jullie steun en vertrouwen.

Liefste Roeland, het is een publiek geheim dat dit proefschrift er zonder jouw onvoorwaardelijke liefde en zorg nooit zou zijn gekomen. De afgelopen jaren heb je jezelf altijd weggecijferd om mij te helpen en begrip getoond voor mijn kluzenaarsgedrag. Ik hoop dat er nu een tijd aanbreekt waarin we samen met Sieb kunnen gaan genieten.